Regulation of SnRK1-dependent energy signaling by sumoylation

Leonor Ribeiro Duarte Margalha

Dissertation presented to obtain the Ph.D degree in Molecular Biology

Instituto de Tecnologia Química e Biológica António Xavier | Universidade Nova de Lisboa

Oeiras,
September, 2015

INSTITUTO
DE TECNOLOGIA
QUÍMICA E BIOLÓGICA
/UNL

Knowledge Creation

Regulation of SnRK1-dependent energy signaling by sumoylation

Leonor Ribeiro Duarte Margalha

Dissertation presented to obtain the Ph.D degree in Molecular Biology

Instituto de Tecnologia Química e Biológica | Universidade Nova de Lisboa

Research work coordinated by

Oeiras,
September,
2015

INSTITUTO
DE TECNOLOGIA
QUÍMICA E BIOLÓGICA
/UNL

Knowledge Creation

Margalha, L.

Regulation of SnRK1-dependent energy signaling
by sumoylation

Ph.D thesis, Instituto Gulbenkian de Ciência,
Universidade Nova de Lisboa, 2015

In English, with abstract in Portuguese
This thesis has been scanned for plagiarism and
there was no conflict with published works

Supervisor:

Elena Baena-González, Ph.D
Plant Stress Signaling
Instituto Gulbenkian de Ciência
Oeiras, Portugal

Examiners:

Jürgen Dohmen, Ph.D
Institute for Genetics, University of Cologne
Cologne, Germany

Filip Rolland, Ph.D
Molecular Plant Biology, KU Leuven
Leuven, Belgium

Isabel Abreu, Ph.D
GPlantS Unit,
Instituto de Tecnologia Química e Biológica António Xavier
Universidade Nova de Lisboa
Oeiras, Portugal

Alekos Athanasiadis, Ph.D
Protein-nucleic acids interactions
Instituto Gulbenkian de Ciência
Oeiras, Portugal

" We shall not cease from exploration
And the end of all our exploring
Will be to arrive where we started
And know the place for the first time."

T.S.Eliot
in *Little Gidding*

"— ... ¿Qué le parece?

— Posible, pero no interesante - respondió Lonnrot-. Usted replicará que la realidad no tiene la menor obligación de ser interesante. Yo le replicaré que la realidad puede prescindir de esa obligación, pero no las hipótesis."

Jorge Luis Borges

"La muerte y la brújula" in *Ficciones*

"Hoje vomitei um líquido esverdeado
Eram as primeiras folhas
Estou prestes a florir "

Jorge de Sousa Braga
"O último girassol" - in *O Poeta Nú*

Declaration/ Declaração

I declare that this dissertation is a result of my own research jointly developed with Dr. Pierre Crozet and carried out between May 2011 and March 2015 in the laboratory of Dr. Elena Baena-González, Instituto Gulbenkian de Ciência in Oeiras, Portugal. Part of chapter 1 has been published in Frontiers in Plant Sciences entitled “Mechanisms of regulation of SNF1/AMPK/SnRK1 protein kinases”, Pierre Crozet, Leonor Margalha, Ana Confraria, Américo Rodrigues, Cláudia Martinho, Mattia Adamo, Carlos A. Elias, Elena Baena-González (2014). Chapters 2, 3, 4 and 5 are part of a manuscript in preparation to be submitted for publication, authored by Pierre Crozet, Leonor Margalha, Rafal Butowt, Noémia Fernandes, Alexandre Elias, Beatriz Orosa, Konstantin Tomanov, Markus Teige, Andreas Bachmair, Ari Sadanandom, Elena Baena-Gonzalez.

Declaro que esta dissertação é o resultado do meu próprio trabalho desenvolvido conjuntamente com o Dr. Pierre Crozet entre Maio de 2011 e Março de 2015 no laboratório da Dra. Elena Baena-González, Instituto Gulbenkian de Ciência em Oeiras, Portugal. Este doutoramento foi realizado no âmbito do Programa Gulbenkian de Doutoramento (edição 2010-2011). Parte do capítulo 1 foi publicado no Frontiers in Plant Sciences como “Mechanisms of regulation of SNF1/AMPK/SnRK1 protein kinases”, Pierre Crozet, Leonor Margalha, Ana Confraria, Américo Rodrigues, Cláudia Martinho, Mattia Adamo, Carlos A. Elias, Elena Baena-González (2014). Os capítulos 2, 3, 4 e 5 estão integrados num manuscrito em preparação para publicação como "SUMOylation represses energy signaling in Arabidopsis" com autoria de Pierre Crozet, Leonor Margalha, Rafal Butowt, Noémia Fernandes, Carlos A. Elias, Beatriz Orosa, Konstantin Tomanov, Markus Teige, Andreas Bachmair, Ari Sadanandom, Elena Baena-Gonzalez.

Financial Support/ Apoio Financeiro

This dissertation had the financial support from FCT, doctoral fellowship SFRH/BD/51627/2011 and Fundação Calouste Gulbenkian.

Esta dissertação teve o apoio financeiro da FCT, bolsa de doutoramento SFRH/BD/51627/2011 e da Fundação Calouste Gulbenkian.

Acknowledgments

Turning the last page in my PhD is a special moment of fulfillment and achievement, and I am filled with gratitude for all those who were present and contributed in several ways to make this an amazing journey.

To my supervisor, Elena Baena-Gonzaléz, I am deeply grateful and honored for being your student. You have opened one way to my happiness and provided the most nurturing environment that allowed me to grow scientifically, engaged in your enthusiasm for science and in your demand for knowledge and excellence. You were always very inspiring, very supportive and kind. I feel fortunate with what I have learned, and will preserve it throughout my life.

It was a privilege to share with Pierre Crozet most of my bench time, a lot of work and scientific discussions. I value your dedication to science and to people, your broad interests and culture. Thank you for the scientific support and great company along these years.

Several people contributed to the work presented in this thesis, and to which I am most grateful: Pierre Crozet, Rafal Butowt, Noémia Fernandes, Alexandre Elias, Konstantin Tomanov, Andreas Bachmair, Ari Sadanandom and Elena Baena-González.

I will always be thankful to Paula Duque for being key in guiding me to science and to what became my scientific home in these last years, the Plant Stress Signaling Laboratory at Instituto Gulbenkian de Ciência.

My lab is made of the amazing people that work and worked there, my colleagues and friends: Elena, our top model boss, thank you for everything. Cláudia Martinho, Rafal Butowt and Américo Rodrigues, my companions at the Big Bang of PSS, thank you for scientific training and laughs. Ana Confraria, thank you for being a scientific "older sister", and for sharing so much knowledge and energy (also *via* delicious food). Pierre Crozet, Mattia Adamo and Alexandre Elias, thank you for extensive experimental support and for making the lab a joy, with music, gardens, pears and gadgets. Titti Valério,

thank you for scientific insights and for spreading enthusiasm. Noémia Fernandes and Fredilson Melo, thank you for crucial experiments and for adorable moments in the lab.

The unifying element amongst all Plant Groups at IGC is Vera Nunes, to whom I am deeply grateful for the amazing plant care, for hilarious moments and for her sweet presence. I thank all the Groups at IGC for sharing reagents, protocols and scientific insights. I am especially grateful to the Plant Molecular Biology Laboratory and to Raquel Carvalho, for providing the nicest atmosphere amongst neighboring groups.

It was an unique opportunity to be part of the IGC PhD program in Integrative Biomedical Sciences (PIBS) 2010, and I much value the gain that such experience brought. My acknowledgements go to Thiago Carvalho and Manuela Cordeiro, and extend to all people involved (from PhD colleagues to scientists, for sharing time and knowledge). I would also like to acknowledge my Thesis Committee, José Feijó and Vasco Barreto, for encouraging me to be critical and independent regarding my research work.

IGC has been a fantastic place to be, and I am grateful to each and everyone that contribute to this rich environment.

I am also very thankful to the scientists that accepted to be part of my PhD jury: Jürgen Dohmen, Filip Rolland, Alekos Athanasiadis and Isabel Abreu.

Other key people in my education and training should be acknowledged in this moment, for their dedication and affection: Prof. Clarisse Borralho, Prof. David Mendes, Dra. Teresa Correia and Dra. Sara Silva Alexandre.

Finally, I am very grateful to my family.

To my dear parents, my adorable brother and sisters, and my precious grandparents, for being part of what I am and for their unlimited support.

To my husband and son, Nuno and Sebastião, for offering me the ground and the sunlight that make me live happily.

Contents

Table of Contents ..... **XV**

List of Figures ..... **XVIII**

Main abbreviations ..... **XX**

Resumo ..... **XXI**

Abstract ..... **XXV**

CHAPTER 1 | **1**

General Introduction **1**

1.1 | Posttranslational regulation by members of the Ubiquitin family **2**

1.2 | SUMO **4**

1.2.1 | SUMO structure 4

1.2.2 | SUMO isoforms 5

1.2.3 | SUMO pathway 9

1.2.4 | SUMO Enzymology 13

1.2.5 | Molecular consequences of sumoylation 26

1.2.6 | SUMO Enigma 31

1.2.7 | Biological consequences of sumoylation 32

1.2.8 | Crosstalk with other posttranslational modifications 33

1.2.9 | Challenges and strategies for the identification of sumoylation substrates and SUMO interactors in Arabidopsis 39

1.3 | Energy sensing and signaling in eukaryotes **41**

1.4 | SnRK1 in the core of plant energy homeostasis **42**

1.4.1 | Stress 47

1.4.2 | Hormones 49

1.4.3 | Metabolism 51

1.4.4 | Growth and Development 55

1.5 | Conserved Structures of SNF1/AMPK/SnRK1 complexes **58**

1.5.1 | α-catalytic subunit 59

1.5.2 | β-regulatory subunit 60

1.5.3 | γ-regulatory subunit 61

1.6 | Regulation of SNF1/AMPK/SnRK1 kinases **62**

1.6.1 | Complex composition 64

1.6.2 | Scaffold proteins 66

1.6.3 | Oligomerization 67

1.6.4 | Subcellular localization 68

1.6.5 | Adenylates, sugars and hormones 70

1.6.6 | Posttranslational modifications 71

1.7 | Aims and thesis scope **101**

CHAPTER 2 | **103**

Sumoylation of the SnRK1 complex **103**
Abstract **105**
2.1 | Introduction **105**
2.2 | Results **107**
2.2.1 | SnRK1α1 bears two high probability SUMO attachment sites 108
2.2.2 | SnRK1α1 catalytic subunit interacts with SCE1 in Yeast two-hybrid assays 109
2.2.3 | Multiple SnRK1 subunits are sumoylated in a heterologous system in *E. coli* 111
2.2.4 | SnRK1 is sumoylated *in planta* 117
2.2.5 | SnRK1 sumoylation is mediated by the E3 ligase SIZ1 *in planta* . 121
2.2.6 | Alternative strategies employed for determining SnRK1 sumoylation in Arabidopsis 123
2.3 | Discussion **132**
2.4 | Materials and Methods **137**
Acknowledgements **146**
References **147**

CHAPTER 3 | **151**

Biochemical and functional outcomes of SnRK1 sumoylation **151**
3.1 | Introduction **154**
3.2 | Results **155**
3.2.1 | Sumoylation inhibits SnRK1 signaling 155
3.2.2 | Sumoylation triggers SnRK1 degradation 163
3.2.3 | Sumoylated SnRK1 is ubiquitylated and degraded by the proteasome 166
3.2.4 | Sumoylation affects SnRK1 complex composition and possibly its oligomerization 168
3.2.5 | Preliminary studies on the genetic interaction between *SIZ1* and *SnRK1α1* in *Arabidopsis thaliana*, and other approaches to address the relevance of SnRK1 sumoylation at the whole plant level 171
3.3 | Discussion **179**
3.4 | Materials and Methods **186**
Acknowledgements **192**
References **192**

CHAPTER 4 | **197**

SnRK1 pathway activation and signal termination **197**
Abstract **199**
4.1 | Introduction **200**
4.2 | Results **202**
4.2.1 | SnRK1 activity triggers its degradation 202
4.2.2 | Sumoylation restores degradation of inactive SnRK1α1 variants . 204

4.2.3 | Preliminary approaches to monitor endogenous SnRK1 protein turnover in energy deprivation (SnRK1 activation) conditions 205
4.2.4 | SnRK1α1 phosphorylates SIZ1 208
4.3 | Discussion 213
4.4 | Materials and Methods 218
Acknowledgements 224
References 224

CHAPTER 5 229

Concluding remarks and future perspectives **229**
References 244

Appendix ..... a

List of Figures

Figure 1.1 | Schematic and three-dimensional ribbon diagrams of mature Ubiquitin and SUMO, evidencing the Ub/UBL β-grasp fold. 5
Figure 1.2 | Primary sequence alignment of *Arabidopsis thaliana* (At) SUMO and Ubiquitin precursors. 6
Figure 1.3 | SUMO and Ubiquitin conjugation pathways. 10
Figure 1.4 | SUMO conjugation reactions. 12
Figure 1.5 | Non-covalent (NC) and covalent (C) interactions between SUMO and substrates. 28
Figure 1.6. | SnRK1 in the interface of Stress, Metabolic, Hormonal, and Developmental signaling pathways. 47
Figure 1.7 | Heterotrimeric structure of the SnRK1 complex. 59
Figure 1.8 | Regulatory mechanisms controlling the SnRK1 kinase. 63
Figure 2.1 | Potential SUMO attachment sites on SnRK1α1 predicted using SUMOplot™. 108
Figure 2.2 | Arabidopsis SnRK1α1 and Drosophila SNF1A interact with the E2 SUMO Conjugating Enzyme 1 (SCE1) in Y2H assays. 111
Figure 2.3 | Multiple SnRK1 subunits, as well as the Drosophila SNF1A catalytic subunit, are sumoylated in a heterologous *E. coli* system. 113
Figure 2.4 | SnRK1α1 residues sumoylated in the *E. coli* assay. 116
Figure 2.5 | Generation of *SnRK1α1-GFP* transgenic plant lines. 118
Figure 2.6 | The SnRK1 complex is sumoylated *in planta*. 121
Figure 2.7 | SIZ1 is required for SnRK1 sumoylation. 122
Figure 2.8 | Detection of SnRK1α1 high molecular weight bands in plant crude extracts (A-B), after nuclear enrichment (C) and in protoplast samples (D-F). 126
Figure 2.9 | Detection of SnRK1α1 high molecular weight forms in SUMO pathway mutants (A) and using the Ubc9 fusion-directed sumoylation (UFDS) methodology in protoplasts (B-C). 130
Figure 2.10 | Processing of SnRK1α1-SUMO conjugates by recombinant Ulp1 SUMO protease. 132
Figure 3.1 | SIZ1-mediated sumoylation of SnRK1α1 represses SnRK1 signaling. 157
Figure 3.2 | SnRK1 signaling overactivation in *siz1-2* is due to lack of SnRK1 sumoylation. 161
Figure 3.3 | Salicylic acid (SA) has no effect on SnRK1 signaling. 162
Figure 3.4 | SnRK1 stability is increased in *siz1-2*. 166
Figure 3.5 | Sumoylation-dependent ubiquitylation of SnRK1 and its degradation by the proteasome. 168
Figure 3.6 | Sumoylation affects SnRK1 complex composition and oligomerization. 170

Figure 3.7 | Generation of *siz1-2 snrk1α1-3* double mutant plant lines. 172
Figure 3.8 | Sugar- and ABA- response phenotypes during early seedling development of *snrk1α1-3, siz1-2 snrk1α1-3, siz1-2, SnRK1α1-OE*, or Col-0 plants..... 176
Figure 3.9 | Generation of *SnRK1α1-SUMO-OE* transgenic plants..... 178
Figure 4.1 | SnRK1 activity triggers its degradation..... 203
Figure 4.2 | Sumoylation restores degradation of inactive SnRK1α1 variants. 205
Figure 4.3 | SnRK1 activity triggers its sumoylation and turnover. 208
Figure 4.4 | SnRK1 phosphorylates SIZ1 *in vitro*..... 210
Figure 4.5 | SnRK1-dependent phosphorylation of SUMO pathway components and possible outcome. 212
Figure 5.1 | Model of SnRK1 turnover mediated by sumoylation. 242

Main abbreviations

ACC	Acetyl-coA carboxylase
AMPK	AMP-activated protein kinase
ASC	Association with SNF1 complex
bZIP	Basic region/leucine zipper motif
CBM	Carbohydrate-binding motif
CIPK15	Calcineurin B–like (CBL)–interacting protein kinase 15
DUB	Deubiquitylating enzyme
DUF	Domain of unknown function
ESD4	Early in short days 4
G1P	Glucose-1-phosphate
G6P	Glucose-6-phosphate
GRIK1/2	Geminivirus Rep-interacting kinase 1/2
HMGR	3-Hydroxy-3-methylglutaryl CoA (HMG-CoA) reductase
KA1	Kinase-associated 1 domain
LKB1	Liver kinase B1 (tumor supressor)
MARD1	Mediator of ABA-regulated dormancy 1
NR	Nitrate reductase
PCNA	Proliferation cellular nuclear antigen
PIAL1/2	Protein inhibitor of activated STAT-like 1/ 2
PP	Protein Phosphatase
PTM	Posttranslational modifications
PRL1	Pleiotropic Regulatory Locus 1
SAE	SUMO activating enzyme
SCE	SUMO conjugating enzyme
SIM	SUMO interacting motif
SKIN	SnRK1A-Interacting Negative Regulator
SnAK1/2	SnRK1 activating kinase 1/2
Snf1	Sucrose non-fermenting 1
SnRK1	Snf1-Related protein Kinase 1
SPS	Sucrose phosphate synthase
STUbL	SUMO-targeted ubiquitin ligase
SUMO	Small ubiquitin-like modifier
TF	Transcription factor
T6P	Trehalose-6-phosphate
TPS	Trehalose Phosphate Synthase
UBA	Ubiquitin-associated domain
UPS	Ubiquitin proteasome system

Resumo

A capacidade de um organismo sentir e reagir a estímulos ambientais, mantendo a homeostasia num meio em constante mudança, é fundamental para a sua sobrevivência. Nas plantas, a SnRK1 (SNF1-related protein kinase 1) é um sensor energético central e um regulador metabólico que integra vários sinais para equilibrar os níveis de energia celular. Ao fazê-lo, a SnRK1 participa na resposta da plantas ao stresse (privação de energia), mas também no crescimento normal e decisões do desenvolvimento da planta. A SnRK1 está conservada em todos os eucariotas. Funciona como um complexo heterotrimérico constituído por uma subunidade catalítica (α) e duas subunidades reguladoras (β e γ). No entanto, apesar da sua importância, a regulação da SnRK1 é ainda pouco compreendida. Em contraste com os homólogos em mamíferos e leveduras, a fosforilação/ desfosforilação da T-loop na subunidade catalítica SnRK1α é necessária, mas não suficiente, para determinar a sua activação/ inactivação, sob stress e uma vez restaurada a homeostasia. Com base em várias evidências, colocámos a hipótese de que outras modificações pós-tradução, nomeadamente sumolização, possam estar envolvidas na regulação da SnRK1.

Mostramos que a SnRK1 interage com a enzima E2 de conjugação do SUMO em ensaios de dois híbridos em levedura, e é sumolizada num sistema heterólogo em *E. coli*. Demonstramos, por imunoprecipitação, que a sumolização da SnRK1 também ocorre na planta, possivelmente como um evento coordenado ao nível do complexo da SnRK1, uma vez que tanto a subunidade catalítica como as reguladoras estão sujeitas a esta modificação. Além disso, identificamos SIZ1 como a enzima E3 de ligação de SUMO responsável pela sumolização da SnRK1 por SUMO1, em Arabidopsis.

A sumolização pode afectar a atividade, estabilidade e/ ou a localização subcelular dos substratos, principalmente através da modulação de interações

proteicas intra- e intermoleculares. Demonstramos que a sumolização regula negativamente a sinalização da SnRK1. No mutante *siz1-2*, a ausência da enzima E3 de ligação de SUMO, SIZ1, conduz a uma maior ativação da via da SnRK1, que pode ser revertida para níveis basais por complementação transiente com SIZ1, mas não com a variante cataliticamente inativa, $SIZ1^{C379A}$. Além disso, a expressão de um constructo que mimetiza a sumolização, através da fusão de SUMO1 e SnRK1α1, restaura os níveis normais de sinalização da SnRK1, reforçando que a sobreativação observada em *siz1-2* é causada pela ausência de sumolização da SnRK1. Observamos também uma maior estabilidade e acumulação de várias subunidades da SnRK1 em *siz1-2*, sugerindo que a sumolização da SnRK1 promove a sua degradação, restringindo assim a sinalização da SnRK1. Com efeito, a activação excessiva da via da SnRK1 em *siz1-2* não é causada por alterações na atividade catalítica intrínseca da quinase, mas sim por uma acumulação da SnRK1 neste mutante.

Mostramos ainda que a SnRK1 é ubiquitinada na planta e encaminhada para degradação pelo proteosoma. Nos imunoprecipitados da SnRK1 são co-purificados conjugados de SUMO e de ubiquitina. No entanto, em *siz1-2*, os conjugados de ubiquitina associados à SnRK1 estão bastante reduzidos, sugerindo uma interação cooperativa entre a sumolização e a ubiquitinação no direcionamento da SnRK1 para degradação. Este processo poderá envolver a ação de ligases de ubiquitina dirigidas para SUMO (STUbLs), responsáveis pela ubiquitinação de substratos multi- ou polisumolizados. Adicionalmente, temos resultados preliminares que sugerem que a sumolização poderá afectar a composição do complexo da SnRK1 e, possivelmente, a organização das subunidades da SnRK1 em complexos heterotriméricos e putativamente oligoméricos.

Finalmente, mostramos que os variantes inativos da SnRK1, $SnRK1^{K48M}$ e $SnRK1^{T175A}$, se acumulam em níveis mais elevados e são mais estáveis do que a proteína ativa, sugerindo uma ligação entre a atividade e a estabilidade da quinase. Para além disso, os variantes inativos $SnRK1^{K48M}$ e $SnRK1^{T175A}$ podem

ser destabilizados se co-transfectados com SnRK1 ativa, ou se expressos como proteínas em fusão com SUMO1, reforçando que a atividade da quinase é essencial para a sua degradação, e sugerindo que a deficiente degradação dos variantes inativos da SnRK1 é causada pela ausência de sumolização. O trabalho aqui descrito revela um mecanismo de feedback negativo pelo qual a atividade da SnRK1 desencadeia a sua própria degradação pelo proteosoma, mediada por sumolização e ubiquitinação, para evitar os efeitos nocivos resultantes de uma sinalização excessiva da SnRK1 na planta. Além disso, mostramos que a SnRK1 fosforila a enzima E3 de ligação de SUMO, SIZ1, *in vitro*. Propomos que esse mecanismo poderá ser o elo de ligação entre o stresse e consequente ativação da SnRK1 e a sua sumolização/ubiquitinação, que resulta na sua subsequente degradação na planta. A apertada regulação da ativação da via da SnRK1, e da acumulação da quinase em condições de privação de energia, poderá estar conservada evolutivamente e ser essencial para o equilíbrio entre respostas ao stresse e defesa, com as atividades biossintéticas, de crescimento e desenvolvimento da planta.

Abstract

The ability of an organism to sense and react to environmental stimuli, maintaining homeostasis under ever-changing conditions, is key for survival. The plant SnRK1 (Snf1-Related protein Kinase 1) is a central energy sensor and metabolic regulator that integrates multiple inputs to balance cellular energy levels. In doing so, it takes part in the plant stress (energy deprivation) response but also on normal plant growth and developmental decisions. The SnRK1 kinase is conserved in all eukaryotes. It functions as a heterotrimer composed of α-catalytic and β- and γ-regulatory subunits. However, despite its importance, SnRK1 regulation is still poorly understood. In contrast to its mammalian and yeast homologues, SnRK1α T-loop phosphorylation/dephosphorylation is required but insufficient to determine its activation under stress and subsequent inactivation once homeostasis is restored. Based on several lines of evidence, we hypothesized that additional posttranslational modifications, like SnRK1 sumoylation, may be involved.

We show that SnRK1 interacts with the E2 SUMO conjugating enzyme in yeast two-hybrid assays and undergoes sumoylation in a heterologous *E. coli* system. Importantly, immunoprecipitation experiments demonstrate that sumoylation of SnRK1 also occurs *in planta*, seemingly as a coordinated event at the whole-complex level, as both catalytic and regulatory subunits undergo this modification. Moreover, we identify SIZ1 as the E3 SUMO ligase responsible for SnRK1 sumoylation by SUMO1 in Arabidopsis.

Sumoylation can affect substrate activity, stability and/or subcellular localization, mainly through modulation of intra- and intermolecular protein interactions. We demonstrate that SnRK1 signaling is negatively regulated by sumoylation. In the *siz1-2* mutant, the absence of the E3 SUMO ligase SIZ1 leads to enhanced SnRK1 pathway activation that can be reverted to wild-type (WT) levels by transient complementation with SIZ1, but not with the

catalytically inactive SIZ1^{C379A} variant. Furthermore, a translational fusion of SUMO1 to SnRK1α1 mimics sumoylation and restores normal SnRK1 signaling in *siz1-2*, supporting that the overactivation of the SnRK1 pathway in this mutant is caused by the lack of SnRK1 sumoylation. We observed increased stability and accumulation of several SnRK1 subunits in *siz1-2*, suggesting SnRK1 sumoylation promotes its degradation and thereby restrains SnRK1 signaling. Indeed, the higher activation of SnRK1 signaling in *siz1-2* was not caused by changes in SnRK1 intrinsic activity, but rather by an enhanced accumulation of the kinase in this mutant background.

We further show that SnRK1 is ubiquitylated *in planta* and targeted for proteasomal degradation. SUMO and ubiquitin conjugates co-purify in SnRK1 immunoprecipitates. However, in the *siz1-2* background, SnRK1-ubiquitin conjugates are greatly reduced, suggesting a cooperative interplay between sumoylation and ubiquitylation in targeting SnRK1 for degradation. This process is likely to involve the action of SUMO-targeted Ubiquitin Ligases (STUbLs), responsible for the ubiquitylation of multi- or polysumoylated substrates. Additionally, preliminary results suggest sumoylation may also affect SnRK1 complex composition, and possibly SnRK1 complex assembly and its putative oligomerization.

Finally, we show that the inactive SnRK1 variants SnRK1^{K48M} and SnRK1^{T175A} accumulate to a greater extent and are more stable than the active WT SnRK1 protein, underpinning a connection between kinase activity and stability. Importantly, inactive SnRK1^{K48M} and SnRK1^{T175A} can be destabilized if co-transfected with active SnRK1α1 or if expressed as translational protein fusions with SUMO1, further supporting that kinase activity is essential for its degradation and suggesting the impaired turnover of inactive SnRK1α1 variants is caused by lack of sumoylation. The work here described has uncovered a negative feedback loop by which SnRK1 activity triggers its own SUMO-mediated proteasomal degradation, to prevent deleterious effects derived from overly high SnRK1 signaling. Furthermore, we show that SnRK1 phosphorylates

the E3 SUMO ligase SIZ1 *in vitro*, and hypothesize that such mechanism may couple stress and SnRK1 activation to its sumoylation/ubiquitylation, and subsequent turnover *in planta*. A tight regulation of SnRK1 pathway activation and kinase accumulation in energy deprivation conditions may be evolutionary conserved and essential for balancing stress and defense responses with biosynthetic activities, growth and development.

CHAPTER 1 |

General Introduction

Posttranslational modifications (PTMs) allow a sensitive, rapid and reversible response to internal or external stimuli, allowing cells to adapt to programmed or unpredicted changes (*1, 2*). The expansion in proteome diversity prompted by PTMs is crucial for an organism plasticity, adaptation and ultimately survival.

1.1 | Posttranslational regulation by members of the Ubiquitin family

Ubiquitin (Ub) was discovered in the mid 1970s and is the founding member and the most prominent one (ubiquitous) of a broad family of protein modifiers (Ubiquitin-like, UBL). Ub an UBLs are transiently conjugated to other proteins, expanding the diversity and versatility of the proteome in eukaryotes (*3*). However, they can also modify prenyl groups or lipids, as it is the case for the membrane-anchored ubiquitin-fold protein (MUB) and the UBL-protein autophagy 8 (ATG8), respectively. The transient conjugation of ATG8 to the autophagosomal membrane is essential for autophagy (*4*).

All members of the ubiquitin family share a robust β-grasp structure, derived from the folding of a conserved ββαβββ secondary motif, with some N- and C-terminal variations or extra helixes/folds, specific to each UBL member (*3, 5, 6*) (**Figure** 1.1). The compact structures of UBLs result in fast assembling and highly stable proteins resistant to harsh environmental conditions. Despite the reduced conservation of the primary structure amongst different UBLs, each UBL member shares a highly conserved sequence, structure, and possibly regulation and regulatory role across different organisms (*3*). UBL modifiers are encoded in the genome and therefore, have been targets of duplication and diversification events during evolution (*7*). Insight regarding the origins of the Ub/UBL family came from the prokaryotic ThiS and MoaD proteins, involved in the biosynthesis of several sulfur-containing enzyme cofactors. These proteins

are structurally related to the β-grasp structure and display surprising mechanistic parallels with the UBL conjugation pathway. Moreover, the eukaryotic UBL ubiquitin-related modifier 1 (URM1), implicated both in sulfur donation to transfer RNAs (tRNAs) and in covalent protein attachment to target proteins, could represent an ancestral bridge between sulfur chemistry and protein conjugation (*1, 3, 5*).

Several proteins have evolved as translational fusions with N-terminal Ub/UBL domains, in a stable association that overcomes the need for subsequent modification. These UBL domains have lost the characteristic C-terminal end and are thus resistant to deconjugation, providing enduring features in protein-protein interactions or folding properties to the whole protein (*3, 5*).

In plants, besides Ub, the UBL family includes the small ubiquitin-like modifier (SUMO), related to ubiquitin (RUB), ATG8 and ATG12, MUB, URM1, ubiquitin-fold modifier 1 (UFM1), and homology to ubiquitin1 (HUB1), whereas other UBL modifiers like the interferon-stimulated gene 15 (ISG15) or HLA-F adjacent transcript 10 (FAT10) are only present in metazoans (*1, 3, 8*).

The biological processes regulated by PTMs of the UBL family, and the specificities associated to each member, have been the focus of intense research and at present, Ub and UBLs are considered major regulators of growth, development, and survival in eukaryotes.

This thesis will focus on posttranslational modification by SUMO, given its prominent role in Snf1-Related protein Kinase 1 (SnRK1) regulation and due to the limitations of covering the entire UBL family here. SUMO regulation of SnRK1 signaling in plants will be addressed in detail in the experimental chapters, while the following introductory sections will provide an overview of the SUMO system and of the SnRK1 pathway.

1.2 | SUMO

SUMO stands for Small Ubiquitin-like Modifier and was discovered in 1996, when a peptide sequence analysis retrieved a protein with two N-termini but just one C-terminal end (*9*). The Ran-GTPase-activating protein 1 (RanGAP1) was the first SUMO substrate described, and the outcome of this modification was a change in the subcellular localization of RanGAP1 (*10*). Since then, a burst in the UBL research area allowed the identification of a myriad of SUMO targets and implicated SUMO in the regulation of crucial biological processes elevating it, together with Ub, as one of the most prominent UBL members.

1.2.1 | SUMO structure

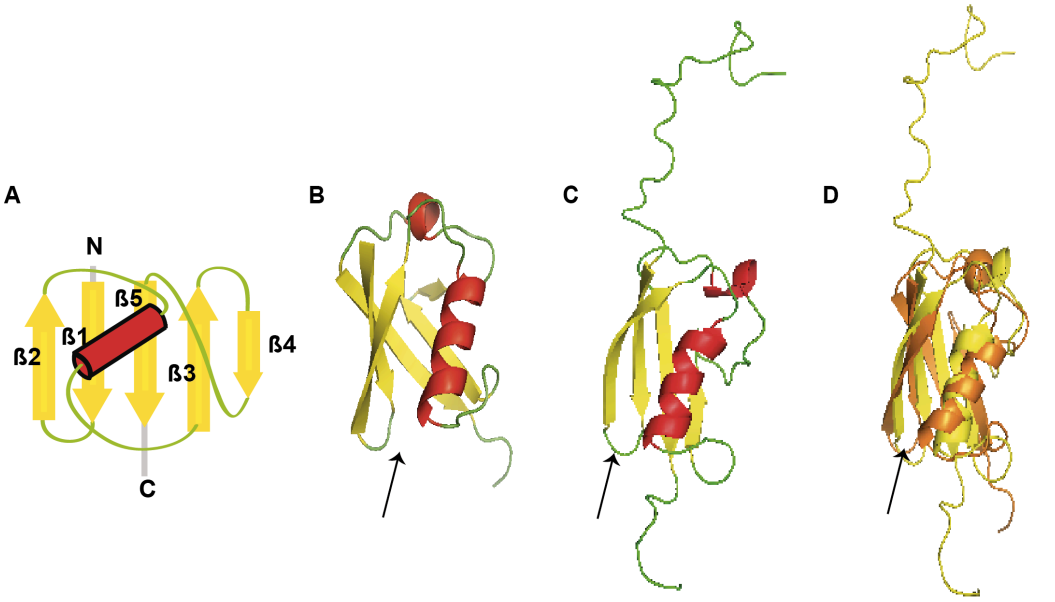

Figure 1.1 | Schematic and three-dimensional ribbon diagrams of mature Ubiquitin and SUMO, evidencing the Ub/UBL β-grasp fold.

A. Schematic arrangement of the α-helix and β-strand secondary structures in the Ub/UBL β-grasp fold. **B.** *Avena sativa* Ub [PDB accession number 1UBQ; (*11*)]. **C.** Human SUMO1 [PDB accession number 1AR5; (*12*)]. **D.** Superimposed structures of Ubiquitin (orange, from **B**) and SUMO (yellow, from **C**). Arrows point to the hydrophobic groove between the β2-strand and α1-helix of Ub/SUMO. In **A**, **B**, and **C**, colors represent different secondary structures (red- helix; yellow- sheet; green- loop). Adapted from (3).

SUMO and Ub share only ~18% amino acid (aa) sequence identity and their overall surface-charge distribution is different (*6, 12-14*). A specific feature of SUMO is an N-terminal unfolded extension that provides unique binding properties to this modifier and precedes the conserved hallmark β-grasp structure of the UBL class (**Figure** 1.1). SUMO is synthesized as a precursor (as most of the UBL members) and is processed to expose a di-Glycine (GG) C-terminal motif through peptide cleavage (*6*). Due to its N-terminal extension, mature SUMO has a few more amino acids (~100 aa) than Ub (76 aa). SUMO protein is around 12KDa but, when conjugated, it contributes to an increment of ~20KDa on the target protein molecular mass. The corresponding delay in migration in SDS-PAGE of the modified protein will also depend on where in the substrate the SUMO conjugation takes place and, for instance, on the occurrence of branching effects (*15-18*).

1.2.2 | SUMO isoforms

Whereas lower eukaryotes possess only one SUMO isoform (Smt3 in *S. cerevisae* or Pmt3 in *S. pombe)*, higher eukaryotes express several SUMO variants possibly with distinct functional properties (*19-21*). In mammals, four SUMO paralogs (SUMO1 to SUMO4) exist, although *SUMO4* has been suggested to be a pseudogene (only its mRNA is detected but not the protein),

and its ability to undergo maturation and conjugation even if expressed, has been questioned (*20, 22*).

In *Arabidopsis thaliana,* eight genes are putatively attributed to SUMO isoforms (*6, 23, 24*), but only 4 SUMO variants are highly, although differentially, expressed: *SUMO1, SUMO2, SUMO3* and *SUMO5* (*6, 25, 26*). *SUMO1* and *SUMO2* are much more abundant (~7 fold) than *SUMO3* and *SUMO5* transcripts (*25, 27*). The transcriptional profile of SUMO isoforms is mostly unchanged in different tissues and developmental stages. Nevertheless, *SUMO3* and *SUMO5* transcripts might be specifically enriched in roots and flowers, respectively, reflecting isoform-specific roles in these tissues (*27*). However, at the protein level there is an enrichment of free SUMO1/2 and of the respective SUMO conjugates, in flowers and siliques (*27*). The *SUMO1* and *SUMO2* genes are constitutively expressed, whereas *SUMO3* can be strongly and widely induced by salicylic acid (SA) and by the defense elicitor Flg22 (*21*). At the cellular level, most of the SUMOs are present in the nucleus as the majority of proteins involved in sumoylation, despite some may display distinct intracellular localizations (*28*).

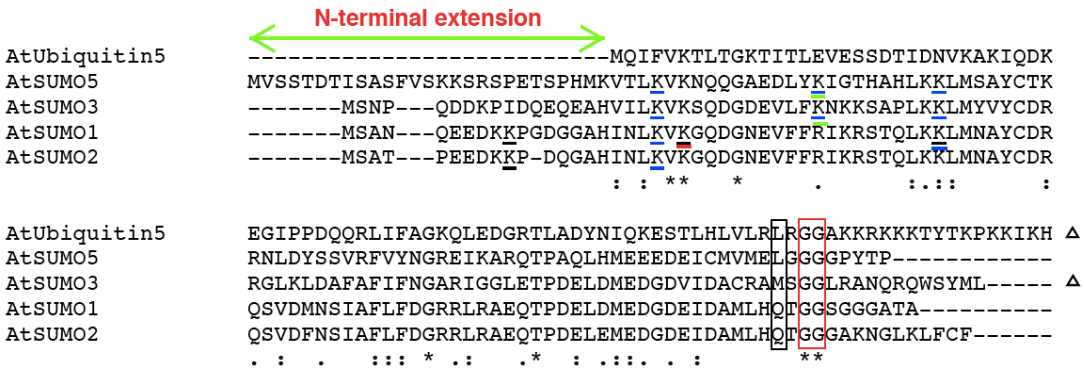

Figure 1.2 | Primary sequence alignment of *Arabidopsis thaliana* (At) SUMO and Ubiquitin precursors.

Proteins were analyzed using the Clustal O (1.2.1) multiple sequence alignment tool

(www.ebi.ac.uk/Tools/msa/clustalo/). A red box highlights the C-terminal di-glycine motif exposed during precursor maturation, and a black box evidences the variable amino acids important for deconjugation rate, at position -4 from the mature isoform C-terminus. Underlined residues represent identified sumoylation (black) and ubiquitylation (red) sites. Additional putative ubiquitylation (blue) and acetylation (green) sites are based on the detection of the respective modification in conserved residues of human SUMO1 and/or SUMO2. Below the alignment, asterisks (*) indicate amino acid residues conserved in all aligned sequences, colon (:) indicates conservation between groups of strongly similar properties, and period (.) indicates conservation between groups of weakly similar properties. The Delta (Δ) symbol in front of AtUbiquitin5 and AtSUMO3 indicates that further downstream amino acids of the precursor were omitted. Adapted from (*7*).

There is a high sequence similarity between SUMO1 and SUMO2 proteins (93%) (*7*) and probably functional equivalence (*21, 23, 27*). Accordingly, a single functional allele of *SUMO1* or *SUMO2* is sufficient for cell viability, whereas double mutants blocking the accumulation of both SUMO1 and SUMO2 are embryo lethal, underpinning an essential role for SUMO conjugation (*21, 27*). At the protein level, SUMO1 and SUMO3 share 53% sequence identity and the more divergent SUMO5 shares only 44% sequence identity with SUMO1 (*7*). Sequence alignment of the different isoforms revealed differences at a glutamine (Q) residue, conserved in most organisms, four amino acids distant from the mature C-terminus. SUMO1, SUMO3 and SUMO5 display Q, methionine (M) or leucine (L) at that position, respectively, and differences in deconjugation between SUMO isoforms *in vitro* were attributed to the identity of this amino acid (Q causing the fastest deconjugation) (**Figure** 1.2). Such type of regulation could result in a different half-life for the different SUMO-specific conjugates *in vivo*, and in diverse roles for the different paralogs (*7, 25, 29*). Besides SUMO proteases that can preferentially desumoylate specific SUMO conjugates (*7*), the SUMO paralog specificity also relies on E3 SUMO ligases and/or substrate interaction surfaces that may favor the binding of one SUMO isoform.

Whereas SUMO1 and SUMO2 can be further modified by SUMO in specific lysine (K) residues [K10, K23 and K42 in SUMO1 (*30, 31*) and K10 in SUMO2 (*7, 25*)], and feature chain assembly, SUMO3 does not share this property or is sumoylated to a much minor extent (**Figure** 1.2). SUMO1/2 chain formation is functionally important in plants, for instance in the crosstalk with the ubiquitin proteasome system (UPS), when Ub and SUMO cooperatively target a protein for degradation (*32*), as similarly reported in yeast and animals (*33, 34*). In plants, there is a free pool of SUMO1/2 protein that is rapidly diminished by conjugation to substrates upon exposure to a diversity of stresses like heat shock, H_2O_2, ethanol and to the aminoacid analog canavanine, whereas the SUMO3 profile does not seem to change in these conditions (*23*).

The differences observed in plant SUMO isoforms occur also in animals, although in this case SUMO2/3 are the highly similar and chain-forming isoforms, more abundant *in vivo* and massively conjugated as part of an early stress response (*35, 36*). Interestingly, mixed-chain formation between all SUMO family members was detected in mammals (*37*). *SUMO1* mRNA levels increase in response to hypoxia in animals (*38, 39*), and higher *SUMO2* transcripts are an indicator of malignancy in human hepatocellular carcinomas (*40*). In animals, a number of lysine residues (K11, K20, K32, K41 and K44) have been identified in SUMO2, as acceptor sites for ubiquitylation (*41*). Some of these residues are conserved in Arabidopsis SUMO isoforms (**Figure** 1.2). SUMO2 monoubiquitylation at its N-terminus primes its polyubiquitylation (*42*) through K63-linked ubiquitin chains that might target SUMO conjugates to insoluble protein inclusions (*41*). Ubiquitylation of AtSUMO1 on K23 was detected in heat stressed plants (*30*). SUMO can also be phosphorylated (*43, 44*) and acetylated (*45*) (**Figure** 1.2). Acetylation of K37 in SUMO1 and K33 in SUMO2 neutralizes a positive charge on SUMO and inhibits its interaction with some SUMO interacting motifs (SIMs), whereas it promotes the interaction of SUMO2 with the bromodomain in p300, indicating that acetylation of SUMO can work as a molecular switch (*28, 46*).

1.2.3 | SUMO pathway

As for other UBLs, the SUMO pathway engages an E1-E2-E3 (and E4) enzymatic cascade that initiates with an inactive precursor processed by specific proteases, and terminates with the covalent attachment of the mature SUMO to a target substrate. The subsequent removal of the modifier by specific proteases confers a transient and versatile nature to the posttranslational modification of substrates by SUMO (**Figure** 1.3). SUMO conjugation requires energy and involves the formation of high-energy thioester bonds.

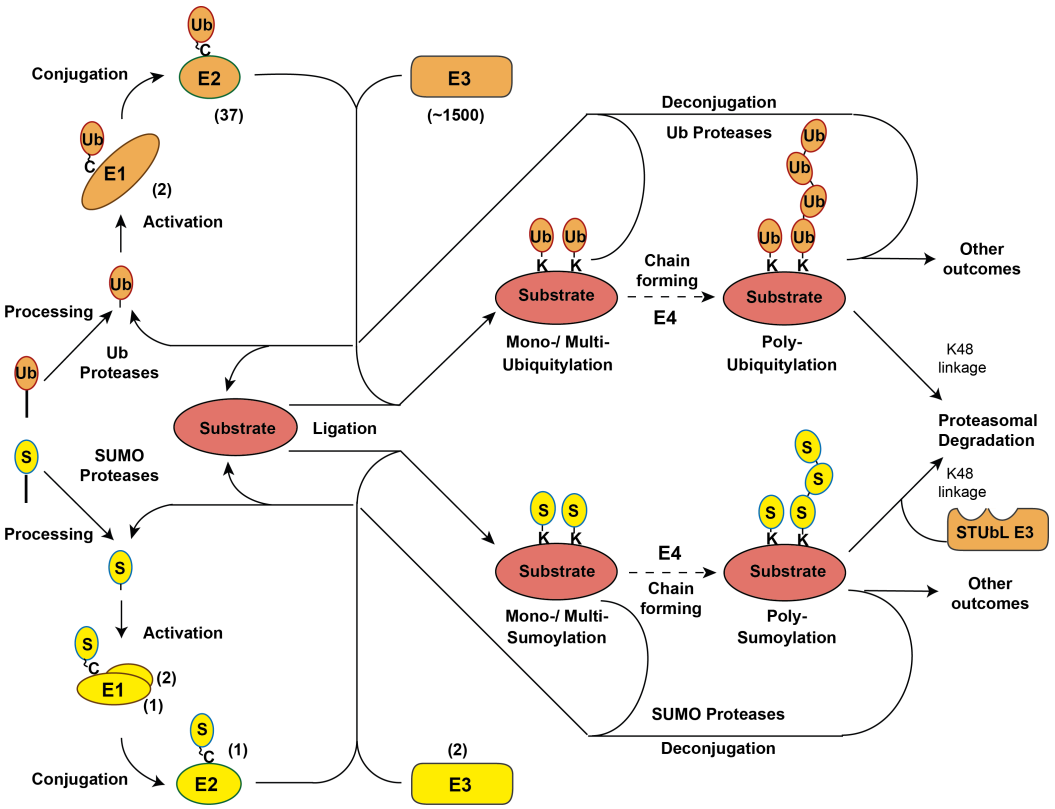

Figure 1.3 | SUMO and Ubiquitin conjugation pathways.

Both SUMO (S, bottom, yellow) and Ubiquitin (Ub, upper, orange) pathways share an E1 (activating), E2 (conjugating), E3 (ligase) and E4 (ligase, involved in chain formation) enzymatic cascade. After processing, the modifier is covalently attached through its C-terminal glycine (G) residues to the ε-amino group of lysine (K) residues in the substrate (red). Modifiers can target single or multiple lysines in the substrate (mono-/multiubiquitylation/sumoylation) and subsequently form chains through different lysine residues of the modifiers (polyubiquitylation/sumoylation). There are diverse outcomes of these modifications that essentially modulate protein-protein interactions. SUMO-targeted ubiquitin ligases (STUbLs) can ubiquitylate SUMO conjugates, and ubiquitin chains with K48 topology target substrates for proteasomal degradation. Modifications can be reversed by Proteases, also involved in the processing of the respective precursors, which control the free pool of the modifier. The enzymes involved are specific for each pathway and there are striking differences in their number (the numbers of enzymes encoded in Arabidopsis are in parentheses). Adapted from (*47*).

1.2.3.1 | SUMO maturation

Most of the newly synthesized UBL isoforms need to be processed to expose a conserved di-glycine motif involved in the covalent attachment to the substrate. SUMO proteases fulfill this role through endopeptidase cleavage of carboxyl-terminal extensions from SUMO inactive precursors (*6*). SUMO proteases can perform both SUMO maturation and SUMO deconjugation, or be specifically engaged in only one of these functions (*48*).

The proteolytic activity of SUMO proteases can target SUMO-specific isoforms (*7, 25, 29*). In fact, *in vitro* pre-SUMO processing activity of the Arabidopsis SUMO proteases ESD4, OTS1 and OTS2, as well as yeast ULP1 and *X. campestris* XopD, was shown to be specific to AtSUMO1 and AtSUMO2 precursors. In this assay AtSUMO3 could only be processed by XopD, whereas AtSUMO5 was not processed at all, suggesting the enrollment of other SUMO proteases in precursor processing in Arabidopsis. The five cysteine proteases tested also showed SUMO-specific isopeptidase activity towards SUMO1 and

SUMO2 conjugates (*7*).

1.2.3.2 | SUMO conjugation/deconjugation

SUMO conjugation follows the same chemistry as Ub conjugation, however significant differences make E1, E2 and E3 enzymes specific for each UBL (*3*). One exception occurs for ATG8 and ATG12 modifiers that are activated by the same E1 (ATG7) but subsequently transferred as thioester intermediates to separate E2s (*3, 5*). E1 SUMO activating enzymes function as heterodimers (SAE1 and SAE2) and activate mature SUMO with the consumption of one ATP. Activated SUMO is transferred to the active site cysteine of SAE2 with the formation of a thioester bond and release of AMP (SAE2~SUMO). A transthiolation reaction allows the transfer of SUMO from SAE2 to the active site cysteine of E2 SCE1 (SCE1~SUMO). SUMO-loaded SCE1 will directly bind the target and conjugate SUMO through an amide (isopeptide) bond to a lysine residue on the substrate. It may modify a single lysine (monosumoylation) or multiple lysine residues (multisumoylation) on the substrate, and it may also result in the formation of SUMO chains (polysumoylation). E3 SUMO ligases facilitate SUMO conjugation and improve specificity either by bringing SCE1 and the substrate together, or by orienting SCE1~SUMO in a way that promotes SUMO transfer (*32, 49*). SUMO-substrate conjugates can be rapidly and specifically deconjugated through the isopeptidase activity of SUMO proteases that replenish the pool of free SUMO and release the substrate from its sumoylated state (**Figure** 1.4).

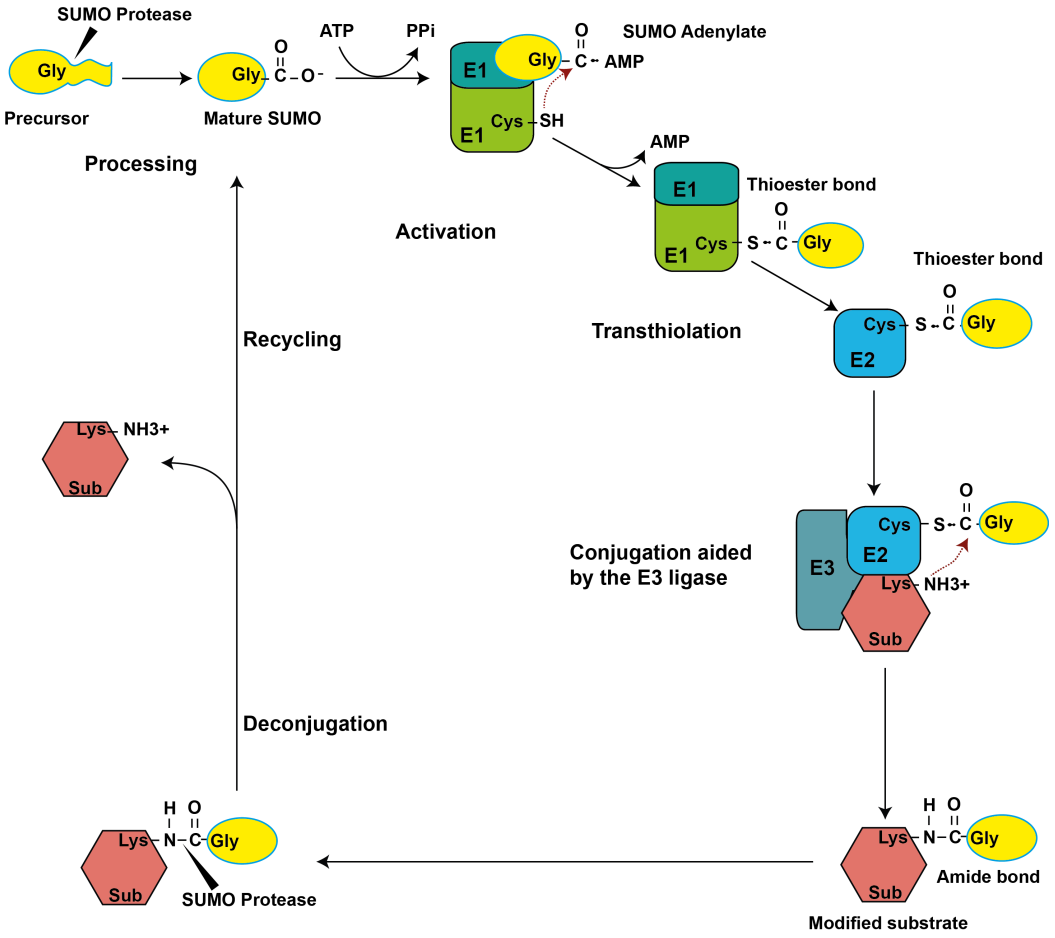

Figure 1.4 | SUMO conjugation reactions.

SUMO precursors are processed by SUMO proteases that expose a C-terminal glycine (Gly) in the SUMO modifier. Mature SUMO is activated with ATP by E1 SAE1, that adenylates the C-terminal carboxyl group of SUMO, forming a high-energy (~) AMP adduct. This intermediate is attacked (red arrow) and covalently bound by the sulfhydryl group of the E1 SAE2 catalytic cysteine, creating a thioester bond and releasing AMP. SUMO is subsequently transferred to the catalytic cysteine of the E2 SCE via a transthiolation reaction. SUMO can thereafter be ligated to a substrate with the help of an E3 SUMO ligase that can position the amino group of a substrate

lysine near the E2-SUMO thioester, catalyzing the transfer of SUMO to the substrate. Following this, SUMO proteases can remove SUMO from substrates, recycling the modifier. Adapted from (*50*).

1.2.4 | SUMO Enzymology

Unlike ubiquitylation, which in Arabidopsis involves 2 E1s, 37 E2s and over 1500 different E3s that provide substrate specificity, the SUMO machinery comprises only two different E1 heterodimers, a single E2, and just two E3s. Therefore, distinct features of the sumoylation process, such as the recognition of specific motifs by the E2 on the target, and a tight regulation must be key to attain specificity. The SUMO conjugation and deconjugation machinery is target of such regulation at the transcript level, protein amount and distribution, as well as through posttranslational modifications (*3, 28*).

1.2.4.1 | E1 SUMO activating enzymes (SAE1 and SAE2)

The yeast *Saccharomyces cerevisiae* has a single E1 enzyme that coordinates the activation of Ub (Uba) while the SUMO activation in the same organism requires an E1 heterodimer (Aos1/Uba2). In Arabidopsis, the heterodimeric complex of E1 SAE is composed of a small subunit (SAE1a or SAE1b; encoded by two genes), and a big subunit (SAE2), that functionally resemble the N- and C-terminal domains of E1 in the Ub system, respectively (*6, 7, 27*). SAE1a and SAE1b share high amino acid sequence identity (81%) and have similar expression patterns in plants, suggesting functional redundancy. Accordingly, a potentially null mutant affecting SAE1a is viable, probably due to redundancy with SAE1b (*27*). SAE1 activates SUMO through the formation of a SUMO adenylate between the carboxyl group of SUMO C-terminal glycine (G) and the α-posphate group of ATP, with the subsequent release of pyrophosphate (PPi). The activated intermediate is then transferred

to the sulfhydryl group of the SAE2 active site cysteine, forming a highly energetic thioester linkage (SAE2~SUMO). Null T-DNA insertion mutants of the single gene encoding SAE2 in Arabidopsis are embryonic lethal, with arrest occurring early in embryo development (*27*).

In Arabidopsis, there is little variation in the mRNA profiles of SAE1a, SAE1b or SAE2 across different tissues and developmental stages, despite some differences at the protein level, for instance with SAE1 levels slightly elevated in flowers (*27*). Regulation at the transcriptional level was described in other organisms, with increased accumulation of *SAE1/Aos1* transcripts in a variety of tissues (e.g., testis and thymus) (*51, 52*), in the *S* phase of the cell cycle (*52*), as well as during embryogenesis in Drosophila (*53*). On the other hand, high *SAE2/Uba2* and *SUMO2* transcript levels were correlated with malignancy in human hepatocellular carcinomas (*40*).

At the protein level, sumoylation of both SAE subunits has been observed in mammals. Sumoylation of SAE2 is thought to be more common and derived from auto-sumoylation or mediated by E2 SCE (*54, 55*). SUMO conjugation on the active site of SAE2 inhibits the transfer of SUMO from E1 to E2 (*56*), whereas sumoylation on the SAE2 C-terminus is important for SAE nuclear retention (*57*). AtSAE2 is also sumoylated *in vivo* (*30*). SAE1 and SAE2 are ubiquitylated and downregulated upon viral infection in the presence of the adenovirus protein Gam1 (*58*). Reversible oxidation, on the other hand, has also been shown to regulate sumoylation. In response to low concentrations of ROS, mammalian E1 SAE2 and E2 SCE1 form a disulfide bond between their catalytic cysteines, preventing SUMO thioester formation (*59*).

1.2.4.2 | E2 SUMO conjugating enzyme (SCE1)

In Arabidopsis, the SUMO machinery comprises a single E2 enzyme (SCE1), whereas more than 30 E2s exist in the Ub system. Therefore, SCE1 must have

relaxed substrate specificity to conjugate all SUMO substrates (and all SUMO isoforms) *in vivo* (*7*). SCE1 is crucial in SUMO conjugation since it binds directly the target on a consensus motif, through a patch surrounding the active site (*60, 61*). The SUMO moiety is then transferred from the thioester bond with SCE1 to the ε-amino group of a target lysine, establishing a covalent amide bond *via* the SUMO C-terminal glycine carboxyl group. This feature of SCE1 allows sumoylation in *in vitro* systems even in the absence of E3 SUMO ligases, despite co-expression of the latter might increase the efficiency of the reaction. SCE1 activity is modulated by the non-covalent binding of E1 (determinant for SCE1~SUMO formation) and of SUMO on a multifunctional binding site on SCE1 (*6, 62*). The consensus motif recognized by SCE, and ultimately the SUMO attachment site (SAS) in the target is ΨKxE/D, where Ψ is a bulky hydrophobic amino acid (mainly valine (V), leucine (L), Isoleucine (I)), x is any amino acid, and where aspartate (D) can also replace the preferable glutamate (E) residue. There are several variations of this classic motif and also inverted motifs (*63*). The negatively charged amino acid-dependent sumoylation motif (NDSM) $\Psi KxE(x)_{2\text{-}3}(E/D)_n$ comprises acidic residues downstream of the core motif that enhance the binding affinity with the positively charged patch of SCE1 (*64*). The same increase in affinity is seen in the phosphorylation-dependent sumoylation motif (PDSM) ΨKxExxS/T, when phosphorylation of the serine (S)/ threonine (T) triggers sumoylation (*65*). A third sumoylation motif, hydrophobic cluster-containing sumoylation motif (HCSM), clusters N-terminal hydrophobic residues upstream of the core motif, $\Psi_n KxE$. Inverted sumoylation motifs have also been described, E/DxKΨ (*66*).

The variation on SAS motifs contributes to the efficiency and specificity of SUMO conjugation at the substrate level in response to varied signaling cues (*63*). There are several algorithms that score the probability of a SAS to become modified by SUMO according to the hydrophobicity and acidity of the amino acids at given positions (e.g., SUMOplot, www.abgent.com; sumosp, http://sumosp.biocuckoo.org/; JASSA v4). Despite not all consensus motifs are

bona fide SUMO targets and sumoylation also occurs outside of canonical high probability SUMO attachment sites (hpSAS), there seems to exist a correlation between hpSAS enrichment and SUMO conjugation. Proteomic analysis of putative SUMO targets reveals that 70% (*25, 67*) or even 80% (*30*) of these proteins contain hpSAS [defined with an arbitrary cutoff value of hpSAS ≥91% (*67*)], compared to the presence of hpSAS in ~40% of the Arabidopsis proteome. Interestingly, in a recent proteomic study, whereas more than half of the identified sumoylation sites matched the SUMO consensus motif in untreated cells, the adherence to the consensus motif dropped moderately for sumoylation sites mapped exclusively after heat-shock treatment, and more drastically after proteasome or SUMO/ubiquitin protease inhibitors treatment (*37*). However, besides the substrate primary sequence, SUMO attachment will also depend on the 3D context of the consensus motif, since it has to be exposed on the surface of the protein and thereby accessible to the sumoylation machinery (*7*). Furthermore, suitable modification sites are frequently outside of functional domains, within flexible regions not conserved, as described for protein group modification events (addressed in a later section) (*47, 60*).

SCE1 is essential not only in plants but in all organisms tested, with the exception of *S. pombe*, in which the mutant lacking the SUMO E2 grows poorly and has severe defects in genome maintenance (with the same phenotypes as *S. pombe* mutants lacking SUMO or E1 subunits) (*6, 27, 68-74*). In Arabidopsis, *SCE1* is the most highly expressed gene of all SUMO conjugation components and there is little variation in its mRNA profile across different tissues and developmental stages, despite its relative enrichment at the protein level in flowers and siliques (*27*). The transcription of SCE1 can be modulated by temperature, as revealed by its induction by heat and repression by cold shock in rice (*75*). SCE is regulated by several posttranslational modifications with an impact on its efficiency and specificity towards different targets. Auto-sumoylation of the mammalian E2-conjugating enzyme Ubc9 at K14 leads to a gain in affinity for the transcriptional regulator Sp100 and to a decreased

interaction with RanGAP1, while not altering its activity towards other targets (*76*). On another report in budding yeast, E2 sumoylation at K153, and its subsequent interaction with the non-sumoylated SUMO-charged E2, promoted SUMO chain formation (*77*). Recently, SUMO conjugation to SCE1 at K15 was shown to be essential for SUMO chain formation in Arabidopsis (*31*). E2s can also be acetylated at K65 and this acetylation selectively reduces sumoylation of NDSM-containing proteins, such as the ETS-domain transcription factor ELK1 (*28, 45*). In response to oxidative stress, mammalian SAE2 (UBA2) and E2 SCE form a disulfide bond between their catalytic cysteines preventing SUMO thioester formation (*59*), whereas ubiquitylation and downregulation of E2 occurs in response to viral infections (*58, 78, 79*).

1.2.4.3 | E3 SUMO ligases

In the Ub system more than one thousand E3 Ub ligases were identified and coupled with specific substrates, whereas few E3 ligases exist in the SUMO pathway (*3*). E3 SUMO ligases are not required for SUMO conjugation in *in vitro* systems but increase the rate and substrate specificity of sumoylation *in vivo* (*32*). SCE1~SUMO and the target substrate can be brought together through binding interfaces in E3 ligases, that by this mean influence SUMO isoform and substrate specificity. This might be particularly relevant in cases when a consensus SAS motif is absent in the substrate, compromising a direct binding of SCE1 that needs to be recruited *via* an interaction with the ligase (*47*). On the other hand, E3 SUMO ligases may interact only with SCE1 and thus orient SCE1~SUMO in such a way to favor the SUMO transfer (*49*). A known SCE interaction domain present in most E3 ligases is the SP-RING domain (*80*), in which a zinc ion is coordinated via a set of conserved cysteine and histidine residues (*32, 81, 82*). The intracellular localization of E3 SUMO ligases is also critical for their function and substrate specificity, and since they possess SUMO

interacting motifs (SIMs) they can concentrate upon sumoylation and trigger a sumoylation chain reaction (*47*).

E3 SUMO ligases are grouped in several distinct types. The best characterized is the SIZ/PIAS (SAP and MIZ/ protein inhibitor of activated STAT) (*83-86*) that displays conserved SAP, PINIT, SP-RING, SUMO binding, and NLS domains (*87*). The PINIT and SP-RING domains are both required for SUMO ligase activity and the SP-RING is determinant for SCE binding (*80, 87, 88*). The SAP domain is composed of a helix-extended loop-helix structure and interacts with DNA (*89*). In the plant homologs of SIZ/PIAS, there is an additional specific Zn-finger domain, the plant homeodomain (PHD), associated with chromatin remodeling complexes (*90*) and contributing to SCE1 binding as well (*91*). Additional types of SUMO E3s include the non-SMC element/methyl methanesulfonate sensitive (NSE2/MMS21) that also belongs to the family of SP-RING ligases, and other structurally unrelated SUMO ligases like RanBP2 (*92*) or Pc2 (*6, 93*). In plants, SIZ1 (*23, 24, 94*) and HPY2/MMS21 (*95, 96*) are the only two E3 SUMO ligases identified and contain the hallmark SP-RING domain (*32*).

1.2.4.3.1 | SIZ1

Arabidopsis SIZ1 was the first SUMO E3 identified in plants, belonging to the SP-RING family, SIZ/PIAS type of SUMO ligases. AtSIZ1 is encoded by a single gene, and several orthologs are predicted in other plant species (*32*). In rice, two paralogs OsSIZ1 and OsSIZ2 have been described (*97, 98*). As determined for other components of the SUMO machinery in Arabidopsis, the relative expression of *SIZ1* mRNA shows little variation across different tissues and developmental stages (*27*). Nevertheless, a relative enrichment of *SIZ1* mRNAs was observed in root compared to shoot (*94*) and in female organs compared to anthers or pollen (*99*). At the cellular level, AtSIZ1 protein localizes predominantly to punctuate structures (speckles) in the nucleus, as described

for PIAS ligases in other organisms (*94, 100*). Despite its predominant role, null mutants of SIZ1 are still viable but have severe and pleiotropic phenotypes. On the other hand, the *siz1-2* and *hpy2-1* double mutant is embryonic lethal (*82*) showing that the combined role of the two ligases is essential for plant development, and questioning the physiological relevance of direct sumoylation by SCE1 via E3-independent mechanisms (*27, 82*).

SIZ1 is implicated in plant vegetative growth and developmental processes, as well as in the response to several biotic and abiotic stresses. Under control conditions, SIZ1 regulates the expression of important sets of genes (*101*). The *siz1* mutants accumulate salicylic acid (SA) to a higher extent (~28 fold) than wild-type (WT) plants (*102, 103*), and many of the phenotypes caused by the absence of SIZ1 are SA-dependent. The *siz1* mutations cause dwarfism and reduced leaf size (*101*) due to a decrease in cell size and number (SA-dependent) (*104*), an early flowering phenotype in short days (SD) (SA-dependent), and reduced fertility, probably due to defects in the female gametophyte (*99*), but also due to anther dehiscence (*98*). SIZ1 sumoylates and represses Flowering Locus D (FLD) activity, required for proper expression of the floral repressor Flowering Locus C (FLC) (*105, 106*). SIZ1 also modulates abscisic acid (ABA) signaling through sumoylation of the transcription factors ABI5 (*107, 108*) and MYB30 (*109*) that operate in parallel pathways to coordinate germination in response to ABA. Consequently, *siz1* mutations cause ABA hypersensitivity with an inhibition of germination and of seedling primary root growth. Plants cope with nutrient imbalance through several molecular mechanisms in which SIZ1 is key. These include the response to Pi starvation, through sumoylation of the transcriptional activator PHR1 and the control of auxin distribution-induced root architecture (*94, 110*), as well as the regulation of copper homeostasis and tolerance (*111*), and sodium sensitivity (*94, 112*). In addition, SIZ1 sumoylates the nitrate reductases NIA1 and NIA2, stimulating their activity and favoring nitrogen assimilation (*113*) and an increase in alternative respiratory bypass pathways (*114*). SIZ1 mediates the

accumulation of SUMO1/2 conjugates required for basal thermotolerance (*94, 115*) and for cold acclimation. Sumoylation-dependent stabilization of the transcription factor ICE1 inhibits MYB15 and activates CBF3/DREB1A downstream responses to low temperature (in a SA-dependent process) (*116-118*). SIZ1 accumulates in response to drought stress, increasing SUMO1/2 conjugation, and thereby inducing transcriptional changes that promote tolerance to water scarcity (*101*). However, a subsequent study reported an decreased stomatal aperture and increased tolerance to drought in the *siz1* mutant, mediated by SA-induced ROS accumulation (*119*). Besides its role in abiotic stress, SIZ1 is also involved in biotic stress responses. *siz1* plants have a constitutive systemic-acquired resistance (SAR), characterized by increased SA accumulation, increased expression of pathogenesis-related (PR) genes and increased resistance to the pathogen *Pseudomonas syringae pv. tomato (Pst) DC3000* (*102, 103*).

Interestingly, several of the *siz1* mutant phenotypes could be attributed to specific domains of the E3 ligase protein, through complementation of *siz1-2* knockout mutants with *SIZ1* alleles harboring point mutations in the predicted domains (*120*). The SP-RING is the most important domain for sumoylation, for the proper nuclear localization of SIZ1, crucial for its activity, and for the control of SA levels. Alterations in the PHD and PINIT domains of SIZ1 had a negative impact on SUMO conjugation and sugar and light perception, whereas mutations in the SAP or SXS domains did not influence the level of SUMO conjugates. The SXS domain, on the other hand, has been implicated in SA-mediated ABA signaling at the level of cotyledon greening and expansion (*120*).

Several posttranslational modifications regulate the SIZ1 E3 ligase and can impact its localization, activity and/or specificity. Different SIZ1 phosphopeptides were retrieved in phosphoproteomic studies (*121-125*), but the role of differentially phosphorylated SIZ1 remains unclear in plants. In other systems, phosphorylation was shown to directly modulate the activity of the human E3 SUMO ligase Pc2 in response to DNA damage (*126*), to affect the localization of

the yeast Siz1 during mitosis (*84*), or to target human PIAS1 to downstream effectors in response to pro-inflammatory stimuli (*28, 127*). In response to environmental stresses, AtSIZ1 is sumoylated in specific lysine residues [K100 (H_2O_2, heat), K479 (H_2O_2), K488 (H_2O_2, heat)] (*30*). Sumoylated SUMO ligases RanBP2 and Siz2 were also detected in Xenopus egg extracts and in yeast, respectively, but the relevance of these modifications requires further clarification (*128, 129*). Several mammalian SUMO ligases are targeted for ubiquitin-dependent proteasomal degradation (*130-132*) and a SUMO-targeted ubiquitin ligase (STUbL) was recently implicated in the degradation of the nuclear pool of the Siz1 ligase in yeast (*133*).

1.2.4.3.2 | HPY2*/* MMS21

The role of yeast and mammalian MMS21 is well documented in DNA repair, chromosome segregation and other cellular processes (*134*), but the Arabidopsis SUMO ligase HPY2/MMS21 was recently identified and is less characterized than SIZ1. HPY2/MMS21 belongs to the family of SP-RING, MMS21-type of E3 SUMO ligases and except for SP-RING, it lacks all the domains characteristic of the SIZ/PIAS-type E3s. Orthologs of *HPY2* were identified in several plants, mostly as single copy genes (*32*). The expression pattern of *HPY2* is distinct and more restricted even if partially overlapping with that of *SIZ1*. Moreover, ectopic expression of SIZ1 driven by the *HPY2* promoter is unable to rescue the dwarf phenotype of *hpy2*, revealing that the two ligases have independent functions (*82*). At the cellular level, HPY2 localizes in the nucleus like the core of SUMO machinery and SUMOs (*95*), although cytoplasmic localization has also been reported (*96*). HPY2 functions primarily in development and may also contribute to stress tolerance since the *hpy2* mutant accumulates less SUMO1/2 conjugates in response to heat stress than WT plants (but more than *siz1-2*). HPY2 modulates cell cycle progression and

meristem development in the PLETHORA1 (PLT1) and PLT2-dependent signaling pathway (*95*), and impacts root development (*96*). HPY2 acts downstream of the auxin pathway to promote cell proliferation (*82*), and negatively modulates cytokinin signaling to control primary root development (*96*). Reported *hpy2* phenotypes are independent of SA signaling, as opposed to SIZ1 (*82*).

1.2.4.4 | E4 SUMO ligases

Besides SIZ1 and HPY2, the Arabidopsis genome encodes two other proteins with a SP-RING domain, PIAS Like1 (PIAL1) and 2 (PIAL2) (*31, 32*), that also possess SUMO interacting motifs (SIMs). They show SUMO ligase activity *in vitro* and promote the formation of SUMO chains through SUMO-SUMO isopeptide bonds on already mono or multisumoylated substrates. Extension of the SUMO chains occurs through modification of K10, K23 and K42 on SUMO1, and occurs less efficiently with SUMO3. Unmodified SUMO substrates are not sumoylated by PIAL1 and PIAL2, but these ligases seem to promote the sumoylation of SCE1 on K15, which strongly favors polysumoylation, as previously described (*129*). Accordingly, in the presence of the mutated and unmodified $SCE1^{K15R}$, PIALs enhance SUMO chain formation to a lesser extent. By analogy with the E4 Ubiquitin ligases that extend polyubiquitin chains in a protein that has been already modified by one or more ubiquitins (*8*), these ligases were designated as E4 SUMO ligases (*31*). Several plants analyzed have at least one homolog of PIAL, more similar to PIAL2 than to PIAL1 (*32*). The analysis of single and double mutants suggests a role for PIAL1 and PIAL2 in the salt and osmotic stress responses, and in sulfur metabolism. PIAL1 and PIAL2 (both with polysumoylation activity) seem to be redundant and do not overlap functionally with SIZ1 (with mono/multisumoylation activity). Surprisingly, *pial1 pial2* double mutants

accumulate SUMO conjugates to the same extent or even more than WT (and *siz1-2*) under normal and heat stress conditions. Since SUMO does not target directly substrates to the proteasome, this unexpected observation led to the proposal that E4 SUMO ligases (through extension of polySUMO chains), together with SUMO-targeted Ubiquitin Ligases (STUbLs) (through recognition, binding, and ubiquitylation of polySUMO chains - or direct ubiquitylation of the sumoylated substrate) (*135*), may target poly- and/ or multisumoylated substrates to proteosomal degradation, attributing a physiological role to SUMO chains in substrates (*31*).

1.2.4.5 | SUMO Proteases

A delicate balance between SUMO conjugation and deconjugation confers precision and reversibility to SUMO signaling and its regulatory mechanisms. SUMO proteases are required for deconjugation of SUMO (or SUMO chains) from modified substrates, through cleavage of the scissile peptide bond between the terminal glycine of mature SUMO and the lysine on the substrate, and for processing SUMO precursors into mature forms. SUMO proteases can edit SUMO chains by removal of just some SUMO moieties (*136*). The pool of free-SUMO will vary in accordance with both proteolytic outcomes of SUMO recycling and maturation. SUMO proteases are cysteine proteases with a papain-like proteinase fold belonging to three distinct classes, based on structural and functional characteristics (*32, 136*). The diversification of SUMO proteases resembles the diversification seen for deubiquitylating enzymes (DUBs). In Arabidopsis, around 70 DUBs have been identified, compared to less then 10 SUMO proteases (*3, 32*). However, the high number of SUMO proteases if compared to SUMO activating (SAE) and conjugating (SCE) enzymes, suggests an important modulation of SUMO signaling at the level of desumoylation (*29, 137*).

The catalytic domain in SUMO proteases contains the triad (sometimes dyad) catalytic residues (Histidine-Aspartate-Cysteine), whereas non-catalytic regions can display one or more SUMO interacting motifs, and have described roles on subcellular localization (*138*), substrate recognition (*139*) and paralog specificity (*140*). The substrate specificity of SUMO proteases, though, is strongly influenced by their subcellular localization (*138*). AtESD4 localizes to the nuclear periphery and interacts with the Nuclear Pore Anchor (NUA) protein to regulate flowering time and other developmental processes (*141-143*). The related SUMO protease ELS1/AtULP1a has extra-nuclear localization and is functionally distinct from ESD4, as shown by distinct mutant phenotypes (*48*). *In vivo*, the SUMO protease ELS1 is predominantly engaged in SUMO maturation and ESD4 in SUMO deconjugation. *esd4* accumulates high levels of SUMO conjugates and its early flowering and pleiotropic shoot development phenotypes are even worsened by supplying mature SUMOs, as opposed to *els1* (*7, 48, 141, 142*). Accordingly, ELS1 (but not ESD4) complements an *ulp1-ts* yeast mutant impaired in SUMO precursor processing, and ESD4 (but not ELS1) complements an *ulp2Δ* yeast mutant impaired in SUMO deconjugation. Recently, it was described that the Ulp2 protease trims SUMO chains with a minimum of three SUMO moieties and from the distal end, since attachment to the N-terminus of the distal SUMO moiety reduces cleavage efficiency (*144*).

Belonging to another group of SUMO proteases, OTS1/AtULP1d and OTS2/AtULP1c are nuclear localized, in association with speckle-like bodies (OTS2) or diffused in the nucleoplasm (OTS1), and act redundantly in the response to salt-stress (*137*). *ots1* and *ots2* single and double mutants accumulate high levels of SUMO1/2 conjugates in basal conditions, and even more in response to salt stress, showing a role for SUMO deconjugation *in vivo*. The *ots1 ots2* double mutant exhibits an early flowering phenotype but has an overall growth similar to WT plants (*137*). Other potential plant SUMO proteases have been predicted but await functional characterization (*23, 32*). Although *in*

vitro deconjugation generally lacks SUMO paralog specificity, Arabidopsis SUMO-specific conjugates, with distinct residues four amino acids upstream of the glycine attached to the substrate, can influence the deconjugation rate by SUMO proteases (*7*). *In vivo,* SUMO paralog specificity relies very often on the accessibility of SUMO proteases to the modified substrate, depending on its localization and competitive binding of other proteins (*136*). In SUMO precursor processing, variable peptide extensions of the immature forms are thought to determine the affinity of specific SUMO proteases (*136*).

An important role for sumoylation in plant-pathogen interactions was uncovered by the SUMO protease activities of plant pathogen virulence factors, like XopD from *Xanthomonas campestris*, towards plant nuclear proteins, leading to deactivation of important biotic stress responses (*7, 145, 146*). Regulation of SUMO proteases can occur at the transcript level, e.g., through binding of hypoxia stress signaling components to response elements located at the promoter region (*147*), or through differential splicing like in human *SENP2* mRNA, with an impact on its localization (*148*). SUMO proteases are also regulated by posttranslational modifications like phosphorylation (*149*) and ubiquitylation, with subsequent proteolytic cleavage (*150*). AtESD4 is sumoylated in oxidative stress conditions (*30*). In response to salt stress, despite no detectable changes at the mRNA level, OTS1 protein levels decrease in a proteasome-dependent manner, suggesting a regulatory negative feedback mechanism (*137*). Some SUMO proteases can be inactivated transiently, through a disulfide bond between the catalytic cysteine of two proteases in response to oxidative stress (*151*), or irreversibly by heat shock-promoted denaturation (*152*). Interestingly, a crosstalk between SUMO proteases and SUMO targeted ubiquitin ligases (STUbLs) has been reported. Depletion of SUMO proteases [ULP2 in yeast (*153*) or SENP6, in human cells (*154*)] rescues the defects caused by depletion of STUbLs (SLX5 or SLX8 in yeast; or RNF4 in human cells, respectively). This was an unexpected observation, since SUMO modification is reversed primarily through

deconjugation by SUMO proteases and, alternatively, by STUbL activity, and suggests that there might exist *in vivo* antagonism between these two players.

Furthermore, a putative metalloproteinase expected to cleave a covalent bond between SUMO and ubiquitin, as suggested for the yeast protein Wss1 (*155*), has been predicted in Arabidopsis (*32*). Such protease might have an important role in the cleavage of mixed SUMO-Ubiquitin chains.

1.2.5 | Molecular consequences of sumoylation

Downstream effects of sumoylation occur primarily through modulation of interactions of the modified substrate with other proteins, since SUMO attachment alters the properties and binding surface of the target.

1.2.5.1 | Promotion of interactions/ Recruiting factors

The most common outcome of sumoylation is to promote protein-protein non-covalent interactions. The molecular basis for this relies on the increased affinity of a specific surface groove of the SUMO moiety on the conjugate, towards a SUMO interacting motif (SIM) present in another protein.

SUMO interacting motifs (SIMs)

SUMO interacting motifs are short sequence elements (less than 10 amino acids) with a hydrophobic core of 3 to 4 amino acids (usually I or V) in the vicinity of acidic amino acids (E or D), or phosphorylated S or T residues. The SIM forms a β-strand that sits in a hydrophobic groove between the β2-strand

and α1-helix of SUMO (**Figure** 1.5). The acidic residues of SIM bind a basic patch on SUMO, and are determinant to strengthen the interaction, to define the orientation of the SIM (parallel or antiparallel to the β2 strand), and to modulate its specificity towards distinct SUMO isoforms (*8, 136, 156-158*). All SIMs dock onto the same site on SUMO and thus belong to a single group, contrasting with over 16 structurally distinct Ub recognition motifs, that bind ubiquitin at several surface sites (*3, 8, 159-161*). According to different consensus sequences, SIMs can be classified in several types: SIMa, ΨΨxΨAcAcAcAcAc, characterized by four consecutive hydrophobic residues (Ψ) (the third hydrophobic residue is not conserved, though) immediately followed by a mixed cluster of acidic (Ac) D/S/E residues; SIMb, ΨΨDLT, with a better conservation, and can have a downtream non-crucial acidic region; and SIMr, AcAcAcAcAcΨxΨΨ, that resembles SIMa but in a reversed orientation (*162*). Despite recent advances, a better insight into biologically active SIMs awaits further criteria, since the residues contacting SUMO are still poorly defined and lead to ambiguous identifications of SUMO-interacting proteins (*135, 157, 163*). SIM-associated S and T residues can be phosphorylated, adding a negative charge that can act as a switch for efficient recognition of SUMO (*158*). This is the case, for example, for PIAS1, PML and PMSCL1, whose SIMs are phosphorylated by CK2, allowing efficient recognition of human SUMO1/2 (*164*). A cluster of multiple SIMs is found in some proteins and can be indicative of non-covalent interactions with polysumoylated or multisumoylated targets.

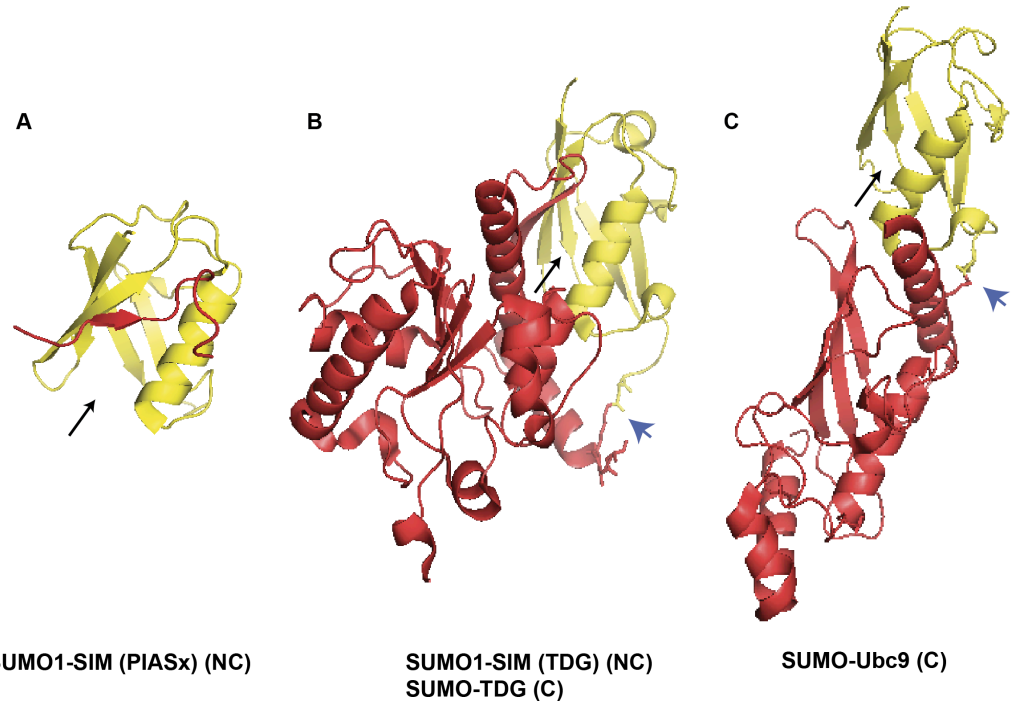

Figure 1.5 | Non-covalent (NC) and covalent (C) interactions between SUMO and substrates.

Shown are ribbon diagrams of SUMO interactions with substrates. **A.** Diagram of the SIMb from PIASx (red) bound to human SUMO1 (yellow) (based on structure PDB: 2ASQ) *(157)*. The SIM β-strand sits in the SUMO hydrophobic groove (marked with a black arrow). **B.** Covalent (blue arrowhead) and non-covalent (SUMO-SIM, arrow) contacts between TDG (red) and SUMO1 (yellow) induce a conformational change essential for the release of TDG from the product DNA (based on structure PDB: 1WYW) (*165*). In the SUMO-SIM interaction, the SIM β-strand from TDG sits in the SUMO hydrophobic groove. **C.** Covalent attachment (blue arrowhead) of SUMO to Ubc9 creates new binding interfaces that can provide a gain in Ubc9 affinity towards specific targets (based on structure PDB: 2VRR) (*76*). In this structure, the SUMO on sumoylated Ubc9 does not participate in any SUMO-SIM non-covalent interaction, and consequently the SUMO hydrophobic groove is free. TDG, thymine/uracil DNA glycosylase; PIAS, protein inhibitor of activated STAT.

SUMO-SIM interactions transduce the biological impact of sumoylation but

are also crucial to regulate the activity and specificity of sumoylation *per se*. SIM motifs are found on the SUMO machinery and in sumoylation substrates (*166*). SCE1 has 2 SIMs (1 SIMa and 1 SIMb), and SIZ1 has 2 SIMs type *a* located in the SAP, PINIT and SP-RING domains. Both SCE1 and SIZ1 were retrieved, together with 6 STUbLs and 6 histone or DNA methyltransferases or demethylases, in large-scale yeast two-hybrid (Y2H) screens to identify Arabidopsis proteins that interact with SUMO isoforms (*167*). A predicted SIMa also exists in the OTS2 SUMO protease. On the other hand, SUMO-SIM non-covalent interactions can be required for the covalent attachment of SUMO to targets. A SIM in Sp100 is required for its enhanced sumoylation, likely through specific recruitment of sumoylated E2 (*76*).

Protein Group sumoylation

When several sumoylated proteins that also have SIMs are in proximity, this can lead to complex assembly and formation of a net of SUMO-SIM connected proteins. Sites of DNA damage, telomeres, promyelocytic leukemia (PML) nuclear bodies (NBs), and ribosome biosynthesis at the nucleolus, are described hot spots of sumoylation in mammalian and yeast cells. For instance, sumoylation of PML promotes the formation of PML NBs and recruitment of associated proteins with SIMs, like Sp100 and the transcriptional repressor Daxx, followed by sumoylation of associated proteins and additional recruitments. E3 SUMO ligases, that also have SIMs, could be enrolled in this wave of sumoylation reactions, crucial in signaling pathways. Still, active and functional complexes could pre-assemble and be further stabilized by sumoylation that would act as “glue" between the different elements/ subunits. The Arabidopsis co-repressors TOPLESS (TPL) and LEUNIG bind to gene-specific repressors and recruit components involved in histone deacetylation. Both TPL and LEUNIG are sumoylated, as almost all of the additional

components of these two transcriptional regulatory circuits (including SEUSS, HDA19, GCN5, and ADA2a and b), suggesting that the entire process is under SUMO control (*30*). When such a web of cooperative bonds is established, individual SUMO-SIM interactions may be redundant or additive, and justify some of the absent or weak phenotypes observed with single SAS or SIM mutations. In the case of protein group sumoylation, specificity is attained through co-localization with the SUMO ligase in the presence of a specific trigger of sumoylation (*6, 47, 168*).

1.2.5.2 | Inhibition of interactions

Besides promoting interactions, the SUMO moiety in a substrate can act as a "repellent", blocking the access of binding partners to the same residue or to a close binding site. A bulky SUMO moiety conjugated to K236 of human SAE2 leads to steric hindrance and interferes with the proper interaction between E1 and E2, and with overall SUMO conjugation to target proteins (*56*). SUMO and ubiquitin can compete for the same residue (K21) on IκBα. SUMO1-modified IκBα cannot be ubiquitylated and is resistant to proteasome-mediated degradation (*169*), constituting an example of antagonism between SUMO and ubiquitin pathways. In Arabidopsis, sumoylation of the transcription factors ICE1, ABI5, and MYB30 results in their stabilization, possibly through reduced ubiquitin-mediated degradation (*108, 109, 117*). However, different modifications of the same residue on a substrate do not necessarily mean competition between PTMs, since they can be sequential and cooperative, or occur in different times, conditioned by distinct stimuli.

1.2.5.3 | Promotion of an intramolecular conformational switch

Finally, substrate sumoylation can lead to a change in its conformation due to the establishment of intramolecular SUMO-SIM interactions with relevant functional consequences. The base excision repair protein uracil/ thymine DNA glycosylase (TDG) is sumoylated after base excision. A subsequent non-covalent intramolecular interaction of the conjugated SUMO with a SIM in TDG (VQEV) induces a conformational change and steric hindrance, with the release of TDG from DNA (*165, 170*). More recently, the same type of mechanism was shown to regulate the Sucrose non-fermenting 1 (Snf1) kinase in yeast. Snf1 is sumoylated and inhibited in response to sugar supply. The non-covalent interaction of the conjugated SUMO with a SIM near the Snf1 active site prompts a conformational change and the rapid inhibition of the kinase (*171*).

1.2.6 | SUMO Enigma

Usually only a minor fraction of a protein pool is sumoylated at a given time point, providing however a global effect. This phenomenon is referred as the SUMO enigma and can be understood if a cycle of sumoylation and desumoylation, rather than persistent attachment of SUMO to the substrate, is required for a functional outcome. In the abovementioned example of TDG, the sumoylation and desumoylation steps are required for each catalytic cycle. SUMO conjugation induces a conformational change in TDG, crucial for its removal from DNA after base-excision repair. Released TDG is rapidly desumoylated and can again bind with high affinity to mismatches in DNA (*14, 172*). On the other hand, the sumoylation-mediated effects may persist after SUMO deconjugation, for instance if sumoylation drives translocation of a substrate to a different subcellular compartment, where it is subsequently desumoylated. In neurons, the SUMO modification of glutamate receptor subunit 6 (GluR6) leads to its endocytosis at the plasma membrane. A large

fraction of GluR6 undergoes SUMO-mediated endocytosis but only a small proportion of sumoylated GluR6 can be detected at a given time point, probably due to its rapid deconjugation after endocytosis (*20, 173*). However, SUMO modification could still act stoichiometrically and correspond to one state whereas desumoylation would restore the original state. In this case, SUMO would get attached to only a minor fraction of structurally and/ or functionally engaged proteins, of a larger total pool (*6, 20*).

1.2.7 | Biological consequences of sumoylation

Through the modulation of protein intra- and intermolecular interactions, sumoylation can have an impact on substrate stability, activity and/or subcellular localization. As previously mentioned, in most organisms the SUMO pathway is essential for viability. The lethality of E1 (SAE2), E2, and double SUMO1/2 mutants, and the severity of E3 SUMO ligase and of some SUMO protease mutants' phenotypes in Arabidopsis, is a corollary of such an essential role in plants. Studies of SUMO pathway mutants implicated SUMO in the regulation of flowering (*105, 142*) and other development processes (*82, 95, 110, 174*), in the cell cycle (*95*), and in signaling through abscisic acid (*107-109, 175*) and other hormones (*110, 176*). A prominent role was also established in nitrogen and sulfur metabolism (*113, 177*) (*31*), in phosphate homeostasis (*94*) and copper tolerance (*111*), as well as in the response to biotic stress (*30, 102, 103*), and the response to heat (*23, 115*), cold (*116-118*), drought (*101, 119, 178*) and salinity (*112, 137*). Despite the importance of sumoylation established by genetics, only recent proteomic approaches have provided detailed insight on the identity of SUMO substrates and their associated processes in Arabidopsis (*25, 30, 67, 167, 179*). Such studies have retrieved sumoylated proteins from a myriad of cellular processes, with an enrichment for SUMO machinery components (SUMO1, SAE2, SCE1, SIZ1, ESD4), and chromatin

remodeling/repair factors (e.g. Histone 2b, GCN5 histone acetyltransferase, HDA19 histone deacetylase, and UBP26 deubiquitylating enzyme), suggesting a role for sumoylation in the plant histone code and chromatin accessibility (*30*). Sumoylation also plays a role in transcription, with transcription factors (TFs) being the most represented elements in the Arabidopsis sumoylome, and with several co-regulators [TPL and LEUNIG] also being sumoylated (*30*). Other categories enriched in SUMO substrates are RNA metabolism, cell cycle regulators (*6, 28*), and nuclear–cytoplasmic shuttling (*6*). Such categories are also enriched in yeast and human sumoylomes and highlight predominant SUMO-regulated processes in a far-reaching SUMO regulatory landscape (*180-183*). Despite the enrichment of SUMO, sumoylation machinery components, and SUMO conjugates in the nuclear compartment, sumoylation occurs also outside the nucleus and sumoylated proteins are found throughout the cell. The Arabidopsis sumoylome responds strongly to biotic and abiotic stress with several types of stress triggering a rapid increase in SIZ1-mediated SUMO1/2 conjugation (*179*). On the other hand, distinct factors, like the ESD4 SUMO protease, WRKY72 transcription factor and LINC1 are specifically sumoylated in response to oxidative stress, heat or basal conditions, respectively (*30*), altogether revealing a pervasive role for SUMO in the plant stress response.

1.2.8 | Crosstalk with other posttranslational modifications

An increasing body of evidence points to an active and dynamic interplay between SUMO and other posttranslational modifications (PTMs), such as phosphorylation, ubiquitylation and acetylation, to coordinately regulate protein function in response to multiple cues (*63*). One layer of crosstalk occurs when the posttranslational modifier (and/or machinery) is itself subjected to posttranslational regulation. As described in previous sections, SUMO itself and the SUMO machinery are modulated through phosphorylation, acetylation,

ubiquitylation and sumoylation. Conversely, sumoylation may intervene in the regulation of other posttranslational modifiers (and/or machinery). Interplay between PTMs can also occur at the substrate level. Frequently, SUMO attachment sites have flanking regions that are also subject to PTMs, dictating the efficiency of sumoylation (e.g., phospho-dependent sumoylation occurs upon phosphorylation of PDSMs). The co-regulation of a given target by SUMO and other modifiers can be competitive or cooperative, and occur in a sequential or simultaneous manner. Since the biological outcomes of sumoylation are mostly transduced via SUMO-SIM interactions, the modification of SIMs by PTMs introduces another variation to the theme [e.g., SIM-associated S and T residues can be phosphorylated, adding a negative charge that can act as a switch for efficient recognition of SUMO (*158*)]. The interplay between SUMO and other posttranslational modifications occurs at different levels of the sumoylation cascade and gives rise to a robust and versatile regulation (*63, 184, 185*).

1.2.8.1 | SUMO and Ubiquitin

SUMO (and SUMO machinery) regulation by mono, multi and polyubiquitylation has been addressed in previous sections. The deubiquitylating enzyme UBP26, which removes Ub bound to histone 2b, is sumoylated in response to oxidative stress, whereas Ub13 is increasingly sumoylated from basal, to oxidative and to heat stress conditions in Arabidopsis (*30*). The biological meaning of such modifications needs further elucidation. At the target level, sumoylation is thought to attenuate HOS1 mediated polyubiquitylation of the transcription factor ICE1. SUMO or ubiquitin conjugation to ICE1 results in either transcription factor activity or degradation, respectively. In response to low temperatures, ICE1 is sumoylated and stabilized, promoting CBF3/DREB1A expression and plant acclimation (*117*). Another example of an antagonistic regulation between SUMO and Ub occurs in

the case of the ABI5 transcription factor. Sumoylation protects ABI5 from proteasomal degradation mediated by AFP and KEG E3 ubiquitin ligase, but renders the transcription factor inactive, negatively modulating ABA signaling (*108, 186, 187*).

SUMO-targeted Ubiquitin ligases

A new class of ubiquitin ligases with a cluster of SIMs and affinity to multi- or polysumoylated substrates was recently described in yeast, animals and plants (*32, 167, 188, 189*). SUMO targeted Ubiquitin ligases (STUbLs) bind poly and/ or multisumoylated substrates through a cluster of SIMs. RING domains on STUbLs recruit the E2 ubiquitin conjugating enzyme, and ubiquitin is directly transferred to the substrate and/or to the attached SUMO moieties (*155, 190*). Consequently, STUbL activity results in proteins that are modified both by SUMO and ubiquitin. Ubiquitylation of sumoylated proteins can target them to proteasomal-mediated degradation (and in fact, STUbL mutants accumulate more SUMO conjugates) or to non-proteolytic fates (*33, 135*). PML protein is ubiquitylated by the STUbL RNF4 in a SUMO-dependent manner and degraded by the proteasome, in response to arsenic treatment (*34, 191*). This crosstalk opens new questions such as whether the conjugated SUMO(s) could fulfill other biological functions prior to SUMO targeted ubiquitylation and signal termination, whether this discrimination could be based on the length and/or topology of the attached SUMO chains, and whether SUMO proteases could still deconjugate SUMO on proteins simultaneously sumoylated and ubiquitylated (*136*). The recently uncovered role of the USP11 ubiquitin protease in removing ubiquitin polymers attached to SUMO chains (counteracting RNF4) (*192*), as well as the described mechanism of SUMO chain trimming by the SUMO protease Ulp2 (*144*), suggest that the modifiers are gradually removed from the distal N-terminus of ubiquitin-SUMO hybrid chains. The processing of such

modified substrate would predict the existence of a protease that cleaves a covalent bond between SUMO and ubiquitin, and this role has been attributed in yeast to the metalloproteinase Wss1 (*155*). An ortholog of Wss1 has been predicted in Arabidopsis (*32*). Arabidopsis STUbLs share a conserved RING domain with *S. pombe* Rfp1/Rfp2 and human RNF4 STUbLs, and contain SIMs of type b and/or type a. Both the RING domain and SIMs are required to complement to various degrees the phenotypes of *S. pombe rfp1/rfp2* mutant. The complementation analysis suggests that AtSTUbL1, 3, and 6 are most similar to *S. pombe* Rfp1/Rfp2, whereas STUbL2 and 4 probably evolved plant-specific functions. All characterized STUbLs localized to the nucleoplasm, but whereas STUbL1, 3 and 4 were strongly localized in the nucleolus, STUbL4 also localized to speckles, and STUbL2 and 6 were excluded from the nucleolus. STUbL4 reduces the protein levels of Cycling DOF Factor 2 (CDF2) with a consequent increase on the *CONSTANS* transcript and the promotion of flowering transition (*167*).

Proteasome inhibition studies show an increased accumulation of both SUMO and ubiquitin conjugates (surprisingly K63 polyubiquitylated substrates are particularly enriched) and underpin an interplay between SUMO and ubiquitin modifiers not only in SUMO-targeted degradation through the UPS, but also in the formation of protein inclusions, as a quality control mechanism for the newly synthesized unfolded/misfolded proteins (*41, 193*).

1.2.8.2 | SUMO and Phosphorylation

SUMO (and the SUMO machinery) can be regulated by phosphorylation. Conversely, sumoylation modulates several kinases, phosphatases and signal transduction pathways (*28, 63*). In response to oxidative stress, there is a coordinated sumoylation and acetylation of homeodomain-interacting protein

kinase 2 (HIPK2) (*194*), whereas phosphorylation triggers the sumoylation of phosphatase PTEN (phosphatase and tensin homolog) (*195, 196*). As previously mentioned, phosphorylation can trigger SUMO covalent attachment through PDSMs on the substrate, and SUMO-SIM non-covalent interactions through phosphorylation of S and T residues associated with SIMs on interacting proteins. Phospho groups add negative charges and increase the affinity of PDSMs with the positively charged patch of SCE1 (*64*), or the affinity of phosphorylated SIMs with a positive patch on SUMO (*158*). Besides the cooperative interplay between phosphorylation and sumoylation, these PTMs can impose opposite fates on a substrate. ABI5 is phosphorylated and activated by SnRK2.2 and SnRK2.3 kinases in response to ABA, whereas SIZ1-mediated sumoylation renders ABI5 inactive, probably by interfering with its phosphorylation (*108*).

1.2.8.3 | SUMO and Acetylation

SUMO (and the SUMO machinery) can be regulated by acetylation. Acetylation neutralizes positive charges on SUMO and E2, and thereby decreases their affinity for negatively charged SIMs or target NDSMs, respectively. Acetylation of K37 in SUMO1 and K33 in SUMO2 decreases the affinity towards some SUMO interacting motifs (SIMs), but promotes the interaction of SUMO2 with the bromodomain in p300 (*28, 46, 63*). The GCN5 histone acetyltransferase and the HDA19 (HD1) histone deacetylase, together with HAC1, ADA2A and ADA2B elements, are some of the factors involved in chromatin modification that are sumoylated in Arabidopsis (*30*). It has been previously mentioned that sumoylation and acetylation cooperate in the regulation of HIPK2 in response to oxidative stress. Oppositely, sumoylation of the tumor suppressor p53 on K386 has a negative impact in the acetylation of K382 by p300/CBP, presumably due to steric hindrance (*63, 197*).

1.2.8.4 | SUMO and Methylation

Several proteins involved in DNA methylation like the SUVR chromatin methylase family and related elements (SUVR1, SUVR2, SUVH2, SUVH9, KTF1, IBM1) are sumoylated in Arabidopsis (*30*). A functional crosstalk between SUMO and methylation probably occurs at the level of several histone or DNA methyltransferases (MT) or demethylases (DMT) that were retrieved as SUMO-interacting proteins in Y2H screens using Arabidopsis SUMO1, 2 and 3 as baits (*167*).

Posttranslational modifications are often combined at the substrate level, generating unique regulatory codes that reflect specific physiological contexts or signaling cues. The tumor suppressor p53 can be heavily modified in its C-terminal regulatory domain by sumoylation, ubiquitylation, neddylation, phosphorylation, acetylation, and methylation (*63*). Phosphorylation of the human flap endonuclease (FEN1) induces SUMO conjugation, leading to a subsequent SUMO-dependent ubiquitylation and proteasomal degradation at the end of S phase (*184, 185*). Sumoylation of ABI5 stabilizes the protein in an inactive state, while phosphorylation induces transcriptional activity, and subsequent ubiquitylation and degradation (*108*). Such intricate networks have tight regulatory roles in fundamental biological processes. Thus, a toolbox of PTMs allows swift molecular switches, enabling sensing, signaling, and ultimately plasticity at the whole organism level.

1.2.9 | Challenges and strategies for the identification of sumoylation substrates and SUMO interactors in Arabidopsis

The low levels of sumoylated proteins and the labile nature of SUMO conjugates due to high SUMO protease activity associated with cell lysis, have hampered until recently the large-scale identification of SUMO substrates in Arabidopsis and other organisms. Several strategies have been developed for enrichment, purification and identification of SUMO substrates and their acceptor sites. These approaches included interactome studies using the Arabidopsis E2 SCE1 and the ESD4 desumoylating protease as baits in Y2H screens, combined with computational analysis of hpSAS on the Arabidopsis proteome (*167*), *in vitro* sumoylation reactions of candidate proteins (*94, 108, 117*), and reconstitution of the Arabidopsis SUMO machinery in *E. coli* (*198*). Despite the enormous advances made with such approaches, they provide low level confidence regarding the *in vivo* sumoylation of the identified targets and its biological relevance (*199*). High confidence analysis of SUMO conjugates employed cells expressing epitope tagged SUMO isoforms, both in transient protoplast assays (*106, 108, 109, 117*) or using genetically modified Arabidopsis (*30, 179*), followed by (tandem) affinity purification and immunoblot detection. In human cells, other alternative approaches have been used, including the use of monoclonal SUMO antibodies for immunoprecipitation and epitope-specific peptides for elution (*54*), and affinity purification with peptides containing SUMO interaction motifs [also called SUMO Binding Entities (SUBEs)] to specifically enrich for polysumoylated proteins (*55, 199-202*). *Bona fide* mass spectrometry identification of sumoylated sites is challenging, since SUMO leaves a large footprint on the modified lysine residue after tryptic digestion (196). Several strategies to interpret complex Mass Spectrometry (MS) data (*66, 203, 204*),

modified protease digestion protocols (*205-208*), or the use of SUMO variants mutated in their C-terminal amino acids have proven useful in such task. In Arabidopsis, a stringent three-step purification procedure to enrich for SUMO conjugates, and a Histidine (H) tagged SUMO1-H89 mutated to arginine (R) variant that generates a smaller footprint (K-QTGG) compared to WT SUMO footprint (K-25 amino acids), allowed the identification of 357 SUMO substrates, although only for 14 of them the SUMO attachment sites were determined (*30*). Recently, isobaric tag for relative and absolute quantification (iTRAQ) MS allowed the quantitative study of sumoylation dynamics in intact Arabidopsis seedlings subjected to stress, and revealed that stress mostly increases the abundance of existing conjugates as opposed to modifying new targets (*179*). The rapid breakdown of SUMO conjugates can be minimized by adding N-ethylmaleimide (NEM) (*175*) that irreversible alkylates and inhibits the active cysteine of SUMO proteases, or through the usage of strong denaturants (e.g., 7 M guanidine chloride or 8 M urea) (*30*), in the cell lysis. The latter approach also avoids that proteins non-covalently bound to SUMO via SUMO-SIM interactions are retrieved in such screens. However, a global insight into the functional and biological outcomes of sumoylation has to integrate both covalent and non-covalent SUMO binding partners. The use of mild conditions in the extraction buffer allows the identification of both type of SUMO interactions, whereas a Y2H screen using a SUMO variant that lacks the terminal di-glycine motif and thus can not be conjugated, identified only proteins non-covalently attached to SUMO (*209*). Arabidopsis SUMO1, 2 and 3 were used as baits in large-scale Y2H screens for identifying SUMO interacting proteins. Fourteen proteins that interacted with SUMO through regions spanning putative SIMs were retrieved, and unraveled predominant nuclear functions for these SUMO interactors. The E2 SCE1 and E3 SIZ1 were identified, together with six histone or DNA methyltransferases (MT) or demethylases (DMT), and six STUbL E3 ligases (*167*).

In the next section, I will describe the central role of the SNF1/AMPK/SnRK1 family of protein kinases in energy signaling in yeast, mammals and plants, respectively. Common and particular features will be analyzed with a special focus on the SnRK1 pathway, in plants. Moreover, the dissection of SNF1/AMPK/SnRK1 regulatory mechanisms will give further insight on these systems, but also reveal the very scarce knowledge on the regulation of the plant counterpart. The activation of the SnRK1 kinase in response to energy stress will be shown to rely on distinct features from the regulatory mechanisms occurring in yeast and mammals in activating conditions. This discloses the need for additional regulatory mechanisms such as posttranslational modifications, namely sumoylation, in the tight regulation of the SnRK1 energy sensor in plants.

1.3 | Energy sensing and signaling in eukaryotes

All organisms need to tightly balance the energy levels of the cell in accordance with the surrounding available resources. The yeast SNF1 (Sucrose non-fermenting 1), mammalian AMPK (AMP-activated protein kinase), and plant SnRK1 (Snf1-related protein kinase 1) are conserved kinases with homologs in almost all eukaryotes. These kinases sense the energy levels of the cell and undergo activation in response to energy depletion, turning off energy-consuming processes and mobilizing energy reserves in an attempt to restore homeostasis (*210*). SNF1/AMPK/SnRK1 are heterotrimeric complexes composed of an α-catalytic subunit (SnRK1α1/α2 in Arabidopsis, also called AKIN10/11 or KIN10/11) and two regulatory subunits, β and γ (*211*).

Genetic studies firstly identified a central role for SNF1 in carbohydrate metabolism in the budding yeast *Saccharomyces cerevisiae* (*212, 213*). Mutants

of the catalytic subunit, *snf1Δ*, failed to grow in the absence of glucose due to their inability to induce genes required for metabolizing alternative carbon sources, or to switch from fermentative to a more energy efficient oxidative metabolism (diauxic shift) (*212-214*). In more complex multicellular organisms, the role of SNF1/AMPK/SnRK1 kinases evolved beyond a conserved cell autonomous regulation of energy homeostasis, to integrate additional metabolic and hormonal cues, balancing energy at the whole body level. In mammals, AMPK activation is crucial for metabolic adaptation to fasting and exercise, when the cellular ATP levels decline (and the AMP/ATP and ADP/ATP ratios increase). In response to peripheral hormones, AMPK activation in the hypothalamus increases appetite and food intake (*215*). The AMPK homolog in the nematode *Caenorhabditis elegans*, AAK, is required for the response to starvation and to other stresses, and promotes lifespan extension (*216, 217*). Similarly, in plants, SnRK1 is important for balancing energy use and storage, and for growth under low energy conditions. The moss *Physcomitrella patens snf1a snf1b* null mutant is deficient in starch accumulation and is only viable if grown under high energy conditions, either in the form of constant illumination or exogenous sugar supply (*210*). Furthermore, it displays altered sensitivity to several phytohormones and premature senescence (*210*). Conversely, SnRK1α1/AKIN10 overexpression in *Arabidopsis thaliana* allows plants to better tolerate conditions of limited photosynthesis and carbohydrate supply, whereas it delays flowering and the onset of senescence under long-day conditions (*218*).

1.4 | SnRK1 in the core of plant energy homeostasis

The early identification of a Snf1-related protein kinase in the endosperm of rye, RKIN1 (*219*), and the remarkable sequence similarity amongst the plant, yeast and mammalian *RKIN1/SNF1/AMPK* genes, respectively, suggested they

belong to an evolutionarily conserved family of protein kinases (*220*). The characterization of *AKIN10* in *Arabidopsis thaliana* revealed a 65% identity to the catalytic domain of yeast Snf1, and showed its ubiquitous expression (*221*). Rye *RKIN1* (*219*), as well as tobacco *NPK5* (*222*), complemented the yeast *snf1* mutant, suggesting a conserved function for the plant kinases in the control of carbon metabolism. The first *in vivo* evidence for such role came from the antisense-mediated silencing of *SnRK1α* in potato (*223, 224*) and wheat embryos (*225*), which resulted in decreased expression of the sucrose synthase (*SUS4*, sucrose-inducible), and α-amylase (α-*AMY2*, glucose-repressible) genes, respectively.

Overtime, different biochemical studies showed the phosphorylation and inactivation of the key metabolic enzymes 3-hydroxy-3-methylglutaryl CoA (HMG-CoA) reductase (HMGR), sucrose phosphate synthase (SPS) and nitrate reductase (NR), in cauliflower (*226, 227*), spinach (*228, 229*) and Arabidopsis (*228*). However, only later it was realized that the kinases responsible for these different phosphorylation events belonged to the same SnRK1 family (*230*). Consequently, besides the abovementioned gene expression regulation, the SnRK1 kinases were also implicated in the control of fundamental metabolic processes through direct enzyme phosphorylation (HMGR, isoprenoid biosynthesis; SPS, sucrose synthesis; and NR, nitrogen assimilation), and in a clear analogy with the SNF1 and AMPK kinases that regulate metabolism in yeast and mammals (*224*). Furthermore, SnRK1, SNF1 and AMPK share similar substrate recognition motifs (*231*) and can phosphorylate several substrates from their counterparts in different organisms. For instance, SnRK1 phosphorylates and inactivates the mammalian HMGR and acetyl-CoA carboxylase (ACC, involved in lipid biosynthesis) in the same sites as AMPK. However, SnRK1 does not phosphorylate the plant ACC, where possibly different regulatory mechanisms have evolved (*226*).

The Arabidopsis SnRK superfamily comprises the SnRK1, SnRK2 and SnRK3 groups (*232*). Whereas the SnRK1 group (with 3 members, SnRK1α1,

α2 and α3) is closely related to the yeast Snf1 and mammalian AMPK, SnRK2 (with 10 members) and SnRK3 (with 25 members) are more divergent plant-specific groups that cannot functionally replace SnRK1, and have been implicated in the osmotic and salt stress responses (*233*).

The identification and characterization of β and γ regulatory subunits associated with SNF1 (*234*)/ AMPK (*235-238*)/ SnRK1 (*239-241*) complexes, and their regulation through different metabolites and through phosphorylation of a conserved threonine residue on the T-loop of the α-subunit (*242-248*), were progressively unraveled as well as the crosstalk with novel metabolic, developmental, and stress response pathways.

Importantly, subsequent studies in *Arabidopsis thaliana* uncovered an unexpectedly wide role for SnRK1 in transcriptional reprogramming, impacting more than a thousand genes in response to energy deprivation *(218, 249)*. KIN10 and KIN11 [SnRK1α1 and α2, respectively; *SnRK1α3* or *KIN12* is poorly expressed in most plant tissues (*218*)] were shown to be activated by energy deprivation caused by unpredicted darkness and other stresses that impair photosynthesis and/or respiration, such as DCMU herbicide treatment and hypoxia. However, the induction of these kinases by stress was blocked by glucose or sucrose supply (*218*). The massive transcriptional changes triggered by SnRK1 activation occurred partly through the S-class of basic region/leucine zipper motif (bZIP) transcription factors (TFs) (*250*). Activation of SnRK1 signaling induced genes related to major catabolic pathways, including cell wall, starch, sucrose, amino acid, lipid, and protein degradation, as well as autophagy and trehalose metabolism genes. Conversely, it repressed genes related to anabolic pathways such as amino acid and protein synthesis, or ribosome biogenesis genes. TFs, chromatin remodeling factors, and signal transduction components were also regulated at the transcript level by SnRK1 (*218*). Furthermore, the transcriptional profile induced by SnRK1 activity largely overlapped with the profiles obtained under a variety of dark and starvation (SnRK1 activating) conditions (*251-254*), and was opposite to the ones in which

sucrose or glucose were fed (inhibiting SnRK1) (*255, 256*). Recently, miRNAs were also implicated in the regulation of specific mRNA targets of the SnRK1 pathway, possibly tuning down particular cellular processes during the stress response (*257*).

Overall, SnRK1 emerged as a global regulator of gene expression in response to energy deprivation, that coupled with direct enzyme regulation, favors energy production and represses energy consuming processes to achieve homeostasis.

SnRK1 appears to be at the interface of several stress, hormone, and metabolic signaling pathways, promoting survival and long-term responses for plant adaptation, growth and development (*218, 233, 249*) (**Figure** 1.6). The next sections will address the centrality of the SnRK1 system and the intricate crosstalk between SnRK1 and other signaling pathways. Furthermore, recent studies highlighting the impact of SnRK1 on plant growth and developmental decisions will be discussed.

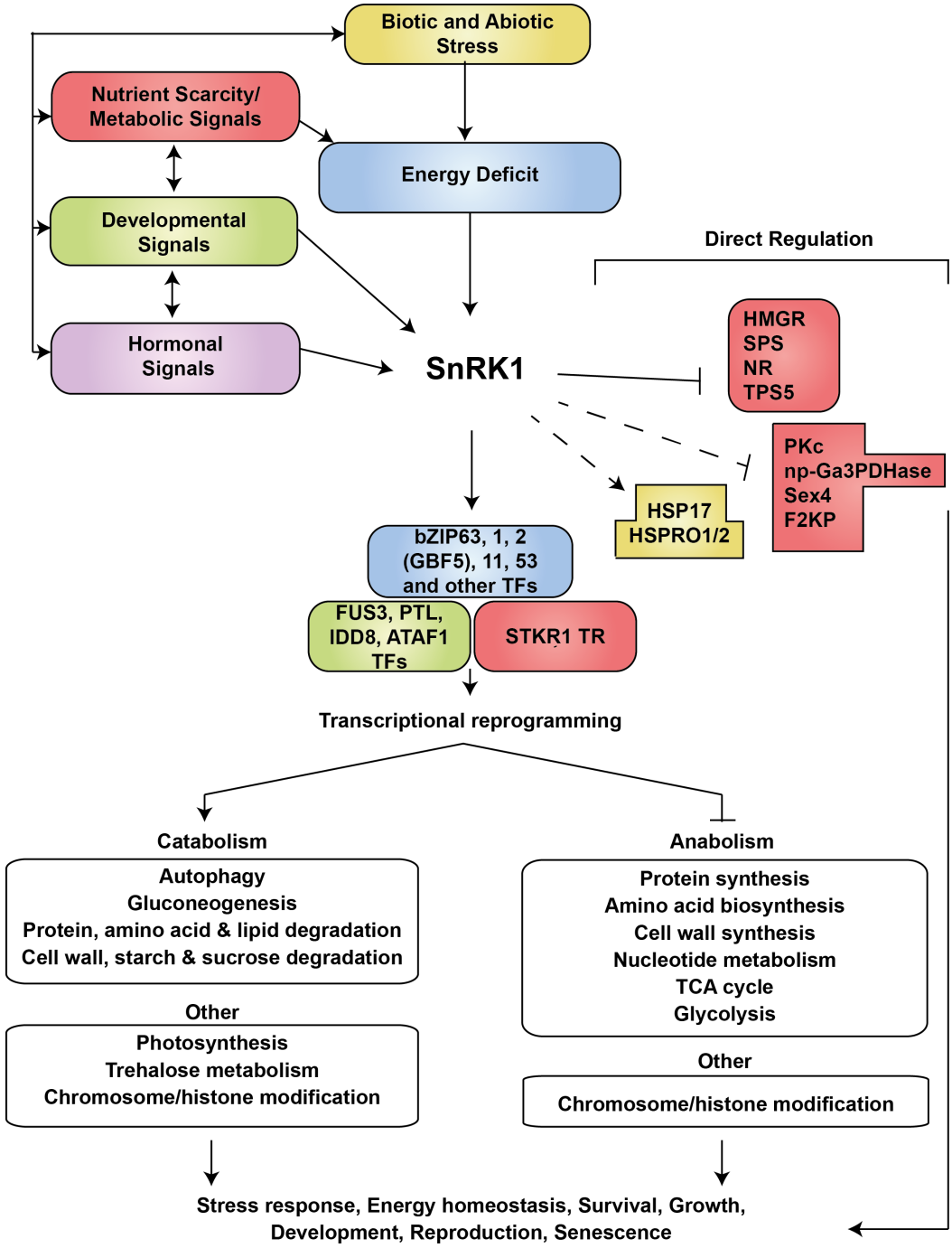
Biotic and Abiotic Stress
Nutrient Scarcity/ Metabolic Signals
Energy Deficit
Developmental Signals
Hormonal Signals
SnRK1
Direct Regulation
HMGR
SPS
NR
TPS5
PKc
np-Ga3PDHase
Sex4
F2KP
HSP17
HSPRO1/2
bZIP63, 1, 2 (GBF5), 11, 53 and other TFs
FUS3, PTL, IDD8, ATAF1 TFs
STKR1 TR
Transcriptional reprogramming
Catabolism
Autophagy
Gluconeogenesis
Protein, amino acid & lipid degradation
Cell wall, starch & sucrose degradation
Other
Photosynthesis
Trehalose metabolism
Chromosome/histone modification
Anabolism
Protein synthesis
Amino acid biosynthesis
Cell wall synthesis
Nucleotide metabolism
TCA cycle
Glycolysis
Other
Chromosome/histone modification
Stress response, Energy homeostasis, Survival, Growth, Development, Reproduction, Senescence

Figure 1.6. | SnRK1 in the interface of Stress, Metabolic, Hormonal, and Developmental signaling pathways.

Several types of biotic and abiotic stresses, as well as nutrient deprivation conditions, converge as an energy deficit signal that triggers SnRK1 activation, alike other hormonal and developmental signals. Upon activation, SnRK1 triggers a vast transcriptional reprogramming that together with direct enzyme regulation promotes energy homeostasis. Through an increase in catabolism and repression of anabolic processes, SnRK1 promotes stress response and survival, growth and development, throughout the plant life cycle. Adapted from (*218, 249*).

1.4.1 | Stress

SnRK1 intervenes in plant responses to abiotic and biotic stress that disrupt energy homeostasis. As previously mentioned, many adverse conditions that interfere with carbon assimilation and/or respiration, such as drought, extreme temperatures, extended darkness, pollutants or flooding, are decoded as energy deficit signals that trigger SnRK1 activation (*218, 249*). One of the first observations connecting environmental stress and SnRK1 was the increased salt sensitivity of potato plants silenced for the *SnRK1β* subunit (*258*). SnRK1 promotes tolerance to submergence stress in rice (*259*) and Arabidopsis (*260*), at least partly because it mediates the induction of important stress genes. The calcineurin B–like (CBL)–interacting protein kinase 15 (CIPK15) acts through the SnRK1A-MYBS1 axis to regulate carbohydrate catabolism and fermentation, allowing rice to grow under floodwater. Furthermore, SnRK1A plays a role in source-sink communication during seedling growth in rice and this contributes to seedling vigor during stress (*259, 261*). Consistent with this, SnRK1 was recently identified as a central hub required for signal integration from multiple stress, hormone and metabolic pathways in rice (*262*). Additionally, SnRK1 has been implicated in the response to Pi starvation in Arabidopsis (*263*) and its ability to interact with and phosphorylate the barley heat shock protein 17 (HSP17), suggests it may also be important for the heat stress response (*264*).

An increasing number of reports highlight a role for SnRK1 also in the biotic stress response. The metabolic status of the host influences the inherent susceptibility to pathogen attack, and in some cases SnRK1 was shown to be a component of the plant resistance to infection. On the other hand, pathogens can hijack host resources and trigger metabolic and energy imbalances. In such scenario, SnRK1 activation triggered by pathogen attack can also elicit a defense response. In other cases, SnRK1 is specifically targeted upon infection, thereby participating in the evolutionary arms race between hosts and pathogens. Several examples are listed below.

In *N. benthamiana*, the SnRK1 homolog AKIN1 increases resistance against tomato golden mosaic virus and beet curly top virus. On the other hand, AL2 and L2 viral proteins interact and inactivate AKIN1, counteracting the plant defense response (*265*). AL2 viral proteins can also repress adenosine kinase (ADK) with a consequent decrease in AMP levels. This may increase the susceptibility of SnRK1 to dephosphorylation and inactivation, and may be an indirect mechanism for SnRK1 downregulation by AL2 (*265, 266*). Arabidopsis SnRK1α2 is inhibited by AC2/C2 geminivirus proteins, and the infection results in broad effects, namely on RNA silencing and autophagy, likely components of antiviral immunity (*267*). Begomovirus and curtovirus AL2/C2 proteins interact with the host geminivirus Rep-interacting kinases (GRIKs), which are upstream activating kinases of SnRK1 (*268, 269*). Moreover, SnRK1 phosphorylates the AL2/C2 proteins *in vitro*, suggesting this as a mechanism by which SnRK1 delays viral DNA accumulation and symptom development during *Arabidopsis thaliana* infection (*270*). SnRK1 also interacts and phosphorylates the βC1 protein encoded by a Geminivirus β-Satellite, as part of the host defense in tomato plants (*271, 272*).

On the other hand, infection of sweet orange plants by *Xanthomonas axonopodis pv. aurantifolii* increased the expression of trehalose biosynthesis enzymes and SNF1-related kinases, likely associated with a defense response (*273*). The AvrBsT protein of *Xanthomonas campestris pv. vesicatoria* targets

SnRK1 and suppresses the hypersensitive response (HR) elicited by the effector protein AvrBs1 in pepper. Intriguingly, SnRK1 is required for AvrBs1-induced HR (*274*). In another case, the plant AvrPto-dependent Pto-interacting protein 3 (Adi3) interacts and phosphorylates the SnRK1β subunit Gal83, with a consequent suppression of SnRK1 activity. Adi3 is a cell-death suppressor with an important role in the resistance of tomato plants to *Pseudomonas syringae pv tomato* (*275*). Furthermore, the plant-specific SnRK1βγ subunit interacts with HSPRO1/2 proteins involved in plant defense and possibly in the leaf senescence program (*276*). HSPRO was shown to participate in a whole-plant change in growth physiology associated with SnRK1 signaling, when *Nicotiana attenuata* seedlings interact with the fungus *Piriformospora indica* (*277, 278*). Interestingly, herbivore attack results in downregulation of *SnRK1β* transcripts in *Nicotiana attenuata* source leaves, and thereby in increased assimilate transport to the roots. Plants with enhanced root reserves prolong reproduction and tolerate better herbivory by allocating reserves to a less vulnerable location within the plant (*279*).

1.4.2 | Hormones

The SnRK1 pathway is intimately associated with plant hormone signaling and several hormones have been shown to control SnRK1 at various levels.

In tomato, expression of the SnRK1γ-regulatory subunit, *LeSNF4,* was induced in response to abscisic acid (ABA) or dehydration, and repressed by gibberellins (GA) or in seeds that had completed germination. In contrast, *SnRK1α* and *β*-subunit genes were constitutively expressed regardless of the developmental, hormonal, or environmental conditions (*280*). Consistent with this, an inhibitor of ABA synthesis repressed *SNF4b* gene expression (*281*) in Medicago. On the other hand, another study showed that auxin and ABA stimulated *Vicia faba SnRK1* promoter activity in Arabidopsis and tobacco

protoplasts (*282*).

Interplay between sugar and ABA signaling has been revealed through extensive connections (*283*), as exemplified by the requirement of *GIN1/ABA2,* involved in ABA synthesis, for the glucose hypersensitivity of SnRK1 overexpressors (*284*).

ABA controls SnRK1 activity also at a posttranscriptional level in a 2C-type protein phosphatase (PP2C)-dependent manner. Two known repressors of the ABA pathway, the PP2Cs ABI1 and PP2CA, interact, dephosphorylate and inactivate SnRK1α. ABA, in turn, inhibits PP2C action, thereby resulting in the activation not only of ABA signaling but also of the SnRK1 pathway (*285*). Consistent with this, SnRK1 and ABA induce largely overlapping transcriptional responses (*285*). On the other hand, *SnRK1* repression via antisense expression causes an ABA insensitive phenotype in pea seeds, suggesting other levels of crosstalk between the two pathways downstream of PP2Cs (*282, 286*).

However, some studies report a negative regulation of ABA on SnRK1 signaling, possibly due to the use of different (autotrophic vs. heterotrophic) plant material or conditions that may determine different SnRK1 complex composition. ABA counteracts SnRK1A signaling in rice seedlings by restricting SnRK1A-Interacting Negative Regulators (SKINs), SnRK1A and MYBS1 to the cytoplasm and thus preventing SnRK1A-MYBS1 nuclear localization and mobilization of nutrient reserves from source tissues (*261*). An antagonistic regulation of the two pathways was also suggested by another study in which SnRK1 repressed salt and ABA-inducible gene expression (*287*). On the other hand, the C-class bZIP63 TF that is phosphorylated by SnRK1 (*288*) and partially mediates SnRK1 transcriptional reprogramming, requires intact ABA signaling for its full repression in high sugar concentrations in Arabidopsis seedlings (*289*). Finally, ABA treatment promoted SnRK1 degradation overtime in wheat roots. However, the amount of phosphorylated SnRK1α remained constant and an increase in the kinase activity was observed (*290*).

Studies using pea seeds with reduced SnRK1 activity also highlighted a cooperative crosstalk between SnRK1 and other hormones, such as auxin and cytokinins, at early stages of seed development, cotyledon emergence and growth (*282, 286, 291*). On the other hand, transcripts related to GA and/or brassinosteroid (BR) synthesis were increased upon silencing of SnRK1 (*286*). In accordance, BR and jasmonate (JAZ) hormone metabolism genes are downregulated upon SnRK1 overexpression in Arabidopsis protoplasts (*218*). Finally, one of the downstream effectors of SnRK1 signaling, the S-class bZIP TFs bZIP11 (*218*), is able to trigger auxin-induced transcription through the recruitment of SAGA-like histone acetyltransferase complexes, *via* ADA2b. This role might be shared by other members of the S-class bZIPs (*292*).

1.4.3 | Metabolism

As early as its identification as part of the SNF1/AMPK/SnRK1 family of protein kinases, SnRK1 was implicated in sugar sensing and signaling pathways in plants. SnRK1 senses the metabolic status of the plant and regulates accordingly metabolism in a cell-autonomous manner, as well as at the whole plant level through crosstalk with hormonal and other signaling pathways.

A first layer of metabolic regulation is exerted by the SnRK1 kinase through direct enzyme regulation of key metabolic components. The inhibitory phosphorylation by SnRK1 of SPS, NR and HMGR implicated this central kinase in the regulation of sucrose synthesis, nitrogen assimilation and sterol/isoprenoid metabolism, respectively (*230*). SnRK1 also phosphorylates the class II trehalose-6-phosphate synthase 5 (TPS5). Phosphorylated TPS5 binds to 14-3-3 proteins but the functional outcome of this regulation needs further clarification (*293*). Further connections between SnRK1 and metabolism come from the phosphorylation of fructose-6-phosphate,2-kinase/ fructose-2,6-biphosphatase (F2KP) by purified AMPK or by an Arabidopsis cell extract (*294*).

Arabidopsis F2KP generates and hydrolyzes fructose-2,6-biphosphate (fru-2,6-P_2), a signaling metabolite in photosynthetic carbon partitioning. Similarly to SPS (*295*), NR (*296*) and TPS5 (*293*), phosphorylation of F2KP causes its binding to 14-3-3 proteins, but whether and how this modifies F2KP function and carbon partitioning requires further investigation. Other examples of direct enzyme regulation come from the potato SnRK1 catalytic subunits PKIN1 and StubSNF1, which interact in yeast-two hybrid assays with the key enzyme of glycolysis, cytosolic pyruvate kinase (PKc). PKc has a consensus SnRK1 motif (*230*) that is phosphorylated by StubSNF1 but not by PKIN1. However, both *PKIN1* and *StubSNF1* silenced lines show diurnal changes in the intensity and periodicity of PKc activity in leaves, compared to WT plants (*297*). Another candidate metabolic target of SnRK1 is nonphosphorylating glyceraldehyde-3-phosphate dehydrogenase (np-Ga3PDHase), a cytosolic unconventional glycolytic enzyme regulated by phosphorylation in heterotrophic tissues. Phosphorylated np-Ga3PDHase is subsequently bound to 14-3-3 proteins and inactivated. Partially purified SnRK1 from wheat endosperm phosphorylates np-Ga3PDHase and impacts carbohydrate and reducing power partitioning and storage (*298*).

Besides direct enzyme regulation, SnRK1 activation also triggers metabolic rearrangements through an extensive transcriptional reprogramming, with implications in primary and secondary metabolism (*218, 249*). The transcriptional regulation exerted by SnRK1 was first acknowledged through its positive impact on sucrose synthase (*219*) and α-amylase (*225*) gene expression. However, SnRK1 regulates the transcription of many other metabolism genes such as plant specific trehalose genes, for instance (*218*). Thus, plants manipulated in the SnRK1 pathway display altered metabolic profiles and changes in carbohydrate storage (*223, 282, 286, 299, 300*). Silencing of *SnRK1* in pea embryos results in defects in sucrose utilization, impaired metabolic fluxes, lower levels of metabolites, and a consequent reduction in sink strength and accumulation of seed reserves (*282*). Similar

implications have been described for AMPK and SNF1 in their respective systems (*233*).

Another example of an intricate SnRK1-carbohydrate regulatory network is the case of ADP-glucose pyrophosphorylase (AGPase), involved in starch synthesis and activated posttranslationally through redox modification. SnRK1 is required for the redox activation of AGPase in response to sucrose and trehalose-6-phosphate (T6P), whereas redox activation in response to glucose seems to involve a separate pathway that depends on hexokinase (*301, 302*).

Conversely, diverse metabolic signals modulate the SnRK1 pathway, in order to adjust and optimize its downstream regulatory response. Several levels of regulation of the SnRK1 pathway by sugars have been reported. For example, sucrose deprivation stimulated *Vicia faba SnRK1* promoter activity in Arabidopsis protoplasts (*282*), and glucose depletion induced *SnRK1β1* expression in germinating *Medicago truncatula* seeds (*281*). *SnRK1β1* expression was also induced by dark (*303*), or ammonia (*304*).

Sugars can also regulate the expression of S-class bZIP transcription factors, downstream effectors of SnRK1 signaling (*305-307*). For example, *bZIP11* expression is induced by sugars, but its translation is repressed by sucrose through a so-called sucrose-induced repression of translation (SIRT) mechanism. Plants with dexamethasone (dex)-inducible nuclear localization of bZIP11 have low T6P levels, changes in trehalose metabolism genes, and altered carbohydrate metabolic profiles that resemble carbon starvation, suggesting a SnRK1-bZIP11-T6P regulatory circuitry that controls growth (*308*). As another example of a posttranscriptional regulation, mRNA decay was also reported as an important mechanism to downregulate *bZIP63* in response to sugar and ABA signals (*289*). On the other hand, glucose deprivation activated SnRK1A posttranscriptionally in rice embryos and suspension cells, and this activation was dependent on the CIPK15 kinase (*309*). SnRK1A protein accumulation was higher after 24h of glucose deprivation, and in the absence of *SnRK1A* transcript changes, a two-fold increase in kinase activity was achieved

in comparison to glucose-fed conditions (*310*). It is important to note that sugar depletion can be the result of unfavorable environmental conditions, but also of an increased demand for photosynthate in other high-priority tissues or organs *(249, 282)*.

In an apparent contradiction, some studies have suggested a positive regulation of SnRK1 activity by sucrose (*223, 224, 301, 311*) or glucose (*284*). Potential explanations for this could be that high sugar concentrations, particularly in the light (where endogenous sugar levels are already elevated), may be perceived as a stress, with the consequent activation of SnRK1. In other studies, the use of heterotrophic tissues or organs (e.g. tubers) as experimental material as opposed to autotrophic mature leaves could explain an opposite mode of SnRK1 regulation (*312*).

T6P is a precursor of trehalose and plays an important signaling role in plant carbohydrate metabolism, growth and development. Increased T6P accumulation generally occurs when sucrose levels are high, and is thus considered an indicator of the sugar status of the plant (*313, 314*). T6P represses SnRK1 activity in physiological amounts, and its inhibition of SnRK1 is mediated by an unknown proteinaceous, heat labile factor, present in young actively growing tissues (*315-323*). Other sugars such as glucose-6-phosphate (G6P) and glucose-1-phosphate (G1P, alone or in synergism with T6P) also inhibit SnRK1, whereas the glycolysis-inhibitor, non-metabolizable sugar, 2-deoxyglucose seems to activate it (*293, 294, 324, 325*).

SnRK1 was also implicated in inositol signaling trough its *in vitro* interaction with the WD40 domain of a myoinositol polyphosphate 5-phosphatase 13 (5PTase13) protein. 5PTase13 is a positive regulator of SnRK1 activity under low-nutrient or -sugar conditions, whereas in severe starvation conditions, it exerts a negative regulation (*326*). Another conserved WD protein, the pleiotropic regulatory locus 1 (PRL1) interacts and inhibits the activity of SnRK1 in Arabidopsis (*311*), possibly through its ubiquitylation and proteasome-mediated degradation (*327*). Accordingly, *prl1* mutants display higher SnRK1

activity and exhibit glucose and sucrose hypersensitivity and transcriptional derepression of glucose responsive genes (*328, 329*). In comparison to WT plants, *prl1* mutants have increased accumulation of isoprenoid products derived from the plastidial isoprenoid pathway, possibly as a consequence of the increased phosphorylation and inactivation of HMGR, the rate-limiting enzyme of the cytosolic pathway for isoprenoid biosynthesis (*330*).

1.4.4 | Growth and Development

SnRK1 energy sensing conveys environmental and metabolic signals towards important developmental decisions in vegetative and reproductive growth. In potato, antisense transcript repression of the α-subunit *PKIN1* (*331*) or the β-subunit *StubGAL83* (*258*) affected tuber and root development. On the other hand, engineered reduction of T6P levels in potato tubers activated SnRK1 and induced down-regulation of genes involved in cell proliferation and growth promotion, and up-regulation of an inhibitor of cell cycle progression (*323*). T6P and SnRK1-mediated signaling are also involved in the repression of new fruit growth by preexisting fruits in cucumber plants (*332*), whereas transgenic tomato plants overexpressing *SnRK1* ripened earlier than the wild-type (*300*). In *Medicago truncatula* seeds, repression of *SNF4b* resulted in reduced seed longevity (*299*).

A developmental role for SnRK1 has been similarly shown in cereals. Antisense repression of *SnRK1* in barley could never be transmitted to the T1 generation (*333*), probably due to the developmental arrest of a starch-depleted pollen (*334*). Wheat SnRK1 marker genes showed different patterns of expression before and during the grain filling period, consistent with changes in T6P content (*319*). On the other hand, SnRK1A protein kinase was also shown to promote seed germination and seedling growth and modulate development in rice (*260, 310*). SnRK1A-Interacting Negative Regulators (SKINs) counteracted

SnRK1A function, inhibiting starch and nutrient mobilization from the endosperm and in consequence seed germination and growth (*261*).

Antisense repression of *SnRK1* in pea seeds caused defects in seed storage and maturation reminiscent of ABA-insensitivity. This included downregulation of genes related to cell proliferation, meristem maintenance and differentiation, leaf formation, and polarity, both through interaction with ABA-dependent and independent pathways (*282, 286*). In agreement with its described transcriptional reprogramming function, SnRK1α1 is predominantly localized to the nucleus in young organs, such as leaf primordia and meristematic zones of roots and shoots. In most other tissues throughout Arabidopsis development, SnRK1α1 is mainly in the cytoplasm and at the plasma membrane (*335*). Additionally, *SnRK1* was identified as a very early marker gene of developing leaf primordia in tomato (*336*).

In Arabidopsis, SnRK1 function in growth and development was assessed employing transient and systemic virus induced gene silencing (VIGS) of *KIN11* in a *kin10* mutant background. This strategy was employed to circumvent the problem of redundancy in single α-subunit mutants, as well as potential lethality problems in stable double mutants. Plants depleted of both KIN10 and KIN11 displayed dramatic growth defects, strong accumulation of anthocyanins and early senescence (*218*). Less severe silencing allowed the formation of inflorescences, although they were rudimentary and unviable. Unlike the *snf1a snf1b* double mutant in moss (*210*), the growth defects of the Arabidopsis SnRK1 loss-of-function plants could not be rescued by constant illumination or exogenous supply of sucrose, suggesting fundamental roles in normal vegetative and reproductive growth beyond a purely metabolic regulation (*218*). Conversely, SnRK1α1 overexpression in Arabidopsis altered inflorescence architecture, delayed flowering, and the onset of senescence under long-day conditions (*218, 260*). In agreement with the strong phenotypes resulting from altered SnRK1 levels, the previously described *prl1* mutants display pleiotropic growth and developmental defects that may be partly attributed to their higher

SnRK1 activity (*328*). Similarly, deficient myristoylation of the SnRK1β1 and β2 subunits in the N-myristoyltransferase mutant *nmt* contributes to malformation of the shoot apical meristem and to developmental arrest (*337*). SnRK1 kinase activity was five fold increased in the *nmt1-1* mutant, that also displayed glucose hypersensitivity (*337*).

AMPK was shown to regulate fundamental cellular functions, such as cell polarity and cell division (*338*). Phosphorylation of the cyclin-dependent kinase inhibitor $p27_{KIP1}$ by AMPK causes its stabilization, and thereby cell-cycle arrest, autophagy or apoptosis (*339-341*). Similarly, SnRK1 phosphorylates the Arabidopsis $p27_{KIP1}$ homologs, KRP6 and KRP7, but this phosphorylation seems to promote cell division. This seemingly counterintuitive function of SnRK1 in promoting cell cycle progression could be unrelated to its energy sensing function, ensuring proper cell division in the absence of stress. It may also serve a coordinating function, allowing an orderly cell cycle arrest in the ensuing G1 phase (*342*).

Recently, SnRK1α1 was shown to interact, phosphorylate and stabilize FUSCA3 (FUS3) TF. SnRK1α1 and FUS3 interact genetically and functionally as positive regulators of ABA signaling, antagonize embryonic-to-vegetative and vegetative-to-reproductive phase transitions, and regulate lateral organ development in Arabidopsis thaliana (*343, 344*). SnRK1 was also shown to interact with the PETAL LOSS (PTL) TF that represses growth in inter-sepal zones of Arabidopsis (*345*), and with the plant-specific NAC TF family member ATAF1. ATAF subfamily members are positive regulators of plant development and accordingly, *ATAF* downregulation leads to dwarfism, sterility and reduced or absent flower initiation (*346*). Recently SnRK1α1 was shown to phosphorylate and repress the indeterminate domain 8 (IDD8) TF, with a consequent delay in flowering (*347*).

1.5 | Conserved Structures of SNF1/AMPK/SnRK1 complexes

The common ancestral functions shared by SNF1/AMPK/SnRK1 kinases in the regulation of energy and carbon metabolism are accompanied by structural similarities (*211, 348, 349*). Purification and characterization of the AMPK complex revealed an heterotrimeric complex composition with an α-catalytic subunit, and a β and γ-regulatory subunits (*350*). Multiple isoforms of the three subunits have been recognized in the genomes of almost all eukaryotes due to a remarkable structural conservation (*220, 234, 239, 351*). The αβγ heterotrimeric complex is assembled through varied combinations of specific α (Snf1 in yeast, α1/α2 in mammals, α1/α2 in plants), β (Sip1/Sip2/Gal83 in yeast; β1/β2 in mammals; β1/β2/β3 in plants) and γ subunit isoforms (Snf4 in yeast; γ1/γ2/γ3 in mammals; *γ*/βγ in plants) (*234, 239, 240, 276, 350*). Some experimental evidence also suggests the existence of atypical complexes, such as in the case of complexes devoid of AMPKγ-regulatory subunits, that interact with the upstream hypothalamic calcium/calmodulin-dependent protein kinase kinase 2 (CaMKK2) independently of the adenine nucleotide ratios (*352, 353*). Even though dimeric complexes of SnRK1 have also been suggested (*335, 354*), more recent studies do not support this (*355, 356*). Finally, alternative transcription initiation or splicing events can further increase the number of subunit variants and thereby the diversity of complexes assembled (*276, 351, 357*). Some insights regarding complex-specific functions, distribution and regulation have emerged but further work is required in this respect (*303, 358*). The catalytic and regulatory subunits of SNF1/AMPK/SnRK1 complexes will be described in more detail in the next sections.

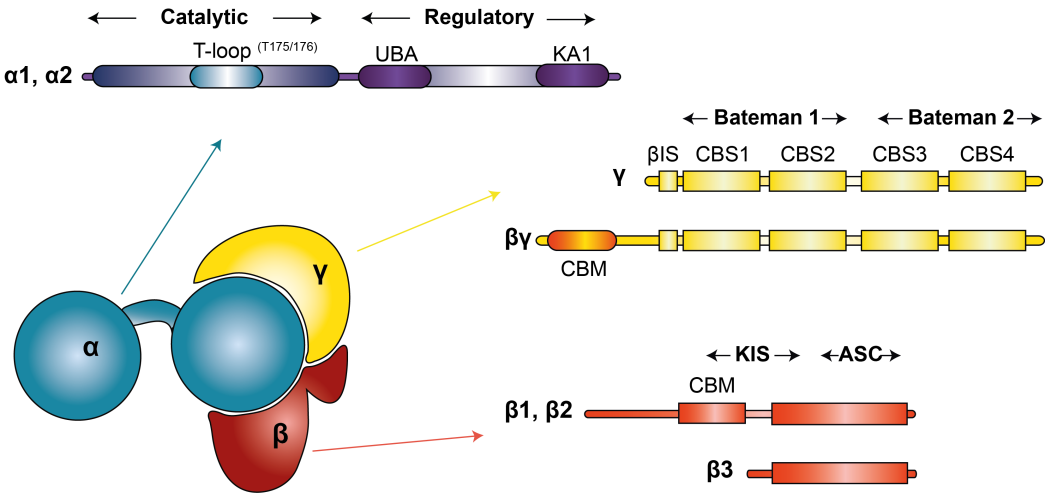

Figure 1.7 | Heterotrimeric structure of the SnRK1 complex.

The α-subunit (in blue) is composed of a catalytic domain (in blue with the T-loop in cyan) and a regulatory domain (in purple-blue), which encompasses an ubiquitin-associated (UBA) domain, and a kinase-associated (KA1) domain for binding the β- and γ-subunits. The γ-subunit (in yellow) is composed of two "Bateman" domains, each of them containing two CBS (cystathionine-β-synthase) domains and a β-interacting sequence (βIS). The plant-specific SnRK1βγ possesses a carbohydrate-binding module (CBM). The β-subunit (in red) harbors an ASC (association to the Snf1 complex) domain, containing the sites of interaction with α and γ, a CBM and an N-terminal extension. The KIS (kinase interacting sequence) domain, traditionally used for designating the region comprising the CBM and the site for interaction with the α-subunit, is no longer used. The plant-specific SnRK1β3 is an atypical β-subunit, as it does not possess the CBM or the N-terminal extension. Adapted from (*359*).

1.5.1 | α-catalytic subunit

The catalytic subunit comprises an N-terminal kinase domain and a C-terminal regulatory domain. It has the highest degree of cross-species

conservation amongst the three subunits, especially in the kinase domain of the protein (*220, 360*). The kinase domain displays a canonical fold (*361*) and contains the activation loop (T-loop), in which the phosphorylation of a conserved threonine (T) by upstream kinases is essential for activity (Snf1^{T210};AMPKα1^{T183}/AMPKα2^{T172};SnRK1α1^{T175}/SnRK1α2^{T176}) (*218, 359, 362-365*). The C-terminal regulatory domain in yeast and mammals harbors an auto-inhibitory sequence (AIS) adjacent to the kinase domain (*366, 367*). This does not seem to be the case in SnRK1 (*365*), where instead an ubiquitin-associated domain (UBA) is present that may mediate the interaction with ubiquitylated proteins (*368, 369*). In addition, these kinases possess a kinase-associated 1 (KA1) domain near the C-terminal end (also referred to as β-subunit interaction domain), responsible for the interaction with the regulatory subunits and the upstream phosphatases, as well as with other interacting proteins (*241, 285, 311, 368, 370-373*) (**Figure** 1.7). A nuclear export sequence (NES) was identified in the C-terminal tail of AMPKα (*374*), whereas a nuclear localization signal (NLS) is present in the end of the kinase domain (*375*). Both signals seem to be conserved in the plant and yeast counterparts. It was shown that the yeast and mammalian α-catalytic subunits can form dimers, as observed in crystals and in *in vivo* co-immunoprecipitation assays (*376-378*), and the same might occur with the plant α-subunits (*325, 379*). However, the physiological relevance of such level of organization is still unclear.

1.5.2 | β-regulatory subunit

A primordial function of the β-regulatory subunit is to act as a scaffold between α- and γ-subunits. It contains a carbohydrate-binding motif [CBM, also referred as glycogen-binding domain (GBD)] in the middle of the protein, shown to interact with glycogen in yeast and mammals (*380-383*). In plants, recent evidence suggests that the CBM of the β-regulatory subunits does not mediate

SnRK1 binding to starch or other carbohydrates, although an opposite conclusion was reached in a previous study (*355, 384*). Work in yeast supports that the CBM domain may exert regulatory functions independently of glycogen interaction (*385, 386*). The CBM domain largely overlaps, but not totally, with the previously assigned kinase interaction sequence (KIS) domain, which is required for the interaction with the regulatory domain of the α-catalytic subunit of yeast SNF1 and plant SnRK1 (*234*). A C-terminal domain, association with SNF1 complex (ASC), mediates the interaction with the γ-subunit of yeast SNF1 and plant SnRK1, and both α- and γ-subunits of mammalian AMPK (*351, 387*). Besides the conserved domains, the β-subunits have variable N-terminal extensions that can determine subcellular localization, extent of activation and substrate specificity of the kinase complexes, through posttranslational modification switches (*303, 348, 388-392*). The plant-specific β3 subunit, contains only the ASC domain (lacking the N-terminal extension and CBM) and is still able to complement the *gal83Δ sip1Δ sip2Δ* yeast mutant devoid of all three β-subunits (*240*). In this atypical β subunit, the ASC domain interacts with both α- and γ- plant subunits (**Figure** 1.7).

1.5.3 | γ-regulatory subunit

γ-subunits harbor two Bateman domains (*393*), comprising four cystathionine-beta-synthase (CBS) repeats that, in mammals, bind adenylates. Whereas CBS2 is free and CBS4 binds AMP non-exchangeably (*394*), CBS1 and CBS3 bind adenylates (ATP/ADP/AMP) interchangeably (*395, 396*), and by this mean control the activity of the AMPK α-catalytic subunit (*348, 349, 397*). The CBS motifs are preceded by a pre-CBS domain in the N-terminus that is highly divergent (*398*).

In plants there is an atypical γ-subunit, apparently derived from a fusion of a CBM sequence present in the β-subunits, to the N-terminus of a γ-subunit (*276,*

354) (**Figure** 1.7). The plant SnRK1βγ protein is able to complement the yeast *snf4Δ* mutant, and it interacts with α- and β-subunits, forming plant-specific SnRK1 complexes (*241, 276, 335, 355, 356, 399*). On the contrary, the SnRK1γ-subunit is unable to rescue *snf4Δ* and does not appear to interact with α- and β-subunits, suggesting that the SnRK1βγ is the only canonical γ-type subunit in plants (*239, 355, 356*).

Crystal structures have revealed the dimerization of γ-subunits in yeast and mammals. Yeast Snf4 and plant SnRK1βγ were also shown to form dimers *in vivo* (*399-401*).

1.6 | Regulation of SNF1/AMPK/SnRK1 kinases

The activity of protein kinases can be regulated at the expression level and also through swift posttranslational modifications (PTMs), such as phosphorylation, acetylation and ubiquitylation, amongst many others. The binding of activating subunits, inhibitor proteins or metabolites can adjust the kinase response to specific cues. Additionally, kinase modulation is also achieved through oligomerization, intracellular translocation or protein cleavage. The possible interconnection between the different modes of regulation further expands the versatility and complexity of the system. Whereas most of the regulatory mechanisms are reversible (e.g. phosphorylation/ dephosphorylation or binding of protein regulators), an irreversible downregulation (e.g. by degradation through the ubiquitin-proteasome system) can dictate signal termination. The commitment to degradation is most often triggered by an active kinase, especially when the activity is sustained (*402*).

The SNF1/AMPK/SnRK1 kinases are controlled by numerous mechanisms that have an impact on kinase activity, stability, and/or subcellular localization. Several layers of regulation of SNF1/AMPK/SnRK1 complexes will be

addressed in the next sections, with a focus on our current knowledge on plants (**Figure** 1.8).

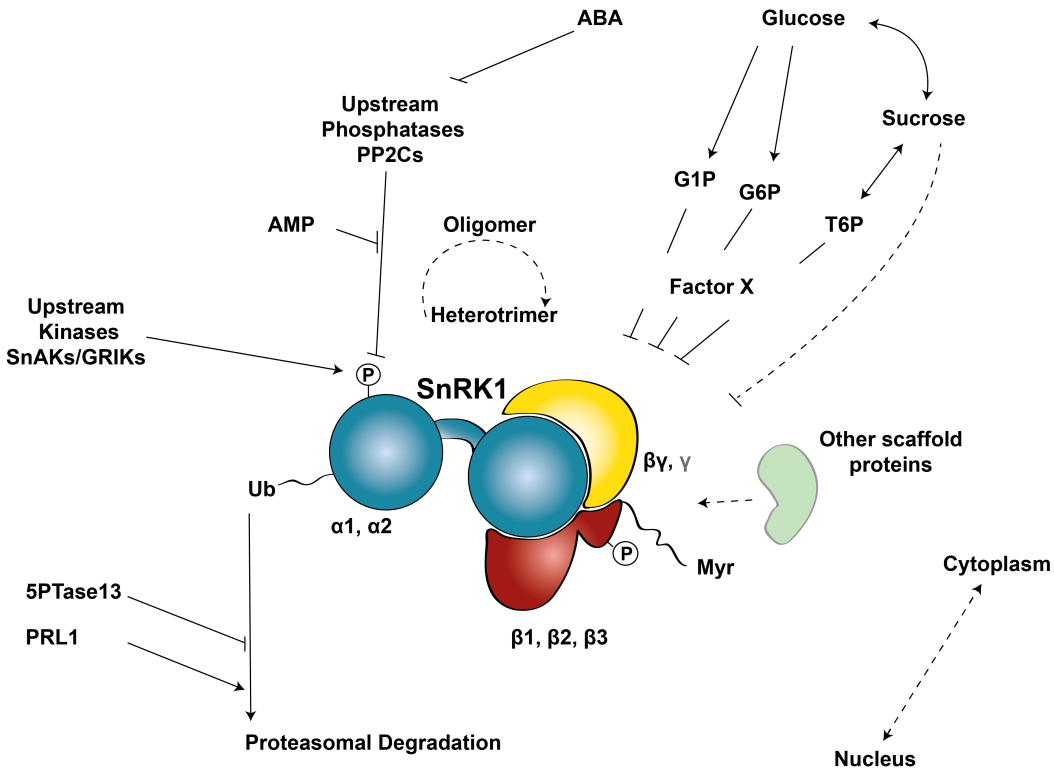

Figure 1.8 | Regulatory mechanisms controlling the SnRK1 kinase.

Multiple factors regulate SnRK1, some of which are conserved across eukaryotic orthologs. Broken lines and full lines designate links that are indirect or require further support, and direct connections, respectively. P, phosphorylation; Ub, ubiquitylation; Myr, myristoylation; SnAKs, SnRK1-activating kinases; GRIKs, Geminivirus Rep-interacting kinases; 5PTase13, myoinositol polyphosphate 5-phosphatase 13; PRL1, Pleiotropic Regulatory Locus 1; PP2C, Protein Phosphatase type 2C; ABA, abscisic acid; G1P, Glucose-1-phosphate; G6P, Glucose-6-phosphate; T6P, Trehalose-6-phosphate.

1.6.1 | Complex composition

Multiple combinations of the different catalytic and regulatory subunits of SNF1/AMPK/SnRK1 heterotrimers lead to a diversity of kinase complexes. Furthermore, the spatiotemporal regulation of individual subunits is determinant for complex composition, which can be a mean to attain specificity. Different upstream regulators and downstream effectors likely recognize different SNF1/AMPK/SnRK1 complexes, and strategies to determine complex composition should be undertaken in the study of the respective signaling pathways.

As previously mentioned, hormones, metabolic and environmental cues, differentially regulate the expression of specific subunits of the SnRK1 complex (e.g. through transcriptional control and alternative splicing). Subunit composition may also be unique to particular subcellular compartments, tissues or developmental stages (*312*). For instance, Arabidopsis SnRK1β genes have specific patterns of expression throughout plant development, and the expression of SnRK1β1 is induced by ammonium (*304*) and dark, and repressed by sugar (*303*). SnRK1β1 containing complexes specifically interact with NR, promoting its phosphorylation and inhibition with a consequent downregulation of nitrogen assimilation (*303*).

The total number of α-, β-, and γ-subunits present in Arabidopsis prompts the possibility of 6 different heterotrimers, taking into account that the γ-subunit does not interact with α- or β-subunits, and that βγ is considered the only canonical γ-type subunit (*403, 404*). Though, the number of possible heterotrimers increases if alternatively spliced variants are considered.

In a study using bean seeds, SnRK1 complexes were separated by size exclusion chromatography and the distribution of SnRK1 activity was evaluated through detection of T-loop phosphorylated and non-phosphorylated catalytic subunits in each fraction. A differential distribution of SnRK1 activity per size/fraction was observed in different developmental stages of bean seeds, and

supports the idea that multiple types of SnRK1 complexes might be present. In the same study, the regulation of SnRK1 activity by metabolites, or in different developmental stages, revealed differences that were dependent on the substrate sequence used in the *in vitro* kinase assays, evidencing a possible substrate specificity conferred by different SnRK1 complexes (*405*). On the other hand, G1P, G6P, and T6P inhibit SnRK1 in young tissues via an intermediary factor that is separable from SnRK1. Since maximal inhibition by G1P and G6P metabolites was found on SnRK1 complexes of the same size as for T6P (~174kDa), it is likely that the SnRK1 complexes inhibited by these metabolites are very similar, requiring possibly the same intermediary factor.

Moreover, plant-specific regulatory subunits β3 and βγ have probably evolved to confer SnRK1 complexes plant-specific functions (*211, 331, 359*). It was suggested that SnRK1 could form heterodimers composed of α and βγ-subunits, and devoid of a β-regulatory subunit (*335, 354*). However, the most recent studies do not support the existence of such SnRK1 dimers (*355, 356*).

In the yeast system, three alternate SNF1 heterotrimeric complexes exist composed of distinct β-subunits, Sip1, Sip2 or Gal83, together with single α- (Snf1) and γ- (Snf4) subunits. The β-subunits have divergent N-termini that confer unique subcellular localization patterns and direct the localization of the catalytic Snf1 subunit, upon glucose deprivation (*348*). The differential distribution of distinct SNF1 complexes within the cell can affect substrate access. Thus, despite of a considerable functional overlap, β-subunits are implicated in distinct processes. For instance, Sip2 is implicated in aging (*406*) whereas Gal83 mediates the interaction of Snf1 with the transcriptional activator Sip4 (*407*), and possibly with the transcriptional apparatus (*408*). The different β-subunits also confer stress-dependent preferences for activation by the upstream kinases Sak1, Tos3, and Elm1 (*348, 409*).

Similarly, AMPK heterotrimers are composed of distinct α-, β-, and γ-subunits that show differential tissue-specific expression and activation. AMPKα2 is highly abundant in skeletal muscle whereas AMPKα1 is more evenly distributed

across different tissues. AMPKβ1 and β2 subunits show an expression profile comparable to AMPKα1 and α2, respectively. Regarding the regulatory γ-subunits, γ1 and γ2 have a more widespread distribution whereas γ3 is mostly restricted to the skeletal muscle (*357*). For instance, it was shown that specific AMPK complexes containing the AMPKα2 catalytic subunit are required for the direct activation of fatty acid oxidation by leptin, in skeletal muscle cells (*375, 410*). On the other hand, the small molecule activator A-769662 is selective for the AMPKβ1 isoform (*358*), exemplifying how complex composition can determine the regulation of specific AMPK heterotrimers (*357*). Some experimental evidence suggests the existence of atypical AMPK complexes, devoid of AMPKγ, that interact with the upstream hypothalamic calcium/calmodulin-dependent protein kinase kinase 2 (CaMKK2) independently of the adenine nucleotide ratios (*352, 353*).

1.6.2 | Scaffold proteins

The binding of adaptor proteins can further increase the versatility of SNF1/AMPK/SnRK1 complexes by bridging their interaction with specific targets or upstream effectors, and also by turning the complex susceptible to regulation by different metabolites. For instance, SnRK1 complex inhibition by T6P requires a yet unknown intermediary factor. Recently, it has been proposed that proteins containing the domain of unknown function 581 (DUF581) may work as auxiliary adaptor modules of SnRK1, providing specificity towards distinct regulators or substrates under certain conditions (*312*). DUF581 proteins interact with Arabidopsis SnRK1α1 and α2 catalytic subunits and their co-expression re-located SnRK1 to different subnuclear loci. The expression of DUF581 genes is differentially regulated by hormonal and environmental cues, indicating possible specialized functions for each of the nineteen DUF581 proteins characterized. DUF581-19, also described as mediator of ABA-

regulated dormancy 1 (MARD1), appears to be a positive regulator of seed dormancy, as *mard1* seeds are less dormant and their radicle protrusion during germination is resistant to external ABA (*411*). This resembles the ABA insensitive phenotypes of SnRK1 silencing in pea seeds (*286*). On the other hand, overexpression of DUF581-18 in Arabidopsis increases resistance to aphids (*412*), and overexpression of a drought-inducible DUF581 wheat protein in Arabidopsis conferred salt and drought tolerance and rendered seeds hypersensitive to ABA (*413*). Furthermore, SnRK1 catalytic subunits and DUF581-18 shared a common target, the storekeeper related 1 (STKR1) transcriptional regulator (*312*), implied in sucrose-regulated gene expression in potato (*414*).

1.6.3 | Oligomerization

The formation of higher order oligomeric complexes can provide an additional layer of kinase regulation (*415*). Yeast SNF1 catalytic (Snf1) and regulatory (Snf4) subunits were shown to form dimers in crystals and *in vivo* (*376, 377, 400*). Dimerization was also observed with mammalian AMPKα or γ subunits (*378, 401*) and with maize βγ-subunits (*399*). The dimerization interface in Snf1 and AMPKα seems to involve extensive hydrophobic interactions around the activation loop of the catalytic subunits (*377, 378*). Importantly, supramolecular assemblies of dimers of heterotrimers have been reported for SNF1 and AMPK (*372, 416, 417*). Furthermore, the expected molecular weights of AMPK and SnRK1 heterotrimers were largely exceeded in size exclusion chromatography analyses (*325, 417*), suggesting higher order oligomers and/or complex assembly with other proteins. It is proposed that the regulation by oligomerization may be particularly important in specific subcellular loci where the kinases are highly concentrated, since dimerization appears to be a reversible and concentration-dependent process (*378, 417*). Higher order

oligomers were associated with an inactive state of the AMPK complex (*378*) and it was also speculated that upon dimerization Snf1 becomes inaccessible for T-loop phosphorylation, rendering the oligomer inactive (*377*). A similar outcome could result from SnRK1 oligomerization since the distribution of T-loop phosphorylation in size fractionation studies reveals a weaker phospho-signal associated with higher order complexes, and a stronger phospho-signal in fractions with the average heterotrimer molecular weight (*325*).

1.6.4 | Subcellular localization

The emergence of subcellular compartments in eukaryotes allowed for new ways of storing nutrients beyond the extracellular and cytosolic boundaries, and required additional sensors to tightly balance and coordinate cellular and whole-organism metabolism (*418*). The mechanisms that regulate SNF1/AMPK/SnRK1 subcellular localization modulate their access to downstream targets or interacting proteins *in vivo* (*374*). Recently, it was suggested that under low nutrient conditions, AMPK activation by the upstream kinase tumor suppressor liver kinase B1 (LKB1) occurs on the surface of the lysosome, through the adaptor protein AXIN. On the other hand, AXIN associates with LAMTOR, a component of the Ragulator complex, shown to promote binding of target of rapamycin complex-1 (mTORC1) to the lysosome under nutrient rich conditions. It was suggested that the Ragulator complex could act as a switch between catabolism (through AMPK activation) and anabolism (through mTORC1 activation) at the lysosomal membrane (*419, 420*).

As previously mentioned, in yeast, the β-subunits direct the localization of the catalytic subunit Snf1 (*348*). All three β-subunits are cytoplasmic in conditions of abundant glucose. However, in response to glucose depletion, the Sip1 β-subunit re-localizes to the vacuolar membrane (*389*), similarly to the lysosome localization of AMPK under low nutrient conditions, and Gal83 re-localizes to the

nucleus, whereas Sip2 remains cytoplasmic (*421*). Whether SnRK1 can similarly localize to the vacuole surface or not is still an open question.

The subcellular localization of SnRK1 can be differentially regulated in various tissues, developmental stages and under various conditions. In agreement with a cytoplasmic role, SnRK1α catalytic subunits associate with β- and βγ-regulatory subunits in the cytoplasm (*399*), and directly target and phosphorylate key metabolic cytoplasmic enzymes. SnRK1 accumulated in Golgi bodies, and a dispersed signal was obtained upon incubation with the Golgi disruptor brefeldin A (*335*). On the other hand, the nuclear localization of some of the subunits of the SnRK1 complex (*218, 276, 335, 345*) is also in accordance with the central role of SnRK1 in transcriptional reprogramming. Both NLS and NES motifs were characterized in AMPKα (*374, 375*), and seem to be conserved in the catalytic subunits of plant (SnRK1α1 and SnRK1α2) and yeast (Snf1). It was hypothesized that the TFs FUS3 and PTL, at least, may retain SnRK1α1 in the nucleus through binding to its C-terminal part and thus masking of the conserved NES in this region (*345*).

Furthermore, the described interaction of SnRK1α1 and SnRK1βγ at the plasma membrane is consistent with the potential assembly of SnRK1 heterotrimeric complexes with membrane-bound myristoylated SnRK1β1 and β2. The atypical subunit SnRK1β3 lacks the conserved N-terminal and CBM domains, is not myristoylated (*240*), and should be absent in membrane-associated complexes (*276, 337*). However, it cannot be excluded the presence of SnRK1β2 and β1 in SnRK1 heterotrimeric nuclear complexes, since SnRK1β2 can co-localize with βγ in the nucleus (*276*), and deletion of the N-terminal myristoylation signal results in nuclear accumulation of SnRK1β1 complexes (*337*). Tissue and subcellular distribution of SnRK1α1 and SnRK1βγ were analyzed throughout development, using a BAC-recombineering strategy in Arabidopsis (*335*). SnRK1βγ had a predominant nuclear localization that overlapped with similar localization of SnRK1α1 in young organs, such as leaf primordia, and meristematic zones of roots and shoots. However, and unlike

SnRK1βγ, SnRK1α1 accumulation was observed in the cytoplasm and at the plasma membrane in most other tissues throughout development (*335*). SnRK1α1 was also reported to localize in chloroplasts and the βγ-subunit has a chloroplast transit peptide (*263*). Finally, it has to be considered that different cues might trigger re-localization of the kinase to yet other subcellular compartments.

1.6.5 | Adenylates, sugars and hormones

The SNF1/AMPK/SnRK1 kinases are regulated by universal signals like adenylates and sugars, whereas more specific hormonal cues have likely evolved to regulate these kinases at the whole organism-level. Adenylates are interconverted from ATP to ADP in energy consuming processes, or from ADP to ATP during catabolism. The adenylate kinase brings AMP to this dynamic equation through the bidirectional reaction 2ADP↔ATP + AMP, favored from left to right in metabolically stressed cells. In such case, the AMP:ATP ratio increases to a greater extent than ADP:ATP. Thus, adenylate ratios (AMP:ATP and ADP:ATP) act as fundamental signals of the energy charge of the cell (*422*). In mammals, increases in AMP/ATP ratio exert a tripartite regulation on AMPK kinase activation. AMP binding to CBS motifs in the γ-regulatory subunit promotes 1) AMPK allosteric activation and 2) phosphorylation by the upstream kinase LKB1, whereas AMP or ADP binding 3) prevents dephosphorylation by upstream phosphatases (*349, 373, 390, 391, 397, 423*). In yeast, ADP is involved in a bipartite regulation of SNF1 activation that is independent of the regulatory subunits, promoting phosphorylation by upstream kinases, but mostly protecting from dephosphorylation by upstream phosphatases (*424*). In plants, SnRK1 regulation by AMP was only associated with protection from dephosphorylation, in an assay with recombinant mammalian PP2C and purified

SnRK1 complex from spinach leaves (*246*). However, the mechanism underlying this regulation is still poorly understood in plants (*359*).

The regulation of SnRK1 signaling by various sugars and hormones, have been addressed in previous sections.

1.6.6 | Posttranslational modifications

Posttranslational modifications (PTMs) allow rapid and dynamic changes on the proteome that do not rely on translation, which besides consuming amino acids, is one of the most energy-demanding processes in the cell (*418, 425*). PTMs regulate the activity, stability and subcellular localization of SNF1/AMPK/SnRK1 kinases, and likely play an important role in the response to environmental and metabolic cues.

Whereas the essential role of T-loop phosphorylation on the catalytic subunit has been extensively characterized, several other PTMs including ubiquitylation, sumoylation, acetylation, myristoylation, and oxidation, have been implicated in the regulation of either catalytic and/or regulatory subunits within SNF1/AMPK/SnRK1 complexes (*359*).

1.6.6.1 | Phosphorylation

Phosphorylation of a conserved threonine (T) residue (Snf1^{T210}; AMPKα1^{T183}/AMPKα2^{T172}; SnRK1α1^{T175}/SnRK1α2^{T176}) in the catalytic subunit is essential for SNF1/AMPK/SnRK1 activity. A size fractionation analysis from Arabidopsis seedlings, revealed a distribution of SnRK1α1^{T175}/SnRK1α2^{T176} phosphorylation with a stronger signal intensity coupled with the main peak of SnRK1 activity, at approximately 100 kDa, suggesting that the phosphorylated catalytic subunit is incorporated into a heterotrimeric complex (*325*). In this study, the majority of SnRK1 activity was attributed to the SnRK1α1 isoform, as

previously observed in preparations from Arabidopsis cell suspension cultures (*284, 325*). In yeast and mammalian systems, differential phosphorylation is observed in high energy (kinase repressing) *versus* low energy (kinase activating) conditions. Yeast cells subjected to glucose deprivation become strongly phosphorylated on Snf1^{T210} rendering the complex active, whereas Snf1^{T210} phosphorylation is undetected in cells grown in abundant glucose (*363*). AMPK allosteric activation by AMP in energy deficit conditions is coupled with reversible phosphorylation of AMPKα^{T172} (*426*). However, unlike the yeast and mammalian counterparts, equal phosphorylation levels of SnRK1α1^{T175}/SnRK1α2^{T176} are detected in control and stress activating conditions in plants (*218, 263, 285, 290*). A finer level of regulation, with tissue or subcellular-specificity, might have been missed with analyses of total plant cell extracts, but additional phospho-residues as well as other mechanisms for controlling activity may also be involved in SnRK1 regulation.

Several of the upstream kinases of SNF1/AMPK/SnRK1 complexes show great homology, highlighting the conservation of these systems. The upstream kinases of SNF1 in yeast, Sak1, Elm1 and Tos3 have partially redundant functions, since growth on alternative carbon sources is only impaired in the triple *elm1Δ sak1Δ tos3Δ* mutant (*427*), but show stress-dependent preferences for particular β-subunit containing SNF1 complexes (*409*). The AMPK upstream kinase tumor suppressor liver kinase B1 (LKB1) was identified based on its sequence similarity with the yeast SNF1 activating kinases, and a CaMKK, CaMKKβ, was shown to phosphorylate AMPKα^{T172}, allowing the input of Ca^{2+} signals into the AMPK pathway (*428, 429*), independently of the adenine nucleotide ratios (*352, 353*). The transforming growth factor β-activated kinase 1 (TAK1) might also be an AMPK upstream kinase, particularly under conditions where reactive oxygen species and redox imbalance are generated (*430, 431*). All AMPK upstream kinases were shown to complement the yeast *elm1Δ sak1Δ tos3Δ* triple mutant (*432*). Sequence comparison, complementation and phosphorylation assays have similarly implicated SnRK1 activating kinase 1 and

2 (SnAK1/2; also called Geminivirus Rep-interacting kinase 2/1, GRIK2/1), as the upstream kinases of SnRK1 in plants (*248, 268, 364, 365*). Similarly to LKB1, SnAKs appear to be constitutively active, and are insensitive to Ca^{2+}, AMP and to the CaMKK-specific inhibitor STO-609, when assayed *in vitro* (*365*). SnAKs autophosphorylate on SnAK1^{T153}/SnAK2^{T154}, and this phosphorylation is required for their activity (*364, 433*). SnRK1 cross-phosphorylates and inactivates SnAK1^{S260}/SnAK2^{S261} *in vitro*, probably as part of a negative feedback loop to tightly control SnRK1 activation (*364*). This kinase cross-regulation may be conserved in the yeast system (*434*). However, along with the lack of *in planta* evidence for SnAKs functional relevance on SnRK1 signaling, SnAKs/GRIKs are only detected in geminivirus-infected mature leaves and in actively proliferating tissues that do not cover the range of detection of SnRK1 phosphorylation (*365*). Proteasomal degradation of SnAKs may justify the undetectably low levels of these proteins in several tissues, but the possible existence of other upstream kinases awaits further exploration (*268, 365*). Mammalian CaMKK can phosphorylate SnRK1 purified from spinach *in vitro* (*246*), and the CIPK15-SnRK1A-MYBS1 circuitry, required for rice seedlings to tolerate flooding (*309*), suggests that endogenous Ca^{2+}-dependent kinases like CIPKs or others may also serve as SnRK1 upstream kinases (*359*).

In the SNF1/AMPK/SnRK1 systems, reversal of T-loop phosphorylation by upstream phosphatases occurs in response to nutrient supply and in energy homeostasis conditions. When glucose is available, the yeast protein phosphatase 1 (PP1) Glc7-Reg1 is able to access and dephosphorylate Snf1^{T210} (*435*), and the PP2A-like phosphatase, Sit4, is also able to dephosphorylate Snf1^{T210} *in vivo* (*436*). PP2A and PP2C phosphatases were reported to dephosphorylate and inactivate mammalian AMPK and plant SnRK1 *in vitro* (*242, 246, 437*). Recently, clade A PP2Cs, ABI1 and PP2CA, were reported to interact and dephosphorylate Arabidopsis SnRK1α1 (*285*). ABI1 and PP2CA are negative regulators of the ABA pathway via their interaction with SnRK2 kinases, and are blocked by the ABA receptors upon ABA binding (*438*).

PP2Cs inactivate SnRK1 in response to sugars and conversely, repression of PP2Cs by the ABA receptors allows the activation of SnRK1 by this phytohormone (*285*). Other PPs were reported to interact with SnRK1α2 *in vitro* and in yeast two-hybrid assays, namely PP2C74 (*439*) and the dual-specificity protein tyrosine phosphatase PTPKIS1 (*440*), although the functional relevance of these interactions is still unknown. PTPKIS1 binds starch through a CBM domain (*441*) and was identified as the component responsible for starch overaccumulation in the *sex4* mutant (*442*), suggesting it may regulate the initial steps of starch degradation at the granule surface (*442, 443*).

In addition to phosphorylation of the conserved T-loop threonine residue, other phosphorylation events have been described in the regulation of SNF1/AMPK/SnRK1 kinases. AMPK phosphorylates and activates the autophagy-initiating kinase Ulk1 (*444*). The cross-phosphorylation of AMPK catalytic and regulatory subunits by Ulk1 and subsequent inactivation, can be part of a negative feedback loop to reset AMPK (*445*). Phosphorylation of AMPKα S485 (*446, 447*) and S173 (*448*) residues inhibits AMPK activity in response to insulin (mediated by Akt/PKB kinase) and to PKA-mediated cAMP signaling, respectively. These phosphorylation events seem to interfere with the phosphorylation of AMPKα^{T172}. Other phosphorylated residues were found in AMPKα- and β-subunits, but the relevance of those modifications is still unclear (*357, 449-451*). Interestingly, the cell death suppressor Adi3, triggered by pathogens in tomato, interacts with SnRK1α1 and phosphorylates the Gal83 β-subunit inhibiting the activity of the SnRK1 complex (*275*). The functional relevance of this mechanism should be determined in response to other types of environmental, metabolic and hormonal cues.

1.6.6.2 | Ubiquitylation

Signal termination in kinase-mediated pathways can be achieved through the ubiquitin-proteasome system (UPS)-mediated protein degradation, and its

impairment may lead to sustained kinase activity with deleterious outcomes. As previously mentioned, the activation of protein kinases can initiate their downregulation, and several mechanisms may signal the kinase activation status to the ubiquitylation machinery. Phosphorylation of active kinases, either through a *cis* or *trans* modification can create a binding site for E3 ligases or a phosphodegron recognized by phospho-dependent Skp1-cullin-F-box (SCF) ligases. Kinase activation may lead to conformational changes that allow the binding of E3 ligases, or expose degrons that were otherwise masked in the inactive state. Importantly, multiple E3 ligases often cooperate to terminate kinase signaling, depending on spatiotemporal and stimuli specificities (*402*). In agreement with this view, the inactive kinases SnRK1α1^{K48M} and T-loop phosphorylation mutant SnRK1α1^{T175A} accumulate to much higher levels than the WT SnRK1α1 protein in Arabidopsis (*218*), suggesting that stability of the SnRK1 protein kinase is connected with its activity and phosphorylation status.

Large proteomic studies to identify ubiquitylated proteins *in planta* detected ubiquitylation of SnRK1α1 (on K20 and K43 of the SnRK1α1.1 and SnRK1α1.2 splice variants, respectively) (*452*), SnRK1α2 and SnRK1βγ (*453*). The extent of ubiquitylation increased substantially upon MG132 treatment, indicating it may be an important signal for proteasomal breakdown of SnRK1 subunits (*453*). Accordingly, SnRK1α1 is targeted for proteasomal degradation in a myoinositol polyphosphate 5-phosphatase (5PTase13)-dependent manner under low nutrient conditions (*326*). SnRK1α1 degradation may also be mediated by the DDB1-CUL4-ROC1-PRL1 E3 ubiquitin ligase, in which PRL1 is the putative substrate receptor of the complex (*454*). SnRK1α1 interacts with PRL1 (*311, 368*) and its proteasomal degradation is slower in *prl1* and *cul4cs* extracts than in the WT, accumulating to a higher extent in these mutants (*454*). On the other hand, PRL1 was reported to compete with SKP1/ASK1 for binding SnRK1α1 and SnRK1α2. SKP1/ASK1 is a component of SCF E3 ubiquitin ligases and although SnRK1 participates in the assembly of a proteasomal complex with this E3 ligase, there is also the possibility that SnRK1 degradation

is mediated either by the SCF complex or the CUL4-DDB1 machinery upon varied conditions (*368, 454*).

During growth on alternative carbon sources, ubiquitylation of yeast Snf1 negatively modulates its stability through proteasome-mediated degradation, as well as phosphorylation and catalytic activity (*455*). The deubiquitylase Ubp8 is part of the histone modifier SAGA complex and was shown to counteract Snf1 ubiquitylation (*455*), whereas the SUMO-targeted ubiquitin ligase (STUbL) Slx5–Slx8 promoted UPS mediated degradation of sumoylated Snf1 (*171*).

The first detection of AMPK ubiquitylation allowed the identification of unusual ubiquitin-chain topologies (like the K29/K33-linked polyubiquitin chains) that might be associated with non-proteolytic outcomes (*456*). Ubiquitylation of AMPKβ with K63-linked chains promoted AMPKβ stability, possibly through its allocation into inclusion bodies and protection from proteolytic turnover. However the latter modification did not affect global AMPK activity (*457*). On the other hand, the cell death-inducing DFF45-like effector (Cidea) forms a complex *in vivo* with AMPK and modulates AMPK stability and activity promoting its ubiquitylation and proteasome-mediated degradation in brown adipose tissue (*458*). Cidea-null mice accumulate higher levels of AMPKα, β, and γ subunits with a consequent increment of AMPKα^{T172} phosphorylation and catalytic activity (*458*).

1.6.6.3 | Sumoylation

Regulation of AMPK and SNF1 by sumoylation was recently described and associated with various outcomes. In AMPK, both catalytic and β2 subunits were identified as SUMO targets (*37, 459*). MS analyses within a large proteomic study detected sumoylated AMPKα1 and AMPKα2 in response to proteasome inhibition, suggesting sumoylation may be implicated in proteasomal degradation of AMPKα subunits. A single lysine residue was modified in AMPKα1 and AMPKα2. In the case of AMPKα1, sumoylated forms

were also retrieved after SUMO protease inhibition and heat shock treatments, and to a lesser extent in control conditions (*37*). In contrast, in another study, sumoylation of AMPKβ2 enhanced AMPK activity by increasing T-loop phosphorylation. It was suggested that sumoylation and ubiquitylation might be antagonistic processes in AMPKβ2 (*459*). On the other hand, Snf1 sumoylation downregulates SNF1, independently of T-loop phosphorylation. In response to glucose, Snf1 is sumoylated at a single lysine residue, and a conformational switch induced by the interaction between the sumoylated residue and a SUMO-interacting motif (SIM), leads to a rapid inhibition of the kinase. In a long-term response, sumoylated Snf1 is ubiquitylated *via* the SUMO-targeted ubiquitin ligase Slx5–Slx8, and targeted for degradation, with the consequent decrease in Snf1 levels in response to glucose sensing (*171*).

Arabidopsis SnRK1α1 interacted with the E2 SUMO conjugating enzyme (SCE1) and with the SUMO protease ESD4 in a yeast two-hybrid screen (*67*). Furthermore, in the same study, SnRK1α1 was found to be sumoylated with both SUMO1 and SUMO3 isoforms in a high-throughput assay in *Escherichia coli*. The fact that SnRK1α1 has high probability SUMO attachment sites (*67*) and that sumoylation has been implicated in the plant abiotic stress response (*460*) suggests that sumoylation may be a conserved mechanism for controlling SNF1/AMPK/SnRK1 activity and stability (*359*).

1.6.6.4 | Acetylation

Modification by acetylation has been described for SNF1 and AMPK. The β-regulatory subunit of SNF1, Sip2, is a substrate of the nucleosome acetyltransferase of H4 complex (NuA4) and was found acetylated *in vitro* and *in vivo* (*461*). Sip2 acetylation stabilizes an inhibitory interaction with the Snf1 catalytic subunit and seems to promote longevity, since Sip2 acetylation mimetics live longer (*462*). AMPKα1 is acetylated *in vitro* by the p300 acetyltransferase (*463, 464*) and AMPKγ1 was also found acetylated in its N-

terminus (*449*). However, the functional relevance of these modifications awaits further clarification. Even though none of SnRK1 subunits was found acetylated until now, the studies in mammals and yeast suggest all three subunits could be subjected to this modification (*359*).

1.6.6.5 | Myristoylation

Myristoylation is the irreversible co-translational conjugation of myristate to proteins, and depends on an N-terminal consensus motif MGxxxS/T, where myristate becomes attached to Glycine2 *via* an amide bond (*337, 465*). Myristoylation of AMPK, SNF1, and SnRK1 modulates their activity and subcellular localization. Both AMPKβ1 and β2 regulatory subunits are myristoylated *in vivo* (*391, 449*). It was proposed that when ATP levels are high, the myristoyl-group binds a hydrophobic region within the AMPK complex, keeping it in an inactive state. In AMPK activating conditions, AMP binding triggers a conformational change and exposes the myristoyl group to the solvent allowing kinase activation and membrane association if required. This model evidences the requirement of myristoylation for the allosteric activation of AMPK by AMP (*390-392*).

Sip1 and Sip2 β-regulatory subunits of SNF1 are also myristoylated. Myristoylation of Sip2 is fundamental for the normal cellular life span of *S. cerevisae* (*466*) and for the proliferative potential during stationary phase (*467*). In young cells, myristoylated Sip2 is located at the plasma membrane and sequesters Snf4, the activating γ-subunit of the SNF1 complex. With aging, Sip2 re-localizes from the plasma membrane to the cytoplasm allowing Snf4/Snf1 entry into the nucleus where the Snf1 catalytic subunit modifies chromatin structure (*466*). Myristoylation of Sip1 regulates its subcellular localization in response to the carbon status of the cell. In glucose grown cells, Sip1 localizes to the cytosol and in response to carbon stress re-localizes to the vacuolar membrane, accompanied by Snf1 (*389*).

Myristoylation of SnRK1 was found to be a critical event for shoot apical meristem differentiation and plant development. In an *nmt1-1* mutant SnRK1 kinase activity and SnRK1β1 transcript levels were five-fold and two-fold higher, respectively, than in wild type plants. In the same study, GFP fusions of either SnRK1β1 or SnRK1β2 localized to the plasma membrane, whereas a G2A substitution preventing myristoylation of the β-subunits re-localized SnRK1β1 to the nucleus and SnRK1β2 to the cytoplasm, mimicking what happens in the *nmt1-1* line. It was hence suggested that myristoylation of β1 or β2 subunits sequesters the complex to the plasma membrane, acting as a negative regulator of the SnRK1 pathway, in accordance with the glucose hypersensitivity of the *nmt1-1* mutant (*337, 468*).

1.6.6.6 | Oxidation

AMPK is regulated by the intracellular redox status through two key cysteine residues in the catalytic subunit. Oxidation leads to the formation of AMPK aggregates through intermolecular disulfide bonds and compromises the interaction with the upstream kinase LKB1, blocking AMPK phosphorylation and activation. On the other hand, thioredoxin 1 reduces these cysteine residues and promotes AMPK activation during energy starvation (*469*). Sequence alignment reveals that these two residues are the only cysteines completely conserved in the respective kinases in yeast, mammals and plants, opening the possibility of a conserved regulation of SNF1/AMPK/SnRK1 by oxidation.

Acknowledgements

I am very grateful to my supervisor, Elena Baena-González, for insights and great support regarding the writing of this Chapter. I thank Pierre Crozet and Nuno Margalha for help with the figures.

References

1. D. C. Schwartz, M. Hochstrasser, in *Trends in Biochemical Sciences*. (2003), vol. 28, pp. 321-328.
2. M. J. Sanders, P. O. Grondin, B. D. Hegarty, M. A. Snowden, D. Carling, *Biochem J.* (2007), vol. 403, pp. 139-148.
3. R. D. Vierstra, in *Plant Physiol*. (2012), vol. 160, pp. 2-14.
4. R. S. Marshall, F. Li, D. C. Gemperline, A. J. Book, R. D. Vierstra, in *Mol Cell*. (2015).
5. M. Hochstrasser, in *Nature cell biology*. (2000), vol. 2, pp. E153-157.
6. E. S. Johnson, in *Annu Rev Biochem*. (2004), vol. 73, pp. 355-382.
7. T. Colby, A. Matthäi, A. Boeckelmann, H.-P. Stuible, in *Plant Physiol*. (2006), vol. 142, pp. 318-332.
8. M. Hochstrasser, in *Nature*. (2009), vol. 458, pp. 422-429.
9. M. J. Matunis, E. Coutavas, G. Blobel, in *J Cell Biol*. (1996), vol. 135, pp. 1457-1470.
10. R. Mahajan, C. Delphin, T. Guan, L. Gerace, F. Melchior, in *Cell*. (1997), vol. 88, pp. 97-107.
11. S. Vijay-Kumar, C. E. Bugg, K. D. Wilkinson, R. D. Vierstra, P. M. Hatfield, W. J. Cook, in *J Biol Chem*. (1987), vol. 262, pp. 6396-6399.
12. P. Bayer, A. Arndt, S. Metzger, R. Mahajan, F. Melchior, R. Jaenicke, J. Becker, in *J Mol Biol*. (1998), vol. 280, pp. 275-286.
13. W.-C. Huang, T.-P. Ko, S. S.-L. Li, A. H.-J. Wang, in *Eur J Biochem*. (2004), vol. 271, pp. 4114-4122.
14. R. Geiss-Friedlander, F. Melchior, in *Nat Rev Mol Cell Biol*. (2007), vol. 8, pp. 947-956.
15. V. Hietakangas, J. K. Ahlskog, A. M. Jakobsson, M. Hellesuo, N. M. Sahlberg, C. I. Holmberg, A. Mikhailov, J. J. Palvimo, L. Pirkkala, L. Sistonen, in *Mol Cell Biol*. (2003), vol. 23, pp. 2953-2968.
16. J. Perdomo, A. Verger, J. Turner, M. Crossley, in *Mol Cell Biol*. (2005), vol. 25, pp. 1549-1559.
17. Y.-H. R. Hsu, K. P. Sarker, I. Pot, A. Chan, S. J. Netherton, S. Bonni, in *J Biol Chem*. (2006), vol. 281, pp. 33008-33018.
18. J. X. Du, A. B. Bialkowska, B. B. McConnell, V. W. Yang, in *J Biol Chem*. (2008), vol. 283, pp. 31991-32002.
19. S. Creton, S. Jentsch, in *CELL*. (2010), vol. 143, pp. 848-848.e841.
20. K. A. Wilkinson, J. M. Henley, in *Biochem. J.* (2010), vol. 428, pp. 133-145.
21. H. A. Van Den Burg, R. K. Kini, R. C. Schuurink, F. L. W. Takken, in *The Plant Cell*. (2010), vol. 22, pp. 1998-2016.
22. H. D. Ulrich, in *Methods Mol Biol*. (2009), vol. 497, pp. 3-16.
23. J. Kurepa, J. M. Walker, J. Smalle, M. M. Gosink, S. J. Davis, T. L. Durham, D.-Y. Sung, R. D. Vierstra, in *J Biol Chem*. (2003), vol. 278, pp. 6862-6872.
24. M. Novatchkova, R. Budhiraja, G. Coupland, F. Eisenhaber, A. Bachmair, in *Planta*. (2004), vol. 220, pp. 1-8.
25. R. Budhiraja, R. Hermkes, S. Müller, J. Schmidt, T. Colby, K. Panigrahi, G. Coupland, A. Bachmair, in *PLANT PHYSIOLOGY*. (2009), vol. 149, pp. 1529-1540.

26. K. Miura, P. M. Hasegawa, in *Trends in Cell Biology*. (2010), vol. 20, pp. 223-232.
27. S. A. Saracco, M. J. Miller, J. Kurepa, R. D. Vierstra, in *PLANT PHYSIOLOGY*. (2007), vol. 145, pp. 119-134.
28. F. Z. Watts, in *Chromosoma*. (2013).
29. R. Chosed, S. Mukherjee, L. M. Lois, K. Orth, in *Biochem J*. (2006), vol. 398, pp. 521-529.
30. M. J. Miller, G. A. Barrett-Wilt, Z. Hua, R. D. Vierstra, in *Proc Natl Acad Sci USA*. (2010), vol. 107, pp. 16512-16517.
31. K. Tomanov, A. Zeschmann, R. Hermkes, K. Eifler, I. Ziba, M. Grieco, M. Novatchkova, K. Hofmann, H. Hesse, A. Bachmair, in *Plant Cell*. (2014), vol. 26, pp. 4547-4560.
32. M. Novatchkova, K. Tomanov, K. Hofmann, H.-P. Stuible, A. Bachmair, in *New Phytol*. (2012), vol. 195, pp. 23-31.
33. K. Uzunova, K. Göttsche, M. Miteva, S. R. Weisshaar, C. Glanemann, M. Schnellhardt, M. Niessen, H. Scheel, K. Hofmann, E. S. Johnson, G. J. K. Praefcke, R. J. Dohmen, in *J Biol Chem*. (2007), vol. 282, pp. 34167-34175.
34. M. H. Tatham, M.-C. Geoffroy, L. Shen, A. Plechanovova, N. Hattersley, E. G. Jaffray, J. J. Palvimo, R. T. Hay, in *Nature cell biology*. (2008), vol. 10, pp. 538-546.
35. Y. Mao, S. D. Desai, L. F. Liu, in *J Biol Chem*. (2000), vol. 275, pp. 26066-26073.
36. H. Saitoh, J. Hinchey, in *J Biol Chem*. (2000), vol. 275, pp. 6252-6258.
37. I. A. Hendriks, R. C. J. D'souza, B. Yang, M. Verlaan-de Vries, M. Mann, A. C. O. Vertegaal, in *Nat Struct Mol Biol*. (2014).
38. K. M. Comerford, M. O. Leonard, J. Karhausen, R. Carey, S. P. Colgan, C. T. Taylor, in *Proc Natl Acad Sci USA*. (2003), vol. 100, pp. 986-991.
39. R. Shao, F.-P. Zhang, F. Tian, P. Anders Friberg, X. Wang, H. Sjöland, H. Billig, in *FEBS Lett*. (2004), vol. 569, pp. 293-300.
40. J.-S. Lee, S. S. Thorgeirsson, in *Gastroenterology*. (2004), vol. 127, pp. S51-55.
41. M. H. Tatham, I. Matic, M. Mann, R. T. Hay, in *Science Signaling*. (2011), vol. 4, pp. rs4.
42. M. H. Tatham, A. Plechanovová, E. G. Jaffray, H. Salmen, R. T. Hay, in *Biochem J*. (2013), vol. 453, pp. 137-145.
43. I. Matic, B. Macek, M. Hilger, T. C. Walther, M. Mann, in *J Proteome Res*. (2008), vol. 7, pp. 4050-4057.
44. A. Skilton, J. C. Y. Ho, B. Mercer, E. Outwin, F. Z. Watts, in *PLoS ONE*. (2009), vol. 4, pp. e6750.
45. Y.-L. Hsieh, H.-Y. Kuo, C.-C. Chang, M. T. Naik, P.-H. Liao, C.-C. Ho, T.-C. Huang, J.-C. Jeng, P.-H. Hsu, M.-D. Tsai, T.-H. Huang, H.-M. Shih, in *The EMBO Journal*. (2013), vol. 32, pp. 791-804.
46. R. Ullmann, C. D. Chien, M. L. Avantaggiati, S. Muller, in *Molecular Cell*. (2012), vol. 46, pp. 759-770.
47. S. Jentsch, I. Psakhye, in *Annu. Rev. Genet.* (2013).
48. R. Hermkes, Y.-F. Fu, K. Nürrenberg, R. Budhiraja, E. Schmelzer, N. Elrouby, R. J. Dohmen, A. Bachmair, G. Coupland, in *Planta*. (2011), vol. 233, pp. 63-73.
49. J. R. Gareau, C. D. Lima, in *Nat Rev Mol Cell Biol*. (2010), vol. 11, pp. 861-871.
50. O. Kerscher, R. Felberbaum, M. Hochstrasser, in *Annu. Rev. Cell Dev. Biol.* (2006), vol. 22, pp. 159-180.

51. O. V. Kovalenko, A. W. Plug, T. Haaf, D. K. Gonda, T. Ashley, D. C. Ward, C. M. Radding, E. I. Golub, in *Proc Natl Acad Sci USA*. (1996), vol. 93, pp. 2958-2963.
52. Y. Azuma, S. H. Tan, M. M. Cavenagh, A. M. Ainsztein, H. Saitoh, M. Dasso, in *FASEB J*. (2001), vol. 15, pp. 1825-1827.
53. C. Donaghue, H. Bates, S. Cotterill, in *Biochim Biophys Acta*. (2001), vol. 1518, pp. 210-214.
54. J. Becker, S. V. Barysch, S. Karaca, C. Dittner, H.-H. Hsiao, M. Berriel Diaz, S. Herzig, H. Urlaub, F. Melchior, in *Nat Struct Mol Biol*. (2013), vol. 20, pp. 525-531.
55. R. Bruderer, M. H. Tatham, A. Plechanovova, I. Matic, A. K. Garg, R. T. Hay, in *EMBO reports*. (2011), vol. 12, pp. 142-148.
56. K. Truong, T. D. Lee, Y. Chen, in *J Biol Chem*. (2012), vol. 287, pp. 15154-15163.
57. K. Truong, T. D. Lee, B. Li, Y. Chen, in *Journal of Biological Chemistry*. (2012), vol. 287, pp. 42611-42619.
58. S. Chiocca, in *Biochem Soc Trans*. (2007), vol. 35, pp. 1419-1421.
59. G. Bossis, F. Melchior, in *Mol Cell*. (2006), vol. 21, pp. 349-357.
60. V. Bernier-Villamor, D. A. Sampson, M. J. Matunis, C. D. Lima, in *CELL*. (2002), vol. 108, pp. 345-356.
61. M. H. Tatham, Y. Chen, R. T. Hay, in *Biochemistry*. (2003), vol. 42, pp. 3168-3179.
62. K. P. Bencsath, M. S. Podgorski, V. R. Pagala, C. A. Slaughter, B. A. Schulman, in *J Biol Chem*. (2002), vol. 277, pp. 47938-47945.
63. X.-J. Yang, C.-M. Chiang, in *F1000Prime Rep*. (2013), vol. 5, pp. 45.
64. S.-H. Yang, A. Galanis, J. Witty, A. D. Sharrocks, in *EMBO J*. (2006), vol. 25, pp. 5083-5093.
65. F. Mohideen, A. D. Capili, P. M. Bilimoria, T. Yamada, A. Bonni, C. D. Lima, in *Nat Struct Mol Biol*. (2009), vol. 16, pp. 945-952.
66. I. Matic, J. Schimmel, I. A. Hendriks, M. A. van Santen, F. van de Rijke, H. van Dam, F. Gnad, M. Mann, A. C. O. Vertegaal, in *Mol Cell*. (2010), vol. 39, pp. 641-652.
67. N. Elrouby, G. Coupland, in *Proc Natl Acad Sci USA*. (2010), vol. 107, pp. 17415-17420.
68. J. L. Epps, S. Tanda, in *Curr Biol*. (1998), vol. 8, pp. 1277-1280.
69. S. Apionishev, D. Malhotra, S. Raghavachari, S. Tanda, R. S. Rasooly, in *Genes Cells*. (2001), vol. 6, pp. 215-224.
70. D. Jones, E. Crowe, T. A. Stevens, E. P. M. Candido, in *Genome Biol*. (2002), vol. 3, pp. RESEARCH0002.
71. K. Tanaka, J. Nishide, K. Okazaki, H. Kato, O. Niwa, T. Nakagawa, H. Matsuda, M. Kawamukai, Y. Murakami, in *Mol Cell Biol*. (1999), vol. 19, pp. 8660-8672.
72. F. al-Khodairy, T. Enoch, I. M. Hagan, A. M. Carr, in *J Cell Sci*. (1995), vol. 108 (Pt 2), pp. 475-486.
73. W. Seufert, B. Futcher, S. Jentsch, in *Nature*. (1995), vol. 373, pp. 78-81.
74. M. Shayeghi, C. L. Doe, M. Tavassoli, F. Z. Watts, in *Nucleic Acids Research*. (1997), vol. 25, pp. 1162-1169.
75. N. Nigam, A. Singh, C. Sahi, A. Chandramouli, A. Grover, in *Mol Genet Genomics*. (2008), vol. 279, pp. 371-383.

76. P. Knipscheer, A. Flotho, H. Klug, J. V. Olsen, W. J. van Dijk, A. Fish, E. S. Johnson, M. Mann, T. K. Sixma, A. Pichler, in *Molecular Cell*. (2008), vol. 31, pp. 371-382.
77. H. Klug, M. Xaver, V. K. Chaugule, S. Koidl, G. Mittler, F. Klein, A. Pichler, in *Molecular Cell*. (2013), vol. 50, pp. 625-636.
78. R. Boggio, R. Colombo, R. T. Hay, G. F. Draetta, S. Chiocca, in *Mol Cell*. (2004), vol. 16, pp. 549-561.
79. P. R. Heaton, A. F. Deyrieux, X.-L. Bian, V. G. Wilson, in *Virus Research*. (2011), vol. 158, pp. 199-208.
80. M. Hochstrasser, in *CELL*. (2001), vol. 107, pp. 5-8.
81. X. Duan, P. Sarangi, X. Liu, G. K. Rangi, X. Zhao, H. Ye, in *Mol Cell*. (2009), vol. 35, pp. 657-668.
82. T. Ishida, M. Yoshimura, K. Miura, K. Sugimoto, in *PLoS ONE*. (2012), vol. 7, pp. e46897.
83. R. T. Hay, in *Molecular Cell*. (2005), vol. 18, pp. 1-12.
84. E. S. Johnson, A. A. Gupta, in *CELL*. (2001), vol. 106, pp. 735-744.
85. T. Kahyo, T. Nishida, H. Yasuda, in *Mol Cell*. (2001), vol. 8, pp. 713-718.
86. A. D. Sharrocks, in *Genes & Development*. (2006), vol. 20, pp. 754-758.
87. K. Miura, J. B. Jin, P. M. Hasegawa, in *Curr Opin Plant Biol*. (2007), vol. 10, pp. 495-502.
88. Y. Takahashi, Y. Kikuchi, in *J Biol Chem*. (2005), vol. 280, pp. 35822-35828.
89. L. Aravind, E. V. Koonin, in *Trends Biochem Sci*. (2000), vol. 25, pp. 112-114.
90. D. A. Bochar, J. Savard, W. Wang, D. W. Lafleur, P. Moore, J. Côté, R. Shiekhattar, in *Proc Natl Acad Sci USA*. (2000), vol. 97, pp. 1038-1043.
91. M. Bienz, in *Trends Biochem Sci*. (2006), vol. 31, pp. 35-40.
92. A. Pichler, A. Gast, J. S. Seeler, A. Dejean, F. Melchior, in *Cell*. (2002), vol. 108, pp. 109-120.
93. M. H. Kagey, T. A. Melhuish, D. Wotton, in *Cell*. (2003), vol. 113, pp. 127-137.
94. K. Miura, A. Rus, A. Sharkhuu, S. Yokoi, A. S. Karthikeyan, K. G. Raghothama, D. Baek, Y. D. Koo, J. B. Jin, R. A. Bressan, D.-J. Yun, P. M. Hasegawa, in *Proc Natl Acad Sci USA*. (2005), vol. 102, pp. 7760-7765.
95. T. Ishida, S. Fujiwara, K. Miura, N. Stacey, M. Yoshimura, K. Schneider, S. Adachi, K. Minamisawa, M. Umeda, K. Sugimoto, in *Plant Cell*. (2009), vol. 21, pp. 2284-2297.
96. L. Huang, S. Yang, S. Zhang, M. Liu, J. Lai, Y. Qi, S. Shi, J. Wang, Y. Wang, Q. Xie, C. Yang, in *Plant J*. (2009), vol. 60, pp. 666-678.
97. H. C. Park, H. Kim, S. C. Koo, H. J. Park, M. S. Cheong, H. Hong, D. Baek, W. S. Chung, D. H. Kim, R. A. Bressan, S. Y. Lee, H. J. Bohnert, D.-J. Yun, in *Plant, Cell & Environment*. (2010), vol. 33, pp. 1923-1934.
98. S. Thangasamy, C.-L. Guo, M.-H. Chuang, M.-H. Lai, J. Chen, G.-Y. Jauh, in *New Phytol*. (2011), vol. 189, pp. 869-882.
99. Y. Ling, C. Zhang, T. Chen, H. Hao, P. Liu, R. A. Bressan, P. M. Hasegawa, J. B. Jin, J. Lin, in *PLoS ONE*. (2012), vol. 7, pp. e29470.
100. J.-S. Seeler, A. Dejean, in *Nature Reviews Molecular Cell Biology*. (2003), vol. 4, pp. 690-699.
101. R. Catala, J. Ouyang, I. A. Abreu, Y. Hu, H. Seo, X. Zhang, N.-H. Chua, in *Plant Cell*. (2007), vol. 19, pp. 2952-2966.
102. J. Lee, K. Miura, R. A. Bressan, P. M. Hasegawa, D.-J. Yun, in *Plant Signal Behav*. (2007), vol. 2, pp. 253-254.

103. J. Lee, J. Nam, H. C. Park, G. Na, K. Miura, J. B. Jin, C. Y. Yoo, D. Baek, D. H. Kim, J. C. Jeong, D. Kim, S. Y. Lee, D. E. Salt, T. Mengiste, Q. Gong, S. Ma, H. J. Bohnert, S.-S. Kwak, R. A. Bressan, P. M. Hasegawa, D.-J. Yun, in *Plant J*. (2007), vol. 49, pp. 79-90.
104. K. Miura, J. Lee, T. Miura, P. M. Hasegawa, in *Plant Cell Physiol*. (2010), vol. 51, pp. 103-113.
105. J. B. Jin, P. M. Hasegawa, in *Plant Signal Behav*. (2008), vol. 3, pp. 891-892.
106. J. B. Jin, Y. H. Jin, J. Lee, K. Miura, C. Y. Yoo, W.-Y. Kim, M. Van Oosten, Y. Hyun, D. E. Somers, I. Lee, D.-J. Yun, R. A. Bressan, P. M. Hasegawa, in *Plant J*. (2008), vol. 53, pp. 530-540.
107. K. Miura, P. M. Hasegawa, in *Plant Signal Behav*. (2009), vol. 4, pp. 1176-1178.
108. K. Miura, J. Lee, J. B. Jin, C. Y. Yoo, T. Miura, P. M. Hasegawa, in *Proc Natl Acad Sci USA*. (2009), vol. 106, pp. 5418-5423.
109. Y. Zheng, K. S. Schumaker, Y. Guo, in *Proc Natl Acad Sci USA*. (2012), vol. 109, pp. 12822-12827.
110. K. Miura, J. Lee, Q. Gong, S. Ma, J. B. Jin, C. Y. Yoo, T. Miura, A. Sato, H. J. Bohnert, P. M. Hasegawa, in *PLANT PHYSIOLOGY*. (2011), vol. 155, pp. 1000-1012.
111. C.-C. Chen, Y.-Y. Chen, I.-C. Tang, H.-M. Liang, C.-C. Lai, J.-M. Chiou, K.-C. Yeh, in *PLANT PHYSIOLOGY*. (2011), vol. 156, pp. 2225-2234.
112. K. Miura, A. Sato, M. Ohta, J. Furukawa, in *Planta*. (2011), vol. 234, pp. 1191-1199.
113. B. S. Park, J. T. Song, H. S. Seo, in *Nature Communications*. (2011), vol. 2, pp. 400.
114. B. S. Park, S.-I. Kim, J. T. Song, H. S. Seo, in *BMB Rep*. (2012), vol. 45, pp. 342-347.
115. C. Y. Yoo, K. Miura, J. B. Jin, J. Lee, H. C. Park, D. E. Salt, D.-J. Yun, R. A. Bressan, P. M. Hasegawa, in *PLANT PHYSIOLOGY*. (2006), vol. 142, pp. 1548-1558.
116. K. Miura, P. M. Hasegawa, in *Plant Signal Behav*. (2008), vol. 3, pp. 52-53.
117. K. Miura, J. B. Jin, J. Lee, C. Y. Yoo, V. Stirm, T. Miura, E. N. Ashworth, R. A. Bressan, D.-J. Yun, P. M. Hasegawa, in *Plant Cell*. (2007), vol. 19, pp. 1403-1414.
118. K. Miura, M. Ohta, in *J Plant Physiol*. (2010), vol. 167, pp. 555-560.
119. K. Miura, H. Okamoto, E. Okuma, H. Shiba, H. Kamada, P. M. Hasegawa, Y. Murata, in *Plant J*. (2012).
120. M. S. Cheong, H. C. Park, M. J. Hong, J. Lee, W. Choi, J. B. Jin, H. J. Bohnert, S. Y. Lee, R. A. Bressan, D.-J. Yun, in *PLANT PHYSIOLOGY*. (2009), vol. 151, pp. 1930-1942.
121. W. R. Engelsberger, W. X. Schulze, in *Plant J*. (2012), vol. 69, pp. 978-995.
122. H. Nakagami, N. Sugiyama, K. Mochida, A. Daudi, Y. Yoshida, T. Toyoda, M. Tomita, Y. Ishihama, K. Shirasu, in *PLANT PHYSIOLOGY*. (2010), vol. 153, pp. 1161-1174.
123. T. Umezawa, N. Sugiyama, F. Takahashi, J. C. Anderson, Y. Ishihama, S. C. Peck, K. Shinozaki, in *Science Signaling*. (2013), vol. 6, pp. rs8.
124. P. Wang, L. Xue, G. Batelli, S. Lee, Y.-J. Hou, M. J. Van Oosten, H. Zhang, W. A. Tao, J.-K. Zhu, in *Proceedings of the National Academy of Sciences*. (2013), vol. 110, pp. 11205-11210.

125. Q. Yao, C. Bollinger, J. Gao, D. Xu, J. J. Thelen, in *Front. Plant Sci.* (2012), vol. 3, pp. 206.
126. A. Roscic, A. Möller, M. A. Calzado, F. Renner, V. C. Wimmer, E. Gresko, K. S. Lüdi, M. L. Schmitz, in *Molecular Cell*. (2006), vol. 24, pp. 77-89.
127. B. Liu, Y. Yang, V. Chernishof, R. R. O. Loo, H. Jang, S. Tahk, R. Yang, S. Mink, D. Shultz, C. J. Bellone, J. A. Loo, K. Shuai, in *CELL*. (2007), vol. 129, pp. 903-914.
128. H. Saitoh, D. B. Sparrow, T. Shiomi, R. T. Pu, T. Nishimoto, T. J. Mohun, M. Dasso, in *Curr Biol*. (1998), vol. 8, pp. 121-124.
129. Y. Takahashi, A. Toh-E, Y. Kikuchi, in *Journal of Biochemistry*. (2003), vol. 133, pp. 415-422.
130. A. Depaux, F. Regnier-Ricard, A. Germani, N. Varin-Blank, in *Oncogene*. (2007), vol. 26, pp. 6665-6676.
131. A. Albor, S. El-Hizawi, E. J. Horn, M. Laederich, P. Frosk, K. Wrogemann, M. Kulesz-Martin, in *J Biol Chem*. (2006), vol. 281, pp. 25850-25866.
132. J. W. Um, D. S. Min, H. Rhim, J. Kim, S. R. Paik, K. C. Chung, in *J Biol Chem*. (2006), vol. 281, pp. 3595-3603.
133. J. W. Westerbeck, N. Pasupala, M. Guillotte, E. Szymanski, B. C. Matson, C. Esteban, O. Kerscher, in *Molecular Biology of the Cell*. (2014), vol. 25, pp. 1-16.
134. P. R. Potts, H. Yu, in *Mol Cell Biol*. (2005), vol. 25, pp. 7021-7032.
135. M. Miteva, K. Keusekotten, K. Hofmann, G. J. K. Praefcke, R. J. Dohmen, in *Subcell Biochem*. (2010), vol. 54, pp. 195-214.
136. C. M. Hickey, N. R. Wilson, M. Hochstrasser, in *Nat Rev Mol Cell Biol*. (2012), vol. 13, pp. 755-766.
137. L. Conti, G. Price, E. O'Donnell, B. Schwessinger, P. Dominy, A. Sadanandom, in *Plant Cell*. (2008), vol. 20, pp. 2894-2908.
138. S.-J. Li, M. Hochstrasser, in *The Journal of Cell Biology*. (2003), vol. 160, pp. 1069-1081.
139. M. H. Lee, A. M. Mabb, G. B. Gill, E. T. H. Yeh, S. Miyamoto, in *Molecular Cell*. (2011), vol. 43, pp. 180-191.
140. N. Kolli, J. Mikolajczyk, M. Drag, D. Mukhopadhyay, N. Moffatt, M. Dasso, G. Salvesen, K. D. Wilkinson, in *Biochem J*. (2010), vol. 430, pp. 335-344.
141. P. H. Reeves, G. Murtas, S. Dash, G. Coupland, in *Development*. (2002), vol. 129, pp. 5349-5361.
142. G. Murtas, P. H. Reeves, Y.-F. Fu, I. Bancroft, C. Dean, G. Coupland, in *Plant Cell*. (2003), vol. 15, pp. 2308-2319.
143. X. M. Xu, A. Rose, S. Muthuswamy, S. Y. Jeong, S. Venkatakrishnan, Q. Zhao, I. Meier, in *Plant Cell*. (2007), vol. 19, pp. 1537-1548.
144. J. Eckhoff, R. J. Dohmen, in *J Biol Chem*. (2015).
145. J.-G. Kim, K. W. Taylor, A. Hotson, M. Keegan, E. A. Schmelz, M. B. Mudgett, in *Plant Cell*. (2008), vol. 20, pp. 1915-1929.
146. A. Hotson, R. Chosed, H. Shu, K. Orth, M. B. Mudgett, in *Molecular Microbiology*. (2003), vol. 50, pp. 377-389.
147. Y. Xu, Y. Zuo, H. Zhang, X. Kang, F. Yue, Z. Yi, M. Liu, E. T. H. Yeh, G. Chen, J. Cheng, in *J Biol Chem*. (2010), vol. 285, pp. 36682-36688.
148. T. Nishida, F. Kaneko, M. Kitagawa, H. Yasuda, in *J Biol Chem*. (2001), vol. 276, pp. 39060-39066.
149. M. L. Baldwin, J. A. Julius, X. Tang, Y. Wang, J. Bachant, in *Cell Cycle*. (2009), vol. 8, pp. 3406-3419.

150. C. Huang, Y. Han, Y. Wang, X. Sun, S. Yan, E. T. H. Yeh, Y. Chen, H. Cang, H. Li, G. Shi, J. Cheng, X. Tang, J. Yi, in *EMBO J*. (2009), vol. 28, pp. 2748-2762.
151. Z. Xu, L. S. M. Lam, L. H. Lam, S. F. Chau, T. B. Ng, S. W. N. Au, in *FASEB J*. (2008), vol. 22, pp. 127-137.
152. M. P. Pinto, A. F. Carvalho, C. P. Grou, J. E. Rodríguez-Borges, C. Sá-Miranda, J. E. Azevedo, in *Biochim Biophys Acta*. (2012), vol. 1823, pp. 1958-1966.
153. J. R. Mullen, M. Das, S. J. Brill, in *Genetics*. (2011), vol. 187, pp. 73-87.
154. D. Mukhopadhyay, A. Arnaoutov, M. Dasso, in *The Journal of Cell Biology*. (2010), vol. 188, pp. 681-692.
155. J. R. Mullen, C.-F. Chen, S. J. Brill, in *Molecular and Cellular Biology*. (2010), vol. 30, pp. 3737-3748.
156. D. Reverter, C. D. Lima, in *Nature*. (2005), vol. 435, pp. 687-692.
157. J. Song, Z. Zhang, W. Hu, Y. Chen, in *J Biol Chem*. (2005), vol. 280, pp. 40122-40129.
158. C.-M. Hecker, M. Rabiller, K. Haglund, P. Bayer, I. Dikic, in *J Biol Chem*. (2006), vol. 281, pp. 16117-16127.
159. B. T. Seet, I. Dikic, M.-M. Zhou, T. Pawson, in *Nat Rev Mol Cell Biol*. (2006), vol. 7, pp. 473-483.
160. J. W. Harper, B. A. Schulman, in *CELL*. (2006), vol. 124, pp. 1133-1136.
161. A. S. Fatimababy, Y.-L. Lin, R. Usharani, R. Radjacommare, H.-T. Wang, H.-L. Tsai, Y. Lee, H. Fu, in *FEBS J*. (2010), vol. 277, pp. 796-816.
162. G. J. K. Praefcke, K. Hofmann, R. J. Dohmen, in *Trends in Biochemical Sciences*. (2012), vol. 37, pp. 23-31.
163. B. Vogt, K. Hofmann, in *Methods Mol Biol*. (2012), vol. 832, pp. 249-261.
164. P. Stehmeier, S. Muller, in *Mol Cell*. (2009), vol. 33, pp. 400-409.
165. D. Baba, N. Maita, J.-G. Jee, Y. Uchimura, H. Saitoh, K. Sugasawa, F. Hanaoka, H. Tochio, H. Hiroaki, M. Shirakawa, in *Nature*. (2005), vol. 435, pp. 979-982.
166. H. Sun, T. Hunter, in *J Biol Chem*. (2012), vol. 287, pp. 42071-42083.
167. N. Elrouby, M. V. Bonequi, A. Porri, G. Coupland, in *Proc Natl Acad Sci USA*. (2013).
168. I. Psakhye, S. Jentsch, in *CELL*. (2012), vol. 151, pp. 807-820.
169. J. M. Desterro, M. S. Rodriguez, R. T. Hay, in *Mol Cell*. (1998), vol. 2, pp. 233-239.
170. O. Kerscher, in *EMBO reports*. (2007), vol. 8, pp. 550-555.
171. K. J. Simpson-Lavy, M. Johnston, in *Proc Natl Acad Sci USA*. (2013).
172. U. Hardeland, R. Steinacher, J. Jiricny, P. Schär, in *The EMBO Journal*. (2002), vol. 21, pp. 1456-1464.
173. S. Martin, A. Nishimune, J. R. Mellor, J. M. Henley, in *Nature*. (2007), vol. 447, pp. 321-325.
174. M. Liu, S. Shi, S. Zhang, P. Xu, J. Lai, Y. Liu, D. Yuan, Y. Wang, J. Du, C. Yang, in *BMC Plant Biol*. (2014), vol. 14, pp. 153.
175. L. M. Lois, C. D. Lima, N.-H. Chua, in *Plant Cell*. (2003), vol. 15, pp. 1347-1359.
176. L. Conti, S. Nelis, C. Zhang, A. Woodcock, R. Swarup, M. Galbiati, C. Tonelli, R. Napier, P. Hedden, M. Bennett, A. Sadanandom, in *Dev Cell*. (2014), vol. 28, pp. 102-110.
177. H. J. Park, W.-Y. Kim, H. C. Park, S. Y. Lee, H. J. Bohnert, D.-J. Yun, in *Mol Cells*. (2011), vol. 32, pp. 305-316.
178. S. Zhang, Y. Qi, M. Liu, C. Yang, in *J Integr Plant Biol*. (2012).

179. M. J. Miller, M. Scalf, T. C. Rytz, S. L. Hubler, L. M. Smith, R. D. Vierstra, in *Mol Cell Proteomics*. (2012).
180. J. T. Hannich, A. Lewis, M. B. Kroetz, S.-J. Li, H. Heide, A. Emili, M. Hochstrasser, in *J Biol Chem*. (2005), vol. 280, pp. 4102-4110.
181. J. A. Wohlschlegel, E. S. Johnson, S. I. Reed, J. R. Yates, in *J Biol Chem*. (2004), vol. 279, pp. 45662-45668.
182. F. Golebiowski, I. Matic, M. H. Tatham, C. Cole, Y. Yin, A. Nakamura, J. Cox, G. J. Barton, M. Mann, R. T. Hay, in *Science Signaling*. (2009), vol. 2, pp. ra24.
183. F. Golebiowski, M. H. Tatham, A. Nakamura, R. T. Hay, in *Nat Protoc*. (2010), vol. 5, pp. 873-882.
184. H. D. Ulrich, in *Mol Cell*. (2012), vol. 47, pp. 335-337.
185. Z. Guo, J. Kanjanapangka, N. Liu, S. Liu, C. Liu, Z. Wu, Y. Wang, T. Loh, C. Kowolik, J. Jamsen, M. Zhou, K. Truong, Y. Chen, L. Zheng, B. Shen, in *Mol Cell*. (2012), vol. 47, pp. 444-456.
186. L. Lopez-Molina, S. Mongrand, N. Kinoshita, N.-H. Chua, in *Genes & Development*. (2003), vol. 17, pp. 410-418.
187. S. L. Stone, L. A. Williams, L. M. Farmer, R. D. Vierstra, J. Callis, in *Plant Cell*. (2006), vol. 18, pp. 3415-3428.
188. A. M. Sriramachandran, R. J. Dohmen, in *Biochim Biophys Acta*. (2013).
189. Y. Yin, A. Seifert, J. S. Chua, J.-F. Maure, F. Golebiowski, R. T. Hay, in *Genes & Development*. (2012), vol. 26, pp. 1196-1208.
190. J. R. Mullen, S. J. Brill, in *J Biol Chem*. (2008), vol. 283, pp. 19912-19921.
191. V. Lallemand-Breitenbach, M. Jeanne, S. Benhenda, R. Nasr, M. Lei, L. Peres, J. Zhou, J. Zhu, B. Raught, H. de The, *Nature cell biology* (2008), vol. 10, pp. 547-555.
192. I. A. Hendriks, J. Schimmel, K. Eifler, J. V. Olsen, A. C. O. Vertegaal, in *J. Biol. Chem.* (2015).
193. M. Castorálová, D. Březinová, M. Svéda, J. Lipov, T. Ruml, Z. Knejzlík, in *Biochim Biophys Acta*. (2012), vol. 1823, pp. 911-919.
194. L. De La Vega, I. Grishina, R. Moreno, M. Krüger, T. Braun, M. L. Schmitz, in *Molecular Cell*. (2012), pp. 1-12.
195. J. González-Santamaría, M. Campagna, A. Ortega-Molina, L. Marcos-Villar, C. F. de la Cruz-Herrera, D. González, P. Gallego, F. Lopitz-Otsoa, M. Esteban, M. S. Rodríguez, M. Serrano, C. Rivas, in *Cell Death Dis*. (2012), vol. 3, pp. e393.
196. C. Bassi, J. Ho, T. Srikumar, R. J. O. Dowling, C. Gorrini, S. J. Miller, T. W. Mak, B. G. Neel, B. Raught, V. Stambolic, in *Science*. (2013), vol. 341, pp. 395-399.
197. S.-Y. Wu, C.-M. Chiang, in *The EMBO Journal*. (2009), vol. 28, pp. 1246-1259.
198. S. Okada, M. Nagabuchi, Y. Takamura, T. Nakagawa, K. Shinmyozu, J.-i. Nakayama, K. Tanaka, in *Plant Cell Physiol*. (2009), vol. 50, pp. 1049-1061.
199. W. Yang, W. Paschen, in *Proteomics*. (2014).
200. V. Lang, F. Aillet, E. Da Silva-Ferrada, W. Xolalpa, L. Zabaleta, C. Rivas, M. S. Rodriguez, in *METHODS*. (2014).
201. E. Da Silva-Ferrada, W. Xolalpa, V. Lang, F. Aillet, I. Martin-Ruiz, C. F. De La Cruz-Herrera, F. Lopitz-Otsoa, A. Carracedo, S. J. Goldenberg, C. Rivas, P. England, M. S. Rodríguez, in *Sci. Rep.* (2013), vol. 3, pp. 1690.
202. E. Da Silva-Ferrada, F. Lopitz-Otsoa, V. Lang, M. S. Rodríguez, R. Matthiesen, in *Biochemistry Research International*. (2012), vol. 2012, pp. 875148.

203. S. M. Jeram, T. Srikumar, X.-D. Zhang, H. Anne Eisenhauer, R. Rogers, P. G. A. Pedrioli, M. Matunis, B. Raught, in *Proteomics*. (2010), vol. 10, pp. 254-265.
204. H.-H. Hsiao, E. Meulmeester, B. T. C. Frank, F. Melchior, H. Urlaub, in *Mol Cell Proteomics*. (2009), vol. 8, pp. 2664-2675.
205. O. Osula, S. Swatkoski, R. J. Cotter, in *J Mass Spectrom*. (2012), vol. 47, pp. 644-654.
206. Q. Dumont, D. L. Donaldson, W. P. Griffith, in *Anal Chem*. (2011), vol. 83, pp. 9638-9642.
207. N. Chicooree, J. R. Griffiths, Y. Connolly, C.-T. Tan, A. Malliri, C. E. Eyers, D. L. Smith, in *Rapid Commun Mass Spectrom*. (2013), vol. 27, pp. 127-134.
208. I. A. Hendriks, R. C. D'Souza, J.-G. Chang, M. Mann, A. C. O. Vertegaal, in *Nat Commun*. (2015), vol. 6, pp. 7289.
209. T. Makhnevych, Y. Sydorskyy, X. Xin, T. Srikumar, F. J. Vizeacoumar, S. M. Jeram, Z. Li, S. Bahr, B. J. Andrews, C. Boone, B. Raught, in *Molecular Cell*. (2009), vol. 33, pp. 124-135.
210. M. Thelander, T. Olsson, H. Ronne, in *EMBO J*. (2004), vol. 23, pp. 1900-1910.
211. C. Polge, M. Thomas, in *Trends Plant Sci*. (2007), vol. 12, pp. 20-28.
212. M. Carlson, D. Botstein, in *CELL*. (1982), vol. 28, pp. 145-154.
213. J. L. Celenza, M. Carlson, in *Science*. (1986), vol. 233, pp. 1175-1180.
214. V. Haurie, H. Boucherie, F. Sagliocco, in *J Biol Chem*. (2003), vol. 278, pp. 45391-45396.
215. U. Andersson, K. Filipsson, C. R. Abbott, A. Woods, K. Smith, S. R. Bloom, D. Carling, C. J. Small, in *J Biol Chem*. (2004), vol. 279, pp. 12005-12008.
216. J. Apfeld, G. O'Connor, T. McDonagh, P. S. DiStefano, R. Curtis, in *Genes & Development*. (2004), vol. 18, pp. 3004-3009.
217. E. L. Greer, A. Brunet, in *Aging Cell*. (2009), vol. 8, pp. 113-127.
218. E. Baena-González, F. Rolland, J. M. Thevelein, J. Sheen, in *Nature*. (2007), vol. 448, pp. 938-942.
219. A. Alderson, P. A. Sabelli, J. R. Dickinson, D. Cole, M. Richardson, M. Kreis, P. R. Shewry, N. G. Halford, in *Proc Natl Acad Sci USA*. (1991), vol. 88, pp. 8602-8605.
220. D. Carling, K. Aguan, A. Woods, A. J. Verhoeven, R. K. Beri, C. H. Brennan, C. Sidebottom, M. D. Davison, J. Scott, in *J Biol Chem*. (1994), vol. 269, pp. 11442-11448.
221. L. Le Guen, M. Thomas, M. Bianchi, N. G. Halford, M. Kreis, in *Gene*. (1992), vol. 120, pp. 249-254.
222. T. Muranaka, H. Banno, Y. Machida, in *Mol Cell Biol*. (1994), vol. 14, pp. 2958-2965.
223. P. Purcell, A. M. Smith, N. G. Halford, in *Plant J* (1998), vol. 14, pp. 195-203.
224. N. G. Halford, D. G. Hardie, in *Plant Mol Biol*. (1998), vol. 37, pp. 735-748.
225. S. Laurie, R. S. McKibbin, N. G. Halford, in *Journal of experimental botany*. (2003), vol. 54, pp. 739-747.
226. R. W. Mackintosh, S. P. Davies, P. R. Clarke, J. Weekes, J. G. Gillespie, B. J. Gibb, D. G. Hardie, in *Eur J Biochem*. (1992), vol. 209, pp. 923-931.
227. K. L. Ball, S. Dale, J. Weekes, D. G. Hardie, in *Eur J Biochem*. (1994), vol. 219, pp. 743-750.
228. P. Douglas, E. Pigaglio, A. Ferrer, N. G. Halfords, C. MacKintosh, in *Biochem J*. (1997), vol. 325 (Pt 1), pp. 101-109.

229. R. W. McMichael, M. Bachmann, S. C. Huber, in *Plant Physiol*. (1995), vol. 108, pp. 1077-1082.
230. C. Sugden, P. G. Donaghy, N. G. Halford, D. G. Hardie, in *Plant Physiol*. (1999), vol. 120, pp. 257-274.
231. S. Dale, W. A. Wilson, A. M. Edelman, D. G. Hardie, in *FEBS Lett*. (1995), vol. 361, pp. 191-195.
232. E. M. Hrabak, C. W. M. Chan, M. Gribskov, J. F. Harper, J. H. Choi, N. Halford, J. Kudla, S. Luan, H. G. Nimmo, M. R. Sussman, M. Thomas, K. Walker-Simmons, J.-K. Zhu, A. C. Harmon, in *PLANT PHYSIOLOGY*. (2003), vol. 132, pp. 666-680.
233. N. G. Halford, S. J. Hey, in *Biochem J*. (2009), vol. 419, pp. 247-259.
234. R. Jiang, M. Carlson, in *Mol Cell Biol*. (1997), vol. 17, pp. 2099-2106.
235. K. I. Mitchelhill, D. Stapleton, G. Gao, C. House, B. Michell, F. Katsis, L. A. Witters, B. E. Kemp, in *J Biol Chem*. (1994), vol. 269, pp. 2361-2364.
236. D. Stapleton, G. Gao, B. J. Michell, J. Widmer, K. Mitchelhill, T. Teh, C. M. House, L. A. Witters, B. E. Kemp, in *J Biol Chem*. (1994), vol. 269, pp. 29343-29346.
237. G. Gao, C. S. Fernandez, D. Stapleton, A. S. Auster, J. Widmer, J. R. Dyck, B. E. Kemp, L. A. Witters, in *J Biol Chem*. (1996), vol. 271, pp. 8675-8681.
238. A. Woods, P. C. Cheung, F. C. Smith, M. D. Davison, J. Scott, R. K. Beri, D. Carling, in *J Biol Chem*. (1996), vol. 271, pp. 10282-10290.
239. J. P. Bouly, L. Gissot, P. Lessard, M. Kreis, M. Thomas, in *Plant J*. (1999), vol. 18, pp. 541-550.
240. L. Gissot, C. Polge, J.-P. Bouly, T. Lemaitre, M. Kreis, M. Thomas, in *Plant Mol Biol*. (2004), vol. 56, pp. 747-759.
241. T. Kleinow, R. Bhalerao, F. Breuer, M. Umeda, K. Salchert, C. Koncz, in *Plant J.* (2000), vol. 23, pp.115-122
242. S. P. Davies, N. R. Helps, P. T. Cohen, D. G. Hardie, in *FEBS Letters*. (1995), vol. 377, pp. 421-425.
243. S. A. Hawley, M. Davison, A. Woods, S. P. Davies, R. K. Beri, D. Carling, D. G. Hardie, in *J Biol Chem*. (1996), vol. 271, pp. 27879-27887.
244. W. A. Wilson, S. A. Hawley, D. G. Hardie, in *Curr Biol*. (1996), vol. 6, pp. 1426-1434.
245. K. Ludin, R. Jiang, M. Carlson, in *Proc Natl Acad Sci USA*. (1998), vol. 95, pp. 6245-6250.
246. C. Sugden, R. M. Crawford, N. G. Halford, D. G. Hardie, in *Plant J*. (1999), vol. 19, pp. 433-439.
247. R. R. McCartney, M. C. Schmidt, in *J Biol Chem.* (2001), vol. 276, pp. 36460-36466.
248. S. Hey, H. Mayerhofer, N. G. Halford, J. R. Dickinson, in *J Biol Chem*. (2007), vol. 282, pp. 10472-10479.
249. E. Baena-González, J. Sheen, in *Trends in Plant Science*. (2008), vol. 13, pp. 474-482.
250. M. Jakoby, B. Weisshaar, W. Dröge-Laser, J. Vicente-Carbajosa, J. Tiedemann, T. Kroj, F. Parcy, b. R. Group, in *Trends Plant Sci*. (2002), vol. 7, pp. 106-111.
251. A. L. Contento, S.-J. Kim, D. C. Bassham, in *Plant Physiol*. (2004), vol. 135, pp. 2330-2347.
252. O. Thimm, O. Bläsing, Y. Gibon, A. Nagel, S. Meyer, P. Krüger, J. Selbig, L. A. Müller, S. Y. Rhee, M. Stitt, in *The Plant Journal*. (2004), vol. 37, pp. 914-939.

253. J.-F. Lin, S.-H. Wu, in *Plant J*. (2004), vol. 39, pp. 612-628.
254. V. Buchanan-Wollaston, T. Page, E. Harrison, E. Breeze, P. O. Lim, H. G. Nam, J.-F. Lin, S.-H. Wu, J. Swidzinski, K. Ishizaki, C. J. Leaver, in *Plant J*. (2005), vol. 42, pp. 567-585.
255. J. Price, A. Laxmi, S. K. St Martin, J.-C. Jang, in *Plant Cell*. (2004), vol. 16, pp. 2128-2150.
256. P. M. Palenchar, A. Kouranov, L. V. Lejay, G. M. Coruzzi, in *Genome Biol*. (2004), vol. 5, pp. R91.
257. A. Confraria, C. Martinho, A. Elias, I. Rubio-Somoza, E. Baena-González, in *Front. Plant Sci.* (2013), vol. 4, pp. 197.
258. A. Lovas, A. Bimbó, L. Szabó, Z. Bánfalvi, in *Plant J*. (2003), vol. 33, pp. 139-147.
259. K. W. Lee, P. W. Chen, C. A. Lu, S. Chen, T. H. Ho, S. M. Yu, in *Sci Signal.* (2009), vol 2, ra61 2/91/ra61 [pii]10.1126/scisignal.2000333.
260. Y.-H. Cho, J.-W. Hong, E.-C. Kim, S.-D. Yoo, in *Plant Physiol*. (2012), vol. 158, pp. 1955-1964.
261. C.-R. Lin, K.-W. Lee, C.-Y. Chen, Y.-F. Hong, J.-L. Chen, C.-A. Lu, K.-T. Chen, T.-H. D. Ho, S.-M. Yu, in *The Plant Cell*. (2014).
262. R. Sharma, D. De Vleesschauwer, M. K. Sharma, P. C. Ronald, in *Mol Plant*. (2013), vol. 6, pp. 250-260.
263. S. Fragoso, L. Espíndola, J. Páez-Valencia, A. Gamboa, Y. Camacho, E. Martínez-Barajas, P. Coello, in *Plant Physiol*. (2009), vol. 149, pp. 1906-1916.
264. S. P. Slocombe, F. Beaudoin, P. G. Donaghy, D. G. Hardie, J. R. Dickinson, N. G. Halford, in *Plant Physiol Biochem*. (2004), vol. 42, pp. 111-116.
265. L. Hao, H. Wang, G. Sunter, D. M. Bisaro, in *The Plant Cell*. (2003), vol. 15, pp. 1034-1048.
266. G. Sunter, J. L. Sunter, D. M. Bisaro, in *Virology*. (2001), vol. 285, pp. 59-70.
267. L. Liu, H. Y. Chung, G. Lacatus, S. Baliji, J. Ruan, G. Sunter. (2014), pp. 1-16.
268. W. Shen, L. Hanley-Bowdoin, in *Plant Physiol*. (2006), vol. 142, pp. 1642-1655.
269. W. Shen, M. I. Reyes, L. Hanley-Bowdoin, in *Plant Physiol*. (2009), vol. 150, pp. 996-1005.
270. W. Shen, M. B. Dallas, M. B. Goshe, L. Hanley-Bowdoin, in *Journal of Virology*. (2014), vol. 88, pp. 10598-10612.
271. Q. Shen, Z. Liu, F. Song, Q. Xie, L. Hanley-Bowdoin, X. Zhou, in *PLANT PHYSIOLOGY*. (2011).
272. Q. Shen, M. Bao, X. Zhou, in *Plant Signal Behav*. (2012), vol. 7, pp. 888-892.
273. R. A. Cernadas, L. R. Camillo, C. E. Benedetti, in *Molecular Plant Pathology*. (2008), vol. 9, pp. 609-631.
274. R. Szczesny, D. Büttner, L. Escolar, S. Schulze, A. Seiferth, U. Bonas, in *New Phytol*. (2010), vol. 187, pp. 1058-1074.
275. J. Avila, O. G. Gregory, D. Su, T. A. Deeter, S. Chen, C. Silva-Sanchez, S. Xu, G. B. Martin, T. P. Devarenne, in *Plant Physiol*. (2012), vol. 159, pp. 1277-1290.
276. L. Gissot, C. Polge, M. Jossier, T. Girin, J.-P. Bouly, M. Kreis, M. Thomas, in *Plant Physiol*. (2006), vol. 142, pp. 931-944.
277. S. Schuck, I. T. Baldwin, G. Bonaventure, in *Plant Signal Behav*. (2013), vol. 8, pp. e23537.
278. S. Schuck, I. Camehl, P. A. Gilardoni, R. Oelmueller, I. T. Baldwin, G. Bonaventure, in *PLANT PHYSIOLOGY*. (2012), vol. 160, pp. 929-943.

279. J. Schwachtje, P. E. H. Minchin, S. Jahnke, J. T. van Dongen, U. Schittko, I. T. Baldwin, in *Proc Natl Acad Sci USA*. (2006), vol. 103, pp. 12935-12940.
280. K. J. Bradford, A. B. Downie, O. H. Gee, V. Alvarado, H. Yang, P. Dahal, in *PLANT PHYSIOLOGY*. (2003), vol. 132, pp. 1560-1576.
281. M. T. J. Buitink, L. Gissot, O. Leprince, in *Plant Cell Environ.* (2003), vol. 27, pp. 55-67.
282. R. Radchuk, R. J. N. Emery, D. Weier, H. Vigeolas, P. Geigenberger, J. E. Lunn, R. Feil, W. Weschke, H. Weber, in *Plant J*. (2010), vol. 61, pp. 324-338.
283. F. Rolland, E. Baena-Gonzalez, J. Sheen, in *Annu Rev Plant Biol*. (2006), vol. 57, pp. 675-709.
284. M. Jossier, J.-P. Bouly, P. Meimoun, A. Arjmand, P. Lessard, S. Hawley, D. Grahame Hardie, M. Thomas, in *Plant J*. (2009), vol. 59, pp. 316-328.
285. A. Rodrigues, M. Adamo, P. Crozet, L. Margalha, A. Confraria, C. Martinho, A. Elias, A. Rabissi, V. Lumbreras, M. González-Guzmán, R. Antoni, P. L. Rodriguez, E. Baena-González, in *The Plant Cell*. (2013), vol. 25, pp. 3871-3884.
286. R. Radchuk, V. Radchuk, W. Weschke, L. Borisjuk, H. Weber, in *Plant Physiol*. (2006), vol. 140, pp. 263-278.
287. J. H. Im, Y.-H. Cho, G.-D. Kim, G.-H. Kang, J.-W. Hong, S.-D. Yoo, in *Plant, Cell & Environment*. (2014), vol. 37, pp. 2303-2312.
288. A. Mair, L. Pedrotti, B. Wurzinger, D. Anrather, A. Simeunovic, C. Weiste, C. Valerio, K. Dietrich, T. Kirchler, T. Nägele, J. Vicente Carbajosa, J. Hanson, E. Baena-González, C. Chaban, W. Weckwerth, W. Dröge-Laser, M. Teige, in *eLife*. (2015), vol. 4.
289. C. C. Matiolli, J. P. Tomaz, G. T. Duarte, F. M. Prado, L. E. V. Del Bem, A. B. Silveira, L. Gauer, L. G. G. Corrêa, R. D. Drumond, A. J. C. Viana, P. D. Mascio, C. Meyer, M. G. A. Vincentz, in *PLANT PHYSIOLOGY*. (2011).
290. P. Coello, E. Hirano, S. J. Hey, N. Muttucumaru, E. Martinez-Barajas, M. A. J. Parry, N. G. Halford, in *Journal of experimental botany*. (2012), vol. 63, pp. 913-924.
291. R. Radchuk, U. Conrad, I. Saalbach, M. Giersberg, R. J. N. Emery, H. Küster, A. Nunes-Nesi, A. R. Fernie, W. Weschke, H. Weber, in *Plant J*. (2010), vol. 64, pp. 715-730.
292. C. Weiste, W. Dröge-Laser, in *Nat Commun*. (2014), vol. 5, pp. 3883.
293. J. E. Harthill, S. E. M. Meek, N. Morrice, M. W. Peggie, J. Borch, B. H. C. Wong, C. Mackintosh, in *Plant J*. (2006), vol. 47, pp. 211-223.
294. A. Kulma, D. Villadsen, D. G. Campbell, S. E. M. Meek, J. E. Harthill, T. H. Nielsen, C. Mackintosh, in *Plant J*. (2004), vol. 37, pp. 654-667.
295. D. Toroser, G. S. Athwal, S. C. Huber, in *FEBS Letters*. (1998), vol. 435, pp. 110-114.
296. S. C. Huber, C. MacKintosh, W. M. Kaiser, *Plant Mol Biol.* (2002), vol. 50, pp.1053-1063.
297. F. Beczner, G. Dancs, A. Sós-Hegedus, F. Antal, Z. Bánfalvi, in *J Plant Physiol*. (2010), vol. 167, pp. 1046-1051.
298. C. V. Piattoni, D. M. Bustos, S. A. Guerrero, A. Á. Iglesias, in *PLANT PHYSIOLOGY*. (2011), vol. 156, pp. 1337-1350.
299. C. Rosnoblet, C. Aubry, O. Leprince, B. L. Vu, H. Rogniaux, J. Buitink, in *Plant J*. (2007), vol. 51, pp. 47-59.

300. X. Wang, F. Peng, M. Li, L. Yang, G. Li, in *Journal of Plant Physiology*. (2012), vol. 169, pp. 1173-1182.
301. A. Tiessen, K. Prescha, A. Branscheid, N. Palacios, R. Mckibbin, N. G. Halford, P. Geigenberger, in *Plant J*. (2003), vol. 35, pp. 490-500.
302. A. Kolbe, A. Tiessen, H. Schluepmann, M. Paul, S. Ulrich, P. Geigenberger, in *Proc Natl Acad Sci USA*. (2005), vol. 102, pp. 11118-11123.
303. C. Polge, M. Jossier, P. Crozet, L. Gissot, M. Thomas, in *PLANT PHYSIOLOGY*. (2008), vol. 148, pp. 1570-1582.
304. X.-F. Li, Y.-J. Li, Y.-H. An, L.-J. Xiong, X.-H. Shao, Y. Wang, Y. Sun, in *J Integr Plant Biol*. (2009), vol. 51, pp. 513-520.
305. F. Rook, N. Gerrits, A. Kortstee, M. van Kampen, M. Borrias, P. Weisbeek, S. Smeekens, in *Plant J.* (1998), vol. 15, pp. 253-263.
306. F. Weltmeier, F. Rahmani, A. Ehlert, K. Dietrich, K. Schutze, X. Wang, C. Chaban, J. Hanson, M. Teige, K. Harter, J. Vicente-Carbajosa, S. Smeekens, W. Droge-Laser, in *Plant Mol Biol*.(2009), vol 69, pp.107-119.
307. A. Wiese, N. Elzinga, B. Wobbes, S. Smeekens, in *Biochem Soc Trans.* (2005), vol. 33, pp. 272-275.
308. J. Ma, M. Hanssen, K. Lundgren, L. Hernández, T. Delatte, A. Ehlert, C.-M. Liu, H. Schluepmann, W. Dröge-Laser, T. Moritz, S. Smeekens, J. Hanson, in *New Phytol*. (2011), vol. 191, pp. 733-745.
309. K.-W. Lee, P.-W. Chen, C.-A. Lu, S. Chen, T.-H. D. Ho, S.-M. Yu, in *Science Signaling*. (2009), vol. 2, pp. ra61.
310. C.-A. Lu, C.-C. Lin, K.-W. Lee, J.-L. Chen, L.-F. Huang, S.-L. Ho, H.-J. Liu, Y.-I. Hsing, S.-M. Yu, in *Plant Cell*. (2007), vol. 19, pp. 2484-2499.
311. R. P. Bhalerao, K. Salchert, L. Bakó, L. Okrész, L. Szabados, T. Muranaka, Y. Machida, J. Schell, C. Koncz, in *Proc Natl Acad Sci USA*. (1999), vol. 96, pp. 5322-5327.
312. M. Nietzsche, I. Schießl, F. Börnke, in *Front Plant Sci*. (2014), vol. 5, pp. 54.
313. J. E. Lunn, R. Feil, J. H. M. Hendriks, Y. Gibon, R. Morcuende, D. Osuna, W.-R. Scheible, P. Carillo, M.-R. Hajirezaei, M. Stitt, in *Biochem. J.* (2006), vol. 397, pp. 139-148.
314. L. E. O'Hara, M. J. Paul, A. Wingler, in *Mol Plant*. (2013), vol. 6, pp. 261-274.
315. H. Schluepmann, M. Paul, in *Arabidopsis Book*. (2009), vol. 7, pp. e0122.
316. H. Schluepmann, T. Pellny, A. van Dijken, S. Smeekens, M. Paul, in *Proc Natl Acad Sci U S A* (2003), vol. 100, pp. 6849-6854.
317. H. Schluepmann, A. van Dijken, M. Aghdasi, B. Wobbes, M. Paul, S. Smeekens, in *Plant Physiol.* (2004), vol. 135, pp. 879-890.
318. L. D. Gomez, S. Baud, A. Gilday, Y. Li, I. A. Graham, in *Plant J.* (2006), vol. 46, pp. 69-84.
319. E. Martínez-Barajas, T. Delatte, H. Schluepmann, G. J. de Jong, G. W. Somsen, C. Nunes, L. F. Primavesi, P. Coello, R. A. C. Mitchell, M. J. Paul, in *Plant Physiol*. (2011), vol. 156, pp. 373-381.
320. M. J. Paul, L. F. Primavesi, D. Jhurreea, Y. Zhang, in *Annu. Rev. Plant Biol.* (2008), vol. 59, pp. 417-441.
321. M. Paul, in *Curr Opin Plant Biol*. (2007), vol. 10, pp. 303-309.
322. Y. Zhang, L. F. Primavesi, D. Jhurreea, P. J. Andralojc, R. A. C. Mitchell, S. J. Powers, H. Schluepmann, T. Delatte, A. Wingler, M. J. Paul, in *Plant Physiol*. (2009), vol. 149, pp. 1860-1871.

323. S. Debast, A. Nunes-Nesi, M. R. Hajirezaei, J. Hofmann, U. Sonnewald, A. R. Fernie, F. Börnke, in *PLANT PHYSIOLOGY*. (2011), vol. 156, pp. 1754-1771.
324. D. Toroser, Z. Plaut, S. C. Huber, in *PLANT PHYSIOLOGY*. (2000), vol. 123, pp. 403-412.
325. C. Nunes, L. F. Primavesi, M. K. Patel, E. Martinez-Barajas, S. J. Powers, R. Sagar, P. S. Fevereiro, B. G. Davis, M. J. Paul, in *Plant Physiol Biochem*. (2013), vol. 63, pp. 89-98.
326. E. A. Ananieva, G. E. Gillaspy, A. Ely, R. N. Burnette, F. L. Erickson, in *PLANT PHYSIOLOGY*. (2008), vol. 148, pp. 1868-1882.
327. J.-H. Lee, W. Terzaghi, G. Gusmaroli, J.-B. F. Charron, H.-J. Yoon, H. Chen, Y. J. He, Y. Xiong, X. W. Deng, in *Plant Cell*. (2008), vol. 20, pp. 152-167.
328. K. Németh, K. Salchert, P. Putnoky, R. Bhalerao, Z. Koncz-Kálmán, B. Stankovic-Stangeland, L. Bakó, J. Mathur, L. Okrész, S. Stabel, P. Geigenberger, M. Stitt, G. P. Rédei, J. Schell, C. Koncz, in *Genes & Development*. (1998), vol. 12, pp. 3059-3073.
329. K. Salchert, R. Bhalerao, Z. Koncz-Kálmán, C. Koncz, in *Philos Trans R Soc Lond, B, Biol Sci*. (1998), vol. 353, pp. 1517-1520.
330. U. Flores-Pérez, J. Pérez-Gil, M. Closa, L. P. Wright, P. Botella-Pavía, M. A. Phillips, A. Ferrer, J. Gershenzon, M. Rodríguez-Concepción, in *Mol Plant*. (2010), vol. 3, pp. 101-112.
331. N. G. Halford, S. Hey, D. Jhurreea, S. Laurie, R. S. McKibbin, M. Paul, Y. Zhang, in *Journal of experimental botany*. (2003), vol. 54, pp. 467-475.
332. Z. Zhang, Y. Deng, X. Song, M. Miao, in *J Plant Physiol*. (2015), vol. 177, pp. 110-120.
333. Y. Zhang, P. R. Shewry, H. Jones, P. Barcelo, P. A. Lazzeri, N. G. Halford, in *Plant J*. (2001), vol. 28, pp. 431-441.
334. N. Sreenivasulu, V. Radchuk, M. Strickert, O. Miersch, W. Weschke, U. Wobus, in *Plant J*. (2006), vol. 47, pp. 310-327.
335. M. Bitrián, F. Roodbarkelari, M. Horváth, C. Koncz, in *Plant J*. (2011), vol. 65, pp. 829-842.
336. S. Pien, J. Wyrzykowska, A. J. Fleming, in *Plant J*. (2001), vol. 25, pp. 663-674.
337. M. Pierre, J. A. Traverso, B. Boisson, S. Domenichini, D. Bouchez, C. Giglione, T. Meinnel, in *THE PLANT CELL ONLINE*. (2007), vol. 19, pp. 2804-2821.
338. T. Williams, J. E. Brenman, in *Trends Cell Biol*. (2008), vol. 18, pp. 193-198.
339. J. Liang, S. H. Shao, Z.-X. Xu, B. Hennessy, Z. Ding, M. Larrea, S. Kondo, D. J. Dumont, J. U. Gutterman, C. L. Walker, J. M. Slingerland, G. B. Mills, in *Nature cell biology*. (2007), vol. 9, pp. 218-224.
340. J. D. Short, R. Dere, K. D. Houston, S.-L. Cai, J. Kim, J. M. Bergeron, J. Shen, J. Liang, M. T. Bedford, G. B. Mills, C. L. Walker, in *Mol. Carcinog.* (2010), vol. 49, pp. 429-439.
341. J. D. Short, K. D. Houston, R. Dere, S.-L. Cai, J. Kim, C. L. Johnson, R. R. Broaddus, J. Shen, S. Miyamoto, F. Tamanoi, D. Kwiatkowski, G. B. Mills, C. L. Walker, in *Cancer Research*. (2008), vol. 68, pp. 6496-6506.
342. T. Guérinier, L. Millan, P. Crozet, C. Oury, F. Rey, B. Valot, C. Mathieu, J. Vidal, M. Hodges, M. Thomas, N. Glab, in *Plant J*. (2013).
343. A. Y.-L. Tsai, S. Gazzarrini, in *Plant J*. (2012), vol. 69, pp. 809-821.
344. A. Y.-L. Tsai, S. Gazzarrini, in *Plant Signal Behav*. (2012), vol. 7, pp. 1238-1242.

345. M. O'Brien, R. N. Kaplan-Levy, T. Quon, P. G. Sappl, D. R. Smyth, in *Journal of Experimental Botany*. (2015).
346. T. Kleinow, Himberta, S, Krenza, B, Jeskea, H, and Koncz, C, in *Plant Science* (2009), vol.177, pp. 360-370.
347. E.-Y. Jeong, P. J. Seo, J. C. Woo, C.-M. Park, in *BMC Plant Biol*. (2015), vol. 15, pp. 110.
348. K. Hedbacker, M. Carlson, in *Front Biosci*. (2008), vol. 13, pp. 2408-2420.
349. D. Carling, C. Thornton, A. Woods, M. J. Sanders, in *Biochem. J.* (2012), vol. 445, pp. 11-27.
350. S. P. Davies, S. A. Hawley, A. Woods, D. Carling, T. A. Haystead, D. G. Hardie, in *Eur J Biochem*. (1994), vol. 223, pp. 351-357.
351. R. Ghillebert, E. Swinnen, J. Wen, L. Vandesteene, M. Ramon, K. Norga, F. Rolland, J. Winderickx, in *The FEBS journal*. (2011).
352. S. Fogarty, S. A. Hawley, K. A. Green, N. Saner, K. J. Mustard, D. G. Hardie, in *Biochem. J.* (2010), vol. 426, pp. 109-118.
353. K. A. Anderson, T. J. Ribar, F. Lin, P. K. Noeldner, M. F. Green, M. J. Muehlbauer, L. A. Witters, B. E. Kemp, A. R. Means, in *Cell Metabolism*. (2008), vol. 7, pp. 377-388.
354. V. Lumbreras, M. M. Alba, T. Kleinow, C. Koncz, M. Pagès, in *EMBO Rep*. (2001), vol. 2, pp. 55-60.
355. S. Emanuelle, M. I. Hossain, I. E. Moller, H. L. Pedersen, A. M. L. van de Meene, M. S. Doblin, A. Koay, J. S. Oakhill, J. W. Scott, W. G. T. Willats, B. E. Kemp, A. Bacic, P. R. Gooley, D. I. Stapleton, in *Plant J*. (2015), vol. 82, pp. 183-192.
356. M. Ramon, P. Ruelens, Y. Li, J. Sheen, K. Geuten, F. Rolland, in *Plant J*. (2013).
357. G. R. Steinberg, B. E. Kemp, in *Physiol Rev*. (2009), vol. 89, pp. 1025-1078.
358. J. W. Scott, B. J. W. van Denderen, S. B. Jorgensen, J. E. Honeyman, G. R. Steinberg, J. S. Oakhill, T. J. Iseli, A. Koay, P. R. Gooley, D. Stapleton, B. E. Kemp, in *Chemistry & Biology*. (2008), vol. 15, pp. 1220-1230.
359. P. Crozet, L. Margalha, A. Confraria, A. Rodrigues, C. Martinho, M. Adamo, C. A. Elias, E. Baena-González, in *Front. Plant Sci.* (2014), vol. 5, pp. 190.
360. N. G. Halford, S. Hey, D. Jhurreea, S. Laurie, R. S. McKibbin, M. Paul, Y. Zhang, in *J Exp Bot.* (2003), vol. 54, pp. 467-475.
361. S. K. Hanks, T. Hunter, Protein kinases 6. in *FASEB J.* (1995), vol. 9, pp. 576-596.
362. S. C. Stein, A. Woods, N. A. Jones, M. D. Davison, D. Carling, in *Biochem J.* (2000), vol. 345, pp. 437-443.
363. R. R. McCartney, M. C. Schmidt, in *J Biol Chem*. (2001), vol. 276, pp. 36460-36466.
364. P. Crozet, F. Jammes, B. Valot, F. Ambard-Bretteville, S. Nessler, M. Hodges, J. Vidal, M. Thomas, in *J Biol Chem*. (2010), vol. 285, pp. 12071-12077.
365. W. Shen, M. I. Reyes, L. Hanley-Bowdoin, in *Plant Physiol.* (2009), vol. 150, pp. 996-1005.
366. T. Pang, B. Xiong, J.-Y. Li, B.-Y. Qiu, G.-Z. Jin, J.-K. Shen, J. Li, in *J Biol Chem*. (2007), vol. 282, pp. 495-506.
367. L. Chen, Z.-H. Jiao, L.-S. Zheng, Y.-y. Zhang, S.-T. Xie, Z.-X. Wang, J.-W. Wu, in *Nature*. (2009), vol. 459, pp. 1146-1149.

368. R. Farrás, A. Ferrando, J. Jásik, T. Kleinow, L. Okrész, A. Tiburcio, K. Salchert, C. del Pozo, J. Schell, C. Koncz, in *The EMBO Journal*. (2001), vol. 20, pp. 2742-2756.
369. K. Hofmann, P. Bucher, in *Trends in Biochemical Sciences*. (1996), vol. 21, pp. 172-173.
370. C.-P. Chiang, C.-H. Li, Y. Jou, Y.-C. Chen, Y.-C. Lin, F.-Y. Yang, N.-C. Huang, H. E. Yen, in *Journal of experimental botany*. (2013), vol. 64, pp. 2385-2400.
371. K. Moravcevic, J. M. Mendrola, K. R. Schmitz, Y.-H. Wang, D. Slochower, P. A. Janmey, M. A. Lemmon, in *Cell*. (2010), vol. 143, pp. 966-977.
372. G. A. Amodeo, M. J. Rudolph, L. Tong, in *Nature*. (2007), vol. 449, pp. 492-495.
373. B. Xiao, M. J. Sanders, E. Underwood, R. Heath, F. V. Mayer, D. Carmena, C. Jing, P. A. Walker, J. F. Eccleston, L. F. Haire, P. Saiu, S. A. Howell, R. Aasland, S. R. Martin, D. Carling, S. J. Gamblin, in *Nature*. (2011), vol. 472, pp. 230-233.
374. N. Kazgan, T. Williams, L. J. Forsberg, J. E. Brenman, in *Mol Biol Cell*. (2010), vol. 21, pp. 3433-3442.
375. A. Suzuki, S. Okamoto, S. Lee, K. Saito, T. Shiuchi, Y. Minokoshi, in *Mol Cell Biol*. (2007), vol. 27, pp. 4317-4327.
376. M. J. Rudolph, G. A. Amodeo, Y. Bai, L. Tong, in *Biochemical and Biophysical Research Communications*. (2005), vol. 337, pp. 1224-1228.
377. V. Nayak, K. Zhao, A. Wyce, M. F. Schwartz, W.-S. Lo, S. L. Berger, R. Marmorstein, in *Structure*. (2006), vol. 14, pp. 477-485.
378. R. Scholz, M. Suter, T. Weimann, C. Polge, P. V. Konarev, R. F. Thali, R. D. Tuerk, B. Viollet, T. Wallimann, U. Schlattner, D. Neumann, in *J Biol Chem*. (2009), vol. 284, pp. 27425-27437.
379. P. Coello, E. Martínez-Barajas, in *Plant Physiol Biochem*. (2014), vol. 80, pp. 153-159.
380. G. Polekhina, A. Gupta, B. J. Michell, B. Van Denderen, S. Murthy, S. C. Feil, I. G. Jennings, D. J. Campbell, L. A. Witters, M. W. Parker, B. E. Kemp, D. Stapleton, in *Curr Biol*. (2003), vol. 13, pp. 867-871.
381. G. Polekhina, A. Gupta, B. J. W. Van Denderen, S. C. Feil, B. E. Kemp, D. Stapleton, M. W. Parker, in *Structure*. (2005), vol. 13, pp. 1453-1462.
382. H. A. Wiatrowski, B. J. W. Van Denderen, C. D. Berkey, B. E. Kemp, D. Stapleton, M. Carlson, in *Mol Cell Biol*. (2004), vol. 24, pp. 352-361.
383. A. McBride, S. Ghilagaber, A. Nikolaev, D. G. Hardie, in *Cell Metabolism*. (2009), vol. 9, pp. 23-34.
384. A. Avila-Castañeda, N. Gutiérrez-Granados, A. Ruiz-Gayosso, A. Sosa-Peinado, E. Martínez-Barajas, P. Coello, in *Front. Plant Sci.* (2014), vol. 5, pp. 199.
385. M. Momcilovic, S. H. Iram, Y. Liu, M. Carlson, in *J Biol Chem*. (2008), vol. 283, pp. 19521-19529.
386. S. Mangat, D. Chandrashekarappa, R. R. McCartney, K. Elbing, M. C. Schmidt, in *Eukaryotic Cell*. (2010), vol. 9, pp. 173-183.
387. T. J. Iseli, M. Walter, B. J. W. Van Denderen, F. Katsis, L. A. Witters, B. E. Kemp, B. J. Michell, D. Stapleton, in *J Biol Chem*. (2005), vol. 280, pp. 13395-13400.
388. K. Hedbacker, M. Carlson, in *Eukaryotic Cell*. (2006), vol. 5, pp. 1950-1956.
389. K. Hedbacker, R. Townley, M. Carlson, in *Molecular and Cellular Biology*. (2004), vol. 24, pp. 1836-1843.

390. J. S. Oakhill, R. Steel, Z.-P. Chen, J. W. Scott, N. Ling, S. Tam, B. E. Kemp, in *Science*. (2011), vol. 332, pp. 1433-1435.
391. J. S. Oakhill, Z.-P. Chen, J. W. Scott, R. Steel, L. A. Castelli, N. Ling, S. L. Macaulay, B. E. Kemp, in *Proc Natl Acad Sci USA*. (2010), vol. 107, pp. 19237-19241.
392. S. M. Warden, C. Richardson, J. O'Donnell, D. Stapleton, B. E. Kemp, L. A. Witters, in *Biochem J*. (2001), vol. 354, pp. 275-283.
393. A. Bateman, in *Trends Biochem Sci*. (1997), vol. 22, pp. 12-13.
394. B. Xiao, M. J. Sanders, E. Underwood, R. Heath, F. V. Mayer, D. Carmena, C. Jing, P. A. Walker, J. F. Eccleston, L. F. Haire, P. Saiu, S. A. Howell, R. Aasland, S. R. Martin, D. Carling, S. J. Gamblin, in *Nature* (2011), vol. 472, pp. 230-233.
395. J. W. Scott, S. A. Hawley, K. A. Green, M. Anis, G. Stewart, G. A. Scullion, D. G. Norman, D. G. Hardie, in *J. Clin. Invest.* (2004), vol. 113, pp. 274-284.
396. B. Xiao, R. Heath, P. Saiu, F. C. Leiper, P. Leone, C. Jing, P. A. Walker, L. Haire, J. F. Eccleston, C. T. Davis, S. R. Martin, D. Carling, S. J. Gamblin, in *Nature* (2007), vol. 449, pp. 496-500.
397. G. J. Gowans, S. A. Hawley, F. A. Ross, D. G. Hardie, in *Cell Metabolism*. (2013), vol. 18, pp. 556-566.
398. R. Viana, M. C. Towler, D. A. Pan, D. Carling, B. Viollet, D. G. Hardie, P. Sanz, in *J Biol Chem*. (2007), vol. 282, pp. 16117-16125.
399. C. López-Paz, B. Vilela, M. Riera, M. Pagès, V. Lumbreras, in *FEBS Lett*. (2009), vol. 583, pp. 1887-1894.
400. M. J. Rudolph, G. A. Amodeo, S. H. Iram, S.-P. Hong, G. Pirino, M. Carlson, L. Tong, in *Structure*. (2007), vol. 15, pp. 65-74.
401. P. Day, A. Sharff, L. Parra, A. Cleasby, M. Williams, S. Hörer, H. Nar, N. Redemann, I. Tickle, J. Yon, in *Acta Crystallogr D Biol Crystallogr*. (2007), vol. 63, pp. 587-596.
402. Z. Lu, T. Hunter, in *Annu Rev Biochem*. (2009), vol. 78, pp. 435-475.
403. M. Ramon, P. Ruelens, Y. Li, J. Sheen, K. Geuten, F. Rolland, in *Plant J*. (2013); published online EpubApr 1 (10.1111/tpj.12192).
404. S. Emanuelle, M. I. Hossain, I. E. Moller, H. L. Pedersen, A. M. van de Meene, M. S. Doblin, A. Koay, J. S. Oakhill, J. W. Scott, W. G. Willats, B. E. Kemp, A. Bacic, P. R. Gooley, D. Stapleton, in *Plant J*. (2015); published online EpubMar 3 (10.1111/tpj.12813).
405. P. Coello, E. Martínez-Barajas, in *Front. Plant Sci.* (2014), vol. 5, pp. 196.
406. K. Ashrafi, S. S. Lin, J. K. Manchester, J. I. Gordon, in *Genes Dev*. (2000), vol. 14, pp. 1872-1885.
407. O. Vincent, M. Carlson, in *The EMBO Journal*. (1999), vol. 18, pp. 6672-6681.
408. S. Kuchin, I. Treich, M. Carlson, in *Proc Natl Acad Sci U S A* (2000), vol. 97, 7916-7920.
409. R. R. McCartney, E. M. Rubenstein, M. C. Schmidt, in *Curr Genet*. (2005), vol. 47, pp. 335-344.
410. Y. Minokoshi, Y.-B. Kim, O. D. Peroni, L. G. D. Fryer, C. Müller, D. Carling, B. B. Kahn, in *Nature*. (2002), vol. 415, pp. 339-343.
411. Y. He, S. Gan, in *Plant Mol Biol*. (2004), vol. 54, pp. 1-9.
412. X. Chen, Z. Zhang, R. G. F. Visser, C. Broekgaarden, B. Vosman, in *PLoS ONE*. (2013), vol. 8, pp. e70914.

413. Y. L. Xiaona Hou, Xiaoliang He, Yinzhu Shen, Zhanjing Huang, in *Plant Mol. Biol. Rep.* (2013), vol. 31, pp. 791–801.
414. M. Zourelidou, M. de Torres-Zabala, C. Smith, M. W. Bevan, in *Plant J*. (2002), vol. 30, pp. 489-497.
415. P. Pellicena, J. Kuriyan, in *Curr Opin Struct Biol*. (2006), vol. 16, pp. 702-709.
416. R. Townley, L. Shapiro, in *Science*. (2007), vol. 315, pp. 1726-1729.
417. U. Riek, R. Scholz, P. Konarev, A. Rufer, M. Suter, A. Nazabal, P. Ringler, M. Chami, S. A. Müller, D. Neumann, M. Forstner, M. Hennig, R. Zenobi, A. Engel, D. Svergun, U. Schlattner, T. Wallimann, in *J Biol Chem*. (2008), vol. 283, pp. 18331-18343.
418. L. Chantranupong, Rachel L. Wolfson, David M. Sabatini, in *CELL*. (2015), vol. 161, pp. 67-83.
419. C.-S. Zhang, B. Jiang, M. Li, M. Zhu, Y. Peng, Y.-L. Zhang, Y.-Q. Wu, T. Y. Li, Y. Liang, Z. Lu, G. Lian, Q. Liu, H. Guo, Z. Yin, Z. Ye, J. Han, J.-W. Wu, H. Yin, S.-Y. Lin, S.-C. Lin, in *Cell Metabolism*. (2014), vol. 20, pp. 526-540.
420. D. G. Hardie, in *Current Opinion in Cell Biology*. (2014), vol. 33C, pp. 1-7.
421. O. Vincent, R. Townley, S. Kuchin, M. Carlson, in *Genes & Development*. (2001), vol. 15, pp. 1104-1114.
422. D. G. Hardie, in *Annu. Rev. Nutr.* (2014), vol. 34, pp. 31-55.
423. J. S. Oakhill, J. W. Scott, B. E. Kemp, in *Trends in Endocrinology & Metabolism*. (2012), vol. 23, pp. 125-132.
424. D. G. Chandrashekarappa, R. R. McCartney, M. C. Schmidt, in *J Biol Chem*. (2013), vol. 288, pp. 89-98.
425. N. Lane, W. Martin, in *Nature*. (2010), vol. 467, pp. 929-934.
426. S. C. Stein, A. Woods, N. A. Jones, M. D. Davison, D. Carling, in *Biochem J*. (2000), vol. 345 Pt 3, pp. 437-443.
427. S.-P. Hong, F. C. Leiper, A. Woods, D. Carling, M. Carlson, in *Proc Natl Acad Sci USA*. (2003), vol. 100, pp. 8839-8843.
428. S. A. Hawley, D. A. Pan, K. J. Mustard, L. Ross, J. Bain, A. M. Edelman, B. G. Frenguelli, D. G. Hardie, in *Cell Metabolism*. (2005), vol. 2, pp. 9-19.
429. A. Woods, K. Dickerson, R. Heath, S.-P. Hong, M. Momcilovic, S. R. Johnstone, M. Carlson, D. Carling, in *Cell Metabolism*. (2005), vol. 2, pp. 21-33.
430. Z. Chen, X. Shen, F. Shen, W. Zhong, H. Wu, S. Liu, J. Lai, in *Mol Cell Biochem*. (2013), vol. 377, pp. 35-44.
431. M. Xie, D. Zhang, J. R. B. Dyck, Y. Li, H. Zhang, M. Morishima, D. L. Mann, G. E. Taffet, A. Baldini, D. S. Khoury, M. D. Schneider, in *Proc Natl Acad Sci USA*. (2006), vol. 103, pp. 17378-17383.
432. M. Momcilovic, S.-P. Hong, M. Carlson, in *J Biol Chem*. (2006), vol. 281, pp. 25336-25343.
433. L.-J. Kong, L. Hanley-Bowdoin, in *Plant Cell*. (2002), vol. 14, pp. 1817-1832.
434. K. Elbing, R. R. McCartney, M. C. Schmidt, in *Biochem J*. (2006), vol. 393, pp. 797-805.
435. E. M. Rubenstein, R. R. McCartney, C. Zhang, K. M. Shokat, M. K. Shirra, K. M. Arndt, M. C. Schmidt, in *J Biol Chem*. (2008), vol. 283, pp. 222-230.
436. A. Ruiz, X. Xu, M. Carlson, in *Proc Natl Acad Sci USA*. (2011), vol. 108, pp. 6349-6354.
437. A. E. Marley, J. E. Sullivan, D. Carling, W. M. Abbott, G. J. Smith, I. W. Taylor, F. Carey, R. K. Beri, in *Biochem J*. (1996), vol. 320 (Pt 3), pp. 801-806.

438. S. R. Cutler, P. L. Rodriguez, R. R. Finkelstein, S. R. Abrams, in *Annu Rev Plant Biol*. (2010), vol. 61, pp. 651-679.
439. D. Tsugama, S. Liu, T. Takano, in *FEBS Lett*. (2012), vol. 586, pp. 693-698.
440. A. P. Fordham-Skelton, P. Chilley, V. Lumbreras, S. Reignoux, T. R. Fenton, C. C. Dahm, M. Pages, J. A. Gatehouse, in *Plant J*. (2002), vol. 29, pp. 705-715.
441. D. Kerk, T. R. Conley, F. A. Rodriguez, H. T. Tran, M. Nimick, D. G. Muench, G. B. G. Moorhead, in *Plant J*. (2006), vol. 46, pp. 400-413.
442. T. Niittylä, S. Comparot-Moss, W.-L. Lue, G. Messerli, M. Trevisan, M. D. J. Seymour, J. A. Gatehouse, D. Villadsen, S. M. Smith, J. Chen, S. C. Zeeman, A. M. Smith, in *J Biol Chem*. (2006), vol. 281, pp. 11815-11818.
443. O. Kötting, D. Santelia, C. Edner, S. Eicke, T. Marthaler, M. S. Gentry, S. Comparot-Moss, J. Chen, A. M. Smith, M. Steup, G. Ritte, S. C. Zeeman, in *Plant Cell*. (2009), vol. 21, pp. 334-346.
444. J. Kim, M. Kundu, B. Viollet, K.-L. Guan, in *Nature cell biology*. (2011), vol. 13, pp. 132-141.
445. A. S. Löffler, S. Alers, A. M. Dieterle, H. Keppeler, M. Franz-Wachtel, M. Kundu, D. G. Campbell, S. Wesselborg, D. R. Alessi, B. Stork, in *autophagy*. (2011), vol. 7, pp. 696-706.
446. S. Horman, D. Vertommen, R. Heath, D. Neumann, V. Mouton, A. Woods, U. Schlattner, T. Wallimann, D. Carling, L. Hue, M. H. Rider, in *J Biol Chem*. (2006), vol. 281, pp. 5335-5340.
447. R. L. Hurley, L. K. Barré, S. D. Wood, K. A. Anderson, B. E. Kemp, A. R. Means, L. A. Witters, in *J Biol Chem*. (2006), vol. 281, pp. 36662-36672.
448. N. Djouder, R. D. Tuerk, M. Suter, P. Salvioni, R. F. Thali, R. Scholz, K. Vaahtomeri, Y. Auchli, H. Rechsteiner, R. e. A. Brunisholz, B. Viollet, T. P. MÄKel&Auml, T. Wallimann, D. Neumann, W. Krek, in *The EMBO Journal*. (2009), vol. 29, pp. 1-13.
449. K. I. Mitchelhill, B. J. Michell, C. M. House, D. Stapleton, J. Dyck, J. Gamble, C. Ullrich, L. A. Witters, B. E. Kemp, in *J Biol Chem*. (1997), vol. 272, pp. 24475-24479.
450. A. Woods, D. Vertommen, D. Neumann, R. Turk, J. Bayliss, U. Schlattner, T. Wallimann, D. Carling, M. H. Rider, in *J Biol Chem*. (2003), vol. 278, pp. 28434-28442.
451. F. S. Oppermann, F. Gnad, J. V. Olsen, R. Hornberger, Z. Greff, G. Kéri, M. Mann, H. Daub, in *Molecular & Cellular Proteomics*. (2009), vol. 8, pp. 1751-1764.
452. R. Maor, A. Jones, T. S. Nühse, D. J. Studholme, S. C. Peck, K. Shirasu, in *Mol Cell Proteomics*. (2007), vol. 6, pp. 601-610.
453. D.-Y. Kim, M. Scalf, L. M. Smith, R. D. Vierstra, in *The Plant Cell*. (2013), vol. 25, pp. 1523-1540.
454. J. H. Lee, W. Terzaghi, G. Gusmaroli, J. B. Charron, H. J. Yoon, H. Chen, Y. J. He, Y. Xiong, X. W. Deng, in *Plant Cell* (2008), vol. 20, pp. 152-167.
455. M. A. Wilson, E. Koutelou, C. Hirsch, K. Akdemir, A. Schibler, M. C. Barton, S. Y. R. Dent, in *Molecular and Cellular Biology*. (2011), vol. 31, pp. 3126-3135.
456. A. K. Al-Hakim, A. Zagorska, L. Chapman, M. Deak, M. Peggie, D. R. Alessi, in *Biochem. J.* (2008), vol. 411, pp. 249-260.
457. D. Moreno, M. C. Towler, D. G. Hardie, E. Knecht, P. Sanz, in *Mol Biol Cell*. (2010), vol. 21, pp. 2578-2588.

458. J. Qi, J. Gong, T. Zhao, J. Zhao, P. Lam, J. Ye, J. Z. Li, J. Wu, H.-M. Zhou, P. Li, in *The EMBO Journal*. (2008), vol. 27, pp. 1537-1548.
459. T. Rubio, S. Vernia, P. Sanz, in *Mol Biol Cell*. (2013), vol. 24, pp. 1801-1811.
460. P. H. Castro, R. M. Tavares, E. R. Bejarano, H. Azevedo, in *Cell Mol Life Sci*. (2012), vol. 69, pp. 3269-3283.
461. Y.-y. Lin, J.-y. Lu, J. Zhang, W. Walter, W. Dang, J. Wan, S.-C. Tao, J. Qian, Y. Zhao, J. D. Boeke, S. L. Berger, H. Zhu, in *CELL*. (2009), vol. 136, pp. 1073-1084.
462. J.-y. Lu, Y.-y. Lin, J.-C. Sheu, J.-T. Wu, F.-J. Lee, Y. Chen, M.-I. Lin, F.-T. Chiang, T.-Y. Tai, S. L. Berger, Y. Zhao, K.-S. Tsai, H. Zhu, L.-M. Chuang, J. D. Boeke, in *CELL*. (2011), vol. 146, pp. 969-979.
463. Y.-y. Lin, S. Kiihl, Y. Suhail, S.-Y. Liu, Y.-h. Chou, Z. Kuang, J.-y. Lu, C. N. Khor, C.-L. Lin, J. S. Bader, R. Irizarry, J. D. Boeke, in *Nature*. (2012), vol. 482, pp. 251-255.
464. Y.-y. Lin, S. Kiihl, Y. Suhail, S.-Y. Liu, Y.-h. Chou, Z. Kuang, J.-y. Lu, C. N. Khor, C.-L. Lin, J. S. Bader, R. Irizarry, J. D. Boeke, in *Nature*. (2013), vol. 503, pp. 146-146.
465. M. D. Resh, in *Biochim Biophys Acta*. (1999), vol. 1451, pp. 1-16.
466. S. S. Lin, in *Journal of Biological Chemistry*. (2003), vol. 278, pp. 13390-13397.
467. K. Ashrafi, T. A. Farazi, J. I. Gordon, in *J Biol Chem*. (1998), vol. 273, pp. 25864-25874.
468. J. A. Traverso, T. Meinnel, C. Giglione, in *Plant Signal Behav*. (2008), vol. 3, pp. 501-502.
469. D. Shao, S.-i. Oka, T. Liu, P. Zhai, T. Ago, S. Sciarretta, H. Li, J. Sadoshima, in *Cell Metabolism*. (2014), vol. 19, pp. 232-245.

1.7 | Aims and thesis scope

The aim of the work described in this thesis was to gain further insight on SnRK1 signaling in plants, namely through dissection of its regulatory mechanisms. We focused on novel posttranslational modifications of the SnRK1 kinase that could explain its activation in response to energy deprivation conditions. Considering 1) the presence of high probability SUMO attachment site (hpSAS) motifs on SnRK1α1 catalytic subunit, 2) the detection of high molecular weight (hMW) SnRK1α1 forms potentially corresponding to SnRK1α1-SUMO conjugates, and 3) the important roles ascribed to the SUMO pathway and SnRK1 signaling in the plant response to various biotic and abiotic stresses (*22, 29, 103, 221, 259, 447, 459*), we hypothesized that SUMO and SnRK1 could be entwined in the plant stress response, namely through sumoylation of the SnRK1 kinase, and possibly through SnRK1-dependent phosphorylation of SUMO pathway components, due to several SnRK1 phosphorylation consensus motifs in these proteins.

Detailed evidence of posttranslational modification of the SnRK1 complex by sumoylation and ubiquitylation, and their functional implications in SnRK1-dependent energy signaling in plants, will be provided. Furthermore, a mechanism of signal termination through sumoylation of activated SnRK1 is proposed based on the obtained results, and suggested to be conserved in the SNF1 and AMPK orthologs as well. The next sections will be organized as follows:

Chapter 2 | *Sumoylation of the SnRK1 complex*

In this chapter we present evidence that SnRK1 is sumoylated at the whole complex level, possibly in multiple residues and/or with (poly)SUMO chains. Using yeast two-hybrid assays, a heterologous system that reconstitutes the Arabidopsis SUMO pathway in *E. coli*, and through immunoprecipitation of SnRK1α1 from plants followed by immunodetection with anti-SUMO1 antibody,

we unravel sumoylation as a new layer of regulation of this central kinase in plant energy signaling. We also show that *in planta* SnRK1 sumoylation by SUMO1 is mediated by the E3 SUMO ligase SIZ1. Finally, considering the data presented, together with the reported sumoylation of Snf1 and AMPK *in vivo*, we suggest sumoylation is a conserved posttranslational regulatory mechanism of the central family of SNF1/AMPK/SnRK1 kinases.

Chapter 3 | *Biochemical and functional outcomes of SnRK1 sumoylation*

In this chapter we present evidence that SnRK1 sumoylation is a novel regulatory mechanism that impacts SnRK1 protein stability and thereby impinges on its activity and SnRK1 signaling *in planta*. We suggest that there is a cooperative interplay between SnRK1 sumoylation and its subsequent ubiquitylation, in targeting the protein kinase towards proteasomal degradation. We also present preliminary evidence supporting sumoylation may affect SnRK1 complex composition and a putative oligomerization state.

Chapter 4 | *SnRK1 pathway activation and signal termination*

In this chapter we present evidence suggesting that the SUMO-dependent degradation of SnRK1 is triggered by its activation, as part of a negative feedback loop to prevent deleterious effects derived from overly high SnRK1 signaling. Furthermore, we show that SnRK1 phosphorylates the E3 SUMO ligase SIZ1 *in vitro*, and hypothesize that such mechanism may couple stress and SnRK1 activation to its sumoylation/ubiquitylation, and subsequent degradation *in planta*.

Chapter 5 | *Concluding remarks and future perspectives*

In this chapter we discuss and integrate the main findings resulting from the work carried out, and summarize possible future experiments to follow this work.

CHAPTER 2 |

Sumoylation of the SnRK1 complex

Authors' Contributions

Leonor Margalha and Pierre Crozet contributed equally to the work presented in this chapter. Pierre Crozet did the *E. coli* sumoylation assays, prepared samples for Mass Spectrometry (MS) analyses and did the model of the SnRK1 structure. Konstantin Tomanov did the MS analyses. Carlos Alexandre Elias characterized the *snrk1α1-3* mutant and generated the *SnRK1α1ΔKA1-GFP* plants.

Abstract

Plants sense and adapt to environmental stresses to promote survival under ever-changing conditions. The plant SnRK1 (Snf1-Related protein Kinase 1) is a central component of the stress response conserved in all eukaryotes. It functions as a heterotrimer composed of α-catalytic and β and γ-regulatory subunits. In contrast to its mammalian and yeast homologues, SnRK1α T-loop phosphorylation/dephosphorylation is required but insufficient to determine its activation under stress and subsequent inactivation once homeostasis is restored. Thus, based on several lines of evidence, we hypothesized that other posttranslational modifications, like SnRK1 sumoylation, may be involved. Here, we show that SnRK1 interacts with the E2 SUMO conjugating enzyme in yeast two-hybrid assays and undergoes sumoylation in a heterologous *E. coli* system. Immunoprecipitation experiments further demonstrate that sumoylation of SnRK1 occurs *in planta*, seemingly as a coordinated event at the whole-complex level, as both catalytic and regulatory subunits undergo this modification. Moreover, poly- and/or multisumoylation events seem to occur on these subunits. We identify SIZ1 as the E3 SUMO ligase responsible for SnRK1 sumoylation by SUMO1 in Arabidopsis, and suggest SnRK1 sumoylation adds a new layer of regulation of this central kinase in plant energy signaling.

2.1 | Introduction

The plant Snf1-related Protein Kinase 1 (SnRK1) is a central component of a sophisticated signaling network, at the interface of several stress, hormonal, and metabolic signaling pathways, that translates plant carbon status into defense, growth and developmental decisions (*1*). SnRK1 is the plant ortholog of the budding yeast SNF1 (Sucrose-non-fermenting 1) and mammalian AMPK (AMP-activated protein kinase). All three enzymes function as heterotrimeric

complexes composed of an α-catalytic and two β- and γ-regulatory subunits, and in all cases kinase activity requires phosphorylation of a conserved T-loop threonine in the α-subunit (*2-6*). However, the clear connection between T-loop phosphorylation and kinase activation in response to declining energy levels observed in SNF1 and AMPK is not established in plants (*2, 7-9*). Moreover, SnRK1 intrinsic kinase activity appears unchanged under conditions that induce SnRK1 signaling as well as in *pp2c* mutants that display deficient repression of the SnRK1 pathway (*2, 7, 9*). Additional regulatory mechanisms may operate in such conditions to modulate SnRK1 signaling accordingly. Finally, the plant enzyme has incorporated unique regulatory subunits and other distinct features, presumably to respond to plant-specific signals and/or to perform plant-specific functions (*4, 5, 10, 11*). These studies reveal the atypical nature of the plant kinase and underscore our lack of knowledge on the factors that determine the signaling lifetime of such a central component.

SUMO (Small Ubiquitin-like Modifier) is a small protein (about 12kDa) that is conjugated posttranslationally to target proteins in a reversible manner to regulate crucial biological processes. Sumoylation is required for normal growth and development, and consequently, mutants defective in the SUMO pathway are either lethal or display strong phenotypes (*12, 13*). In addition, exposure to environmental or metabolic stresses induces a dramatic accumulation of SUMO conjugates, constituting what is considered to be a cellular protective response in all eukaryotes (*14*). Accordingly, many SUMO targets identified in Arabidopsis are stress-related components (*15-17*) and sumoylation is important for a wide range of plant stress responses (*18*). Diverse biochemical functions have been ascribed to sumoylation, including changes in stability, activity, and subcellular localization, primarily through the modulation of intra- and intermolecular protein interactions (*19, 20*).

Sumoylation requires the maturation of the SUMO moiety by a SUMO protease, exposing a characteristic C-terminal di-glycine motif. Mature SUMO is then activated by the SUMO activating enzyme (E1 enzyme, SAE1/2 in

Arabidopsis), with the formation of a thioester bond, and transferred to the SUMO conjugating enzyme (E2 enzyme, SCE1 in Arabidopsis) through a transthiolation reaction. Finally, SCE conjugates SUMO to a target lysine, either alone or with the help of an E3 SUMO ligase (SIZ1 and HPY2, in Arabidopsis) (*21*). Substrates can carry single SUMO moieties or SUMO polymers, and in Arabidopsis, two E4 SUMO ligases were recently implicated in the assembly of such SUMO chains (*22*). SUMO chains have various roles and can trigger ubiquitylation via SUMO-targeted ubiquitin ligases (STUbLs), hence targeting the protein for proteasomal degradation (*23, 24*).

The work here described aimed at deciphering additional posttranslational regulatory mechanisms of the SnRK1 kinase. We focused on the modification of SnRK1 by SUMO due to the presence of high probability SUMO attachment site (hpSAS) motifs on the SnRK1α1 catalytic subunit, and to the detection of high molecular weight (hMW) SnRK1α1 forms, potentially corresponding to SnRK1α1-SUMO conjugates. Recently, SnRK1α1 was identified as an interactor of two SUMO machinery components, the E2 SUMO conjugating enzyme 1 (SCE1), and the SUMO protease Early in Short Days 4 (ESD4) (*16*). SUMO substrates can be directly recognized and bound on their target lysines *in vitro* by the E2 conjugation enzyme, and thus the SnRK1α1-SCE1 interaction also suggests that SnRK1α1 may be a target of sumoylation. Furthermore, SUMO pathway and SnRK1 signaling share important roles in the plant response to various biotic and abiotic stresses (*2, 15, 17, 18, 25-27*). In this chapter, we present evidence that SnRK1 is sumoylated at the whole complex level *in planta*, hence adding a new layer of regulation of this central kinase in plant energy signaling.

2.2 | Results

2.2.1 | SnRK1α1 bears two high probability SUMO attachment sites

Analysis of the primary structure of Arabidopsis SnRK1α1 with the bioinformatic tool SUMOplot™ (www.abgent.com) retrieved two high probability SUMO attachment sites (hpSAS), latter defined with an arbitrary cutoff value of hpSAS ≥91% (*16*). Both hpSAS, involving lysine(s) (K) 471 and 144, matched the canonical ΨKxE motif (**Introduction**- SCE1). Other putative sumoylation sites, but with a lower probability score, were retrieved at K465, K230, K292 and K421. The predicted target K(s) on SnRK1α1 are listed in descending order of probability of SUMO attachment (**Figure** 2.1). In accordance with the high level of conservation within the kinase domain (*28*), the hpSAS motif encompassing K144 was fully conserved amongst SnRK1 orthologs in yeast, moss, Drosophila and mammals. None of the other predicted SUMO attachment sites were conserved amongst SnRK1α1 orthologs in opisthokonts (**Appendix - Figure** 1).

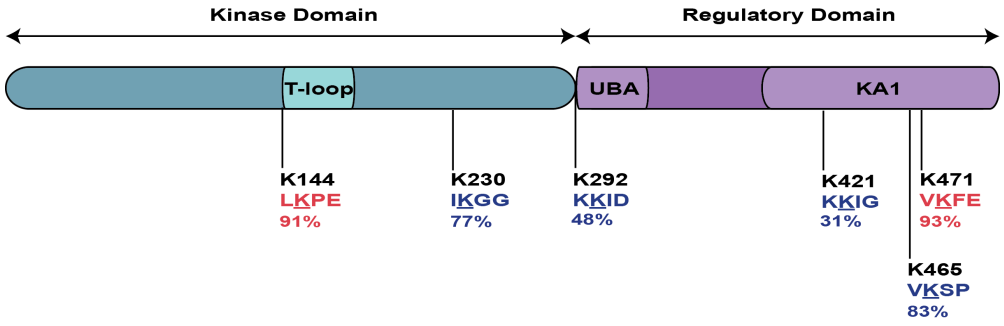

Figure 2.1 | Potential SUMO attachment sites on SnRK1α1 predicted using SUMOplot™.

Predicted SUMO target lysines (K) are identified on SnRK1α1 domains. Numbers below SUMO attachment site (SAS) motifs depict their probability scores. In red, hpSAS (≥91%), and in blue, SAS with a probability score lower than 91%. UBA, ubiquitin associated domain; KA1, kinase associated domain 1.

2.2.2 | SnRK1α1 catalytic subunit interacts with SCE1 in Yeast two-hybrid assays

The E2 SUMO conjugating enzyme 1 (SCE1) is crucial in SUMO conjugation and binds directly the target through a patch surrounding the active site (*29, 30*). As a first approach to test whether SnRK1 is modified by sumoylation, we assayed the interaction between the Arabidopsis E2 SCE1 and SnRK1α1 by yeast two-hybrid assays (Y2H). We observed that SnRK1α1 interacts with SCE1 and that this interaction occurs through the regulatory domain (RD) of SnRK1α1. Yeast cells transformed with SCE1 and SnRK1α1-RDΔKA1, or with SnRK1α1 kinase domain (KD) were also able to grow but in less stringent selection media. Collectively, these data indicate that several regions of SnRK1α1 interact with SCE1 in Y2H assays (**Figure** 2.2A), and that SnRK1α1 is potentially sumoylated on the kinase and regulatory domains.

We also tested if SCE1 could interact with the ortholog of SnRK1α1 in Drosophila, SNF1A. Interestingly, the full-length (FL) catalytic subunit SNF1A interacted with SCE1 in the Y2H assay, suggesting that SNF1A may also be regulated by sumoylation (**Figure** 2.2B).

A proteome-wide Y2H screen for SUMO substrates in Arabidopsis, using the E2 SCE1 or ESD4 SUMO protease as baits, retrieved subsequently the interaction between FL SnRK1α1 with both referred SUMO machinery components (*16*). The results obtained by Elrouby et al. strengthened our own results and reinforced the possibility of SnRK1 being sumoylated.

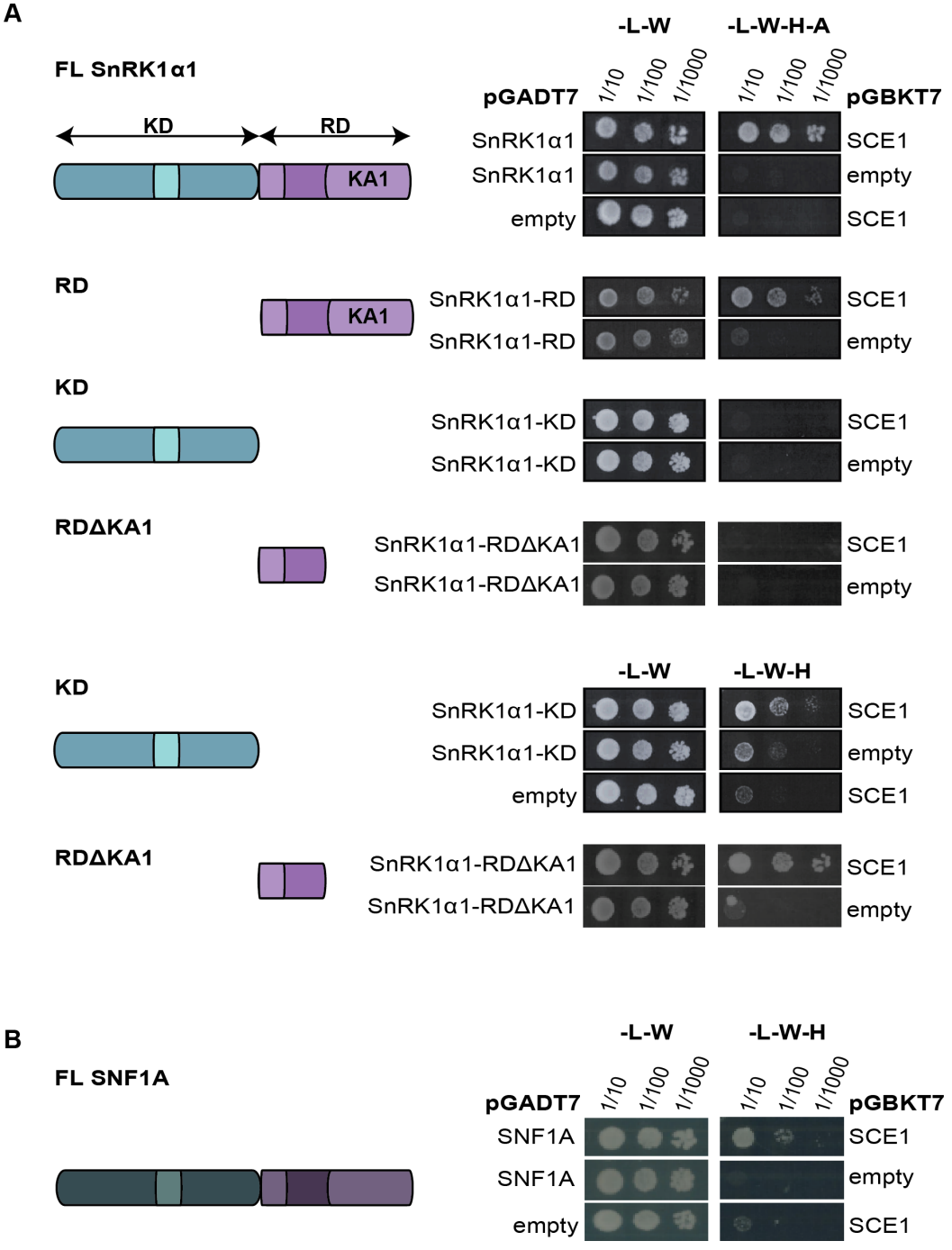
A
FL SnRK1α1
KD
RD
KA1
-L-W
-L-W-H-A
1/10
1/100
1/1000
pGADT7
pGBKT7
SnRK1α1
SCE1
SnRK1α1
empty
empty
SCE1
RD
KA1
SnRK1α1-RD
SCE1
SnRK1α1-RD
empty
KD
SnRK1α1-KD
SCE1
SnRK1α1-KD
empty
RDΔKA1
SnRK1α1-RDΔKA1
SCE1
SnRK1α1-RDΔKA1
empty
KD
-L-W
-L-W-H
SnRK1α1-KD
SCE1
SnRK1α1-KD
empty
empty
SCE1
RDΔKA1
SnRK1α1-RDΔKA1
SCE1
SnRK1α1-RDΔKA1
empty
B
FL SNF1A
-L-W
-L-W-H
1/10
1/100
1/1000
pGADT7
pGBKT7
SNF1A
SCE1
SNF1A
empty
empty
SCE1

Figure 2.2 | Arabidopsis SnRK1α1 and Drosophila SNF1A interact with the E2 SUMO Conjugating Enzyme 1 (SCE1) in Y2H assays.

The full-length coding sequence (FL), C-terminal Regulatory Domain (RD) encompassing the KA1 domain, C-terminal RD without the KA1 domain (RDΔKA1) or the N-terminal Kinase Domain (KD) of SnRK1α1 (**A**), as well as FL SNF1A (**B**), were cloned into pGADT7 in fusion with the GAL4 activation domain (AD) and co-transfected with pGBKT7 harboring either the GAL4 binding domain (BD) alone (empty) or in fusion with the full-length SCE1. The growth of transformed AH109 yeast cells was assessed in permissive [-Leucine (L), -Tryptophan (W)], selective [-L-W-Histidine (H)], or more stringent [-L-W-H,-Adenine (A)] media. A representative experiment of a minimum of two independent assays is shown.

2.2.3 | Multiple SnRK1 subunits are sumoylated in a heterologous system in *E. coli*

To investigate whether the interaction between SnRK1α1 and SCE1 results into SnRK1 sumoylation, we first employed a heterologous system in which the Arabidopsis sumoylation machinery is reconstituted and co-expressed with individual potential substrates in *E. coli* (*31*). In the presence of mature SUMO1 (SUMO1-GG) or mature SUMO3 (SUMO3-GG), SnRK1α1 displayed a clear sumoylation signal characterized by the presence of high molecular weight (hMW) SnRK1α1 forms (marked by red arrowheads) in Western-blot (WB) analyses. This signal was absent when the corresponding non-conjugatable isoforms (SUMO-AA) were used as negative controls (**Figure** 2.3A).

Sumoylation often targets groups of functionally engaged proteins that may pre-assemble upon given stimuli, regulating entire signaling networks (*19*). Thus, we next decided to explore if the regulatory subunits of the SnRK1 heterotrimeric complex could also be sumoylated. Using the *E. coli* heterologous system, we could observe sumoylation of both SnRK1β1 and SnRK1β2 regulatory subunits, but not of the γ-type regulatory subunit, SnRK1βγ (**Figure** 2.3A). SnRK1γ was also clearly sumoylated (**Figure** 2.3A). However, the

functional connection of this potential γ-subunit to SnRK1 remains uncertain, as it does not interact with the other established subunits [**Figure** 2.6C, (*10, 11*)]. In all sumoylated substrates, multiple bands with slower migration could be detected, indicating multi- and/or polysumoylation events. SUMO1 and SUMO3 isoforms generated similar sumoylation patterns within the same substrate (for SnRK1γ only SUMO3 was tested), but in most cases the intensity of the signal was stronger with SUMO3. Altogether, these results indicate that in the *E. coli* heterologous system, SUMO is conjugated to several and specific components of the SnRK1 complex in Arabidopsis.

To obtain further insight regarding a conserved regulation by sumoylation amongst SnRK1 orthologs, we also tested if the Drosophila catalytic subunit SNF1A could be a target of sumoylation using the same system. Indeed, we could detect sumoylation of the SNF1A C-terminal domain in the presence of the SUMO3 conjugatable isoform (**Figure** 2.3B). Since human AMPK (*32*) (*33*) and yeast SNF1 (*34*) were recently identified as sumoylation targets as well, it is possible that all members of the eukaryotic SNF1/AMPK/SnRK1 family of protein kinases are similarly regulated by sumoylation.

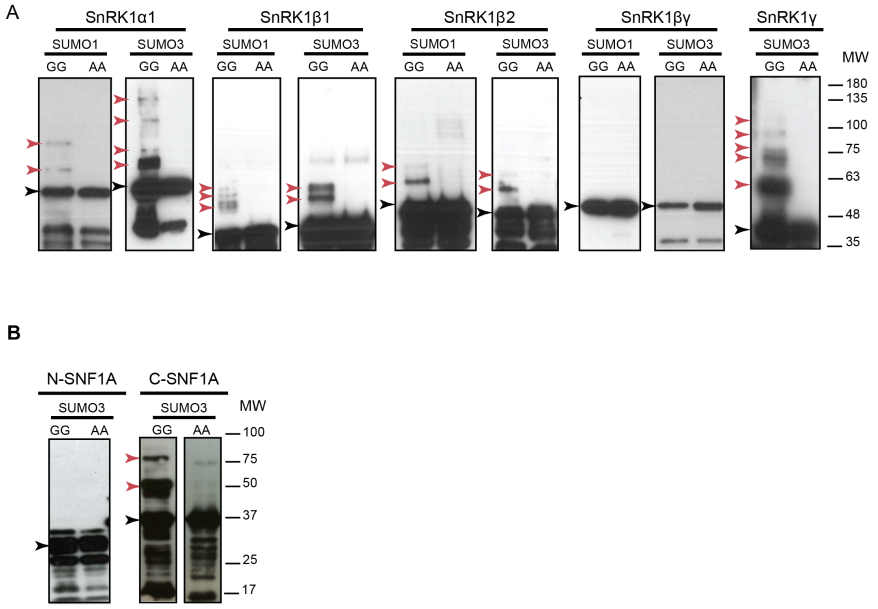

Figure 2.3 | Multiple SnRK1 subunits, as well as the Drosophila SNF1A catalytic subunit, are sumoylated in a heterologous *E. coli* system.

A-B. SnRK1 or SNF1A subunits harboring 6*Histidine (His) and T7 tags were co-expressed in *E. coli* with the indicated SUMO isoform together with the SUMO-activating (AtSAE1a/AtSAE2) and SUMO-conjugating (AtSCE1) enzymes. SnRK1 subunits were purified via the His-tag by immobilized metal ion affinity chromatography (IMAC) and immunoblotted against their T7 tag. GG and AA refer to conjugatable and non-conjugatable SUMO variants, respectively. Unmodified SnRK1 subunits have an approximate molecular weight (MW) of 58kDa (α1), 30kDa (β1), 32kDa (β2), 53kDa (βγ) and 48kDa (γ), whereas unmodified SNF1A N- and C-terminal regions have a MW of 33kDa (N) and 31kDa (C), respectively. His- and T7 tags give a small increment of 2kDa to the respective protein MW, and a single SUMO moiety can contribute with an average increment of 20kDa (*20*). Black and red arrowheads designate non-sumoylated and sumoylated proteins, respectively.

In order to better understand the molecular mechanism of SnRK1 sumoylation, we decided to identify the target lysine (K) residue(s) in SnRK1α1 catalytic subunit using the *E. coli* sumoylation assay. Several sumoylation events were observed with constructs expressing only the kinase domain (KD; 1-293) or the regulatory domain (RD; 294-512) (**Figure** 2.4A), suggesting that SnRK1α1 is sumoylated on several residues of both domains (**Figure** 2.4B), in agreement with the results obtained from the Y2H assay (**Figure** 2.2A). Mutation of both hpSAS residues K471 and K144 to arginine (R) did not prevent SnRK1α1 sumoylation in the *E. coli* assay (**Figure** 2.4C), suggesting that other residues might be involved. Therefore, to identify the target K residues, we performed Liquid Chromatography-Tandem Mass Spectrometry (LC-MS/MS) of sumoylated SnRK1α1 KD and RD (**Figure** 2.4D). To this end, we employed regular mature SUMO3 (SUMO3-GG) and a variant ($SUMO3^{S91R}$-GG) that yields a small tryptic footprint and thereby facilitates LC-MS/MS analyses (*31*). We focused these analyses on SUMO3 due to the stronger signal intensity but similar sumoylation pattern compared with SUMO1, allowing a better yield. We uncovered nine sumoylated residues (including K144 but not K471), of which

two are located in the KA1 domain and seven in the KD (**Figure** 2.4A and 2.4E). The structural model of the SnRK1 complex predicts that all of these residues are accessible (**Figure** 2.4E, residues indicated). A single K390R mutation and a double K34R/K63R mutation were sufficient to abrogate sumoylation of the RD and KD, respectively (**Figure** 2.4F). Furthermore, sumoylation could no longer be detected in the full-length SnRK1α1$^{K34/63/390R}$ triple mutant (**Figure** 2.4G), suggesting that these three K residues could be the genuine targets of sumoylation *in vivo*.

LC-MS/MS analysis was also performed on sumoylated C-terminal SNF1A (**Figure** 2.3B), and retrieved four sumoylated residues (SNF1A K447, K456, K469 and K505). However, none of these sumoylated K(s) are conserved amongst SnRK1α1 and SNF1A kinases (**Appendix - Figure** 1).

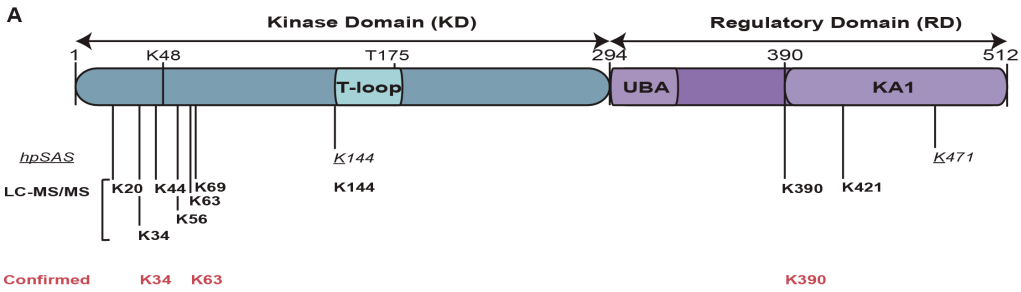

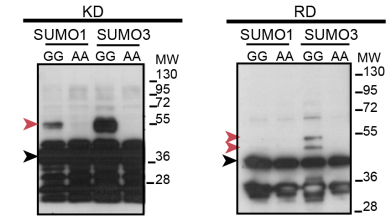

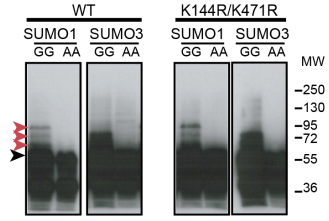

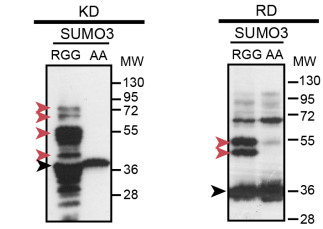

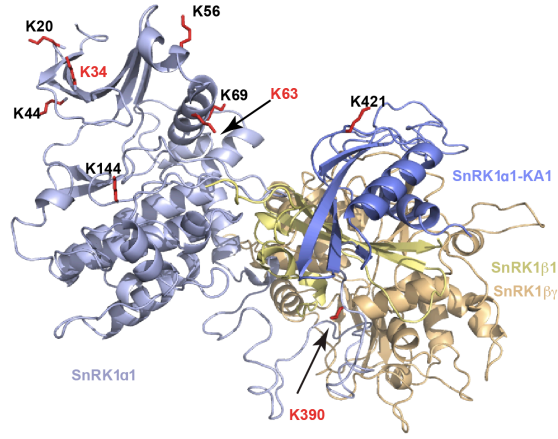

SUMO3	K in KD	K in RD
GG	20, 34, 56, 69 144	390
RGG	20, 34, 44, 56, 63, 69, 144	390, 421

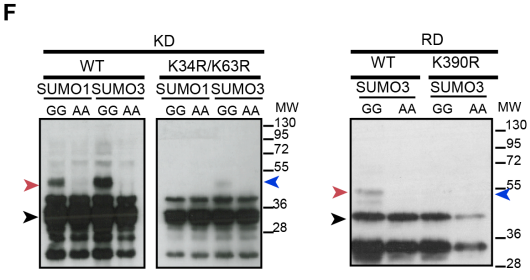

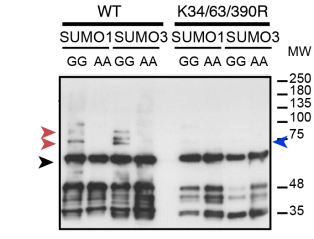

Figure 2.4 | SnRK1α1 residues sumoylated in the *E. coli* assay.

A. Schematic representation of SnRK1α1. K48 (catalytic phospho-transfer) and T175 (activating T-loop phosphorylation) are two residues crucial for SnRK1 enzymatic activity. Predicted hpSAS residues [**Figure** 2.1, (*16*); results in **C**], residues found by LC-MS/MS analysis (from sample shown in **D**), and residues confirmed to be crucial for sumoylation in *E. coli* (results in **F** and **G**) are indicated. Numbering corresponds to gene model At3g01090.1 according to TAIR. **B-D, F-G**. Sumoylation assay using the Arabidopsis SUMO machinery reconstituted in *E. coli*. The indicated SnRK1α1 variants harboring 6*His and T7 tags were co-expressed in *E. coli* with the indicated SUMO isoform together with the SUMO-activating (AtSAE1a/AtSAE2) and SUMO-conjugating (AtSCE1) enzymes. GG and AA refer to conjugatable and non-conjugatable SUMO variants, respectively. Sumoylation was assessed by Western-blot (WB) using antibodies against the T7-tag. **B**. Several residues are sumoylated in SnRK1α1, as shown by the positive sumoylation signal with truncated SnRK1α1 variants harboring only the KD or RD. Black and red arrowheads designate non-sumoylated and sumoylated proteins, respectively. **C**. Mutation of predicted hpSAS residues (**A**, "*hpSAS*") does not abolish SnRK1α1 sumoylation. **D**. WT SnRK1α1 samples used to identify the sumoylated residues. SnRK1α1KD and SnRK1α1RD were purified via the His tag by IMAC and immunoblotted against the T7 tag. Bands corresponding to sumoylated SnRK1α1 (red arrowhead) were excised and analyzed by LC-MS/MS. "RGG", mature SUMO3 mutated at the C-terminus to generate smaller tryptic peptides more amenable for MS analyses. **E**. The structure of the SnRK1 complex in cartoon representation was modeled with the Swiss model portal using the AMPK structure as a template (2Y94). SnRK1α1 is in blue [with the KA1 domain in dark blue; residues 14 to 395 coupled to a model of the KA1 (*9*) from 396 to 512], SnRK1β1 is in yellow (209-281), and SnRK1βγ is in wheat (152-486). SnRK1α1 K residues found to be sumoylated by LC-MS/MS (**A**, "**LC-MS/MS**") are shown with their side chains in stick representation in red. The three K numbered in red correspond to the three lysines confirmed to be crucial for the sumoylation signal using a site-directed mutagenesis approach (**A**, "**Confirmed**"; see panel **F-G**). **F**. Same analysis as in **B**, on total soluble protein extract from bacteria expressing the indicated SnRK1α1 domains mutated or not for the K(s) shown. An area pointed out with a blue arrowhead indicates where the sumoylated protein should be in the mutated variant (compare to red arrowhead in the WT control of the same panel). **G**. Validation of the mutational analysis in **F** using affinity-purified protein from bacteria expressing a full length SnRK1α1 mutated or not for the three confirmed K(s) (K34/63/390). KD, Kinase domain; RD, Regulatory Domain; KA1, Kinase Associated 1 domain; UBA, Ubiquitin-Associated domain, MW, Molecular Weight.

2.2.4 | SnRK1 is sumoylated *in planta*

To determine if SnRK1 sumoylation also occurs *in planta*, we first generated transgenic Arabidopsis lines expressing SnRK1α1-GFP to pull down SnRK1α1 *via* its GFP-tag, and to assess the presence of SUMO-conjugates by immunodetection with anti-SUMO1 antibody. These lines express SnRK1α1 to a similar level than wild-type (WT) plants and were produced by complementing a *snrk1α1* knockout mutant with SnRK1α1 fused to GFP and controlled by its own upstream and downstream regulatory regions (*pSnRK1α1::SnRK1α1-GFP::tSnRK1α1/snrk1α1-3*; hereafter referred as *SnRK1α1-GFP*; **Figure** 2.5A-D).

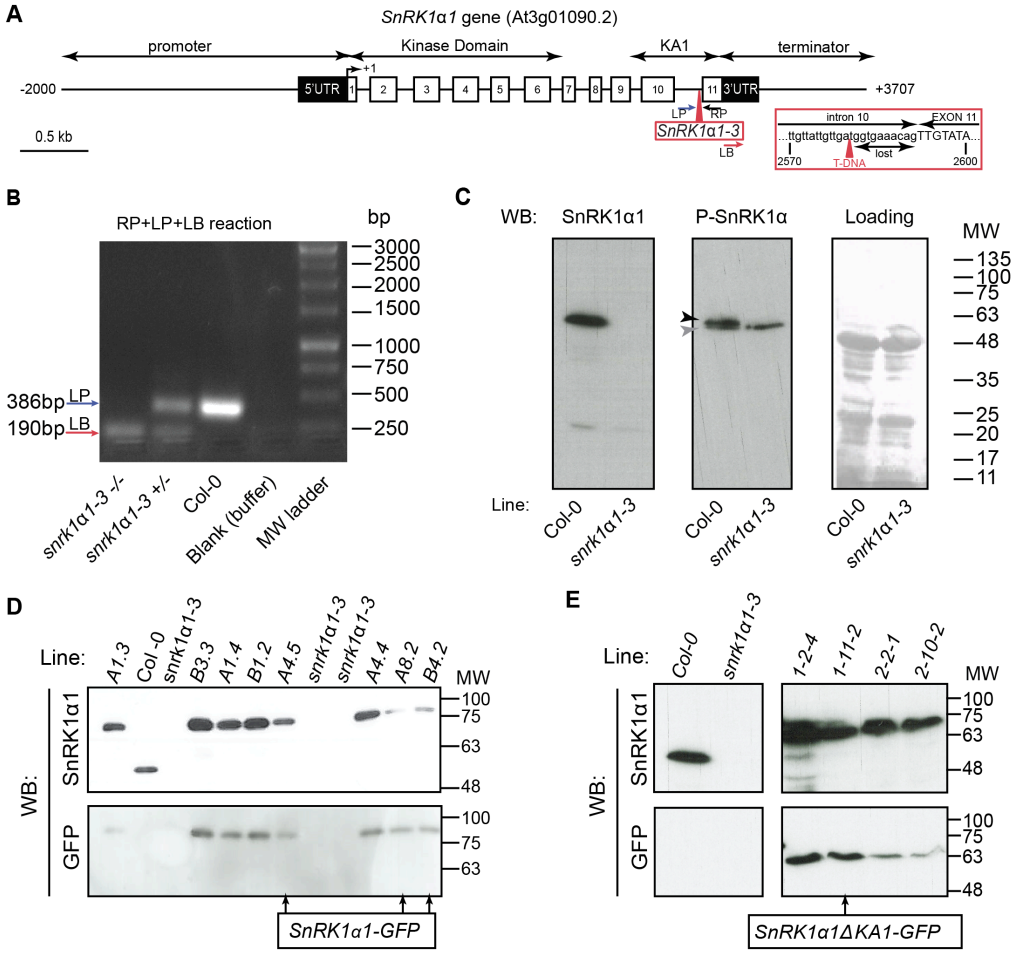

Figure 2.5 | Generation of *SnRK1α1-GFP* transgenic plant lines.

A. Structure of the *SnRK1α1* gene (At3g01090.2 gene model). All indicated positions have the start codon (noted +1) as a reference. The promoter (2kb upstream of the start codon) and terminator (1kb downstream of the stop codon) regions used, as well as the kinase and KA1 domains, are indicated. The location of the T-DNA insertion defining the *snrk1α1-3* mutant line (GABI-KAT: 579E09) is indicated as well as the position of the three genotyping primers (LP, Left Primer; RP, Right Primer; LB, Left Border; **Appendix Table 1**). The sequence providing the exact location of the insertion (2583) is indicated inside the red box ("lost" denotes the 11 bases lost due to the insertion). White boxes correspond to exons and the straight lines between them to introns. Black boxes correspond to UTR regions and the straight lines outside are regulatory regions. **B**. Genotyping PCR using primers LP, RP, and LB, shown in **A**. The expected sizes of the two products are indicated on the left (LP: LP-RP reaction, 386bp indicates WT allele; LB: LB-RP reaction, 190bp indicating a mutant allele). **C**. Total proteins from adult Arabidopsis leaves of Col-0 or the *snrk1α1-3* mutant were analyzed by Western-blot (WB) using antibodies against SnRK1α1 or P-AMPK (recognizing the phosphorylated T175/176 of SnRK1α1/α2, respectively). The black and grey arrowheads indicate phospho-SnRK1α1 and phospho-SnRK1α2, respectively. Equal loading is shown by Coomassie staining of the membrane ("loading"). **D**. *SnRK1α1-GFP* transgenic lines were generated by transformation of the *snrk1α1-3* mutant with the pBm43GW,0 MultiSite Gateway Binary vector, containing the promoter, the genomic coding region (exons-introns) fused to GFP, and the terminator of the SnRK1α1 gene (At3g01090.2; indicated in A). Several transformants were tested for the presence of SnRK1α1-GFP by WB using antibodies against SnRK1α1 and GFP. The selected lines (presenting a SnRK1α1 signal close to Col-0) are indicated with arrows. **E**. *SnRK1α1ΔKA1-GFP* transgenic lines analyzed as in **D**. Several transformants were tested for the presence of SnRK1α1ΔKA1-GFP by WB using antibodies against SnRK1α1 and GFP. MW, Molecular Weight.

Expression of SnRK1α1-GFP in these lines allowed the rapid immunoprecipitation of SnRK1α1 under mild denaturing conditions, which is a prerequisite for detecting the scarce and otherwise extremely labile SUMO conjugates (*35*). As shown in **Figure** 2.6A, SUMO1 conjugates were detected in immunoprecipitates from *SnRK1α1-GFP* (FL) plants but not from control *35S-GFP* plants (Ctrl). Interestingly, SUMO1 conjugates associated with SnRK1α1-GFP were not resolved as distinct bands, but rather as a high molecular weight (hMW) ladder, suggesting the formation of (poly)SUMO chains and/or the

sumoylation of multiple residues. The same SUMO1 pattern was obtained with two other independent *SnRK1α1-GFP* lines (**Figure** 2.6B). The presence of hMW SnRK1α1 forms in the SnRK1α1 immunoblot further supported a possible sumoylation of SnRK1α1 (**Figure** 2.6A, middle panel). Immunodetection with SnRK1β1, SnRK1β2 and SnRK1βγ antibodies confirmed the association of these subunits with SnRK1α1-GFP (**Figure** 2.6C). We could detect hMW forms of SnRK1β1 and SnRK1β2 but not of SnRK1βγ, suggesting that the only SnRK1 regulatory subunits sumoylated *in planta* are the β(s), in accordance with the results obtained in the *E. coli* assay (**Figure** 2.3A). To assess the contribution of β−subunits to the overall SnRK1 sumoylation, we generated a transgenic line expressing a truncated SnRK1α1 variant lacking the KA1 domain (*9*), required for the interaction with β and γ regulatory subunits (*36, 37*) (*pSnRK1α1::SnRK1α1ΔKA1-GFP::tSnRK1α1/snrk1α1-3*; hereafter referred as *SnRK1α1ΔKA1-GFP*, **Figure** 2.5A and E). As expected, we could not detect SnRK1β1, SnRK1β2 or SnRK1βγ associated with SnRK1α1ΔKA1-GFP (Δ) (**Figure** 2.6C). Interestingly, the lack of regulatory subunits was accompanied by a dramatic reduction in SUMO1 conjugates and hMW SnRK1α1 forms (**Figure** 2.6A and C), indicating that the regulatory subunits contribute significantly to the overall sumoylation of the SnRK1 complex. Nevertheless, even if reduced, the presence of SnRK1α1 hMW forms and SUMO1 conjugates in SnRK1α1ΔKA1-GFP immunoprecipitates suggests that the interaction with the regulatory subunits is not strictly necessary for SnRK1α1 sumoylation.

In accordance with previous observations (*10, 11*), SnRK1γ did not co-purify with SnRK1α1-GFP catalytic subunit, immunoprecipitated through its GFP tag (**Figure** 2.6D). Therefore, the putative sumoylation of SnRK1γ does not contribute to the overall sumoylation signal observed for SnRK1.

Collectively, these results suggest that several subunits of the SnRK1 complex are sumoylated *in planta* and that this may involve the formation of SUMO chains and/or the modification of multiple residues.

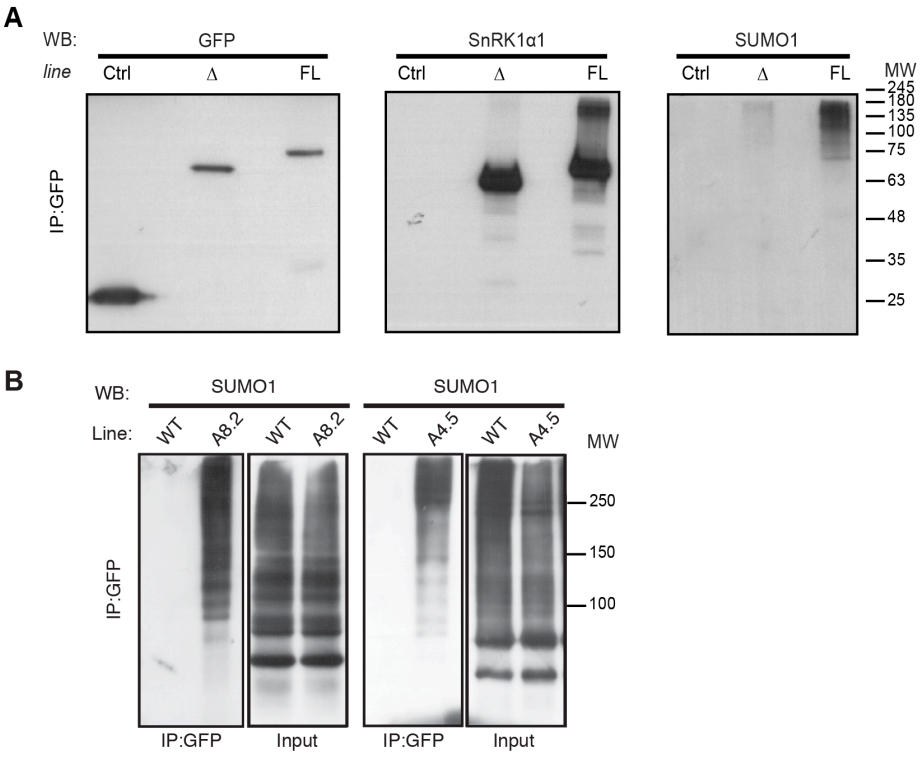
A
WB:
GFP
SnRK1α1
SUMO1
line
Ctrl
Δ
FL
MW
245
180
135
100
75
63
48
35
25
IP:GFP
B
WB:
SUMO1
SUMO1
Line:
WT
A8.2
WT
A8.2
WT
A4.5
WT
A4.5
MW
250
150
100
IP:GFP
IP:GFP
Input
IP:GFP
Input
C
WB:
SnRK1α1
SnRK1β1
SnRK1β2
SnRK1βγ
SUMO1
line
Δ
FL
MW
245
180
135
100
75
63
48
35
IP:GFP
D
WB:
SnRK1β1
SnRK1γ
Sample
Input
IP
Input
IP
line
Ctrl
FL
MW
75
50
37
IP:GFP

Figure 2.6 | The SnRK1 complex is sumoylated *in planta*.

A-D. Leaf crude extracts of plants expressing 35S-GFP (Ctrl), SnRK1α1ΔKA1-GFP (Δ) and full length SnRK1α1-GFP (FL), or WT Col-0 (**B**), were used for GFP immunoprecipitation (IP). Immunoprecipitates were analyzed by Western-Blot (WB) using antibodies against GFP, SnRK1α1 and SUMO1 in **A,** against SUMO1 in **B**, against SnRK1α1, SnRK1β1, SnRK1β2, SnRK1βγ, and SUMO1 in **C**, or against SnRK1β1 and SnRK1γ in **D**. In **B**, two distinct *SnRK1α1-GFP* lines (A8.2 and A4.5, described in **Figure** 2.5D) show the same SUMO1 profile as the one observed after GFP IP of the *SnRK1α1-GFP* line used in **A** (B4.2) and throughout the following work. **D**. SnRK1γ does not co-purify with SnRK1α1-GFP by anti-GFP IP. Co-immunoprecipitation of SnRK1β1 was used as a positive control. In **B** and **D**, the input corresponds to the soluble protein extracts used for IP. Black arrowheads indicate the respective SnRK1 subunits non-sumoylated. Grey brackets designate high molecular weight (hMW) forms of the indicated protein that may correspond to SUMO conjugates. MW, Molecular Weight.

2.2.5 | SnRK1 sumoylation is mediated by the E3 ligase SIZ1 *in planta*

We next decided to identify the E3 ligase(s) responsible for SnRK1 sumoylation *in planta*. Even though SCE1 is sufficient for conjugating the SUMO peptide to a substrate *in vitro*, E3 SUMO ligases are important for substrate specificity and sumoylation efficiency *in vivo* (*38*). In Arabidopsis, only two E3 SUMO ligases have been identified, SIZ1 and HPY2/MMS21 (*39-41*). Given the strong association of SIZ1 with plant stress responses and the involvement of HPY2 mostly in developmental processes (*18*), we first tested if SnRK1 sumoylation could be mediated by SIZ1. To test this, we introduced the *pSnRK1α1::SnRK1α1-GFP::tSnRK1α1* construct previously described (**Figure** 2.5D) in *siz1-2*, a null mutant of SIZ1 (*39*) [hereafter referred as *SnRK1α1-GFP*$_{siz1-2}$ (**Figure** 2.7A)], and performed GFP pull-downs and immunoblot analyses as previously (**Figure** 2.6). As shown in **Figure** 2.7B, SnRK1α1-GFP could be pulled-down from both *SnRK1α1-GFP* ("WT") and *SnRK1α1-GFP*$_{siz1-2}$ ("*siz1-2*") plants. However, immunodetection with anti-SUMO1 antibody revealed the complete absence of SUMO1 conjugates in SnRK1α1-GFP$_{siz1-2}$

immunoprecipitates, demonstrating that SIZ1 is responsible for SnRK1 sumoylation by SUMO1 *in planta*. Importantly, the relative abundance of hMW SnRK1α1 forms in *SnRK1α1-GFP*$_{siz1-2}$ was strongly reduced (more than 50%) when compared to *SnRK1α1-GFP* plants, indicating that a significant proportion of these forms correspond to sumoylated SnRK1α1 (**Figure** 2.7B). Collectively, these results show that SnRK1 is sumoylated *in planta* and that this modification occurs in a SIZ1 dependent manner.

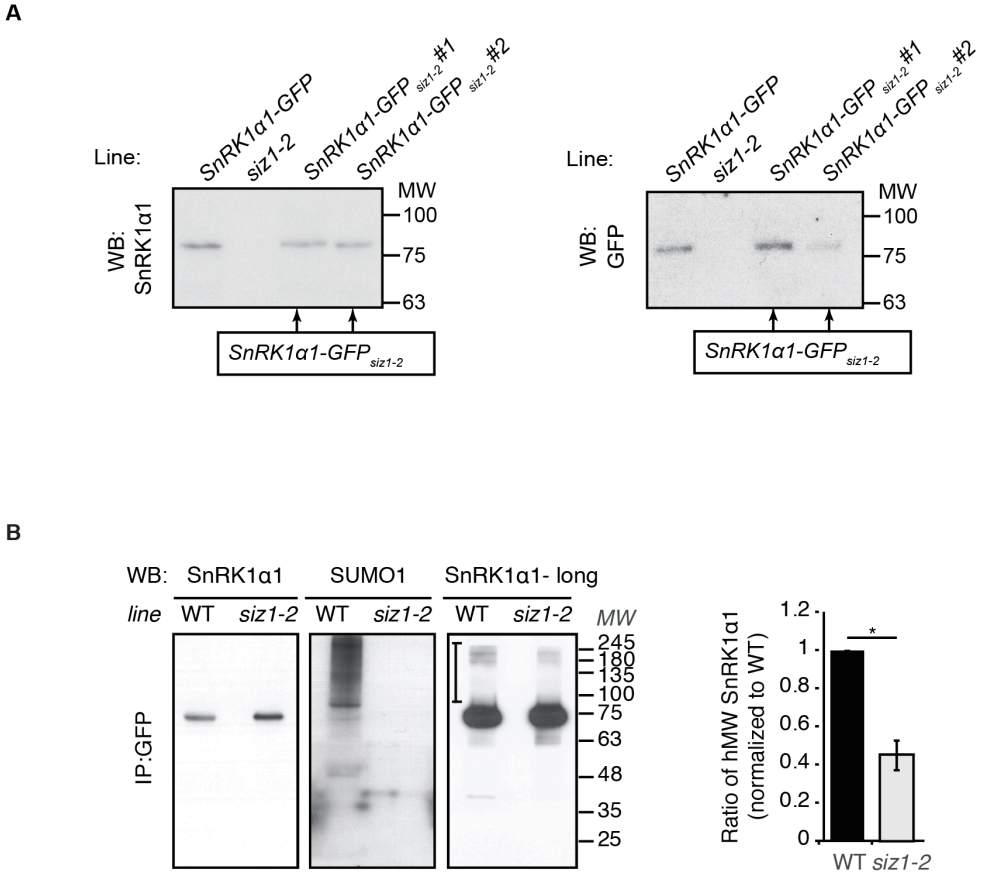

Figure 2.7 | SIZ1 is required for SnRK1 sumoylation.

A. *SnRK1α1-GFP*$_{siz1-2}$ transgenic lines were generated by transformation of the *siz1-2* mutant with the pBm43GW,0 MultiSite Gateway Binary construct described in **Figure** 2.5D. Several

transformants were tested for the presence of SnRK1α1-GFP by Western-blot (WB) using antibodies against SnRK1α1 and GFP. The selected lines are indicated with arrows. **B**. SnRK1α1-GFP was immunoprecipitated (IP) from leaf crude extracts of *SnRK1α1-GFP* ("WT") and *SnRK1α1-GFP*$_{siz1-2}$ ("*siz1-2*") and analyzed by Western-Blot (WB) using antibodies against SnRK1α1 and SUMO1. The quantification of hMW SnRK1α1 forms in both genotypes is presented on the right and corresponds to the ratio of hMW forms (indicated with a bracket in the "α1-long" longer exposure) per unmodified SnRK1α1 ("SnRK1α1" shorter exposure). The values are normalized to the ratio in control plants ("WT"). Stars denote statistical significance, as determined by ratio pair *t*-test prior to normalization (n=4; error bars=SEM; * $p<0.05$). MW, Molecular Weight.

2.2.6 | Alternative strategies employed for determining SnRK1 sumoylation in Arabidopsis

The detection of SUMO substrates *in vivo* is particularly challenging, explaining why sumoylation was discovered relatively late (*42, 43*). One main reason for this is that usually, only a minor fraction of the total pool of a protein is sumoylated at a given time point. Furthermore, the already scarce SUMO conjugates are compromised with an increased lability due to high SUMO protease activity associated with cell lysis (*35*). In addition, sumoylation may occur only in response to particular stimuli (*25, 44*).

We could determine SnRK1 sumoylation *in planta* using a rapid immunoprecipitation of SnRK1α1 from Arabidopsis rosette extracts, under mild denaturing conditions (**Section** 2.2.4). However, alternative strategies had previously been undertaken that suffered technical limitations and were hence unable to detect, or provided a low-level confidence regarding the *in vivo* sumoylation of SnRK1. Some of these approaches will be described in this section.

We could observe SnRK1α1 high molecular weight (hMW) bands in crude plant extracts from wild type (WT) (**Figure** 2.8A) or *SnRK1α1-HA* overexpressing (OE) (**Figure** 2.8B) plants grown under control conditions, using anti-SnRK1α1 and anti-HA antibodies, respectively. The extensive SUMO1 conjugation detected in the same plant extracts spanned a broad range of MWs (**Figure** 2.8A-B), thereby precluding any correlation between a particular SnRK1α1 hMW form and a particular SUMO1 signal. To indirectly test whether SnRK1α1 hMW forms could correspond, at least partially, to SUMO conjugates, we decided to monitor variations in the abundance and profile of these bands 1) through nuclear enrichment and through manipulation of protein subcellular localization strategies, and 2) using a genetic approach, with several SUMO machinery mutant plants.

SUMO, sumoylation machinery components, and SUMO conjugates are particularly enriched in the nuclear compartment and have been implicated in diverse nuclear processes (*17, 45*). On the other hand, SnRK1α1 localizes in the nucleus and cytoplasm, and its distribution varies with tissue and developmental stage, and possibly upon different stimuli (*46*). SnRK1α1 hMW bands could be detected in "soluble" and nuclear enriched fractions obtained after differential centrifugation (**Figure** 2.8C, gray arrowheads). Interestingly, the amount of hMW forms relative to unmodified SnRK1α1 was higher in the nuclear fraction, supporting the notion they could correspond to nuclear enriched, putatively sumoylated SnRK1α1.

Transient co-expression of a protein of interest with SUMO in cell cultures is frequently used to induce sumoylation and to demonstrate that the protein is a sumoylation target (*47-49*). Following the same rationale we tested the Arabidopsis protoplast (leaf mesophyll cells with digested cell walls) expression system (*50*) as a tool to study SnRK1 sumoylation. However, we could not detect SnRK1α1 hMW bands in a clear and consistent manner, from protoplasts transiently expressing epitope tagged SnRK1α1 and mature SUMO isoforms, alone (**Figure** 2.8D-E) or in combination with SCE1 and/or SUMO ligases to

enhance sumoylation (**Figure** 2.8F). SnRK1α1 constructs were co-transfected with mature SUMO1, a mature SUMO1 variant mutated in a conserved glutamine (Q) residue (SUMO1Q90A) that exhibits a slower deconjugation rate compared to WT SUMO1 (*51*) (**Figure** 2.8E-F and 2.9B-C), or with a mature SUMO3 [with a methionine (M) in the respective Q position of SUMO1], to further enrich for *in vivo* SUMO substrates (see **Introduction** - SUMO isoforms). Several SnRK1α1 constructs were tested, including variants mutated in potential nuclear localization signal (NLS) (*52*) and nuclear export signal (NES) (*53*) motifs. Manipulation of SnRK1α1 localization in these variants was expected to potentially influence its sumoylation status, with the underlying hypothesis that nuclear localization could promote or enrich SnRK1α1 sumoylation (*17, 45*). A parallel strategy included the use of SnRK1α1 variants mutated in the regulatory threonine residue of the T-loop. Phospho-mimetic (active) and phospho-mutant (inactive) versions of this residue were expressed with the expectation that kinase activity could influence its putative sumoylation (*54, 55*). Finally, N-terminal and C-terminal tagged constructs of SnRK1α1 variants were tested, to minimize effects due to the position of the tag. We also incubated transfected cells with the nuclear export inhibitor leptomycin or with the proteasome inhibitor MG132, in the latter case, with the underlying hypothesis that SUMO conjugation to SnRK1 could trigger its proteasomal degradation (*23, 24*). However, while taking advantage of the versatility of the protoplast system by testing several constructs and incubation conditions, SnRK1α1 hMW bands could not be observed in a clear and conclusive manner (**Figure** 2.8D-F, and not shown).

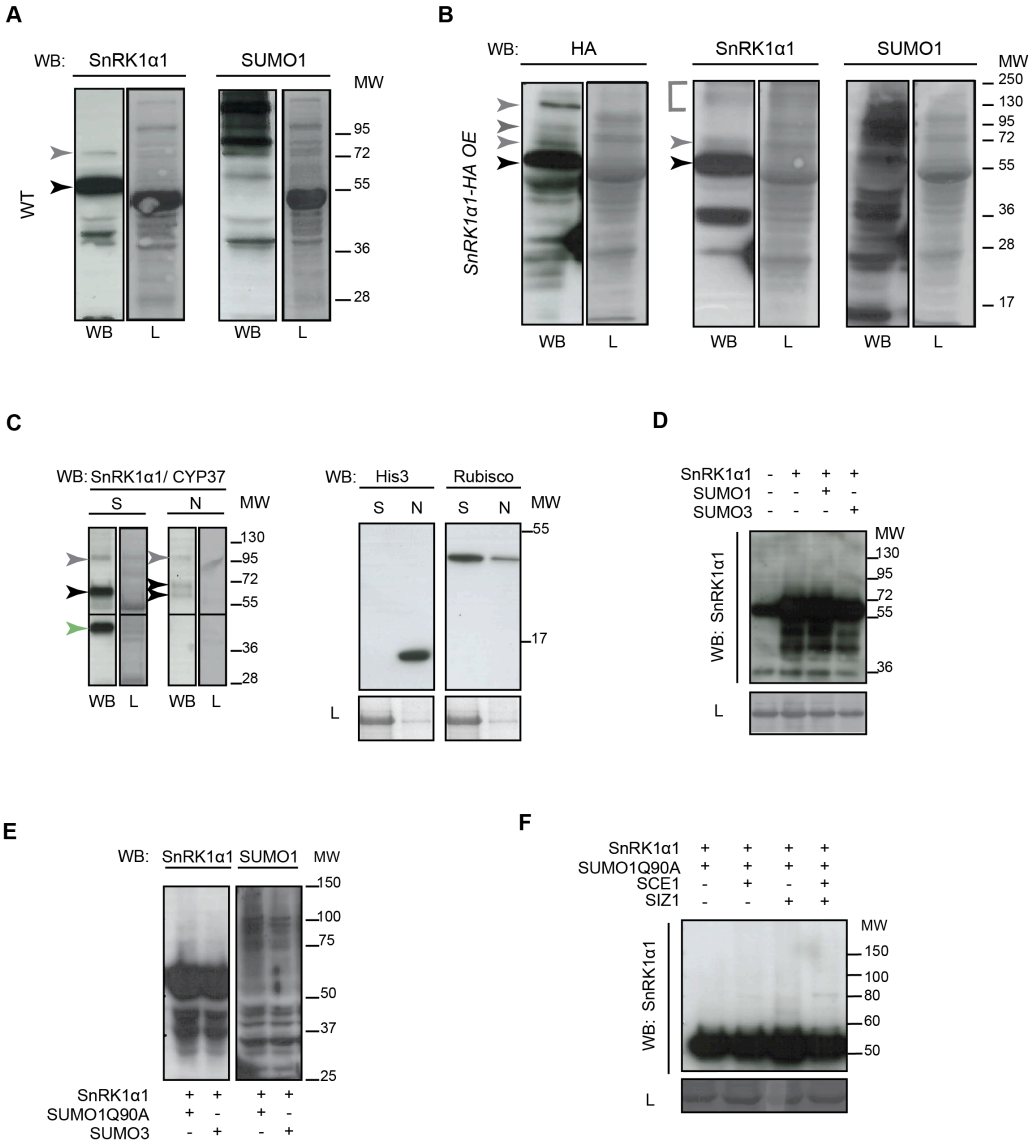

Figure 2.8 | Detection of SnRK1α1 high molecular weight bands in plant crude extracts (**A-B**), after nuclear enrichment (**C**) and in protoplast samples (**D-F**).

A-B. Plant crude extracts from Arabidopsis leaves of 5-week old WT (**A**) or *SnRK1α1-HA OE* (**B**) plants, were analyzed by Western-Blot (WB) using antibodies against SnRK1α1, SUMO1 or

HA (the latter, in **B**). Grey arrowheads or bracket indicate SnRK1α1 high molecular weight (hMW) bands. Black arrowheads indicate SnRK1α1 main band, with the expected size of SnRK1α1 protein. **C**. A full rosette (~30 leaves) of 6-week-old Col-0 subjected to 1 hour of night extension (SnRK1α1 activation condition) was used to separate soluble (S) and nuclei-enriched (N) fractions. These fractions were subsequently analyzed by SDS-PAGE and by immunodetection with antibodies against SnRK1α1 and CYP37, a protein localized in the chloroplast that should be absent in the nuclear fraction. Green arrowhead indicates CYP37 protein, only present in "Soluble", black arrowhead indicates SnRK1α1 main band, and grey arrowhead indicates SnRK1α1 hMW bands. In **C**, the panel on the right evidences nuclear enrichment in "N" with the immunodetection with anti-Histone3 (His3) and anti-Rubisco antibodies, using the same protocol but in a parallel nuclear enrichment experiment. **D-F.** Protoplast samples were transfected with constructs expressing HA-tagged SnRK1α1, SCE1 and/or SIZ1 (in **F**), together with FLAG constructs of mature forms of SUMO1, SUMO1Q90A (in **E-F**), or SUMO3. Immunodetection was done with anti-SnRK1α1 and anti-SUMO1 (in **E**) antibodies. L, loading; MW, Molecular Weight; WB, Western-blot.

We next decided to investigate the presence of hMW SnRK1α1 forms in plant extracts from mutants of the two Arabidopsis E3 SUMO ligases (*siz1-2* and *hpy2-1*), and from the *esd4* SUMO protease [shown to interact with SnRK1α1 in a Y2H screen (*16*)] mutant, where putative SnRK1α1 SUMO conjugates could be potentially diminished (*39, 40*) or enriched (*56*), respectively. These samples were compared to *SnRK1α1 RNAi,* WT, and *SnRK1α1-HA OE* plants that accumulate different SnRK1α1 amounts. For this purpose, we used a buffer with a strong denaturing agent (8M urea) to minimize breakdown of SUMO conjugates during cell lysis and to discard SUMO non-covalent interactions (*57*). However, we could not observe clear differences in the accumulation of SnRK1α1 hMW forms relative to SnRK1α1 main band, amongst the genotypes analyzed (**Figure** 2.9A). Besides possible technical limitations, further characterization is required regarding other stimuli that could be more suitable to trigger differences in putative SnRK1α1-SUMO conjugates, amongst the different genotypes.

In a totally different approach, we made use of the Ubc9 fusion-directed sumoylation (UFDS) methodology (*58-60*) to identify if SnRK1α1 could be a target of this modification. The UFDS system consists in the direct fusion of the E2 SUMO conjugating enzyme to the target protein being analyzed, bypassing the requirement for E3 SUMO ligases. This strategy dramatically enhances sumoylation and facilitates the study of weakly and/or transiently modified SUMO substrates. UFDS has been successfully used to demonstrate both constitutive and stimulus-dependent sumoylation. Half of the proteins sumoylated through UFDS were shown to be sumoylated in an UFDS-independent manner, and in specific SUMO attachment sites (*58-60*). Hence, we generated protein fusions of SCE1 with SnRK1α1 or SnRK1α1ΔKA1 in both N- and C-terminal orientations, and expressed them transiently in Arabidopsis protoplasts. We could detect SnRK1α1 hMW bands in the presence of both mature SUMO1Q90A ("1") and SUMO3 ("3") isoforms, and for both orientations of the UFDS constructs (**Figure** 2.9B, lower panel, red marks). The improved detection with the SUMO1 variant is at least partly due to a higher expression level of this construct (not shown). We could also detect these hMW bands in UFDS constructs in which the SCE1 was mutated in two subsequently identified SUMO attachment sites (K15 and K154) (*17, 22*) (**Figure** 2.9C, red asterisks). However, due to the translational fusion between SCE1 and SnRK1α1, and since mutated SCE1 (SCE1**) alone still exhibits hMW bands, we cannot exclude that the observed SCE1**-SnRK1α1 hMW bands are due to modification of some additional residues on SCE1** (**Figure** 2.9C). On the other hand, SCE1 does not seem to be sumoylated by SUMO3 (**Figure** 2.9B, upper panel), whilst for the SCE1-SnRK1α1ΔKA1 fusion protein a shift in size can be observed with both SUMO1 and SUMO3 (**Figure** 2.9B, lower panel). This suggests that the observed sumoylation with SUMO3 using the UFDS constructs is strictly SnRK1 dependent.

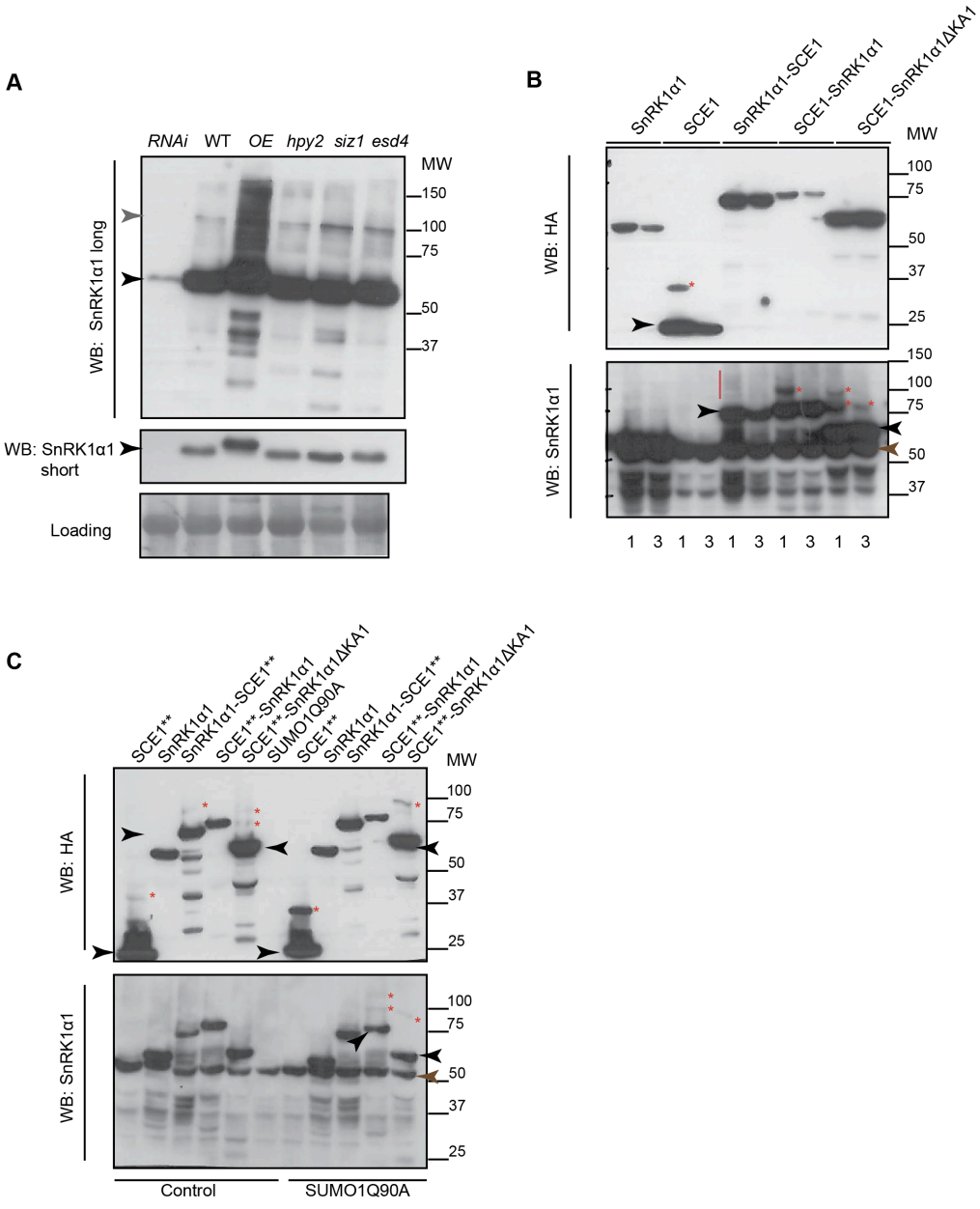
A
RNAi WT OE hpy2 siz1 esd4
MW
150
100
75
50
37
WB: SnRK1α1 long
WB: SnRK1α1 short
Loading
B
SnRK1α1
SCE1
SnRK1α1-SCE1
SCE1-SnRK1α1
SCE1-SnRK1α1ΔKA1
MW
100
75
50
37
25
150
WB: HA
WB: SnRK1α1
1 3 1 3 1 3 1 3 1 3
C
SCE1**
SnRK1α1
SnRK1α1-SCE1**
SCE1**-SnRK1α1
SCE1**-SnRK1α1ΔKA1
SUMO1Q90A
MW
100
75
50
37
25
WB: HA
WB: SnRK1α1
Control
SUMO1Q90A

Figure 2.9 | Detection of SnRK1α1 high molecular weight forms in SUMO pathway mutants (**A**) and using the Ubc9 fusion-directed sumoylation (UFDS) methodology in protoplasts (**B-C**).

A. Detached leaves from *SnRK1α1 RNAi (RNAi)*, Col-0 (WT), *SnRK1α1-HA* (*OE*), *hpy2-1* (*hpy2*), *siz1-2* (*siz1*), or *esd4* plants were processed in 8M urea extraction buffer. Immunodetection was done with anti-SnRK1α1 antibody and short and long exposures are shown. Black arrowhead indicates SnRK1α1 main bands, and grey arrowhead, SnRK1α1 hMW bands. **B-C**. Protoplast samples were transfected with HA tagged constructs of SnRK1α1, SCE1, SnRK1α1-SCE1, SCE1-SnRK1α1 or SCE1-SnRK1α1ΔKA1, together with FLAG constructs of mature SUMO1Q90A ("1", **B-C**), mature SUMO3 ("3", in **B**), or with control DNA (in **C**). In **C**, the SCE1 used in the respective constructs is mutated in two SUMO attachment sites, $SCE1^{K15/K154R}$ ("SCE**"). Immunodetection was done with anti-SnRK1α1 and anti-HA antibodies. Black arrowheads indicate each construct's main band; red asterisks and red line indicate its respective hMW bands (putative SUMO conjugates). Brown arrowheads indicate endogenous SnRK1α1 main band. MW, Molecular Weight; WB, Western-blot.

The requirement to address the specificity and identity of SnRK1α1 hMW bands, urged us to use an immunoprecipitation (IP) step in the analysis of crude plant extracts. Similarly, protoplasts transfected with differentially tagged SUMO and SnRK1α1 constructs, alone or with other SUMO machinery components, were purified through immunoprecipitation of one of the tagged proteins (SnRK1α1 or SUMO). The subsequent detection with an antibody against the other tagged construct (SUMO or SnRK1α1), could be a mean to assign identity to hMW bands with the same size (SnRK1α1-SUMO conjugates). However, as previously mentioned, it was always very hard to detect SnRK1α1 hMW bands and an associated SUMO signal from protoplast samples. Our efforts focused then in the IP analyses from crude extracts of Arabidopsis rosettes (**Figure** 2.6).

The buffer composition used in cell lysis, proved to be determinant for detecting SnRK1 sumoylation *in vivo*. The alkylating agent and inhibitor of SUMO proteases N-Ethylmaleimide (NEM) (*61*) and the proteasome inhibitor MG132 (through a direct inhibition of proteasomal dependent degradation of

SUMO conjugates (*23, 24*), or *via* an indirect mechanism) proved to be crucial. We employed a lysis buffer with some denaturing properties conferred by the ionic detergents sodium dodecyl sulfate (SDS) and sodium deoxycholate, since the usage of strong denaturants would compromise the subsequent IP step. The ionic and nonionic (IGEPAL CA-630) detergents present in the buffer allowed the extraction of cytoplasmic, membranar and nuclear proteins. However, in this case, both covalent and non-covalent (SUMO and others) interactions can be retrieved in the immunoprecipitates. As already shown, SnRK1β regulatory subunits co-purify with SnRK1α1, contributing to the overall SUMO1 signal (**Figure** 2.6A-B).

In order to confirm the identity of SnRK1α1 hMW bands as SnRK1α1-SUMO conjugates, we incubated *SnRK1α1-GFP* immunoprecipitates with the commercially available SUMO protease Ulp1 (recombinant fragment), from *Saccharomyces cerevisiae*. SUMO conjugates (and SnRK1α1 hMW bands) should decrease upon SUMO protease treatment, which was the case when SnRK1α1 sumoylated in *E. coli* was used as a positive control (**Figure** 2.10A). However, when SnRK1α1-GFP immunoprecipitates were used as substrates, no clear differences were observed in SUMO1 and SnRK1α1 immunoprofiles between Ulp1-treated and non-treated samples (**Figure** 2.10B). Ulp1 has a predominant role in SUMO precursor maturation whereas the SUMO protease Ulp2 is mainly associated with SUMO chain processing *in vivo* (*62-64*). Thus, it is possible that despite Ulp1 is able to cleave the SUMO moiety from sumoylated SnRK1α1 purified from *E. coli*, Ulp1 becomes inefficient to remove SUMO moieties from the endogenous SnRK1α1, possibly because it harbors multiple sumoylated residues or SUMO chains. Furthermore, the *in vitro* processing of SnRK1α1-GFP SUMO conjugates by Ulp1 may be additionally hindered by co-purified components or extra modifications that can occur in the N-terminus of sumo moieties (e.g. ubiquitylation). In such scenario, prior processing through distinct machinery would be required, as recently described for Ulp2 proteolytic activity (*65*).

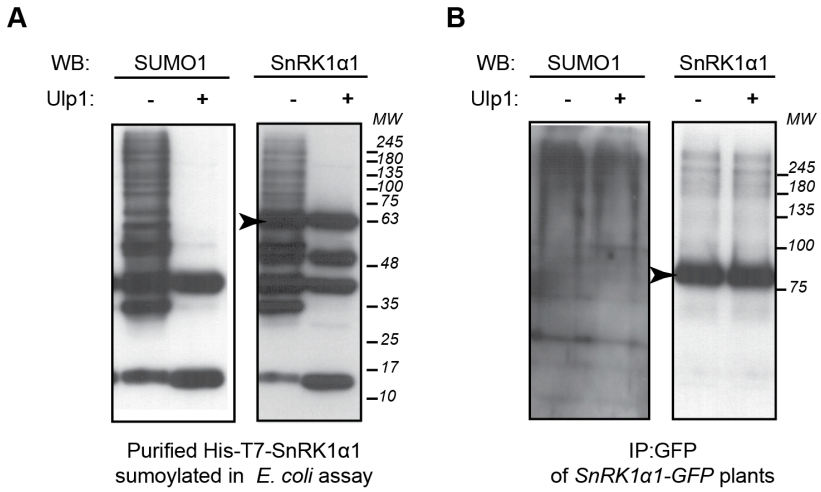

Figure 2.10 | Processing of SnRK1α1-SUMO conjugates by recombinant Ulp1 SUMO protease.

A-B. Purified recombinant SnRK1α1 eluates and plant immunoprecipitates of SnRK1α1 were incubated with (+) or without (-) a recombinant fragment of Ulp1 SUMO protease in 1x SUMO protease buffer for 1h at 25ºC. Samples were analyzed by immunoblot with anti-SUMO1 and anti-SnRK1α1 antibodies. **A**. His-T7-SnRK1α1 catalytic subunit was sumoylated in the *E. coli* system as shown in **Figure** 2.3 and purified via the His-tag by immobilized metal ion affinity chromatography (IMAC) prior to SUMO protease assay. In **A**, after immunodetection with anti-SUMO1 antibody, the same membrane was re-probed with anti-SnRK1α1 antibody. **B**. Immunoprecipitates from *SnRK1α1-GFP* plants were obtained as shown in **Figure 2.6** and subjected to the SUMO protease assay. Immunodetection was done with anti-SUMO1 and anti-SnRK1α1 antibodies.

2.3 | Discussion

Protein kinases are swiftly regulated by posttranslational modifications (PTMs) that adjust the kinase activity and/or its stability and subcellular localization, in line with the cellular and whole organism demands. Unlike yeast Snf1 and mammalian AMPK, the phosphorylation of a conserved residue in the T-loop of SnRK1α1 is unchanged in control and stress conditions that activate SnRK1 signaling (*2, 7-9*). Here, we discovered that the SnRK1 complex (catalytic and multiple regulatory subunits) is sumoylated and hypothesize that this PTM may be important for the regulation of SnRK1 activity.

We have shown that SnRK1α1 interacts through several domains with SCE1 in Y2H assays (**Figure** 2.2), and that SnRK1α1, SnRK1β1 and SnRK1β2 are sumoylated in a heterologous system that reconstitutes the Arabidopsis sumoylation machinery in *E. coli*. SnRK1γ is also sumoylated, although this subunit is not an established component of the SnRK1 complex (*31*) (**Figure** 2.3). The SnRK1βγ regulatory subunit was not sumoylated, and SnRK1α2 and SnRK1β3 subunits remain to be tested regarding a putative sumoylation using the *E. coli* system. LC-MS/MS analyses revealed that nine lysines are sumoylated both in the kinase and regulatory domains of SnRK1α1. We could determine that three lysines (K34, K63 and K390) were the major targets of sumoylation in *E. coli*, since this modification could no longer be detected in the SnRK1α1$^{K34/K63/K390R}$ triple mutant (**Figure** 2.4), and hypothesize that these residues are the genuine targets of sumoylation *in vivo*. SnRK1α1 has two high probability SUMO attachment sites (**Figure** 2.1) but, despite their apparently favorable 3D context, none of these residues seems to be crucial for SnRK1α1 sumoylation (K144, **Figure** 2.4D; K471, not shown). Potential SUMO substrates are enriched in high probability SUMO attachment sites (hpSAS) [70% compared to 40% of the Arabidopsis proteome (*16*)], but an increasing number of studies report sumoylation at noncanonical motifs (*32*). Other factors, besides the sequence of the SUMO attachment motif, may be required to fulfill sumoylation.

In order to study a possible conservation of sumoylation as a posttranslational regulatory mechanism amongst SNF1/AMPK/SnRK1 family of protein kinases, we analyzed if SNF1A, the ortholog of SnRK1α1 in Drosophila, could be a target of this modification. Recent reports have shown the sumoylation of mammalian AMPK catalytic and regulatory subunits (*32, 33*), and yeast Snf1 catalytic subunit (*34*). Similarly to SnRK1α1, SNF1A interacted with SCE1 in Y2H assays (**Figure** 2.2B) and was sumoylated in the *E. coli* system (**Figure** 2.3B). Since both systems use the Arabidopsis SUMO machinery, the fact that sumoylation of Drosophila SNF1A still occurs probably reflects the high level of conservation of the SUMO pathway, as well of SnRK1 orthologs. However, none of the four sumoylated residues identified through MS in the regulatory domain of SNF1A (K447, K456, K469 and K505) are conserved in SnRK1α1.

In protein group sumoylation events, several proteins of a particular complex are targeted synchronously and often at multiple sites by the sumoylation machinery. The sumoylation of SnRK1 catalytic and regulatory subunits suggests this might be the case in the SnRK1 complex, and possibly also in its orthologs (*32, 33*). In the cases of protein group sumoylation, SUMO attachment occurs on multiple sites on a protein and these sites tend to not be conserved in orthologs of other species (*44*). Furthermore, structural studies suggest that the SUMO consensus motif needs to adopt an extended conformation in order to facilitate the interaction with SCE, and function as a *bona fide* sumoylation site. Consequently, sumoylation often occurs outside of folded, functional domains, and thus is less likely to interfere with the intrinsic activities of the modified proteins (*44*). These pieces of evidence might help to explain the lack of conservation between SNF1A and SnRK1α1 sumoylation sites. Similarly, in yeast, Snf1 sumoylation occurs in a single residue in its regulatory domain (RD) (Snf1 K549) (*34*), and this sumoylation site is not conserved in SnRK1α1 or SNF1A. However, we cannot exclude that other sumoylated residues would have been found in SNF1A if targeted by the Drosophila SUMO machinery. On

the other hand, AMPKα1 and α2 were found sumoylated in a single residue (*32*) conserved in SnRK1α1, and crucial for its sumoylation (SnRK1α1 K390) (**Figure** 2.3E and F). In the latter case, sumoylation of a conserved site may be required to achieve a specific molecular or functional outcome. For instance, sumoylation of yeast proliferation cellular nuclear antigen (PCNA) targets a conserved K164 residue that is also a conserved acceptor site for PCNA ubiquitylation in eukaryotes, leading to different repair pathways upon DNA damage (*19, 66*).

After employing several strategies, we were able to show SnRK1 sumoylation *in vivo*, using a rapid GFP immunoprecipitation step from Arabidopsis rosettes of *SnRK1α1-GFP* plants. In this approach, the buffer optimization was crucial to enrich for the extremely labile SUMO conjugates. We were able to observe the sumoylation of SnRK1α1 catalytic subunit and probably of SnRK1β1 and SnRK1β2 regulatory subunits *in vivo*. Immunodetection with subunit-specific antibodies revealed that the three SnRK1 subunits display high molecular weight bands that partially overlap with the signal obtained with SUMO1 immunodetection from the same sample. Importantly, SnRK1α1 high molecular weight bands were strongly diminished in the *siz1-2* background, impaired in SIZ1-dependent sumoylation (**Figure** 2.7B). The detected ladder of SUMO1 conjugates suggests that several subunits are sumoylated *in vivo*, possibly either on multiple sites, involving the formation of (poly)SUMO1 chains, or both. SnRK1βγ co-purified with SnRK1α1 but was not sumoylated, whereas SnRK1γ did not associate with the SnRK1α1 catalytic subunit (**Figure** 2.6C-D). SnRK1βγ has two putative SUMO interacting motifs (SIM; 1 SIMa, LLGL, 484-487; 1SIMr, SSSLPIL, 324-330) (**Introduction** - SUMO interacting motifs). Despite not being covalently modified by SUMO, SnRK1βγ may have increased affinity for sumoylated proteins through non-covalent SUMO-SIM interactions, and can thus be an important signal transducer downstream of SnRK1α and SnRK1β sumoylation. On the other hand, SnRK1γ has a hydrophobic motif followed by acidic residues (VVDVD, 95-99) that may be a SIM (*67*). However, this motif does not appear to be

sufficient to promote SnRK1γ interaction with sumoylated SnRK1α and β-subunits (**Figure** 2.6C). Overall, the results obtained *in planta* validate the previously determined SnRK1 sumoylation in *E. coli*.

Interestingly, a significant fraction of the SUMO signal seems to associate with SnRK1 regulatory subunits, since removal of the KA1 domain, through which regulatory proteins interact, leads to a strong decrease (but not disappearance) of the SUMO signal. It is also possible that proteins other than the regulatory subunits bind SnRK1α1 through its KA1 domain (*9, 36, 68, 69*), also contributing to the SUMO1 signal associated with *SnRK1α1-GFP* IPs. Moreover, SnRK1α1ΔKA1 (1-389) loses the residue K390 shown to be crucial for SnRK1α1 sumoylation in *E. coli*, and K421, also sumoylated in this system, as well as other downstream K(s) that might contribute to SUMO signal intensity *in planta*. However, to conclusively demonstrate sumoylation of a particular SnRK1 subunit, future analyses should employ plants expressing His-tagged SUMO1 or SUMO3 (*17, 51*) to perform SUMO pulldowns under denaturing conditions followed by immunoblots for the protein of interest. This would retrieve only components covalently bound to SUMO (as opposed to components interacting through non-covalent protein-protein interactions).

Despite SnRK1 sumoylation occurs in the absence of SUMO ligase(s) and with several SUMO isoforms in the *E. coli* heterologous system (**Figure** 2.3 and 2.4), SUMO ligases, SUMO proteases, additional PTMs on the substrate, and others, may confer specificity to SnRK1 sumoylation *in vivo*. Importantly, we were able to identify SIZ1 as the E3 SUMO ligase responsible for SnRK1 sumoylation by SUMO1 *in planta*. When SnRK1α1-GFP was immunoprecipitated from the *SnRK1α1-GFP*$_{siz1-2}$ plants that lack SIZ1, the SUMO signal was completely abolished and a clear reduction in SnRK1α1 hMW bands was observed, confirming that many of these bands correspond indeed to SUMO1 conjugates of SnRK1α1 (**Figure** 2.7). On the other hand, a good antibody tool is required to better dissect a possible sumoylation of SnRK1 by SUMO3, or even SUMO5 *in planta*, and a putative role for the E3 SUMO ligase

HPY2 in such scenario. Nevertheless, in accordance with our results of SnRK1 sumoylation, an increase in SUMO1 and SUMO2 conjugates, associated with several types of stresses, is mainly driven by the E3 SUMO ligase SIZ1 (*12*). Also, given the high similarity and probably functional equivalence between SUMO1 and SUMO2 isoforms (*12, 25, 70, 71*), we could not uncouple the modification of SnRK1 by either SUMO1 or SUMO2 *in planta*.

Overall, we were able to show the SIZ1-dependent sumoylation of SnRK1 by SUMO1, through its catalytic and regulatory subunits, in Arabidopsis. Therefore, considering the data presented here, together with the reported sumoylation of Snf1 and AMPK *in vivo*, sumoylation emerges as a posttranslational regulatory mechanism of the central family of SNF1/AMPK/SnRK1 kinases, across eukaryotes.

2.4 | Materials and Methods

A list of all primers, cloning steps, and constructs used in this study, is provided in **Appendix Table** 1.

2.4.1 | Plant Material, Growth Conditions and Transformation

Unless otherwise specified, plants were grown in soil under a 12h light (100µE), 22°C/12h dark, 18°C regime. *Arabidopsis thaliana* plants used in this study are in the Columbia (Col-0) background, except for the *35S-SnRK1α1-HA* (*SnRK1-OE*) and *SnRK1α1 RNAi* lines that are in the Landsberg erecta (Ler) background. The *siz1-2* (SALK_065397) (*72, 73*), *hpy2-1 (40), 35S-SnRK1α1 (2)* and *SnRK1α1 RNAi* (*2*) plants have been previously described. *esd4* (GABI_216D08) homozygous plants were selected after kanamycin selection

and subsequent genotyping for the presence of the insertion in both alleles of the *ESD4* gene (AT4G15880; not shown). A homozygous insertion line for the *SnRK1α1* gene (At3g01090), was identified in the GABI-KAT collection (GABI_579E09; **Figure** 2.5A-C) and was designated as *snrk1α1-3* [previously described *snrk1α1-1* and *snrk1α1-2* mutants are not null (*74*)]. Genotyping was performed using primers *snrk1α1*-GABIa and *snrk1α1*-GABIb in combination with a left border T-DNA primer (GABI-08409-LB). To determine the T-DNA exact insertion site a genomic DNA fragment was amplified by PCR with a forward primer binding to the *SnRK1α1* locus (SnRK1α1-seqF Fw) and a reverse primer binding to the T-DNA right border (GABI1-RB-seq Rv). Sequencing reactions were subsequently performed on the gel-purified PCR product using the same primers. The T-DNA insertion was mapped to position 2583-2593, immediately before the last exon. The last 11 bases of the intron at the insertion site are missing. The potential presence of a second insertion in the *IMS2* gene (AT5G23020), as annotated in the GABI-Kat site, was ruled out by genotyping with primers IMS2-Fw and IMS2-Rv in combination with the GABI-08409-LB primer. The absence of SnRK1α1 protein in *snrk1α1-3* plants was confirmed by immunoblotting with antibodies recognizing epitopes well before the T-DNA insertion, an SnRK1α1-specific antibody and an AMPKα-pT172 antibody recognizing the phosphorylated T-loop of SnRK1α1 and SnRK1α2 [T175 and T176, respectively; (*75*)].

The *pSnRK1α1::SnRK1α1-GFP::tSnRK1α1* and *pSnRK1α1::SnRK1α1ΔKA1-GFP::tSnRK1α1* constructs are in the pBm43GW,0 MultiSite Gateway Binary vector (*76*) and the corresponding areas of the gene are indicated in **Figure** 2.5. Both constructs were generated using a pDONR-P4P1R harboring the *SnRK1α1* upstream regulatory region (*pSnRK1α1*, 2000bp upstream of the *SnRK1α1* start codon in the At3g01090.2 gene model; amplified using primers PROM-5'UTR_gSnRK1α1 attB4 Fw and PROM-5'UTR_gSnRK1α1 attB1r Rv) and a pDONR-P2RP3 harboring the SnRK1α1 downstream regulatory region

(*tSnRK1α1*, 1000bp downstream of the *SnRK1α1* stop codon in the At3g01090.2 gene model; amplified using primers TERM-3'UTR_gSnRK1α1 attB2r Fw and TERM-3'UTR_gSnRK1α1 attB3 Rv). In *pSnRK1α1::SnRK1α1-GFP::tSnRK1α1* the middle pDONR221-P1P2 contained the full genomic sequence of *SnRK1α1* fused to GFP (primers gSnRK1α1-GFP attB1 Fw and gSnRK1α1-GFP attB2 Rv), whereas in *pSnRK1α1::SnRK1α1ΔKA1-GFP::tSnRK1α1,* it contained the coding sequence of *SnRK1α1* truncated at the KA1 domain and fused to GFP (primers gSnRK1α1-GFP attB1 Fw and gSnRK1α1-GFP attB2 Rv). The *pSnRK1α1::SnRK1α1-GFP::tSnRK1α1* and *pSnRK1α1::SnRK1α1ΔKA1-GFP:tSnRK1α1* constructs were introduced into *Agrobacterium tumefaciens* (GV3101) and *snrk1α1-3 or siz1-2* plants were transformed by the floral dip method (*77*) to generate *pSnRK1α1::SnRK1α1-GFP::tSnRK1α1/snrk1α1-3* (referred as *SnRK1α1-GFP*) and *pSnRK1α1::SnRK1α1ΔKA1-GFP::tSnRK1α1/snrk1α1-3* (referred as *SnRK1α1ΔKA1-GFP*). BASTA-resistant transformants were selected based on their segregation ratio (T2) and homozygosity (T3). Homozygous T3 or T4 generation transgenic lines were used.

2.4.2 | Cloning and site-directed mutagenesis

All cloning steps and primers are detailed in **Appendix Table1**. To generate point mutations, PCR was performed using primers carrying the intended mutation and annealing to the same sequence on opposite strands of the original plasmid template. A 25µl reaction mix [primers (25ng each), template plasmid (50ng), 250µM of dNTPs, Pfu polymerase (1.25U, Promega M7745) and 1XPfu buffer] was split in two tubes (12.5µl each); one was incubated in a thermocycler [95°C - 3min; (95°C -30s, 55°C-40s, 68°C-2min/kb) x 14] while the other was kept at 4°C. Ten units of DpnI (NEB) were thereafter added to both

and incubated at 37°C for 12h prior to bacteria transformation (4µL typically used). Positive clones were always confirmed by sequencing.

2.4.3 | Antibodies and Protein Expression Analyses

The SnRK1α1 (1/500, anti-AKIN10, AS10919), SnRK1β1 (1/500, anti-AKINB1, AS09460), SnRK1β2 (1/500, anti-AKINB2, AS09 462), SnRK1βγ (1/1000, anti-AKINBG, AS09463), SnRK1γ (1/2000, anti-AKING1, AS09613), Rubisco (1/5000, anti-RbcL, AS03037), Histone 3 (1/1000, anti-H3, AS10710) and CYP37 (1/2000, anti-PPIase CYP37, AS101589) antibodies were purchased from Agrisera. Phospho-SnRK1α1/2 (T175/176) was detected with an anti–phosphoT172-AMPKα antibody (1/1000 in 5% BSA-TBS-Tween, referred to as P-AMPK; #2535, Cell Signaling). SUMO1 (1/5000, ab5316, Abcam) antibody was used to detect the respective protein modification. Anti-HA (1/1000, Roche, #11867423001), and anti-T7 (1/10000, #69522-3, Novagen) antibodies were used to detect the corresponding tagged proteins.

For immunoblotting all primary antibodies were diluted in 1% non-fat Milk in TBS (unless otherwise stated) and incubated with the membrane under gentle shaking for 12h at 4°C. Secondary antibodies (Jackson ImmunoResearch Lab, inc) were used at 1/10000 in 1% non-fat Milk in TBS for 1h at room temperature (RT). In the case of immunoprecipitated samples, secondary antibodies subsequently used in the immunodetection were against the light chain of IgG.

2.4.4 | Protoplast Transient Expression Assays

Protoplasts from Col-0 plants were isolated and transfected as already described (*78*). All effector constructs (**Appendix Table** 1) were generated by cloning the corresponding coding sequences into a pHBT95 vector harboring a N-terminal FLAG (for SUMO constructs) or C-terminal HA (*78*), for the remaining

constructs. The indicated mutations were introduced by site-directed mutagenesis and verified by sequencing. For protein expression analyses, protoplasts were directly resuspended in 4X Laemmli solubilization buffer (*79*) and boiled for 5min at 95°C. Leptomycin (Sigma, L2913, methanol: water (7:3) stock) and MG132 (Sigma, C2211; DMSO stock) solutions were used at a final concentration of 2µM and 50µM, respectively.

2.4.5 | GFP, SnRK1α1-GFP and SnRK1α1ΔKA1-GFP Immunoprecipitation

Proteins from 5-week-old *SnRK1α1-GFP*, *SnRK1α1ΔKA1-GFP,* or *35S-GFP* plant leaves were extracted with immunoprecipitation (IP) buffer [50mM Tris-HCl pH8.0, 50mM NaCl, 1% (V/V) Igepal CA-630, 0.5% (w/V) Sodium deoxycholate, 0.1% (w/V) SDS, 1mM EDTA pH8.0, 50µM MG132, 50mM *N*-Ethylmaleimide and cOmplete protease inhibitor cocktail (one tablet/10mL)]. After clearing samples by centrifugation (6,785*g*, 2°C, 10min), 800µL of supernatant were supplemented with fresh MG132 (50µM) and incubated at 4°C for 1h with 40µL of µMACS Anti-GFP MicroBeads (µMACS GFP Isolation Kit, Miltenyi, 130-091-125). Samples were thereafter loaded in µColumns (Miltenyi, 130-042-701) pre-equilibrated with 1ml of IP buffer, and allowed to flow through. Columns were washed four times with 200µL of IP buffer and proteins eluted with 80µL of Elution Buffer (Miltenyi, 130-091-125) at 95°C. For SUMO protease assays, columns were washed further with 1ml of 20mM Tris-HCl pH8.0 and eluted with 50µL of 20mM Tris-HCl pH8.0 at RT prior to incubation with SUMO protease (**2.4.8.** SUMO protease assays). β-Mercapto-Ethanol (2%) was added to the eluates prior to boiling for 5 min at 95°C. Proteins were resolved by SDS-PAGE, wet-transferred to a PVDF membrane (30V, 16h at 4°C), and analyzed by

immunoblotting with SnRK1α1, SnRK1β1, SnRK1β2, SnRK1βγ, SnRK1γ, SUMO1, and GFP antibodies. For each GFP immunoprecipitation experiment, immunodetection with different antibodies was done using equal loading on independent membranes.

2.4.6 | Nuclear enrichment

Full rosettes from 6-week-old Col-0 plants were ground in liquid nitrogen and extracted with 15ml/rosette of Nuclear Enrichment Extraction buffer (EB) [20mM Tris-HCl pH6.8, 25% Glycerol (V/V), 1% Triton-X (V/V), 2.5mM $MgCl_2$, 20mM KCl, 2mM EDTA, 8.8% Sucrose (w/V), 0.5mM Spermidine, 30mM β-Mercapto-Ethanol, cOmplete protease inhibitor cocktail (one tablet/25mL), 1/500 (v/v) phosphatase inhibitor 2 (Sigma P5726) and 3 (Sigma P0044), 10mM NEM]. Liquid and homogenous plant extracts were filtered through four layers of Miracloth and kept on ice for 15-20min. Samples were thereafter cleared by centrifugation using a swing-out rotor (1000*g*, 4ºC, 10min). The supernatant, containing the "soluble fraction" was frozen (15-20µl of supernatant loaded per gel), and the pellet containing the nuclei was gently washed three times with 3ml of Nuclei Resuspension buffer (RB) [20mM Tris-HCl pH6.8, 25% Glycerol (V/V), 2.5mM $MgCl_2$, 0.5mM Spermidine, 30mM β-Mercapto-Ethanol, cOmplete protease inhibitor cocktail (one tablet/25mL), 1/500 (v/v) phosphatase inhibitor 2 (Sigma P5726) and 3 (Sigma P0044), 10mM NEM], and resuspended in 60ul of RB (20µl of nuclei enriched fraction loaded per gel). Prior to SDS-PAGE analysis, samples were boiled for 5min at 95°C with 4X Laemmli solubilization buffer (*79*).

2.4.7 | Protein extraction under denaturing conditions

Leaves from WT Col-0, *SnRK1α1-OE*, *SnRK1α1 RNAi, siz1-2, hpy2-1* and *esd4* plants were collected and flash-frozen. Leaves were ground in liquid nitrogen and extracted with approximately the same volume of Urea Lysis Buffer [8M Urea, 100mM $NaH_2PO_4.2H_2O$, 10mM Tris-HCl pH8.0, 0.1% (V/V) Triton X-100, 0.1%SDS, 1mM β-Mercapto-Ethanol, cOmplete protease inhibitor cocktail (one tablet/100mL), 10mM NEM]. Plant extracts were transferred to a fresh tube, resuspended by vortexing, incubated 10min at room temperature and 2min at 95ºC. Extracts were then centrifuged (20,000*g*, 25°C, 15 min) and the supernatants collected. Proteins were quantified prior to SDS-PAGE analysis with the 2D Quant Kit (GE Healthcare, #80-6483-56), according to the manufacturer's instructions, and equal protein amounts were loaded.

2.4.8 | *E. coli* heterologous sumoylation assay

Constructs for reconstituting the *Arabidopsis thaliana* SUMO machinery in *E. coli* were kindly provided by Katsunori Tanaka (*80*). pET28a was used to express potential SUMO targets (SnRK1α1 and its truncated and mutant variants, SnRK1β1, SnRK1β2, SnRK1βγ, and SnRK1γ). BL21(DE3) cells were transformed with pACYCDuet-AtSAE1a-AtSAE2 and selected on 34μg/ml chloramphenicol (Cm) LB Agar plates. 100μl of pACYCDuet-AtSAE1a-AtSAE2 transformed BL21(DE3) competent cells were co-transformed with 30-50ng of pCDFDuet-AtSUMO1/3(AA or GG)-AtSCE1a and pET28a-SnRK1α1 (and its truncation and mutation variants)/SnRK1β1/SnRK1β2/SnRK1γ/SnRK1βγ and then selected on 17μg/mL Cm, 15μg/mL Kanamycin (Kan) and 25μg/mL Spectinomycin (Spec) LB Agar plates. Transformed cells were incubated in 34μg/mL Cm, 30μg/mL Kan and 50μg/mL Spec LB liquid media at 25°C, 200rpm, until Abs^{600nm} reached 0.5-0.8. The expression of recombinant proteins was induced with 0.15mM IPTG (PROMV3955, Promega) at 25°C for 12h.

For analyzing total soluble proteins, cells were harvested from 3mL cultures and lysed with 100µL of BugBuster Protein Extraction Reagent (Novagen) supplemented with 2µL of ProteoBlock (#R1321, Fermentas), 2µL of Lysozyme (L1667, Sigma) and 2µL of DNAse (PROMM6101, Promega). Samples were incubated 20min at RT and cleared by centrifugation (20,000*g*, 4°C, 25min). About 100µg of soluble protein (estimated by Abs^{280nm}) were subjected to SDS-PAGE and immunoblotting with an anti-T7 antibody. For analyses from purified proteins, bacteria were pelleted at 4000*g* for 30min at 4°C, resuspended in Lysis buffer [50mM Hepes-NaOH pH7.25, 0.1M NaCl, antiprotease cOmplete without EDTA (1 tablet/50mL)], and sonicated. After centrifugation (20,000*g* for 30min at 4°C) the soluble fraction was subjected to IMAC purification (Ni-NTA agarose, Qiagen, 30210). Beads were pre-equilibrated in Lysis buffer and incubated with the soluble protein extract under gentle shaking for 1h at RT. Beads were thereafter washed under gravity flow with Lysis buffer (5 BV, bed volume) and then with 50mM Hepes-NaOH pH7.25 until Abs^{230nm} reached 0 or stabilized at less than 0.1. A final wash was applied with 50mM Hepes-NaOH pH7.25, 20mM imidazole. Three consecutive elutions with 50mM Hepes-NaOH pH7.25 supplemented with 100, 200 or 500mM of imidazole were performed during at least 20min at RT under gentle shaking. Eluates were dialyzed to reach a 20mM imidazole concentration, concentrated on 30kDa Amicon columns (Millipore), and analyzed (20µg) by SDS-PAGE and immunoblotting with anti-T7.

2.4.9 | Mass spectrometry analyses

For Mass spectrometry analyses, 15-30µg of concentrated eluates were resolved on SDS-PAGE (8%) and stained with Coomassie Brilliant Blue R250 (VWR: 443283M, 0.2% w/V in 14% Acetic Acid, 14% ethanol) and destained (10% Acetic Acid, 25% ethanol) until the bands were clearly visible. Bands were excised, alkylated with iodoacetamide (carbamidomethylation of cysteines), and

digested with trypsin. Eluted peptides were separated by liquid chromatography and detected with an Orbitrap Velos Pro Hybrid Ion Trap Mass Spectrometer (Thermo Scientific). An initial hit search was done in the NCBI non-redundant database with "Arabidopsis thaliana" as a query organism. Approximately 3400 queries were made for each sample, with peptide mass tolerance ± 3ppm and fragment mass tolerance ± 0.8Da. For a more refined validation, a micro-database was created containing *in silico* predicted masses of the branched peptides resulting from sumoylation, and was compared manually to the data set.

2.4.10 | SUMO protease assay

SnRK1α1-GFP immunoprecipitates (in 21.25µl of 20mM Tris-HCl pH8.0), or 2µg of purified and concentrated eluates of recombinant SnRK1α1 (in 21.25µl of 20mM Tris-HCl pH8.0) sumoylated with SUMO1GG in the *E. coli* assay, were incubated with 1X SUMO protease buffer + Salt (2.5 µl, final salt concentration of 150mM NaCl) and with or without 1.25µl of SUMO protease (1.25U, recombinant fragment of Ulp1, Life Technologies, #12588-018), for 1hour at RT. Prior to SDS-PAGE analysis, samples were boiled for 5min at 95°C with 4X Laemmli solubilization buffer (*79*). Immunodetection was done with anti-SnRK1α1 and anti-SUMO1 antibodies.

2.4.11 | Y2H Assays

Y2H assays were performed as described (*81*). The full-length coding sequence of SnRK1α1 and the various deletions were cloned into pGADT7 in fusion with the GAL4 activation domain. pGADT7 constructs were faced with

pGBKT7 harboring full-length SCE1 fused to the DNA binding domain of GAL4. The empty vectors were used as negative controls. The growth of transformed AH109 yeast cells was assessed in permissive (-Leucine, -Tryptophan), selective (-Leucine, -Tryptophan, -Histidine), or more stringent (-Leucine, -Tryptophan, -Histidine, -Adenine) media.

2.4.12 | Statistical Analyses

Statistical analyses were performed with the GraphPad Prism 6 software (GraphPad softwares).

2.4.13 | Accession Numbers

Sequence data can be found in the Arabidopsis Genome Initiative database under the following accession numbers: *SnRK1α1*, At3g01090; *SnRK1β1*, At5g21170; *SnRK1β2*, At4g16360; *SnRK1βγ*, At1g09020; *SnRK1γ*, At3g48530; *SIZ1*, At5g60410; *HPY2*, At3g15150; *ESD4,* At4g15880*; SUMO1*, At4g26840; *SUMO3*, At5g55170; *SCE1*, At3g57870.

Supplemental data

Supplemental Data includes Supplemental Figure 1 and Supplemental Table 1.

Acknowledgements

I would like to acknowledge Elena Baena-González for guidance throughout all the work and careful reading of the chapter, and Pierre Crozet for contributing for the work here presented, for helping with figures and reading the chapter. I would like to acknowledge Américo Rodrigues for training me in the Y2H assay, Rafal Butowt for contributing and training me in the *E. coli* sumoylation assay, Ari Sadanandom for training me with the GFP IPs, and Konstantin Tomanov and Andreas Bachmair for the MS analyses. I acknowledge Carlos Alexandre Elias for characterizing the *snrk1α1-3* mutant and for generating the *SnRK1α1ΔKA1-GFP* plants. I am thankful to K. Miura, K. Tanaka, and M. Thomas for kindly providing the *siz1-2* mutant, the plasmids for the *E. coli* sumoylation assay, and the constructs for expression of recombinant SnRK1 subunits, respectively. Furthermore, I am grateful to all Plant Stress Signaling group members for fruitful discussions and to Vera Nunes for great plant care.

References

1. J. Lastdrager, J. Hanson, S. Smeekens, in *Journal of Experimental Botany*. (2014).
2. E. Baena-González, F. Rolland, J. M. Thevelein, J. Sheen, in *Nature*. (2007), vol. 448, pp. 938-942.
3. P. Crozet, F. Jammes, B. Valot, F. Ambard-Bretteville, S. Nessler, M. Hodges, J. Vidal, M. Thomas, in *J Biol Chem*. (2010), vol. 285, pp. 12071-12077.
4. P. Crozet, L. Margalha, A. Confraria, A. Rodrigues, C. Martinho, M. Adamo, C. A. Elias, E. Baena-González, in *Front. Plant Sci.* (2014), vol. 5, pp. 190.
5. C. Polge, M. Thomas, in *Trends Plant Sci*. (2007), vol. 12, pp. 20-28.
6. W. Shen, M. I. Reyes, L. Hanley-Bowdoin, in *Plant Physiol*. (2009), vol. 150, pp. 996-1005.
7. P. Coello, E. Hirano, S. J. Hey, N. Muttucumaru, E. Martinez-Barajas, M. A. J. Parry, N. G. Halford, in *Journal of experimental botany*. (2012), vol. 63, pp. 913-924.
8. S. Fragoso, L. Espíndola, J. Páez-Valencia, A. Gamboa, Y. Camacho, E. Martínez-Barajas, P. Coello, in *Plant Physiol*. (2009), vol. 149, pp. 1906-1916.
9. A. Rodrigues, M. Adamo, P. Crozet, L. Margalha, A. Confraria, C. Martinho, A. Elias, A. Rabissi, V. Lumbreras, M. González-Guzmán, R. Antoni, P. L.

Rodriguez, E. Baena-González, in *The Plant Cell*. (2013), vol. 25, pp. 3871-3884.
10. S. Emanuelle, M. I. Hossain, I. E. Moller, H. L. Pedersen, A. M. L. van de Meene, M. S. Doblin, A. Koay, J. S. Oakhill, J. W. Scott, W. G. T. Willats, B. E. Kemp, A. Bacic, P. R. Gooley, D. I. Stapleton, in *Plant J*. (2015), vol. 82, pp. 183-192.
11. M. Ramon, P. Ruelens, Y. Li, J. Sheen, K. Geuten, F. Rolland, in *Plant J*. (2013).
12. S. A. Saracco, M. J. Miller, J. Kurepa, R. D. Vierstra, in *PLANT PHYSIOLOGY*. (2007), vol. 145, pp. 119-134.
13. R. Geiss-Friedlander, F. Melchior, in *Nat Rev Mol Cell Biol*. (2007), vol. 8, pp. 947-956.
14. C. Guo, J. M. Henley, in *IUBMB Life*. (2014).
15. M. J. Mazur, H. A. Van Den Burg, in *Front. Plant Sci.* (2012), vol. 3, pp. 215.
16. N. Elrouby, G. Coupland, in *Proc Natl Acad Sci USA*. (2010), vol. 107, pp. 17415-17420.
17. M. J. Miller, G. A. Barrett-Wilt, Z. Hua, R. D. Vierstra, in *Proc Natl Acad Sci USA*. (2010), vol. 107, pp. 16512-16517.
18. P. H. Castro, R. M. Tavares, E. R. Bejarano, H. Azevedo, in *Cell Mol Life Sci*. (2012), vol. 69, pp. 3269-3283.
19. S. Jentsch, I. Psakhye, in *Annu. Rev. Genet.* (2013).
20. E. S. Johnson, in *Annu Rev Biochem*. (2004), vol. 73, pp. 355-382.
21. H. J. Park, W.-Y. Kim, H. C. Park, S. Y. Lee, H. J. Bohnert, D.-J. Yun, in *Mol Cells*. (2011), vol. 32, pp. 305-316.
22. K. Tomanov, A. Zeschmann, R. Hermkes, K. Eifler, I. Ziba, M. Grieco, M. Novatchkova, K. Hofmann, H. Hesse, A. Bachmair, in *Plant Cell*. (2014), vol. 26, pp. 4547-4560.
23. G. J. K. Praefcke, K. Hofmann, R. J. Dohmen, in *Trends in Biochemical Sciences*. (2012), vol. 37, pp. 23-31.
24. N. Elrouby, M. V. Bonequi, A. Porri, G. Coupland, in *Proc Natl Acad Sci USA*. (2013).
25. J. Kurepa, J. M. Walker, J. Smalle, M. M. Gosink, S. J. Davis, T. L. Durham, D.-Y. Sung, R. D. Vierstra, in *J Biol Chem*. (2003), vol. 278, pp. 6862-6872.
26. R. Catala, J. Ouyang, I. A. Abreu, Y. Hu, H. Seo, X. Zhang, N.-H. Chua, in *Plant Cell*. (2007), vol. 19, pp. 2952-2966.
27. N. G. Halford, S. J. Hey, in *Biochem J*. (2009), vol. 419, pp. 247-259.
28. S. K. Hanks, T. Hunter, Protein kinases 6. *FASEB J* (1995), vol. 9, pp. 576-596.
29. V. Bernier-Villamor, D. A. Sampson, M. J. Matunis, C. D. Lima, in *CELL*. (2002), vol. 108, pp. 345-356.
30. M. H. Tatham, Y. Chen, R. T. Hay, in *Biochemistry*. (2003), vol. 42, pp. 3168-3179.
31. S. Okada, M. Nagabuchi, Y. Takamura, T. Nakagawa, K. Shinmyozu, J.-i. Nakayama, K. Tanaka, in *Plant Cell Physiol*. (2009), vol. 50, pp. 1049-1061.
32. I. A. Hendriks, R. C. J. D'souza, B. Yang, M. Verlaan-de Vries, M. Mann, A. C. O. Vertegaal, in *Nat Struct Mol Biol*. (2014).
33. T. Rubio, S. Vernia, P. Sanz, in *Mol Biol Cell*. (2013), vol. 24, pp. 1801-1811.
34. K. J. Simpson-Lavy, M. Johnston, in *Proc Natl Acad Sci USA*. (2013).
35. H. D. Ulrich, *SUMO Protocols*. J. M. Walker, Ed., METHODS IN MOLECULAR BIOLOGY (Humana Press, New York, 2009), vol. 497.

36. R. P. Bhalerao, K. Salchert, L. Bakó, L. Okrész, L. Szabados, T. Muranaka, Y. Machida, J. Schell, C. Koncz, in *Proc Natl Acad Sci USA*. (1999), vol. 96, pp. 5322-5327.
37. T. Kleinow, R. Bhalerao, F. Breuer, M. Umeda, K. Salchert, C. Koncz, *Plant J.* (2000), vol. 23, pp.115-122.
38. M. Novatchkova, K. Tomanov, K. Hofmann, H.-P. Stuible, A. Bachmair, in *New Phytol*. (2012), vol. 195, pp. 23-31.
39. K. Miura, A. Rus, A. Sharkhuu, S. Yokoi, A. S. Karthikeyan, K. G. Raghothama, D. Baek, Y. D. Koo, J. B. Jin, R. A. Bressan, D.-J. Yun, P. M. Hasegawa, in *Proc Natl Acad Sci USA*. (2005), vol. 102, pp. 7760-7765.
40. T. Ishida, S. Fujiwara, K. Miura, N. Stacey, M. Yoshimura, K. Schneider, S. Adachi, K. Minamisawa, M. Umeda, K. Sugimoto, in *Plant Cell*. (2009), vol. 21, pp. 2284-2297.
41. T. Ishida, M. Yoshimura, K. Miura, K. Sugimoto, in *PLoS ONE*. (2012), vol. 7, pp. e46897.
42. M. J. Matunis, E. Coutavas, G. Blobel, in *J Cell Biol*. (1996), vol. 135, pp. 1457-1470.
43. R. Mahajan, C. Delphin, T. Guan, L. Gerace, F. Melchior, in *Cell*. (1997), vol. 88, pp. 97-107.
44. I. Psakhye, S. Jentsch, in *CELL*. (2012), vol. 151, pp. 807-820.
45. J.-S. Seeler, A. Dejean, in *Nature Reviews Molecular Cell Biology*. (2003), vol. 4, pp. 690-699.
46. M. Bitrián, F. Roodbarkelari, M. Horváth, C. Koncz, in *Plant J*. (2011), vol. 65, pp. 829-842.
47. K. Miura, J. B. Jin, J. Lee, C. Y. Yoo, V. Stirm, T. Miura, E. N. Ashworth, R. A. Bressan, D.-J. Yun, P. M. Hasegawa, in *Plant Cell*. (2007), vol. 19, pp. 1403-1414.
48. K. Miura, J. Lee, J. B. Jin, C. Y. Yoo, T. Miura, P. M. Hasegawa, in *Proc Natl Acad Sci USA*. (2009), vol. 106, pp. 5418-5423.
49. Y. Zheng, K. S. Schumaker, Y. Guo, in *Proc Natl Acad Sci USA*. (2012), vol. 109, pp. 12822-12827.
50. S.-D. Yoo, Y.-H. Cho, J. Sheen, in *Nat Protoc*. (2007), vol. 2, pp. 1565-1572.
51. R. Budhiraja, R. Hermkes, S. Müller, J. Schmidt, T. Colby, K. Panigrahi, G. Coupland, A. Bachmair, in *PLANT PHYSIOLOGY*. (2009), vol. 149, pp. 1529-1540.
52. A. Suzuki, S. Okamoto, S. Lee, K. Saito, T. Shiuchi, Y. Minokoshi, in *Mol Cell Biol*. (2007), vol. 27, pp. 4317-4327.
53. N. Kazgan, T. Williams, L. J. Forsberg, J. E. Brenman, in *Mol Biol Cell*. (2010), vol. 21, pp. 3433-3442.
54. A. Roscic, A. Möller, M. A. Calzado, F. Renner, V. C. Wimmer, E. Gresko, K. S. Lüdi, M. L. Schmitz, in *Molecular Cell*. (2006), vol. 24, pp. 77-89.
55. C. H. Lin, S. Y. Liu, E. H. Y. Lee, in *Oncogene*. (2015).
56. R. Hermkes, Y.-F. Fu, K. Nürrenberg, R. Budhiraja, E. Schmelzer, N. Elrouby, R. J. Dohmen, A. Bachmair, G. Coupland, in *Planta*. (2011), vol. 233, pp. 63-73.
57. W. Yang, W. Paschen, in *Proteomics*. (2014).
58. R. Niedenthal, in *Biochem Soc Trans*. (2007), vol. 35, pp. 1430-1432.
59. A. Jakobs, J. Koehnke, F. Himstedt, M. Funk, B. Korn, M. Gaestel, R. Niedenthal, in *Nat Methods*. (2007), vol. 4, pp. 245-250.

60. A. Jakobs, F. Himstedt, M. Funk, B. Korn, M. Gaestel, R. Niedenthal, in *Nucleic Acids Research*. (2007), vol. 35, pp. e109.
61. L. M. Lois, C. D. Lima, N.-H. Chua, in *Plant Cell*. (2003), vol. 15, pp. 1347-1359.
62. S. J. Li, M. Hochstrasser, in *Mol Cell Biol*. (2000), vol. 20, pp. 2367-2377.
63. S. J. Li, M. Hochstrasser, in *Nature*. (1999), vol. 398, pp. 246-251.
64. I. Schwienhorst, E. S. Johnson, R. J. Dohmen, in *Mol Gen Genet*. (2000), vol. 263, pp. 771-786.
65. J. Eckhoff, R. J. Dohmen, in *J Biol Chem*. (2015).
66. C. Hoege, B. Pfander, G.-L. Moldovan, G. Pyrowolakis, S. Jentsch, in *Nature*. (2002), vol. 419, pp. 135-141.
67. H. Sun, T. Hunter, in *J Biol Chem*. (2012), vol. 287, pp. 42071-42083.
68. R. Farrás, A. Ferrando, J. Jásik, T. Kleinow, L. Okrész, A. Tiburcio, K. Salchert, C. del Pozo, J. Schell, C. Koncz, in *The EMBO Journal*. (2001), vol. 20, pp. 2742-2756.
69. M. O'Brien, R. N. Kaplan-Levy, T. Quon, P. G. Sappl, D. R. Smyth, in *Journal of Experimental Botany*. (2015).
70. T. Colby, A. Matthäi, A. Boeckelmann, H.-P. Stuible, in *Plant Physiol*. (2006), vol. 142, pp. 318-332.
71. H. A. Van Den Burg, R. K. Kini, R. C. Schuurink, F. L. W. Takken, in *The Plant Cell*. (2010), vol. 22, pp. 1998-2016.
72. J. M. Alonso, A. N. Stepanova, T. J. Leisse, C. J. Kim, H. Chen, P. Shinn, D. K. Stevenson, J. Zimmerman, P. Barajas, R. Cheuk, C. Gadrinab, C. Heller, A. Jeske, E. Koesema, C. C. Meyers, H. Parker, L. Prednis, Y. Ansari, N. Choy, H. Deen, M. Geralt, N. Hazari, E. Hom, M. Karnes, C. Mulholland, R. Ndubaku, I. Schmidt, P. Guzman, L. Aguilar-Henonin, M. Schmid, D. Weigel, D. E. Carter, T. Marchand, E. Risseeuw, D. Brogden, A. Zeko, W. L. Crosby, C. C. Berry, J. R. Ecker, *Science* (2003), vol. 301, pp. 653-657.
73. K. Miura, A. Rus, A. Sharkhuu, S. Yokoi, A. S. Karthikeyan, K. G. Raghothama, D. Baek, Y. D. Koo, J. B. Jin, R. A. Bressan, D. J. Yun, P. M. Hasegawa, *Proc Natl Acad Sci U S A* (2005), vol. 102, pp. 7760-7765.
74. A. Y. Tsai, S. Gazzarrini, *Plant J.* (2012), vol. 69, pp. 809-821.
75. E. Baena-Gonzalez, Rolland, F., J. M. Thevelein, J. Sheen, *Nature* (2007), vol. 448, pp. 938-942.
76. M. Karimi, B. De Meyer, P. Hilson, *Trends Plant Sci.* (2005), vol. 10, pp. 103-105.
77. S. J. Clough, A. F. Bent, *Plant J* (1998), vol. 16, pp. 735-743.
78. S. D. Yoo, Y. H. Cho, J. Sheen, *Nat Protoc.* (2007), vol. 2, pp. 1565-1572.
79. U. K. Laemmli, *Nature* (1970), vol. 227, pp. 680-685.
80. S. Okada, M. Nagabuchi, Y. Takamura, T. Nakagawa, K. Shinmyozu, J. Nakayama, K. Tanaka, *Plant Cell Physiol.* (2009), vol. 50, pp.1049-1061.
81. A. Saez, A. Rodrigues, J. Santiago, S. Rubio, P. L. Rodriguez, *Plant Cell* (2008), vol. 20, pp. 2972-2988.

CHAPTER 3 |

Biochemical and functional outcomes of SnRK1 sumoylation

Authors' Contributions

Leonor Margalha and Pierre Crozet contributed equally to the work presented in this chapter. Pierre Crozet did the *in vitro* kinase assays and generated the *siz1-2 snrk1α1* double mutant plants. Noémia Fernandes contributed to the qRT-PCR experiments.

Abstract

Many protein kinases are regulated by sumoylation, often with interplay between SUMO and other posttranslational modifications. Sumoylation functions mainly through modulation of intra- and intermolecular protein interactions, thereby affecting a protein activity, stability and/or subcellular localization. We show that absence of the SUMO E3-ligase SIZ1 leads to enhanced SnRK1 activity in the *siz1-2* mutant, that can be reverted to wild-type (WT) levels by transient complementation with SIZ1, but not with the catalytically inactive $SIZ1^{C379A}$ variant. Furthermore, a translational fusion of SUMO1 to SnRK1α1 mimics sumoylation and restores SnRK1 signaling in *siz1-2*, supporting that the overactivation of the SnRK1 pathway in this mutant is caused by lack of SnRK1 sumoylation. We observed increased stability and accumulation of several SnRK1 subunits in *siz1-2*, suggesting SnRK1 sumoylation promotes its degradation, thereby restraining SnRK1 signaling. We further show that SnRK1 is ubiquitylated *in planta* and targeted for proteasomal degradation. SUMO and ubiquitin conjugates co-purify in SnRK1 immunoprecipitates. However, in the *siz1-2* background, SnRK1-ubiquitin conjugates are greatly reduced, suggesting interplay between sumoylation and ubiquitylation in targeting SnRK1 for degradation. Additionally, preliminary results suggest sumoylation may affect also SnRK1 complex composition, and possibly SnRK1 complex assembly and its putative oligomerization.

3.1 | Introduction

The attachment of small ubiquitin-like modifier (SUMO) to substrate proteins is involved in a wide range of biological functions, and allows modulation of various pathways and processes in all eukaryotes, including plants (*1*). Downstream effects of sumoylation occur primarily through modulation of interactions of the modified substrate with other proteins, since SUMO attachment alters the properties and binding surface of the target. The most common outcome of sumoylation is to promote protein-protein non-covalent interactions, but the SUMO moiety in a substrate can also act as a "repellent", blocking the access of binding partners to the same residue or to a close binding site. On the other hand, substrate sumoylation can lead to a change in its conformation due to the establishment of intramolecular SUMO-SIM interactions with relevant functional consequences. By any of these means, sumoylation can have an impact on substrate stability, activity, and/or subcellular localization.

Many protein kinases are regulated by sumoylation, often through interplay between SUMO and other posttranslational modifications (PTMs), allowing a robust and versatile response to specific physiological contexts or signaling cues (*2-4*). Increasing reports evidence a crosstalk between sumoylation and ubiquitylation at the substrate level. In many cases, multi- or poly-sumoylation and poly-ubiquitylation occur sequentially and in a cooperative manner to bring protein targets for proteasomal degradation (*5-7*). Novel classes of modulators such as E4 SUMO ligases that promote SUMO chain extension (*8*), SUMO targeted Ubiquitin ligases (STUbLs) that bind and ubiquitylate multi- or poly-sumoylated targets (*9, 10*), and specific deubiquitylases that revert STUbLs' action by deubiquitylating hybrid SUMO-ubiquitin chains (*11*), are being unraveled at a fast pace, helping to clarify the mechanisms of SUMO and ubiquitin interplay. Here, we show sumoylation impacts SnRK1 protein stability

and consequently SnRK1 signaling *in planta*. Sumoylation-dependent ubiquitylation of SnrK1 is shown to target the protein kinase towards proteolytic degradation. Furthermore, we analyze a possible impact of sumoylation in SnRK1 complex composition and putative oligomerization.

3.2 | Results

3.2.1 | Sumoylation inhibits SnRK1 signaling

To investigate whether sumoylation has an impact on SnRK1 signaling, we focused on the major catalytic subunit SnRK1α1, as it accounts for nearly 90% of SnRK1 activity *in planta* (*12*). To this end, we used a cell-based (protoplast) assay in which SnRK1 activity is measured as an induction of the *pDIN6::LUC* reporter and transient SnRK1α1 overexpression is sufficient to trigger strong activation of the SnRK1 pathway (*13, 14*). We assessed whether co-expression of SUMO machinery components (E2 SCE1, E3 SIZ1, or E3 HPY2) and mature SUMO variants (mSUMO1 or mSUMO3) in this assay could promote SnRK1α1 sumoylation and thereby alter SnRK1 signaling. A similar approach was successfully used to demonstrate sumoylation of the plant transcription factors ICE1, ABI5 and MYB30 *in vivo* (*15-17*), where the overexpression with SUMO isoforms was sufficient to stimulate sumoylation. SnRK1α1 overexpression resulted, as expected, in strong activation of the SnRK1 pathway. However, no increase or reduction of SnRK1 signaling could be observed upon co-expression of SnRK1α1 with E2 SCE1 (SCE) alone or with mature SUMO variants (mS1, mS3) (**Figure** 3.1A).

Since SnRK1 sumoylation is totally abolished in the *siz1-2* mutant (**Figure** 2.7), we next decided to co-express SnRK1α1 and SUMO1 or SUMO3 with the

E3 ligase SIZ1. Interestingly, SnRK1 pathway activation was reduced to half in the presence of SIZ1 and mature SUMO1, but not when SnRK1α1 was co-expressed with SIZ1 and mature SUMO3 (**Figure** 3.1B). Furthermore, by co-expressing SnRK1α1 with the E3 ligase HPY2 using the same settings, we could no longer observe an impact on SnRK1 pathway activation (**Figure** 3.1C). Altogether, these results suggest that SnRK1α1 sumoylation represses SnRK1 signaling in Arabidopsis. In agreement with our previous findings (**Figure** 2.7), SIZ1 is responsible for this sumoylation and requires specifically the SUMO1 isoform.

The SnRK1 pathway can also be activated downstream of the SnRK1 kinase, through overexpression of the GBF5 transcription factor (*13, 14*). To assess whether SIZ1-mediated repression of SnRK1 signaling occurs at the kinase level or downstream of it, we monitored *pDIN6::LUC* reporter activation by GBF5 in the presence or absence of SIZ1 and mature SUMO1. A similar response was observed when overexpressing GBF5 alone or in combination with SIZ1 and mature SUMO1 (**Figure** 3.1D), indicating that SIZ1 acts upstream of GBF5 on SnRK1 signaling, presumably on SnRK1 itself.

We next decided to test if a SnRK1α1$^{K34/63/390R}$ triple mutant (SnRK1α1^{3K}), which is not sumoylated in the *E.coli* system, could escape the repression by SIZ1 and SUMO1 (**Figure** 2.4F). However, the SnRK1α1^{3K} variants were comparable to the WT kinase in their susceptibility to SIZ1-dependent repression of SnRK1 signaling (**Figure** 3.1E). Furthermore, a SnRK1α1 variant mutated in all sumoylated lysines detected in the *E. coli* system (SnRK1α1^{8K}), except K144 as this mutation abolishes kinase activity [(*18*) and data not shown], induced the reporter normally (**Figure** 3.1F). The same was observed for the SnRK1α1^{3K} variant, whereas an inactive SnRK1α1^{T175A} kinase (*13*) had no effect. These results suggest that SnRK1α1 can be sumoylated on other residues *in planta*, and/or that sumoylation of other components of the complex (e.g. the β-regulatory subunits) is sufficient to exert SUMO function.

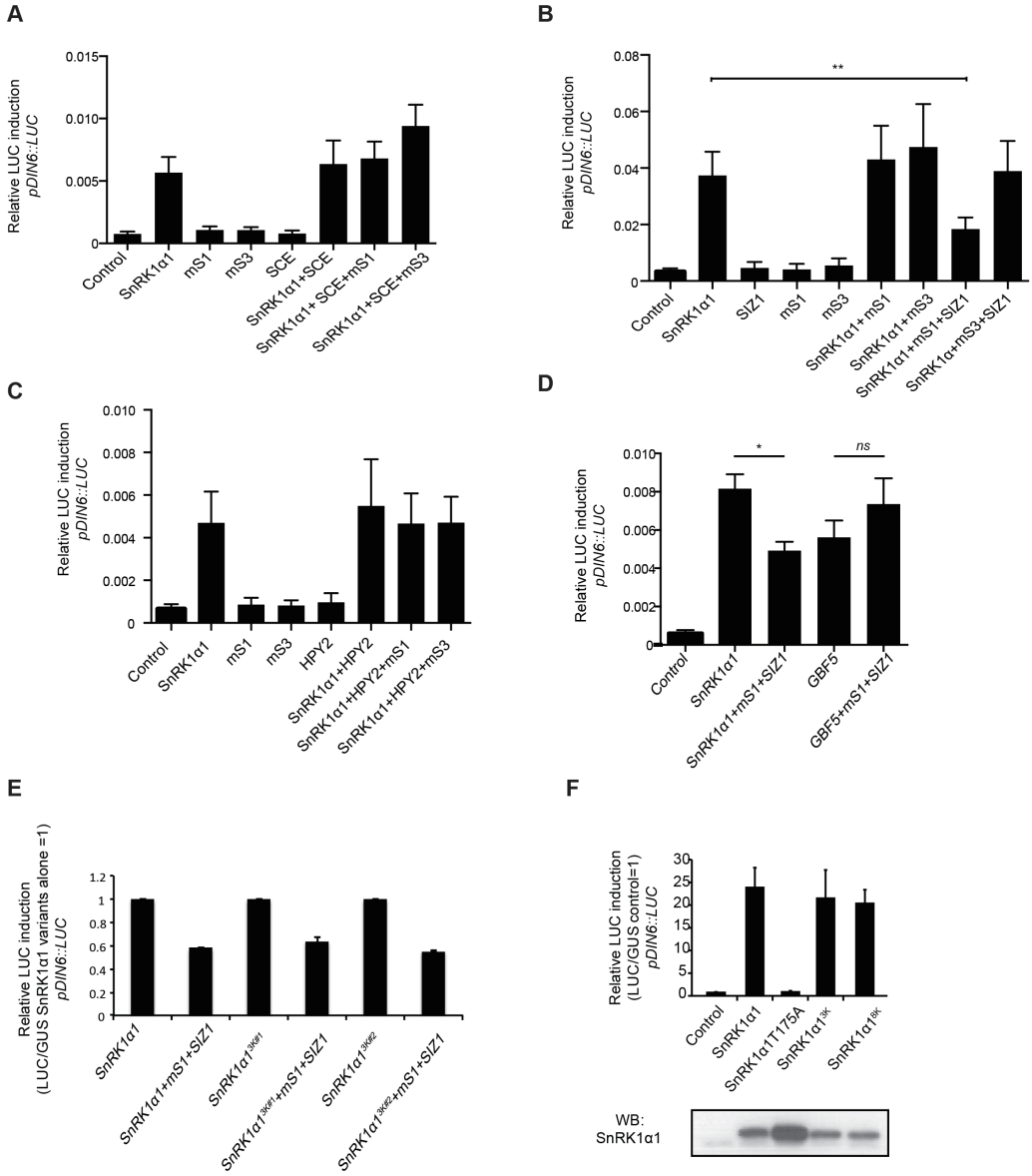

Figure 3.1 | SIZ1-mediated sumoylation of SnRK1α1 represses SnRK1 signaling.

A. Normal induction of SnRK1 signaling by SnRK1α1 in the presence of the E2 SUMO conjugating enzyme SCE1 (SCE) and mature SUMO isoforms. Co-expression of SCE and mature SUMO1 (mS1) or SUMO3 (mS3) does not alter the ability of SnRK1α1 to induce the *pDIN6::LUC*

reporter. **B**. Repression of SnRK1 signaling by SIZ1 and SUMO1. Co-expression of E3 SUMO ligase SIZ1 and mature SUMO1 (mS1) but not SUMO3 (mS3) represses the ability of SnRK1α1 to induce the *pDIN6::LUC* reporter. **C**. Normal induction of SnRK1 signaling by SnRK1α1 in the presence of HPY2 and mature SUMO isoforms. Co-expression of E3 SUMO ligase HPY2 and mature SUMO1 (mS1) or SUMO3 (mS3) does not alter the ability of SnRK1α1 to induce the *pDIN6::LUC* reporter. **D**. The ability of GBF5 to induce SnRK1 signaling is not altered by the presence of SIZ1 and mature SUMO1. Co-expression of E3 SUMO ligase SIZ1 and mature SUMO1 (mS1) represses the ability of SnRK1α1, but not of GBF5, to induce the *pDIN6::LUC* reporter. **E**. Normal repression of SnRK1 signaling by SIZ1 and mature SUMO1 in SnRK1α1 lysine mutants. Co-expression of E3 SUMO ligase SIZ1 and mature SUMO1 (mS1) represses the ability of WT SnRK1α1 and of a SnRK1α1^{3K} variant to induce the *pDIN6::LUC* reporter (#1 and #2 denote two independent clones). 3K, K34R/K63R/K390R. **F**. Normal induction of SnRK1 signaling by SnRK1α1 multiple-lysine mutants. Expression of SnRK1α1 in Arabidopsis mesophyll protoplasts triggers SnRK1 signaling, as measured by induction of the *pDIN6::LUC* reporter. Mutation of K residues found to be sumoylated in the *E. coli* system does not alter the ability of SnRK1α1 to induce the *pDIN6::LUC* reporter. 3K, K34R/K63R/K390R; 8K, K20R/K34R/K44R/K56R/K63R/K69R/K390R/K421R. An inactive T-loop phosphomutant (T175A) is used as a negative control. **A-F** n≥3, in **E** one representative biological experiment is shown. Error bars=SEM. Stars denote statistical significance, as determined by ratio paired t-test (ns $p>0.05$, *$p<0.05$, **$p<0.005$).

As an alternative strategy to globally block sumoylation of the SnRK1 complex and to assess its functional relevance, we decided to compare SnRK1 signaling in Col-0 (WT) and *siz1-2* plants, impaired in SnRK1 sumoylation (**Figure** 2.7). To this end, we treated plants with control (3h light) or SnRK1 activating conditions (3h darkness) and measured the expression of SnRK1 target genes by quantitative RT-PCR (qRT-PCR), as readout of SnRK1 pathway activation (*13, 14*). As expected, exposure to darkness triggered a strong induction of SnRK1 target genes (*AXP, DIN6* and *TPS8*) in Col-0 plants (**Figure** 3.2A). This induction was two-fold higher in the *siz1-2* mutant, showing that, in accordance with the SIZ1-mediated repression of SnRK1 signaling observed in

Col-0 protoplasts (**Figure** 3.1C), SIZ1 is a negative regulator of SnRK1 signaling in Arabidopsis.

Given the compromised growth and pleiotropic phenotypes of the *siz1-2* plants (*19*), we next employed the cell-based system to rule out potential secondary effects of the long-term depletion of SIZ1 on SnRK1 activity in the mutant. To this end, we isolated protoplasts from Col-0 and *siz1-2* plants and monitored activation of the *pDIN6::LUC* reporter by SnRK1α1. As expected, SnRK1α1 overexpression in Col-0 protoplasts triggered a strong activation of the reporter. However, reporter activation was roughly 3-fold higher in the *siz1-2* mutant (**Figure** 3.2B), consistent with the analyses of endogenous gene expression. We next complemented the *siz1-2* mutant by transiently co-expressing SIZ1, or a catalytically inactive SIZ1 variant ($SIZ1^{C379A}$) that lacks SUMO E3 ligase activity (*20*), with SnRK1α1. Whilst co-expression of SIZ1 or $SIZ1^{C379A}$ did not alter reporter activity in Col-0 cells, the overactivation of the reporter in *siz1-2* could be reverted to Col-0 levels by SIZ1 but not by $SIZ1^{C379A}$ expression (**Figure** 3.2B). This result further supports that the E3 ligase activity of SIZ1 restrains SnRK1 signaling *in vivo*.

On the other hand, *pDIN6::LUC* reporter activation by GBF5 in *siz1-2* was normal, and a similar response was observed by co-expressing SIZ1 or $SIZ1^{C379A}$, as in Col-0 cells (**Figure** 3.2C). These results evidence that SIZ1-mediated repression of SnRK1 signaling occurs upstream of GBF5, namely on SnRK1, as previously suggested (**Figure** 3.1D).

As a complementary strategy to restore normal SnRK1 pathway activation in *siz1-2*, we generated a SnRK1α1 ”SUMO mimetic”, through a translational fusion of SnRK1α1 to a non-conjugatable mature SUMO1-AA isoform (SnRK1α1-SUMO1) (*21*), and tested its ability to induce the *pDIN6::LUC* reporter. Fusion of SUMO1 to SnRK1α1 restored SnRK1 signaling in *siz1-2* to the levels observed in Col-0 cells (**Figure** 3.2D), further supporting that the overactivation of SnRK1 signaling in the *siz1-2* mutant is caused by lack of SnRK1α1 sumoylation.

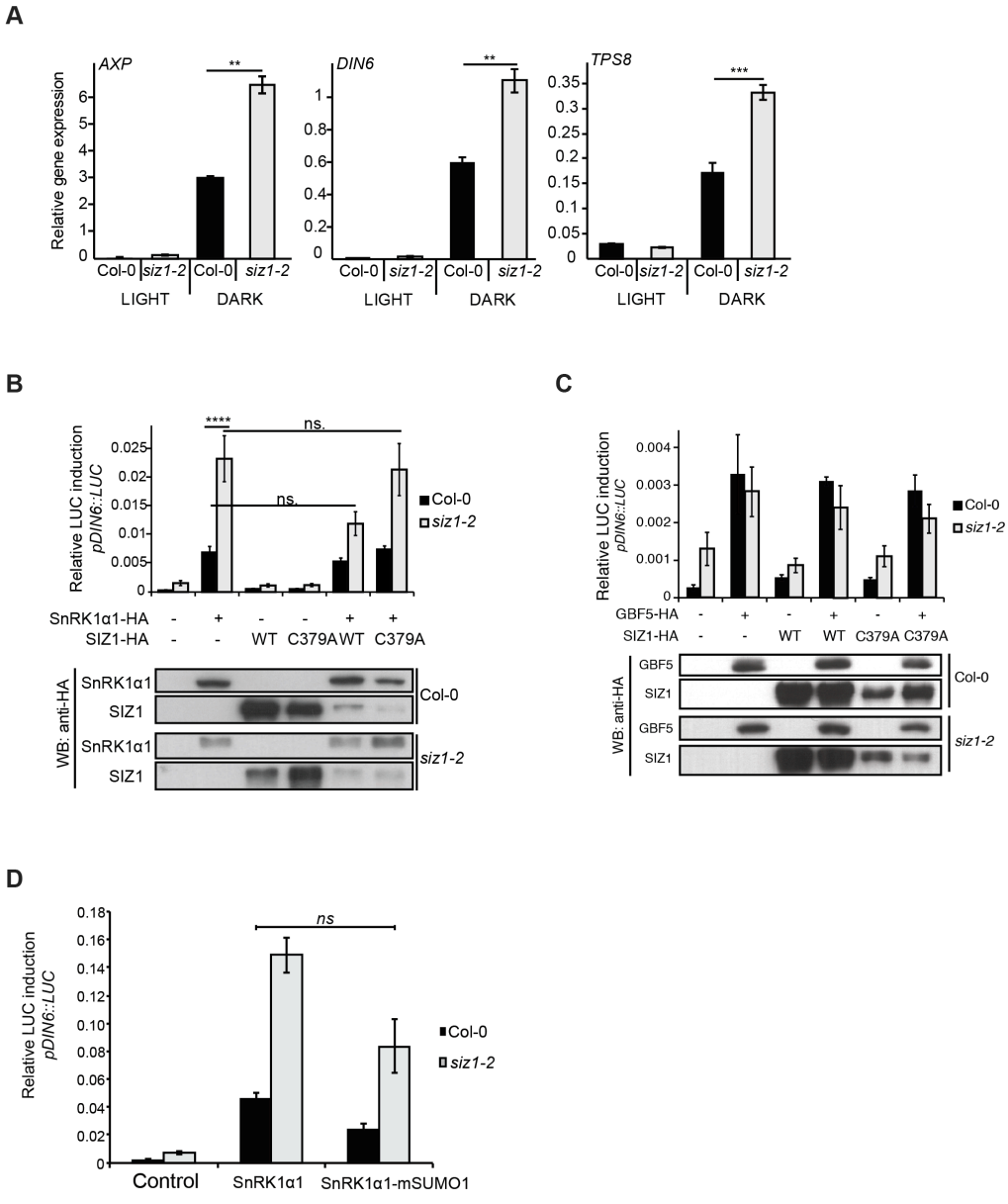
A
AXP
DIN6
TPS8
Relative gene expression
Col-0
siz1-2
LIGHT
DARK
B
Relative LUC induction
pDIN6::LUC
SnRK1α1-HA
SIZ1-HA
WT
C379A
WB: anti-HA
SnRK1α1
SIZ1
C
GBF5-HA
GBF5
D
Control
SnRK1α1
SnRK1α1-mSUMO1
ns

Figure 3.2 | SnRK1 signaling overactivation in *siz1-2* is due to lack of SnRK1 sumoylation.

A. Overinduction of SnRK1 signaling in the *siz1-2* mutant. Relative gene expression of SnRK1 marker genes (*AXP, DIN6, TPS8*) in Col-0 or *siz1-2* mutant plants treated under control (Light) or energy stress (Dark) conditions. Stars denote statistical significance, as determined by paired t-test (n=4; error bars=SEM; **p<0.01; ***p<0.001). **B**. Overinduction of SnRK1 signaling in *siz1-2* is rescued to WT levels by the E3 ligase activity of SIZ1. Expression of SnRK1α1 triggers a three-fold higher induction of the *pDIN6::LUC* reporter in *siz1-2* than in Col-0 protoplasts. Normal *pDIN6::LUC* expression is recovered by co-expression of SIZ1, but not of a catalytically inactive $SIZ1^{C379A}$ variant. **C**. Induction of SnRK1 signaling downstream of SnRK1 is normal in *siz1-2*. Expression of the GBF5 transcription factor triggers similar induction of the *pDIN6::LUC* reporter in Col-0 and *siz1-2* protoplasts. Stars (**B,C**) denote statistical significance, as determined by two-way ANOVA (n=3; error bars=SEM; ns., p>0.05; **p<0.01; ****p<0.0001). **D**. A SnRK1α1 SUMO-mimetic restores normal SnRK1 signaling in *siz1-2* protoplasts. Expression of SnRK1α1 triggers a three-fold higher induction of the *pDIN6::LUC* reporter in *siz1-2* than in Col-0 protoplasts. Expression of SnRK1α1-mSUMO1 fusion protein mimics SnRK1α1 sumoylation in *siz1-2* cells and rescues *pDIN6::LUC* induction to the levels of the WT protein in Col-0 protoplasts. Statistical significance was determined by paired t-test (n=3; error bars=SEM; ns. p>0.05).

Several phenotypes of *siz1-2*, such as diminished plant size, heightened innate immunity, and drought- or basal thermo-tolerance, amongst others, are largely due to the elevated salicylic acid (SA) levels of the mutant (*19, 22-27*). Thus, we next asked if the effect of the *siz1-2* mutation on SnRK1 signaling was indirect, and more specifically induced by SA. To test this, we treated Col-0 protoplasts transfected with the *pDIN6::LUC* reporter and SnRK1α1 with SA or mock control. As shown in **Figure** 3.3A, SA had no effect on SnRK1 signaling during a short (2h) or extended (overnight, 15h) incubation. Furthermore, examination of public microarray datasets with the Genevestigator tool (*28*) revealed that various SA treatments that induce systemic acquired resistance (SAR) marker genes, do not affect SnRK1 marker genes (*DIN6*, *AXP* and *TPS8*) (**Figure** 3.3B), ruling out an indirect effect of the *siz1-2* mutation on SnRK1 signaling mediated by SA.

Overall, the results presented show that SIZ1 inhibits SnRK1 signaling *in vivo*, most probably through sumoylation of the SnRK1 complex.

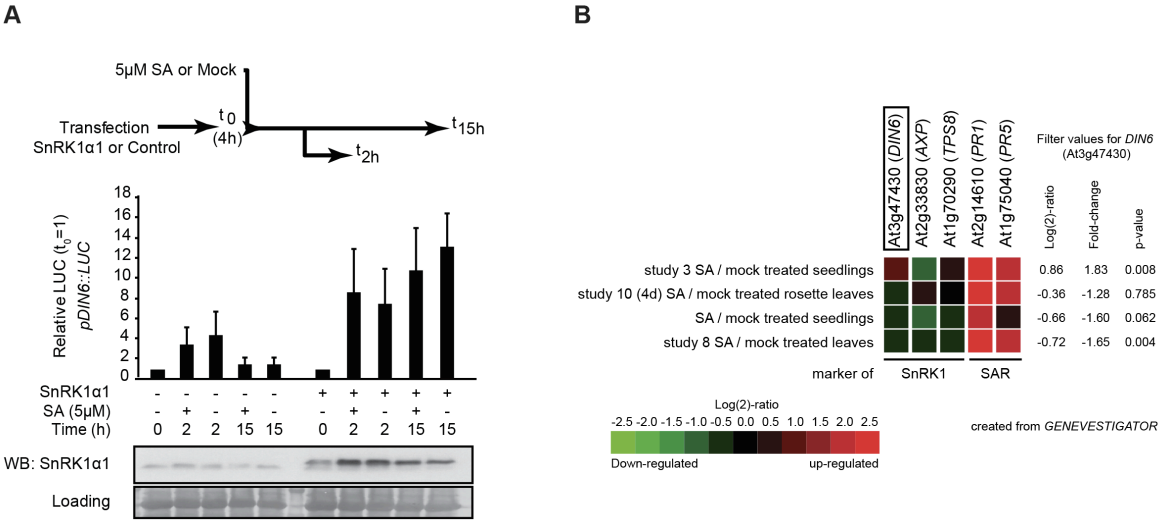

Figure 3.3 | Salicylic acid (SA) has no effect on SnRK1 signaling.

A. SA does not alter SnRK1 reporter gene induction in protoplasts. The *pDIN6::LUC* reporter for SnRK1 signaling is induced by SnRK1α1 expression, but this induction is similar in mock- and SA-treated cells. Protoplasts were transfected with a plasmid expressing SnRK1α1 or control DNA, incubated for 4h and thereafter treated with SA (5µM) or ethanol (mock control) and the t_0 was collected. After 2h or 15h, the cells were collected for luciferase/ glucuronidase activity assays. Expression was confirmed by Western blot (WB) with anti-SnRK1α1 antibody. Data presented are means and error bars are SEM (n=3). **B**. Various SA treatments induce the expression of two marker genes of Systemic Acquired Resistance (SAR), *PR1* (At2g14610) and *PR5* (At1g75040), but not of SnRK1 marker genes *DIN6* (At3g47340), *AXP* (At2g33830), and *TPS8* (At1g70290). The data are from four independent studies and were obtained using *Genevestigator* (https://genevestigator.com/gv/).

3.2.2 | Sumoylation triggers SnRK1 degradation

Proteins modified by SUMO acquire novel molecular features that can affect their stability, activity, and/or subcellular localization, primarily through altered interactions with other proteins (*29*). To determine whether the SIZ1-dependent inhibition of SnRK1 signaling involved changes on SnRK1 specific activity, we performed *in vitro* kinase assays using ABF2 as a peptide substrate (*14*). To minimize potential cross-contamination with other related kinases (e.g. SnRK2 kinases) we used SnRK1α1 immunoprecipitated from Col-0 or *siz1-2* plants instead of total protein extracts. As shown in **Figure** 3.4A, ABF2 phosphorylation was two-fold higher with SnRK1 immunoprecipitated from the *siz1-2* mutant than from the Col-0 control. However, despite starting from identical amounts of total protein in both Col-0 and *siz1-2* extracts, the higher activity was fully explained by the two-fold higher amount of SnRK1α1 immunoprecipitated from *siz1-2* plants (**Figure** 3.4A, lower panel). This shows that the overactivation of SnRK1 signaling in *siz1-2* plants is not caused by changes in SnRK1 specific activity, but rather by an enhanced accumulation of the kinase in the *siz1-2* background. Furthermore, the reduced induction of SnRK1 signaling by SnRK1α1-mSUMO1 (see also **Figure** 3.2D) correlated with a decreased accumulation of the "sumo mimetic" protein in comparison to WT SnRK1α1, in Col-0 cells (**Figure** 3.4B).

To determine more precisely SnRK1 protein levels in Col-0 and *siz1-2* genotypes, we performed immunoblot analyses using total protein extracts. These analyses confirmed that SnRK1α1 is about 2.5-fold more abundant in *siz1-2* than in Col-0 plants (**Figure** 3.4C). As a result of increased accumulation, SnRK1α1 T-loop phosphorylation is also 2.5-fold higher in the *siz1-2* mutant, consistent with a similar SnRK1 specific activity in Col-0 and *siz1-2* plants. T-loop phosphorylation was detected with an antibody (P-AMPK) that recognizes both SnRK1α1 and SnRK1α2 phosphorylated on their regulatory T-loop threonine (T175 and T176, respectively) (*13*). The levels of phosphorylated

SnRK1α2 were also higher in *siz1-2* (**Figure** 3.4C), suggesting that regulation of kinase stability through sumoylation may also apply to the SnRK1α2 isoform.

In accordance with our previous indications that sumoylation could target several SnRK1 subunits (**Figure** 2.3A and 2.6B), we also detected an increase in SnRK1β1 protein amounts in *siz1-2*, whereas SnRK1β2 accumulation was unchanged in both genotypes (**Figure** 3.4D). Similar comparisons were not possible for SnRK1βγ since the available antibodies recognize multiple bands in total protein extracts (not shown), despite being adequate for analyzing SnRK1 immunoprecipitates (**Figure** 2.6B). Interestingly, and although SnRK1γ is not fully established as a SnRK1 subunit, it displayed a 3.5-fold accumulation in the *siz1-2* mutant (**Figure** 3.4E).

To investigate the cause of enhanced SnRK1α1 accumulation in *siz1-2*, we next performed protein half-life measurements, using protoplasts isolated from *siz1-2* or Col-0 plants and transfected with a plasmid expressing SnRK1α1. Following 6h of incubation to allow protein expression, translation was blocked by the addition of cycloheximide and SnRK1α1 protein levels were quantified after 2 and 4 hours. As shown in **Figure** 3.4F, SnRK1α1 degradation was significantly reduced in *siz1-2* compared to Col-0 cells. Importantly, the SnRK1α1-mSUMO1 fusion protein that mimics SnRK1α1 sumoylation and restores SnRK1 signaling in *siz1-2* protoplasts (**Figure** 3.2D), recovered SnRK1α1 degradation in *siz1-2* to a similar extent as in Col-0 cells.

Collectively, the data presented suggests that SIZ1-dependent sumoylation of SnRK1α1 has an impact on the kinase stability, namely promoting its degradation.

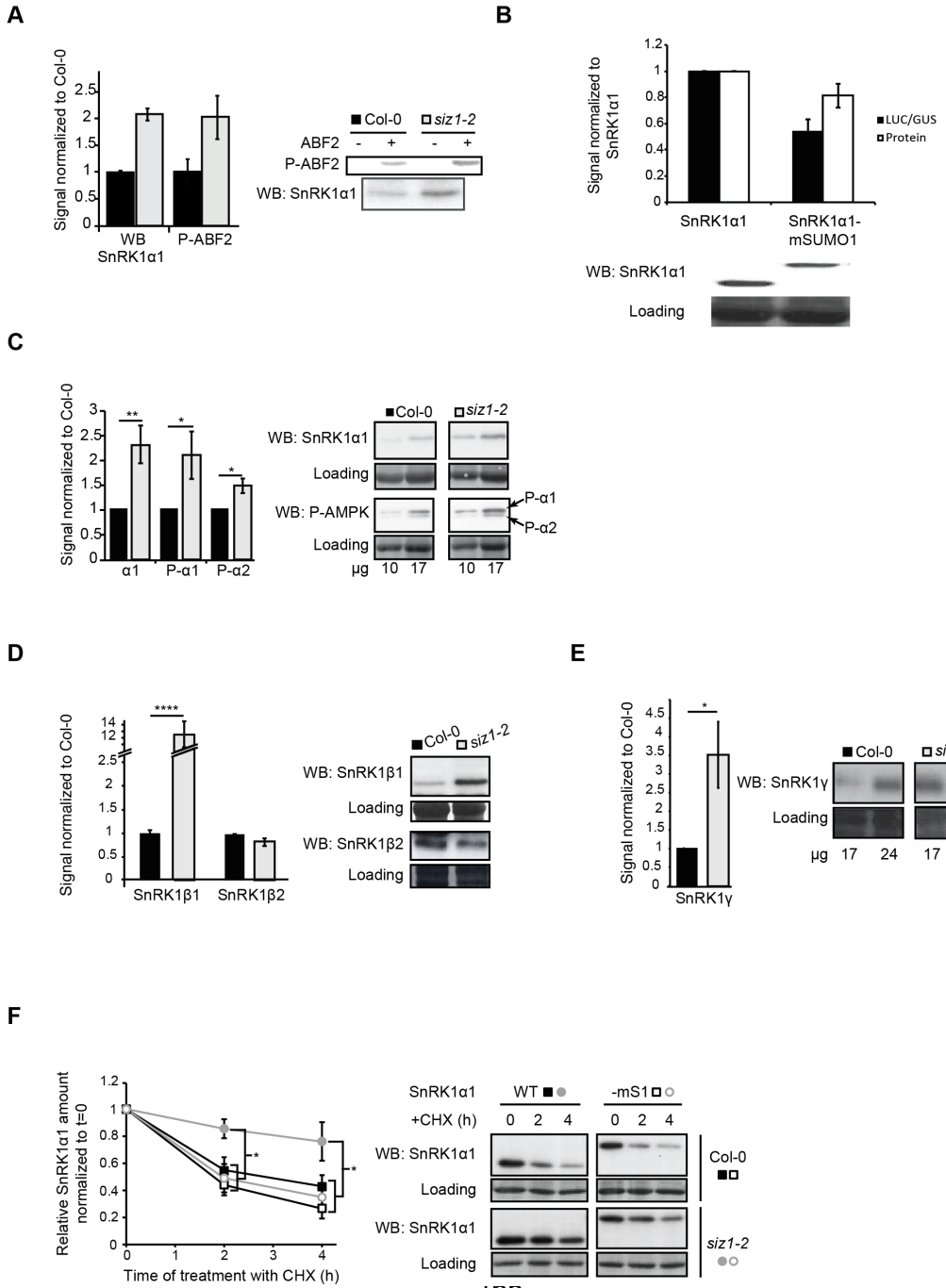
A
Signal normalized to Col-0
WB SnRK1α1
P-ABF2
Col-0
siz1-2
ABF2
P-ABF2
WB: SnRK1α1
B
Signal normalized to SnRK1α1
LUC/GUS
Protein
SnRK1α1
SnRK1α1-mSUMO1
WB: SnRK1α1
Loading
C
Signal normalized to Col-0
α1
P-α1
P-α2
WB: SnRK1α1
Loading
WB: P-AMPK
μg 10 17 10 17
D
Signal normalized to Col-0
SnRK1β1
SnRK1β2
WB: SnRK1β1
WB: SnRK1β2
E
Signal normalized to Col-0
SnRK1γ
WB: SnRK1γ
μg 17 24 17 24
F
Relative SnRK1α1 amount normalized to t=0
Time of treatment with CHX (h)
SnRK1α1
WT
-mS1
+CHX (h)
0 2 4 0 2 4
WB: SnRK1α1
Loading
Col-0
siz1-2

Figure 3.4 | SnRK1 stability is increased in *siz1-2*.

A. SnRK1 specific activity is not altered in the *siz1-2* mutant. SnRK1α1 was immunoprecipitated from Col-0 and *siz1-2* leaf extracts and incubated in the presence of γ-^{32}P-ATP and an ABF2 substrate. SnRK1α1 levels and ABF2 phosphorylation were quantified by Western-blot (WB) and by autoradiography (P-ABF2), respectively. n=3; error bars=SEM. **B**. SnRK1α1 "SUMO mimetic" accumulates less than WT SnRK1α1. Col-0 protoplasts were transfected with SnRK1α1 or with a SnRK1α1 variant fused to mature SUMO1 (SnRK1α1-mSUMO1). Luciferase/ glucuronidase activity assays were performed using the *pDIN6::LUC* reporter as in **Figure** 3.2D, and protein accumulation was analyzed by Western-blot (WB) with anti-SnRK1α1 antibody, considering the loading control. Quantified signals were normalized to SnRK1α1 (n≥2; error bars=SEM). **C**-**E**. SnRK1 accumulation in the *siz1-2* mutant. Total leaf protein extracts of Col-0 and *siz1-2* plants were analyzed by Western-blot (WB) using antibodies against SnRK1α1 and the phosphorylated T-loop of SnRK1α1 and SnRK1α2 (P-α1/P-α2, P-AMPK) (**C**), or against the SnRK1β1 and SnRK1β2 (**D**), or SnRK1γ subunits (**E**). The signals were quantified and normalized to loading. The average quantification in *siz1-2* normalized to Col-0 is presented. **F**. Reduced SnRK1α1 degradation in *siz1-2* is restored in a SUMO-mimetic SnRK1α1 variant. SnRK1α1 fused to mature SUMO1 (-mS1, empty marks) or not (WT, filled marks) was expressed in Col-0 (squares) or *siz1-2* (circles) protoplasts. Protoplasts were thereafter treated with cycloheximide (CHX), samples were harvested at the indicated time points, and analyzed by Western-blot (WB) using anti-SnRK1α1 antibody. The signal was quantified and normalized to the t=0 for each kinetics. Stars denote statistical significance, as determined by ratio paired t-test prior to normalization (**C**-**E**; n=3; error bars=SEM), or by one-way ANOVA (**F**) (n=5; error bars=SEM); *p<0.05; **p<0.01; ****p<0.0001.

3.2.3 | Sumoylated SnRK1 is ubiquitylated and degraded by the proteasome

Given the increasing association between sumoylation, ubiquitylation and proteasomal degradation (*5*-*7*), we next asked whether SnRK1α1 degradation, observed in Col-0 and diminished in *siz1-2* protoplasts (**Figure** 3.4F), occurred via the ubiquitin proteasome system. To this end, we determined SnRK1α1

turnover in the presence of the proteasome inhibitor MG132 or DMSO (mock control). In accordance with previous results [**Figure** 3.4F and degradation assays in cell extracts (*30, 31*)], we could observe a strong reduction in SnRK1α1 levels, 3h after the addition of cycloheximide (**Figure** 3.5A). However, this degradation was significantly blocked in cells treated with MG132, showing that SnRK1α1 protein turnover is largely dependent on the proteasome (**Figure** 3.5A).

To address whether SnRK1 is ubiquitylated *in planta*, we employed the same system as for assessing SnRK1 sumoylation (**Figure** 2.6A-C) and performed GFP immunoprecipitation from *SnRK1α1-GFP*, *SnRK1α1ΔKA1-GFP*, and *35S-GFP* control plants, to check for the presence of ubiquitin conjugates. These analyses revealed a higher accumulation of ubiquitin conjugates in immunoprecipitates from *SnRK1α1-GFP* plants than in those from *SnRK1α1ΔKA1-GFP* plants, while none were detected in the *35S-GFP* control (**Figure** 3.5B). This pattern is clearly similar to that of SUMO conjugates (**Figure** 2.6A), suggesting that SnRK1 ubiquitylation and sumoylation might be interconnected. To test whether SnRK1 sumoylation is a prerequisite for its ubiquitylation, we next immunoprecipitated SnRK1α1-GFP from *SnRK1α1-GFP*$_{siz1-2}$ plants and checked for the presence of ubiquitin conjugates. As shown in **Figure** 3.5C, ubiquitin conjugates were markedly reduced in SnRK1α1-GFP immunoprecipitates from *SnRK1α1-GFP*$_{siz1-2}$ plants, indicating that SnRK1 sumoylation is at least partially required for its subsequent ubiquitylation.

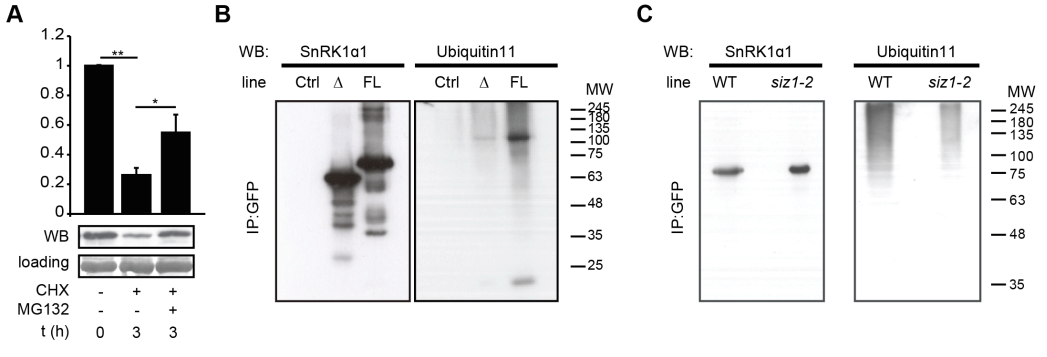

Figure 3.5 | Sumoylation-dependent ubiquitylation of SnRK1 and its degradation by the proteasome.

A. SnRK1α1 is degraded through the proteasome. SnRK1α1 was expressed in Col-0 protoplasts and its levels were assessed by Western-blot (WB), following a 3h treatment with cycloheximide (CHX) in the presence or absence of the proteasome inhibitor MG132. Quantified levels were normalized to t=0. Stars denote statistical significance, as determined by ratio pair t-test prior to data normalization (**p<0.01; *p<0.05). n=3; error bars=SEM. **B**. The SnRK1 complex is ubiquitylated *in planta*. Leaf crude extracts of plants expressing 35S-GFP (Ctrl), SnRK1α1ΔKA1-GFP (Δ) and full length SnRK1α1-GFP (FL) were used for GFP immunoprecipitation (IP). Immunoprecipitates were analyzed by Western-Blot (WB) using antibodies against SnRK1α1 and Ubiquitin11. **C**. SnRK1 ubiquitylation is largely dependent on SIZ1. SnRK1α1-GFP was immunoprecipitated (IP) from leaf crude extracts of *SnRK1α1-GFP* (WT) and *SnRK1α1-GFP*$_{siz1-2}$ (*siz1-2*) plants and analyzed by Western-Blot (WB) using antibodies against SnRK1α1 and Ubiquitin11. MW, Molecular Weight.

3.2.4 | Sumoylation affects SnRK1 complex composition and possibly its oligomerization

We have shown that SnRK1 sumoylation triggers its degradation through the ubiquitin proteasome system. However, the *siz1-2* mutation affects differentially SnRK1β1 and SnRK1β2 protein accumulation (**Figure** 3.4D), despite both regulatory subunits are likely sumoylated *in planta*. In order to determine if sumoylation could promote selective degradation or stabilization of specific SnRK1 complexes, we analyzed SnRK1α1-GFP immunoprecipitates from *SnRK1α1-GFP* and *SnRK1α1-GFP*$_{siz1-2}$ plants. Surprisingly, the abundance of both SnRK1β1 and SnRK1β2 subunits co-purifying with SnRK1α1-GFP was markedly reduced in *SnRK1α1-GFP*$_{siz1-2}$ when compared to *SnRK1α1-GFP* plants (**Figure** 3.6A). On the other hand, the abundance of SnRK1βγ, relative to

the immunoprecipitated SnRK1α1-GFP catalytic subunit, was the same in both genotypes (**Figure** 3.6A). A similar pattern was obtained while analyzing SnRK1α1 immunoprecipitates from Col-0 or *siz1-2* plants (**Figure** 3.6B), ruling out artifacts potentially derived from the GFP-tagged protein. Due to the unavailability of an anti-SnRK1β3 antibody, we could not determine how the absence of SIZ1-dependent sumoylation in the *siz1-2* background influences SnRK1β3-subunit containing complexes.

Several studies have suggested that oligomerization of SNF1/AMPK/SnRK1 complexes may play a role in the control of kinase activity (see **Introduction**), and, in plants, the βγ-regulatory subunit was shown to homodimerize *(32)*. Consistent with this view, we were able to detect the interaction between two SnRK1α1 subunits in Y2H assays (**Figure** 3.6C). Furthermore, SnRK1α2 was co-immunoprecipitated with SnRK1α1-GFP from *SnRK1α1-GFP* plants, but this interaction was strongly diminished in $SnRK1\alpha1\text{-}GFP_{siz1\text{-}2}$ immunoprecipitates (**Figure** 3.6A). These results suggest that, likewise the yeast Snf1 and mammalian AMPKα kinases, SnRK1 α-catalytic subunits have the ability to dimerize (*33, 34*). On the other hand, it remains to be assessed if the dimerization can be determined by the composition of the constituent trimers. Hence, based on these preliminary results, and besides overall accumulation of individual SnRK1 subunits, sumoylation appears to also affect their assembly into SnRK1 heterotrimeric complexes, as well as a putative complex oligomerization.

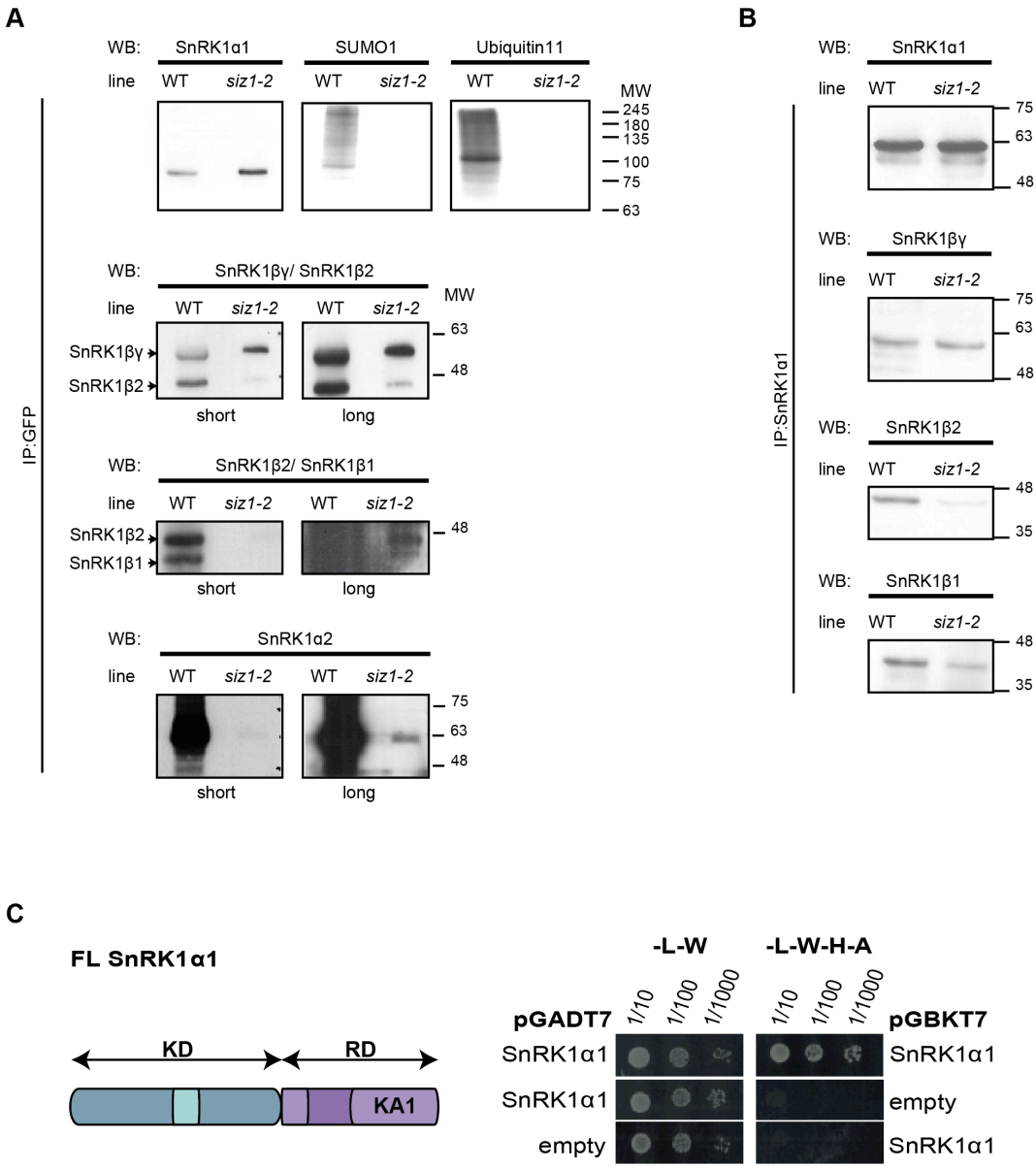

Figure 3.6 | Sumoylation affects SnRK1 complex composition and oligomerization.

A. SnRK1α1-GFP was immunoprecipitated through its GFP tag (IP:GFP) from leaf crude extracts of *SnRK1α1-GFP* (WT) and *SnRK1α1-GFP*$_{siz1-2}$ (*siz1-2*) plants and analyzed by Western-Blot (WB) using antibodies against SnRK1α1, SUMO1, Ubiquitin11, SnRK1βγ, SnRK1β2,

SnRK1β1 and SnRK1α2. **B**. SnRK1α1 was immunoprecipitated using SnRK1α1 antibody (IP: SnRK1α1) from leaf crude extracts of Col-0 (WT) and *siz1-2*, and analyzed by Western-Blot (WB) using antibodies against SnRK1α1, SnRK1βγ, SnRK1β2, and SnRK1β1. MW, Molecular Weight. **C**. SnRK1α1 homodimerizes in a Y2H assay. Full length (FL) SnRK1α1 was cloned in pGBKT7 and co-transfected with FL SnRK1α1 in pGADT7. The growth of transformed AH109 yeast cells was assessed in permissive (-L, -W) or stringent (-L-W-H-A) media. A representative experiment of a minimum of two independent assays is shown.

3.2.5 | Preliminary studies on the genetic interaction between *SIZ1* and *SnRK1α1* in *Arabidopsis thaliana*, and other approaches to address the relevance of SnRK1 sumoylation at the whole plant level

In order to better understand the physiological implications of SnRK1 sumoylation at the whole plant level, we first undertook a "loss-of-function" approach and analyzed phenotypically the *siz1*-2 plants (*35, 36*). A more specific approach, through mutation of several target lysines on SnRK1 α-catalytic subunit, thus blocking directly sumoylation at the substrate level, proved to be unsuccessful in the protoplast system (**Figure** 3.1F). The abrogation of SIZ1-dependent sumoylation leads to an accumulation of SnRK1 in the *siz1-2* mutant, and consequent overactivation of SnRK1 signaling in this background (**Figure** 3.4 and **Figure** 3.2, respectively). *siz1-2* plants were compared with Col-0 (WT), *SnRK1α1* overexpressor [*SnRK1α1-OE*, (*13*)], and *SnRK1α1* knockout [*snrk1α1-3* (**Figure** 2.5A-B)] plants, in an attempt to correlate the various levels of SnRK1α1 expression with phenotypic traits in the different backgrounds. Furthermore, we generated double mutant *siz1-2 snrk1α1-3* plants, by crossing *siz1-2* with *snrk1α1-3* (**Figure** 3.7A). *siz1-2 snrk1α1-3* double mutant plants were also analyzed.

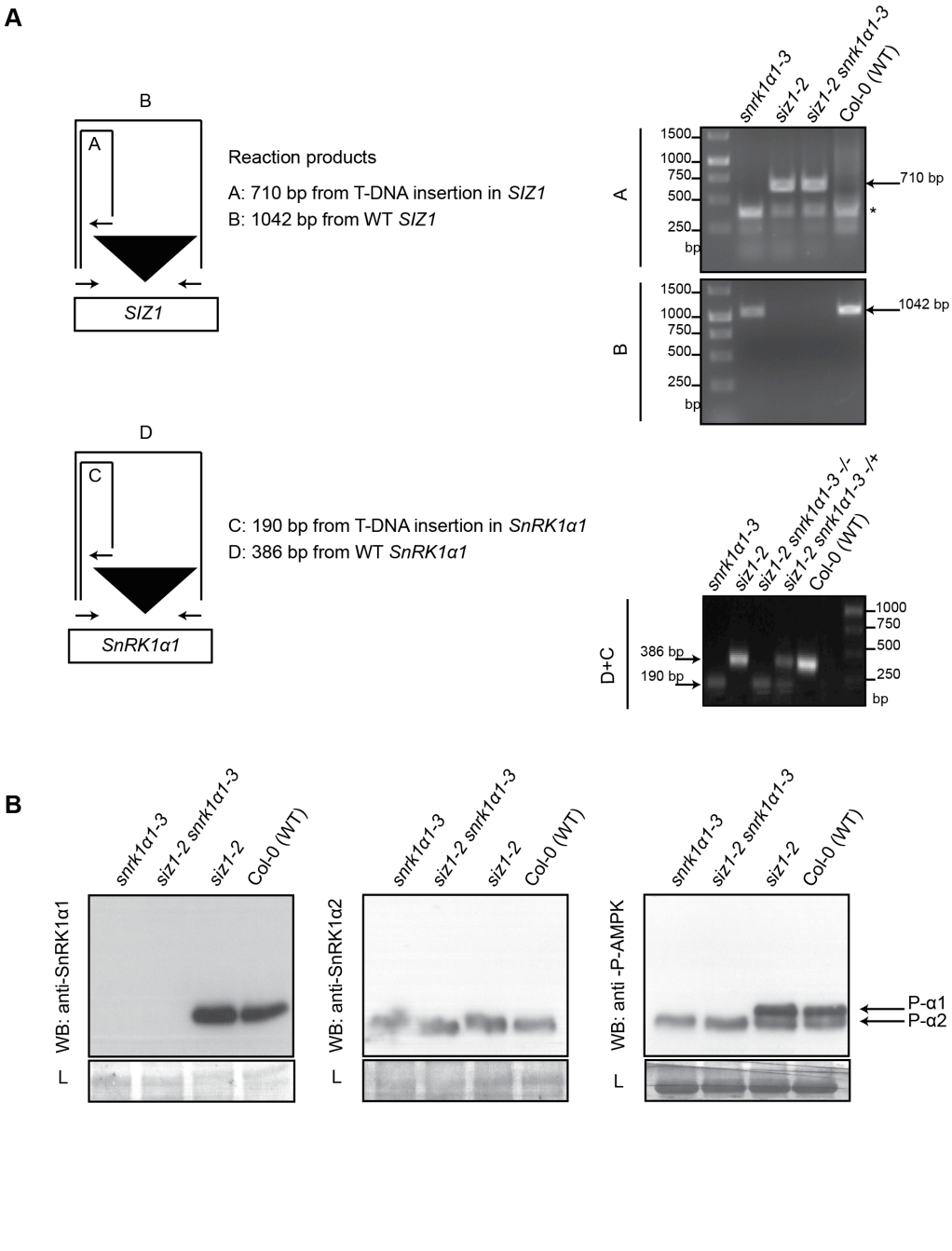

Figure 3.7 | Generation of *siz1-2 snrk1α1-3* double mutant plant lines.

A. Representation of *SIZ1* and *SnRK1α1* genes with a T-DNA insertion defining the *siz1-2* (SALK_065397) and *snrk1α1-3* mutant parent lines (GABI-KAT: 579E09) (**Figure** 2.5A-B).

Genotyping reactions were done using *snrk1α1-3, siz1-2*, *siz1-2 snrk1α1-3* and Col-0 (WT) plant extracts, and are represented as A to D. Reaction A allows the detection of the T-DNA insertion in *SIZ1*, and in B, of the WT *SIZ1* gene. C and D reactions can amplify respectively *SnRK1α1* with a T-DNA insertion or the WT *SnRK1α1 gene*. Genotyping primers are indicated in **Appendix Table 1**. For *SIZ1*, a 710bp band indicates a mutant allele (A reaction) and a 1042bp band indicates a WT allele (B reaction). Unspecific bands were amplified in reaction A and are annotated with an asterisk (*). For *SnRK1α1*, a 190bp band indicates a mutant allele and a 386bp band indicates WT allele (C+D reaction). **B**. Total proteins from adult Arabidopsis leaves of *snrk1α1-3*, *siz1-2 snrk1α1-3*, *siz1-2* or Col-0 were analyzed by Western-blot (WB) using antibodies against SnRK1α1, SnRK1α2 or P-AMPK (recognizing the phosphorylated T175/176 of SnRK1α1/α2, respectively, and annotated as "P- α1"/"P- α2"/). "L", loading is shown by Coomassie staining of the membrane; bp, base-pairs.

Regarding overall plant growth, *siz1-/+ snrk1α1-/-* sesquimutants exhibited a "WT" phenotype, like the one observed for *snrk1α1-3* plants. On the other hand, *siz1-/- snrk1α1-/-* double homozygous (*siz1-2 snrk1α1-3*) plants displayed a "*siz1*" phenotype, with dwarfism and reduced leaf size (*37*) (not shown). We decided to analyze if the differential accumulation of SnRK1α1 in the different backgrounds would impact sugar-responsive phenotypes during early seedling development, due to the relevance of SnRK1 in sugar sensing and signaling in plants (*38*). We could observe the glucose hypersensitivity previously described for the *SnRK1α1-OE* seedlings (*14*) and the same sugar hypersensitivity was also observed for *siz1-2* seedlings in the presence of 6% glucose (**Figure** 3.8A). However, *siz1-2 snrk1α1* double mutants retained the glucose hypersensitivity displayed by *siz1-2*. Moreover, a mild enhancement of the *siz1-2* glucose hypersensitivity occurred upon introduction of *snrk1α1-3* into this genetic background (**Figure** 3.8A). We also tested if the ABA hypersensitivity described for *siz1-2* in early seedling development (*16, 20*) could be ameliorated in the *siz1-2 snrk1α1-3* genetic background, since *SnRK1α1-OE* seedlings also display to some extent ABA hypersensitivity (**Figure** 3.8B, left panel). However, as for the sugar sensitivity, *siz1-2 snrk1α1-3* double mutants retained, even with

mild enhancement (not shown), the ABA hypersensitivity displayed by *siz1-2* ((**Figure** 3.8B, right panel). We also tested starch accumulation in the different backgrounds, since it has been previously suggested SnRK1 might have a role in starch mobilization at night (*13*). However, no consistent differences were observed amongst the different plants analyzed (not shown). For other conditions such as flowering time (*13, 26, 39, 40*), or dark induced senescence, *SnRK1α1-OE* and *siz1-2* plants have opposite phenotypes. *SnRK1α1-OE* and *siz1-2* plants have delayed or accelerated dark induced senescence, respectively (not shown), and an opposite behavior is also expected regarding flowering time. For that reason, we did not pursuit the analysis of *siz1-2 snrk1α1-3* double mutants in those conditions.

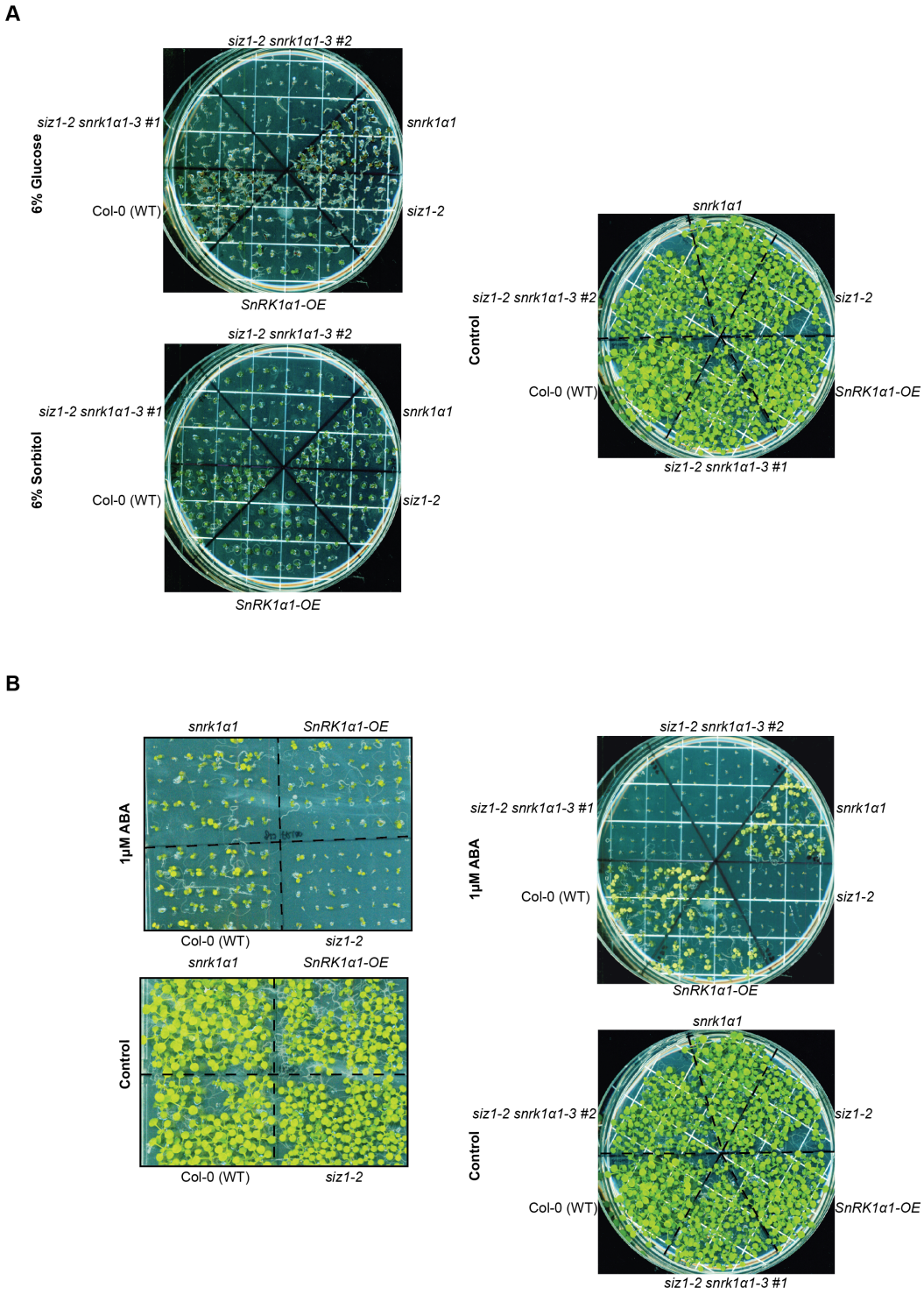
A
siz1-2 snrk1α1-3 #2
siz1-2 snrk1α1-3 #1
snrk1α1
6% Glucose
Col-0 (WT)
siz1-2
SnRK1α1-OE
siz1-2 snrk1α1-3 #2
siz1-2 snrk1α1-3 #1
snrk1α1
6% Sorbitol
Col-0 (WT)
siz1-2
SnRK1α1-OE
snrk1α1
siz1-2 snrk1α1-3 #2
siz1-2
Control
Col-0 (WT)
SnRK1α1-OE
siz1-2 snrk1α1-3 #1
B
snrk1α1
SnRK1α1-OE
1μM ABA
Col-0 (WT)
siz1-2
snrk1α1
SnRK1α1-OE
Control
Col-0 (WT)
siz1-2
siz1-2 snrk1α1-3 #2
siz1-2 snrk1α1-3 #1
snrk1α1
1μM ABA
Col-0 (WT)
siz1-2
SnRK1α1-OE
snrk1α1
siz1-2 snrk1α1-3 #2
siz1-2
Control
Col-0 (WT)
SnRK1α1-OE
siz1-2 snrk1α1-3 #1

Figure 3.8 | Sugar- and ABA- response phenotypes during early seedling development of *snrk1α1-3, siz1-2 snrk1α1-3, siz1-2, SnRK1α1-OE*, or Col-0 plants.

A. Altered glucose response of *siz1-2 snrk1α1-3* and *siz1-2* knockout mutants, and of *SnRK1α1-OE* plants, showing hypersensitivity to 6% glucose during early seedling development, compared to Col-0 or *snrk1α1-3* plants. The sorbitol osmotic control (6%) and control plates with 0.2% of glucose are also shown. All plates have 0.5xMS media. **B.** ABA response of *snrk1α1-3*, *siz1-2 snrk1α1-3*, and *siz1-2* knockout mutants, and of *SnRK1α1-OE* and Col-0 plants during early seedling development. *siz1-2* and *siz1-2 snrk1α1-3* show high hypersensitivity to 1μM ABA. All plates have 0.5xMS media with 0.2% of glucose. Control plates are devoid of ABA.

SIZ1 is a key component of the SUMO machinery that has a determinant impact in the Arabidopsis sumoylome. The *siz1-2* mutant abrogates sumoylation of many protein targets, explaining its pleiotropic phenotype, and thus fails to be an exclusive readout of impaired SnRK1 sumoylation. SIZ1 regulates SnRK1 protein turnover and consequently SnRK1 pathway activation, but there are additional players in the SIZ1 sugar- or ABA- response during early seedling development. This is evidenced by the lack of dependence on *SnRK1α1* regarding the abovementioned phenotypes, as demonstrated by their persistence in the *siz1-2 snrk1α1-3* double mutant. On the other hand, the *siz1-2 snrk1α1-3* double mutant still retains SnRK1 kinase activity through the SnRK1α2 catalytic subunit (**Figure** 3.7B), which may partially compensate for the loss of SnRK1α1.

Using a different approach, we introduced *35S-SnRK1α1* into the *siz1-2* mutant background, by crossing *SnRK1α1-OE* and *siz1-2* plants. However, the selection of double homozygous plants from this cross is still ongoing. Our expectation is that *SnRK1α1-OE*$_{siz1-2}$ will have enhanced sugar hypersensitivity compared to *SnRK1α1-OE* plants, due to an even higher accumulation of SnRK1α1 and higher SnRK1 pathway activation. Whereas in *SnRK1α1-OE*, sumoylation-dependent degradation of SnRK1 should restrain to some extent SnRK1 signaling, such molecular mechanism should be absent in *SnRK1α1-*

OE$_{siz1-2}$ plants, allowing even higher SnRK1 pathway activation. This would also explain the weakness of most phenotypes displayed by the *SnRK1-OE* plants, which are not in accordance with a strong constitutive activation of such a central stress response pathway.

In order to address the functional relevance of SnRK1 sumoylation at the whole plant level we have also undertaken a "gain-of-function" approach and generated *SnRK1α1-SUMO* mimetic overexpressor plants (*35S-SnRK1α1-SUMO* in the *snrk1α1-3* genetic background; referred as *SnRK1α1-SUMO-OE* plants). Several lines were generated with fusions of SUMO1 and SUMO3, mature and non-conjugatable isoforms, and in the N- and C-terminal position of SnRK1α1 (**Figure** 1.3A). In parallel, we also generated several GFP-SUMO overexpressing plants (with fusions of SUMO1 or SUMO3, mature and non-conjugatable isoforms, and in the N- or C-terminal position of GFP) (not shown), to control for possible effects derived from the constitutive overexpression of non-conjugatable SUMO isoforms at the plant level. In the future, SnRK1α1 protein turnover and accumulation, SnRK1 pathway activation, and *SnRK1α1-OE* associated phenotypes, such as glucose hypersensitivity amongst others, will be compared in *SnRK1α1-OE* and *SnRK1α1-SUMO-OE* plants. The expectation is that *SnRK1α1-SUMO-OE* will behave as a weak overexpressor of SnRK1α1 due to the repressive effect associated with SnRK1α1 sumoylation. These plants may also prove useful for assessing potential alterations in SnRK1 complex composition inflicted by sumoylation.

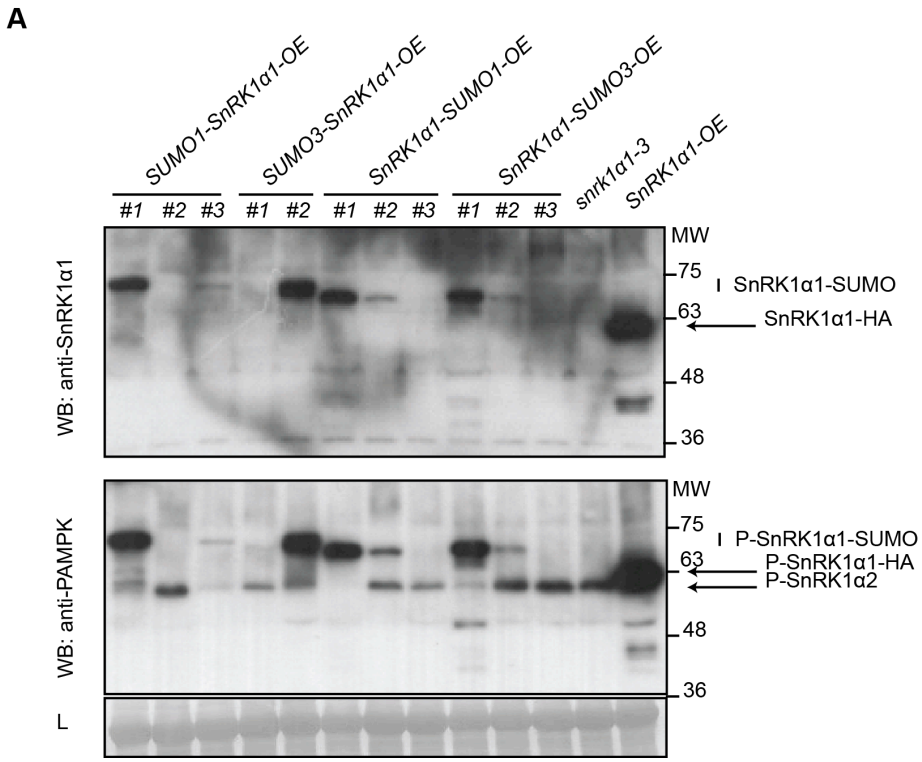

Figure 3.9 | Generation of *SnRK1α1-SUMO-OE* transgenic plants.

A. *SnRK1α1-SUMO-OE* transgenic lines were generated by transformation of the *snrk1α1-3* mutant with the pCB302-derived minibinary expression vector, containing the coding sequence of SnRK1α1 (At3g01090.1) fused with the coding sequence of mature SUMO1 (At4g26840) or mature SUMO3 (At5g55170) non-conjugatable isoforms. SUMO fusion constructs were generated in both orientations (**Appendix Table 1**). Several transformants were tested for the presence of SnRK1α1-SUMO variants. Total proteins from adult Arabidopsis leaves of *SnRK1α1-OE*, different insertion lines *(#1-#3*) of *SUMO1-SnRK1α1-OE*, *SUMO3-SnRK1α1-OE*, *SnRK1α1-SUMO1-OE* and *SnRK1α1-SUMO3-OE* transgenic plants, or from the *snrk1α1-3* mutant, were analyzed by Western-blot (WB) using antibodies against SnRK1α1 or P-AMPK (recognizing the phosphorylated T175/176 of SnRK1α1/α2, respectively). In the first panel, several plants that express SnRK1α1-SUMO variants are identified as well as SnRK1α1-HA (in *SnRK1α1-OE* line), through WB with anti-SnRK1α1 antibody. In the second panel, the same membrane used in the previous panel was incubated with anti-P-AMPK, allowing the detection of endogenous phospho-SnRK1α2 [(phospho)-SnRK1α1 is absent in the *snrk1α1-3* background] in the different lines.

Possible phospho-SnRK1α1-HA (in the *SnRK1α1-OE* line) and phospho-SnRK1α1-SUMO fusions are identified, despite we cannot discard the contribution from the preceding anti-SnRK1α1 immunodetection. Equal loading is shown by Coomassie staining of the membrane ("L").

3.3 | Discussion

In the previous chapter we showed that several SnRK1 subunits are sumoylated, supporting the view that sumoylation occurs at the level of the whole SnRK1 complex. This is in agreement with an increasing number of studies showing that SUMO ligases often act on preassembled protein complexes, hence modifying groups of physically interacting components rather than individual proteins (*29, 41*).

In order to address the functional outcome of SnRK1 sumoylation we co-expressed SUMO isoforms and SUMO machinery components with the SnRK1α1 catalytic subunit, using the protoplast system to monitor SnRK1 pathway activation. Co-expression of the E3 SUMO ligase SIZ1 and mature SUMO1 specifically repressed the ability of SnRK1α1 to induce SnRK1 signaling (**Figure** 3.1C). However, we could not observe any effect with the SUMO3 isoform or with the co-expression of the E3 SUMO ligase HPY2 with either of the two SUMO isoforms (**Figure** 3.1A-C), altogether suggesting that SnRK1α1 sumoylation leads to a downregulation of the kinase and that this requires both SIZ1 activity and SUMO1. This is also in accordance with the absence of SnRK1-SUMO1 conjugates in *siz1-2* plants (**Figure** 2.7B). On the other hand, the induction of SnRK1 signaling by the downstream GBF5 transcription factor was unaltered in the presence of SIZ1 and SUMO1, further supporting that sumoylation occurs at the kinase level (**Figure** 3.1D).

We next aimed to address the relevance of this posttranslational modification by attempting to abolish SnRK1 sumoylation through mutation of specific SUMO

attachment residues on SnRK1α1. However, similarly to the WT kinase, SIZ1-dependent repression of SnRK1 signaling was still observed with SnRK1α1^{3K} (**Figure** 3.1E), and SnRK1α1^{3K} and SnRK1α1^{8K} induced normally SnRK1 signaling in Col-0 cells (**Figure** 3.1F). It has been noted the paradoxical discrepancy between strong phenotypes of SUMO pathway mutants and the lack of phenotypes obtained while mutating specific SUMO acceptor K(s) on substrates. In several instances this can be explained by the fact that sumoylation of other functionally engaged interacting proteins (*29, 41*) compensates for the lack of sumoylation in these K mutants. This appears to be the case in the SnRK1 complex, since mutation of the target K residues in a single subunit (SnRK1α1) is presumably compensated by sumoylation of the remaining subunits [SnRK1β(s)]. The K residues identified in *E. coli* may also be different from the ones sumoylated *in planta*, as the absence of an E3 ligase in the *E. coli* assay may compromise the specificity of the SUMO machinery (*42*). To add further complexity, non-lysine attachment has been observed for ubiquitin, where the free N-terminal amino group or internal cysteine, serine and threonine residues can function as acceptors (*43-45*). However, it remains unknown if the same happens with other ubiquitin-like modifiers.

Using a different approach to block SnRK1 sumoylation, we analyzed *siz1-2* plants that lack the E3 SUMO ligase required for SnRK1 sumoylation *in vivo*. SnRK1 signaling pathway was overactivated in *siz1-2* in comparison to Col-0 plants, and the E3 SUMO ligase activity of SIZ1 inhibited specifically SnRK1 *in vivo*. First, endogenous SnRK1 target genes were overinduced in *siz1-2* plants in response to dark stress conditions (**Figure** 3.2A). Second, a *pDIN6::LUC* reporter gene was overinduced by SnRK1α1 in *siz1-2* cells (**Figure** 3.2B), whilst *pDIN6::LUC* induction by the downstream GBF5 transcription factor was normal (**Figure** 3.2C). Third, SnRK1 pathway overactivation in *siz1-2* cells could be rescued to Col-0 levels by transient expression of SIZ1 but not of a catalytically inactive SIZ1^{C379A} variant (*20*) (**Figure** 3.2C), ruling out long-term pleiotropic effects of the *siz1-2* mutation on SnRK1 function. Similarly, mimicking SnRK1α1

sumoylation by using a SnRK1α1 "SUMO mimetic" in *siz1-2* cells rescued SnRK1 signaling to WT levels (**Figure** 3.2D). Furthermore, SnRK1 pathway overactivation in *siz1-2* seems to be independent of the SA accumulation in this mutant (*22, 46*) (**Figure** 3.3A-B).

Using a combination of immunoprecipitation, *in vitro* kinase assays and immunodetection, we could show that the cause of SnRK1 pathway overactivation in the *siz1-2* mutant is enhanced SnRK1 accumulation (**Figures** 3.4A, C-E). The *siz1-2* mutant accumulates two-fold higher amounts of SnRK1α1 and displays a proportional increase in T-loop phosphorylation in both SnRK1α1 and SnRK1α2 subunits. This confirms that SnRK1 complexes are in an active state in the *siz1-2* mutant and suggests that both SnRK1α isoforms are similarly regulated by SIZ1 (**Figure** 3.4C). The *siz1-2* mutant also accumulated higher levels of SnRK1β1, although in this case the accumulation exceeded nearly six-fold that of the SnRK1α1 subunit (**Figure** 3.4D). This is probably because, in addition to the effect of SIZ1 on SnRK1β1 protein accumulation, SnRK1 activation induces SnRK1β1 gene expression (*13*). Interestingly, we observed a 3.5-fold accumulation of SnRK1γ in the *siz1-2* mutant (**Figure** 3.4E) even though, in agreement with previous reports (*47, 48*), we could not detect SnRK1γ in SnRK1α1 immunoprecipitates (**Figure** 2.6C). Whether this accumulation reflects a functional interaction with the SnRK1 complex and whether this is related to the potential sumoylation of the SnRK1γ subunit (**Figure** 2.3A) remains an open question. Surprisingly, SnRK1β2 subunit accumulated to the same extent in Col-0 and *siz1-2* plants (**Figure** 3.4D), despite being sumoylated in the *E. coli* system and most probably *in planta* (**Figure** 2.3A and 2.6B). Whereas sumoylation seems to negatively affect SnRK1β1 accumulation, a distinct biochemical outcome of SnRK1β2 sumoylation remains to be clarified. This observation suggests that sumoylation may differentially impact SnRK1β1 and SnRK1β2 subunit-containing complexes. In such scenario, an interplay between complex composition and posttranslational modification would dictate the physiological outcome of

sumoylation, in which a putative destabilized SnRK1β1 subunit would *a priori* selectively enrich for SnRK1β2 and/or SnRK1β3 subunit-containing complexes. Surprisingly, the *siz1-2* mutant is strongly depleted of both SnRK1β1- and SnRK1β2-subunit containing complexes, as well as of putative higher-order complexes containing α1 and α2 catalytic subunits (**Figure** 3.6A-B). One possible scenario is that SnRK1β3 is the preferential β-regulatory subunit present in SnRK1α1 complexes in *siz1-2* (to be determined upon antibody availability). However, we can neither exclude that the α1-catalytic subunit is associated with a γ-type regulatory subunit alone (βγ), or even devoid of any regulatory subunit, upon sumoylation abrogation in the *siz1-2* mutant. On the other hand, heterotrimer composition of SnRK1α2 containing complexes remains to be addressed in both genotypes, for instance through SnRK1α2 immunoprecipitation followed by immunodetection of the different regulatory subunits. Since SnRK1β1 accumulation in *siz1-2* is not accompanied by an increased association with SnRK1α1, a possible scenario is that it rather assembles into SnRK1α2-containing complexes, or that is not incorporated in heterotrimers and accumulates as a single subunit. Future efforts should aim to unravel the differential distribution of each SnRK1 complex constituent, ranging from the single subunit to heterotrimeric or even higher order oligomeric states, in WT and *siz1-2* plants. Size-exclusion chromatography, blue native gels and other separation techniques followed by Western-blot and mass spectrometry analyses may provide insights in this regard and disclose an unexpected additional role for sumoylation in heterotrimer and oligomer assembly. Moreover, forthcoming advances in our understanding of the interplay between sumoylation and SnRK1 complex composition should be integrated with the observed SnRK1 signaling overactivation in the *siz1-2* background.

Protein half-life measurements of SnRK1α1 revealed that the reason for enhanced SnRK1α1 accumulation in *siz1-2* cells was deficient protein degradation (**Figure** 3.4F). Furthermore, mimicking SnRK1α1 sumoylation was sufficient to rescue its degradation in the *siz1-2* mutant (**Figure** 3.4F), indicating

that the cause of impaired SnRK1α1 degradation is the lack of sumoylation. SnRK1 seems to be degraded by the 26S proteasome, as it is strongly ubiquitylated (**Figure** 3.5B) and its degradation is largely blocked by the proteasome inhibitor MG132 (**Figure** 3.5A). This is consistent with the identification of SnRK1α1 as a target of ubiquitylation in high-throughput analyses as well as its stabilization by MG132 (*30, 31, 49, 50*). On the other hand, we were able to show that SnRK1 ubiquitylation is largely dependent on sumoylation, as the presence of ubiquitin conjugates in SnRK1α1 immunoprecipitates was greatly reduced in the *siz1-2* background (**Figure** 3.5C). How sumoylated SnRK1 is ubiquitylated and targeted to proteasomal degradation is currently unknown but the process is likely to involve the action of SUMO-targeted Ubiquitin Ligases (STUbLs), responsible for the ubiquitylation of multi- or poly-sumoylated substrates (*9*). The recently uncovered E4 SUMO ligases, responsible SUMO chain extension (*8*), may also be implicated, as suggested from the presence of extremely high molecular weight SUMO1 conjugates in SnRK1α1 immunoprecipitates (**Figure** 2.6A-B). Alternative mechanisms for targeting sumoylated SnRK1 for degradation could depend, for instance, on a conformational modification on SnRK1 upon sumoylation, that would expose a degron or create a binding site for E3 ligases (*51*).

Besides sumoylation-dependent ubiquitylation of SnRK1, we cannot exclude other biological functions of the conjugated SUMO(s) prior to targeted ubiquitylation and degradation (or even prior to an eventual SUMO chain extension). Further studies employing SUMO protease, E4 SUMO ligase, and STUbL mutants will help to clarify such scenario.

The fact that in the *siz1-2* mutant there was a reduction but we still could detect hMW SnRK1α1 forms (**Figure** 2.7B), as well as SnRK1α1-associated ubiquitin conjugates (**Figure** 3.5C), supports the existence of SUMO-independent ubiquitylation events. Indeed, protein kinases are often targeted by more than one E3 ubiquitin ligase (*51*). SnRK1α1 interacts with Pleiotropic Regulatory Locus 1 (PRL1) (*52*) and SnRK1α1 degradation is mediated by the

DDB1-CUL4-ROC1-PRL1 E3 ubiquitin ligase, in which PRL1 is the putative substrate receptor of the complex (*30*). On the other hand, PRL1 was reported to compete with SKP1/ASK1 for binding SnRK1α1 and SnRK1α2. SKP1/ASK1 is a component of the SCF E3 ubiquitin ligase and participates with SnRK1 in the assembly of a proteasomal complex (*52, 53*). Proteasomal degradation of SnRK1α1 was also shown to occur in a Myoinositol Polyphosphate 5-Phosphatase 13 (5PTase13)-dependent manner (*31*). Different E3 ubiquitin ligases and other components may act in an interdependent manner to trigger substrate degradation, but they may also be part of independent pathways that operate specifically under distinct cellular and environmental conditions. However, whether SCF or CUL4-DDB1 E3 ubiquitin ligases, 5PTase13, and SIZ1 act in the same pathway or in parallel ones towards SnRK1 degradation is currently unknown.

Sumoylation has been recently described for SnRK1 orthologs in mammals (AMPK) and yeast (SNF1), affecting these kinases in various ways. In AMPK, both catalytic (α1/α2) subunits were found sumoylated using high-resolution MS (*54*). Sumoylation of AMPKα2 was detected only in the presence of MG132, whereas AMPKα1 sumoylation was significantly increased by proteasome inhibition, suggesting sumoylation may tag both catalytic subunits for degradation. On the other hand, as reported in a different study, AMPKβ2 sumoylation did not affect its degradation rate but instead enhanced AMPK activity. Furthermore, AMPKβ2 sumoylation and ubiquitylation appeared to be antagonistic (*55*). Interestingly, a similar mechanism may be operating in the plant system, where sumoylation of SnRK1α1 catalytic subunit triggers its degradation (**Figure** 3.4F) but a putative SnRK1β2 sumoylation does not seem to affect its stability (**Figure** 3.4D). In the case of the yeast SNF1, sumoylation of Snf1 catalytic subunit was reported to downregulate the kinase in two independent ways. Firstly, a conformational switch induced by interaction of the sumoylated residue with a SUMO-interacting motif (SIM) on Snf1 causes a rapid inhibition of the kinase specific activity. It is unlikely that such a mechanism is

conserved as the two SIMs and the target lysine (Snf1 K549) implicated in this regulation are poorly conserved (**Appendix**- **Figure** 1). Secondly, Snf1 sumoylation induces its degradation through the ubiquitin proteasome system (*56*).

Collectively, the work presented here and studies in yeast and mammals, suggest a conserved outcome for sumoylation of SNF1/AMPK/SnRK1 catalytic subunits, in targeting these protein kinases for proteasomal degradation. Specific SNF1/AMPK/SnRK1 complexes, attained through multiple combinations of catalytic and regulatory subunits, may determine the interaction with different molecular players and diversify the downstream consequences of sumoylation. For instance, the suggested interdependence between SnRK1β1 sumoylation and its degradation may rely on the interaction with STUbLs, whereas sumoylated SnRK1β2 may recruit other interacting proteins that do not affect its stability. How sumoylation of specific individual subunits integrates with the dynamics of the whole complex regulation requires further investigation. Furthermore, specific cellular and environmental stimuli may determine the pool of protein that is sumoylated at a given moment and/or allocate the regulation through sumoylation to specific loci within the cell.

In an attempt to unravel the functional relevance of SnRK1 sumoylation at the whole plant level we analyzed the loss of SnRK1 (SIZ1-dependent) sumoylation using the *siz1-2* mutant. We hypothesized that some phenotypic traits observed in *siz1-2* could be due to the overaccumulation of SnRK1α1 in this background. However, *SnRK1α1* did not mediate both sugar and ABA hypersensitivity in *siz1-2*, due to their persistence in the *siz1-2 snrk1α1-3* double mutant (**Figure** 3.8). Additional components may contribute to these phenotypes, underpinning the pervasive consequences of blocking SIZ1-dependent sumoylation at the whole plant level. Future studies to decipher the functional and biological implications of SIZ1-dependent sumoylation of SnRK1 *in planta* will make use of *SnRK1α1-OE*$_{siz1-2}$ and *SnRK1α1-SUMO-OE* plants (**Figure** 3.9). Whole plant studies of the biological role of SnRK1 sumoylation

may also be facilitated by the identification of the components involved in the intermediary steps of the sumoylation-ubiquitylation-degradation cycle (e.g. E4 SUMO ligases, STUbLs, DUBs, or others) and the phenotypic analyses of the corresponding mutants.

3.4 | Materials and Methods

A list of all primers, cloning steps, and constructs used in this study, is provided in **Appendix Table** 1.

3.4.1 | Plant Material, Growth Conditions, Transformation, and Early Seedling Development Assays

Unless otherwise specified, plants were grown in soil under a 12h light (100µE), 22°C/12h dark, 18°C regime. *Arabidopsis thaliana* plants used in this study are in the Columbia (Col-0) background. The *siz1-2* (SALK_065397) (*35, 36*) and *SnRK1α1*-OE lines (*12*) have been previously described. The *siz1-2 snrk1α1-3* double mutant was generated by crossing *siz1-2* and *snrk1α1-3* (GABI-KAT: 579E09) parent lines, and genotyped for the presence of an insertion in both alleles for each gene. *SnRK1α1-SUMO-OE*, or *GFP-SUMO-OE*, transgenic lines were generated by transformation of the *snrk1α1-3* mutant by the floral dip method (*57*), with *Agrobacterium tumefaciens* (GV3101) containing the pCB302-derived minibinary expression vector (*58*) with the coding sequence of SnRK1α1 (At3g01090.1), or GFP, fused with the coding sequence of a non-conjugatable mature SUMO1 (At4g26840) or mature SUMO3 (At5g55170). SUMO fusion constructs were generated in both orientations (**Appendix Table** 1). BASTA-resistant transformants were selected

based on their segregation ratio (T2) and homozygosity (T3). Homozygous T3 lines were analyzed regarding the presence of SnRK1α1-SUMO variants.

For phenotypical analyses, *siz1-2*, *snrk1α1-3, siz1-2 snrk1α1-3, SnRK1α1-OE*, or Col-0 plants were grown in horizontal plates with 0.5xMS media with 0.2% glucose (control), or with the indicated concentrations of glucose or sorbitol, and ABA in a 16h light (100μE), 22°C/8h dark, 18°C regime. Approximately 2-week old seedlings were analyzed.

3.4.2 | Antibodies and Protein Expression Analyses

The SnRK1α1 (1/500, anti-AKIN10, AS10919), SnRK1β1 (1/500, anti-AKINB1, AS09460), SnRK1β2 (1/500, anti-AKINB2, AS09 462), and SnRK1γ (1/2000, anti-AKING1, AS09613) were purchased from Agrisera. Phospho-SnRK1α1/2 (T175/176) was detected with an anti–phosphoT172-AMPKα antibody (1/1000 in 5% BSA-TBS-Tween, referred to as P-AMPK; #2535, Cell Signaling). SUMO1 (1/5000, ab5316, Abcam) and Ubiquitin11 (1/10000, AS08307, Agrisera) antibodies were used to detect the respective protein modifications. Anti-HA (1/1000, Roche, #11867423001) antibody was used to detect the corresponding tagged proteins.

For immunoblotting, all primary antibodies were diluted in 1% non-fat Milk in TBS (unless otherwise stated) and incubated with the membrane under gentle shaking for 12h at 4°C. Secondary antibodies (Jackson ImmunoResearch Lab, inc) were used at 1/10000 in 1% non-fat Milk in TBS for 1h at RT. In the case of immunoprecipitated samples, secondary antibodies subsequently used in the immunodetection were against the light chain of IgG.

3.4.3 | Protoplast Transient Expression Assays

Protoplasts from Col-0 and *siz1-2* plants were isolated and transfected as already described (*59*). All effector constructs (**Appendix Table** 1) were generated by cloning the corresponding coding sequences into a pHBT95 vector harboring a C-terminal HA (*59*), except for the SnRK1-SUMO construct that has no tag. The indicated mutations were introduced by site-directed mutagenesis and verified by sequencing. For protein expression analyses, protoplasts were directly resuspended in 4X Laemmli solubilization buffer (*60*) and boiled for 5min at 95°C. Cyclohexamide (Biochemica, A0879/0001; Ethanol stock) and MG132 (Sigma, C2211; DMSO stock) solutions were used at a final concentration of 2μM and 50μM, respectively.

3.4.4 | Gene Expression Analyses

Fully expanded rosettes of 4-5-week old Col-0 and *siz1-2* plants were incubated on sterile MilliQ water in Petri dishes under control (3h Light, 100μE) or SnRK1 signaling activating conditions (3h Dark). The treatment was always initiated 3h after the onset of the light period. Total RNA was extracted using TRIzol reagent (Life Technologies), treated with RNase-Free DNase (Promega), and reverse transcribed (1μg) using SuperScriptIII Reverse Transcriptase (Life Technologies), as previously described (*14*). Quantitative real-time RT-PCR (qPCR) analyses were performed using a CFX384TM Real-Time System (Bio-Rad), the iTaqTM Universal SYBR® Green Supermix (BioRad), and the $2^{-\Delta\Delta Ct}$ method for relative quantification (*61*). Expression values of SnRK1 target genes were normalized using the CT values obtained for the *ACT2* reference gene.

3.4.5 | Quantification of immunoblot results

Membranes were analyzed by immunoblotting and then stained with Coomassie Brilliant Blue R250. Band intensity was quantified using Image J (http://imagej.nih.gov/ij/) and Gel Quant Net (http://biochemlabsolutions.com/GelQuantNET.html) softwares. The immunoblot intensities were normalized to the Coomassie staining intensity (referred as "loading"). Quantifications were normalized to the t=0 of each kinetics or to SnRK1α1 in **Figure** 3.4B.

3.4.6 | Statistical Analyses

All statistical analyses were performed with the GraphPad Prism 6 software (GraphPad softwares). For analyses of qPCR data, the statistical significance of the indicated changes was assessed employing log2-transformed relative expression values (*61, 62*).

3.4.7 | GFP, SnRK1α1-GFP and SnRK1α1ΔKA1-GFP Immunoprecipitation

Proteins from 5-week-old *SnRK1α1-GFP*, *SnRK1α1ΔKA1-GFP,* or *35S-GFP* plant leaves were extracted with immunoprecipitation (IP) buffer [50mM Tris-HCl pH8.0, 50mM NaCl, 1% (V/V) Igepal CA-630, 0.5% (w/V) Sodium deoxycholate, 0.1% (w/V) SDS, 1mM EDTA pH8.0, 50µM MG132, 50mM *N*-Ethylmaleimide and cOmplete protease inhibitor cocktail (one tablet/10mL)]. After clearing

samples by centrifugation (6,785*g*, 2°C, 10min), 800µL of supernatant were supplemented with fresh MG132 (50µM) and incubated at 4°C for 1h with 40µL of µMACS Anti-GFP MicroBeads (µMACS GFP Isolation Kit, Miltenyi, 130-091-125). Samples were thereafter loaded in µColumns (Miltenyi, 130-042-701) pre-equilibrated with 1ml of IP buffer, and allowed to flow through. Columns were washed four times with 200µL of IP buffer and proteins eluted with 80µL of Elution Buffer (Miltenyi, 130-091-125) at 95°C. β-Mercapto-Ethanol (2%) was added to the eluates prior to boiling for 5 min at 95°C. Proteins were resolved by SDS-PAGE, wet-transferred to a PVDF membrane (30V, 16h at 4°C), and analyzed by immunoblotting with anti-SnRK1α1 and anti-Ubiquitin11 antibodies. For each GFP immunoprecipitation experiment, immunodetection with different antibodies was done using equal loading on independent membranes.

3.4.8 | SnRK1α1 Immunoprecipitation and *in vitro* Kinase Assays

For measurements of endogenous SnRK1α1 activity, SnRK1α1 was immunoprecipitated from leaves of 5-week-old Col-0 or *siz1-2* plants. Plant material (1g) was extracted in 2 volumes of Buffer C [50mM Hepes, pH7.25, 150mM NaCl, 1mM EDTA, 0.05% Triton X-100, cOmplete protease inhibitor cocktail (one tablet/50mL, Roche 11697498001) and 1/500 (v/v) phosphatase inhibitor 2 (Sigma P5726) and 3 (Sigma P0044)]. After two successive centrifugations (20,000*g*, 4°C, 10min), the supernatant was recovered, and 1 mg of total protein was incubated with gentle shaking for 3h at 4°C with 15µL beads of protein A–antibody complex prepared as follows. For each immunoprecipitation, 15µL (bed volume) of protein A–agarose (Roche #11719408001) was equilibrated in 1XPBS (Sigma-Aldrich P5493) and incubated with 1.5µg of anti-SnRK1α1 antibody (anti-AKIN10) in 500µL of 1X

PBS for 1h at room temperature with gentle shaking. After three washes in buffer C, the beads were used for immunoprecipitation. After incubation for 3h at 4°C under shaking, the beads were washed five times with buffer C, and one-third (5µL) was kept for immunoblot analyses with anti-SnRK1α1 antibody. The remaining 10µL were used to determine the specific activity of SnRK1 in 30µL of kinase buffer (50mM Hepes-NaOH, pH7.25, 20mM $MgCl_2$, 0.5mM DTT and 100mM ATP) with His-ΔC ABF2 (1µg) for 1 h at 30°C in the presence of 2µCi of γ^{32}P-ATP. The reaction products were resolved by 12% SDS-PAGE and detected using a phosphor image system (STORM 860, GE Healthcare).

3.4.9 | Recombinant Protein Production and Purification

Recombinant His-ΔC ABF2 (residues 1–173) was produced and purified as previously described (*14*). Successful protein production and purification was verified by immunoblotting with an anti-T7 antibody.

3.4.10 | Y2H Assays

Y2H assays were performed as described (*63*). The full-length (FL) coding sequence of SnRK1α1 was cloned in pGBKT7 and co-transfected with FL SnRK1α1 in pGADT7. The empty vectors were used as negative controls. The growth of transformed AH109 yeast cells was assessed in permissive (-Leucine, -Tryptophan) or selective (-Leucine, -Tryptophan, -Histidine, -Adenine) media.

3.4.11 | Accession Numbers

Sequence data can be found in the Arabidopsis Genome Initiative database under the following accession numbers: *SnRK1α1*, At3g01090; *SnRK1β1*, At5g21170; *SnRK1β2*, At4g16360; *SnRK1γ*, At3g48530; *GBF5*, At2g18160; *SCE1*, At3g57870; *SIZ1*, At5g60410*; HPY2*, At3g15150; *SUMO1*, At4g26840; *SUMO3*, At5g55170; *DIN6*, At3g47340; *AXP*, At2g33830; *TPS8*, At1g70290; *ACT2*, At3g18780; *UBQ10*, At4g05320; *PR1*, At2g14610; *PR5*, At1g75040.

Supplemental data

Supplemental Data includes **Appendix Table** 1 and **Appendix Figure** 1.

Acknowledgements

I would like to acknowledge Elena Baena-González for guidance throughout all the work and careful reading of the chapter, and Pierre Crozet for contributing for the work here presented. I acknowledge Noémia Fernandes for her contribution to the qRT-PCR experiments. Finally, I would like to acknowledge all Plant Stress Signaling group members for fruitful discussions. Furthermore, I am very thankful to Vera Nunes for great plant care.

References

1. N. Elrouby, G. Coupland, in *Proc Natl Acad Sci USA*. (2010), vol. 107, pp. 17415-17420.
2. X.-J. Yang, C.-M. Chiang, in *F1000Prime Rep*. (2013), vol. 5, pp. 45.

3. H. D. Ulrich, in *Mol Cell*. (2012), vol. 47, pp. 335-337.
4. Z. Guo, J. Kanjanapangka, N. Liu, S. Liu, C. Liu, Z. Wu, Y. Wang, T. Loh, C. Kowolik, J. Jamsen, M. Zhou, K. Truong, Y. Chen, L. Zheng, B. Shen, in *Mol Cell*. (2012), vol. 47, pp. 444-456.
5. M. Miteva, K. Keusekotten, K. Hofmann, G. J. K. Praefcke, R. J. Dohmen, in *Subcell Biochem*. (2010), vol. 54, pp. 195-214.
6. K. Uzunova, K. Göttsche, M. Miteva, S. R. Weisshaar, C. Glanemann, M. Schnellhardt, M. Niessen, H. Scheel, K. Hofmann, E. S. Johnson, G. J. K. Praefcke, R. J. Dohmen, in *J Biol Chem*. (2007), vol. 282, pp. 34167-34175.
7. G. J. K. Praefcke, K. Hofmann, R. J. Dohmen, in *Trends in Biochemical Sciences*. (2012), vol. 37, pp. 23-31.
8. K. Tomanov, A. Zeschmann, R. Hermkes, K. Eifler, I. Ziba, M. Grieco, M. Novatchkova, K. Hofmann, H. Hesse, A. Bachmair, in *Plant Cell*. (2014), vol. 26, pp. 4547-4560.
9. N. Elrouby, M. V. Bonequi, A. Porri, G. Coupland, in *Proc Natl Acad Sci USA*. (2013).
10. M. Novatchkova, K. Tomanov, K. Hofmann, H.-P. Stuible, A. Bachmair, in *New Phytol*. (2012), vol. 195, pp. 23-31.
11. I. A. Hendriks, J. Schimmel, K. Eifler, J. V. Olsen, A. C. O. Vertegaal, in *J. Biol. Chem.* (2015).
12. M. Jossier, J.-P. Bouly, P. Meimoun, A. Arjmand, P. Lessard, S. Hawley, D. Grahame Hardie, M. Thomas, in *Plant J*. (2009), vol. 59, pp. 316-328.
13. E. Baena-González, F. Rolland, J. M. Thevelein, J. Sheen, in *Nature*. (2007), vol. 448, pp. 938-942.
14. A. Rodrigues, M. Adamo, P. Crozet, L. Margalha, A. Confraria, C. Martinho, A. Elias, A. Rabissi, V. Lumbreras, M. González-Guzmán, R. Antoni, P. L. Rodriguez, E. Baena-González, in *The Plant Cell*. (2013), vol. 25, pp. 3871-3884.
15. K. Miura, J. B. Jin, J. Lee, C. Y. Yoo, V. Stirm, T. Miura, E. N. Ashworth, R. A. Bressan, D.-J. Yun, P. M. Hasegawa, in *Plant Cell*. (2007), vol. 19, pp. 1403-1414.
16. K. Miura, J. Lee, J. B. Jin, C. Y. Yoo, T. Miura, P. M. Hasegawa, in *Proc Natl Acad Sci USA*. (2009), vol. 106, pp. 5418-5423.
17. Y. Zheng, K. S. Schumaker, Y. Guo, in *Proc Natl Acad Sci USA*. (2012), vol. 109, pp. 12822-12827.
18. J. H. Im, Y.-H. Cho, G.-D. Kim, G.-H. Kang, J.-W. Hong, S.-D. Yoo, in *Plant, Cell & Environment*. (2014), vol. 37, pp. 2303-2312.
19. K. Miura, J. Lee, T. Miura, P. M. Hasegawa, in *Plant Cell Physiol*. (2010), vol. 51, pp. 103-113.
20. M. S. Cheong, H. C. Park, M. J. Hong, J. Lee, W. Choi, J. B. Jin, H. J. Bohnert, S. Y. Lee, R. A. Bressan, D.-J. Yun, in *PLANT PHYSIOLOGY*. (2009), vol. 151, pp. 1930-1942.
21. H. D. Ulrich, *SUMO Protocols*. J. M. Walker, Ed., METHODS IN MOLECULAR BIOLOGY (Humana Press, New York, 2009), vol. 497.
22. J. Lee, J. Nam, H. C. Park, G. Na, K. Miura, J. B. Jin, C. Y. Yoo, D. Baek, D. H. Kim, J. C. Jeong, D. Kim, S. Y. Lee, D. E. Salt, T. Mengiste, Q. Gong, S. Ma, H. J. Bohnert, S.-S. Kwak, R. A. Bressan, P. M. Hasegawa, D.-J. Yun, in *Plant J*. (2007), vol. 49, pp. 79-90.

23. M. S. Cheong, H. C. Park, H. J. Bohnert, R. A. Bressan, D.-J. Yun, in *Plant Signal Behav*. (2010), vol. 5.
24. K. Miura, H. Okamoto, E. Okuma, H. Shiba, H. Kamada, P. M. Hasegawa, Y. Murata, in *Plant J*. (2012).
25. K. Miura, M. Ohta, in *J Plant Physiol*. (2010), vol. 167, pp. 555-560.
26. J. B. Jin, Y. H. Jin, J. Lee, K. Miura, C. Y. Yoo, W.-Y. Kim, M. Van Oosten, Y. Hyun, D. E. Somers, I. Lee, D.-J. Yun, R. A. Bressan, P. M. Hasegawa, in *Plant J*. (2008), vol. 53, pp. 530-540.
27. B. S. Park, J. T. Song, H. S. Seo, in *Nature Communications*. (2011), vol. 2, pp. 400.
28. T. Hruz, O. Laule, G. Szabo, F. Wessendorp, S. Bleuler, L. Oertle, P. Widmayer, W. Gruissem, P. Zimmermann, in *Advances in Bioinformatics*. (2008), vol. 2008, pp. 420747.
29. S. Jentsch, I. Psakhye, in *Annu. Rev. Genet.* (2013).
30. J.-H. Lee, W. Terzaghi, G. Gusmaroli, J.-B. F. Charron, H.-J. Yoon, H. Chen, Y. J. He, Y. Xiong, X. W. Deng, in *Plant Cell*. (2008), vol. 20, pp. 152-167.
31. E. A. Ananieva, G. E. Gillaspy, A. Ely, R. N. Burnette, F. L. Erickson, in *PLANT PHYSIOLOGY*. (2008), vol. 148, pp. 1868-1882.
32. C. López-Paz, B. Vilela, M. Riera, M. Pagès, V. Lumbreras, in *FEBS Lett*. (2009), vol. 583, pp. 1887-1894.
33. M. J. Rudolph, G. A. Amodeo, Y. Bai, L. Tong, in *Biochemical and Biophysical Research Communications*. (2005), vol. 337, pp. 1224-1228.
34. R. Scholz, M. Suter, T. Weimann, C. Polge, P. V. Konarev, R. F. Thali, R. D. Tuerk, B. Viollet, T. Wallimann, U. Schlattner, D. Neumann, in *J Biol Chem*. (2009), vol. 284, pp. 27425-27437.
35. J. M. Alonso, A. N. Stepanova, T. J. Leisse, C. J. Kim, H. Chen, P. Shinn, D. K. Stevenson, J. Zimmerman, P. Barajas, R. Cheuk, C. Gadrinab, C. Heller, A. Jeske, E. Koesema, C. C. Meyers, H. Parker, L. Prednis, Y. Ansari, N. Choy, H. Deen, M. Geralt, N. Hazari, E. Hom, M. Karnes, C. Mulholland, R. Ndubaku, I. Schmidt, P. Guzman, L. Aguilar-Henonin, M. Schmid, D. Weigel, D. E. Carter, T. Marchand, E. Risseeuw, D. Brogden, A. Zeko, W. L. Crosby, C. C. Berry, J. R. Ecker, in *Science*. (2003), vol. 301, pp. 653-657.
36. K. Miura, A. Rus, A. Sharkhuu, S. Yokoi, A. S. Karthikeyan, K. G. Raghothama, D. Baek, Y. D. Koo, J. B. Jin, R. A. Bressan, D.-J. Yun, P. M. Hasegawa, in *Proc Natl Acad Sci USA*. (2005), vol. 102, pp. 7760-7765.
37. R. Catala, J. Ouyang, I. A. Abreu, Y. Hu, H. Seo, X. Zhang, N.-H. Chua, in *Plant Cell*. (2007), vol. 19, pp. 2952-2966.
38. F. Rolland, E. Baena-Gonzalez, J. Sheen, in *Annu Rev Plant Biol*. (2006), vol. 57, pp. 675-709.
39. S. P. Williams, P. Rangarajan, J. L. Donahue, J. E. Hess, G. E. Gillaspy, in *Front. Plant Sci.* (2014), vol. 5, pp. 324.
40. J. B. Jin, P. M. Hasegawa, in *Plant Signal Behav*. (2008), vol. 3, pp. 891-892.
41. I. Psakhye, S. Jentsch, in *CELL*. (2012), vol. 151, pp. 807-820.
42. K. Miura, P. M. Hasegawa, in *Trends in Cell Biology*. (2010), vol. 20, pp. 223-232.
43. R. D. Vierstra, in *Plant Physiol*. (2012), vol. 160, pp. 2-14.
44. J. Gilkerson, D. R. Kelley, R. Tam, M. Estelle, J. Callis, in *PLANT PHYSIOLOGY*. (2015), vol. 168, pp. 708-720.

45. A. Ciechanover, R. Ben-Saadon, in *Trends in Cell Biology*. (2004), vol. 14, pp. 103-106.
46. J. Lee, K. Miura, R. A. Bressan, P. M. Hasegawa, D.-J. Yun, in *Plant Signal Behav*. (2007), vol. 2, pp. 253-254.
47. M. Ramon, P. Ruelens, Y. Li, J. Sheen, K. Geuten, F. Rolland, in *Plant J*. (2013).
48. S. Emanuelle, M. I. Hossain, I. E. Moller, H. L. Pedersen, A. M. L. van de Meene, M. S. Doblin, A. Koay, J. S. Oakhill, J. W. Scott, W. G. T. Willats, B. E. Kemp, A. Bacic, P. R. Gooley, D. I. Stapleton, in *Plant J*. (2015), vol. 82, pp. 183-192.
49. D.-Y. Kim, M. Scalf, L. M. Smith, R. D. Vierstra, in *The Plant Cell*. (2013), vol. 25, pp. 1523-1540.
50. R. Maor, A. Jones, T. S. Nühse, D. J. Studholme, S. C. Peck, K. Shirasu, in *Mol Cell Proteomics*. (2007), vol. 6, pp. 601-610.
51. Z. Lu, T. Hunter, in *Annu Rev Biochem*. (2009), vol. 78, pp. 435-475.
52. R. P. Bhalerao, K. Salchert, L. Bakó, L. Okrész, L. Szabados, T. Muranaka, Y. Machida, J. Schell, C. Koncz, in *Proc Natl Acad Sci USA*. (1999), vol. 96, pp. 5322-5327.
53. R. Farrás, A. Ferrando, J. Jásik, T. Kleinow, L. Okrész, A. Tiburcio, K. Salchert, C. del Pozo, J. Schell, C. Koncz, in *The EMBO Journal*. (2001), vol. 20, pp. 2742-2756.
54. I. A. Hendriks, R. C. J. D'souza, B. Yang, M. Verlaan-de Vries, M. Mann, A. C. O. Vertegaal, in *Nat Struct Mol Biol*. (2014).
55. T. Rubio, S. Vernia, P. Sanz, in *Mol Biol Cell*. (2013), vol. 24, pp. 1801-1811.
56. K. J. Simpson-Lavy, M. Johnston, in *Proc Natl Acad Sci USA*. (2013).
57. S. J. Clough, A. F. Bent, Floral dip: a simplified method for Agrobacterium-mediated transformation of Arabidopsis thaliana. *Plant J.* (1998), vol. 16, pp. 735-743.
58. C. Xiang, P. Han, I. Lutziger, K. Wang, D. J. Oliver, in *Plant Mol Biol*. (1999), vol. 40, pp. 711-717.
59. S.-D. Yoo, Y.-H. Cho, J. Sheen, in *Nat Protoc*. (2007), vol. 2, pp. 1565-1572.
60. U. K. Laemmli, Cleavage of structural proteins during the assembly of the head of bacteriophage T4. *Nature.* (1970), vol. 227, pp. 680-685.
61. K. J. Livak, T. D. Schmittgen, in *METHODS*. (2001), vol. 25, pp. 402-408.
62. I. Rieu, S. J. Powers, in *Plant Cell*. (2009), vol. 21, pp. 1031-1033.
63. A. Saez, A. Rodrigues, J. Santiago, S. Rubio, P. L. Rodriguez, HAB1-SWI3B interaction reveals a link between abscisic acid signaling and putative SWI/SNF chromatin-remodeling complexes in Arabidopsis. *Plant Cell.* (2008), vol. 20, pp. 2972-2988.

CHAPTER 4 |

SnRK1 pathway activation and signal termination

Authors' Contributions

Leonor Margalha and Pierre Crozet contributed equally to the work presented in this chapter. Pierre Crozet did the *in vitro* kinase assays, prepared samples for Mass Spectrometry (MS) analyses and did the Phos-tag SDS-PAGE analysis. Elena Baena-González did the *SnRK1α2* and *GFP* Virus-induced gene silencing (VIGS) of *snrk1α1-3* plants.

Abstract

The Snf1-Related protein Kinase 1 (SnRK1) is a central component of the plant stress response that promotes catabolism and represses anabolism, in order to restore energy homeostasis upon energy deprivation conditions (*1, 2*). However, both SnRK1 overexpression and its downregulation impact plant growth and developmental transitions (*1*). Hence, a tight regulation of the SnRK1 signaling pathway is required for a responsive and accurate system, though preventing its excessive activation.

Sumoylation is implied in the regulation of several protein kinases where there is often interplay between SUMO and other posttranslational modifications (*3-5*). We have previously shown that SnRK1 sumoylation triggers its ubiquitylation and subsequent proteasomal degradation (**Chapter** 3). Here we show that the inactive SnRK1 variants SnRK1^{K48M} and SnRK1^{T175A} (impaired in ATP binding and T-loop phosphorylation, respectively) accumulate to a greater extent and are more stable than the active WT SnRK1 protein. Importantly, inactive SnRK1^{K48M} and SnRK1^{T175A} can be destabilized if co-transfected with active SnRK1α1 or if expressed as a translational protein fusion with SUMO1, further supporting that kinase activity is essential for its degradation and suggesting the impaired turnover of inactive SnRK1α1 variants is caused by lack of sumoylation. We suggest that SUMO-dependent SnRK1 degradation is triggered by SnRK1 activity as part of a negative feedback loop to prevent deleterious effects derived from overly high SnRK1 signaling. Furthermore, we show SnRK1 phosphorylates the E3 SUMO ligase SIZ1 *in vitro*, and hypothesize that such mechanism may couple stress and SnRK1 activation to its sumoylation/ubiquitylation, and subsequent degradation *in planta*.

4.1 | Introduction

The activity of protein kinases can be regulated at the expression level and also through swift posttranslational modifications (PTMs) such as phosphorylation, acetylation and ubiquitylation, amongst many others. The binding of activating subunits, inhibitor proteins or metabolites can adjust the kinase response to specific cues, and kinase modulation is also achieved through oligomerization, intracellular translocation or protein cleavage (*6*). Furthermore, the possible interconnection between different modes of regulation expands the system versatility. Most of the kinase regulatory mechanisms, either positive or negative, are reversible (e.g. phosphorylation/ dephosphorylation, or binding of protein regulators), but an irreversible downregulation (e.g. through ubiquitin-mediated proteasomal degradation) can dictate signal termination. The commitment to degradation is most often triggered by an active kinase, especially if the activity is sustained (*6*).

Sumoylation is implied in the regulation of several protein kinases. Protein kinase sumoylation can be phosphorylation-dependent, when the negative charges added by phospho groups increase the affinity of phospho-dependent sumoylation motifs (PDSMs) to the positively charged patch of SCE1 (*7*). Another mechanism of phosphorylation-dependent sumoylation may rely on SUMO-SIM non-covalent interactions. Phosphorylated serine and threonine residues associated with SUMO interacting motifs (SIMs) have higher affinity towards a positive patch on SUMO, and may modulate the proximity between SUMO machinery and potential substrate proteins. Besides the cooperative interplay between phosphorylation and sumoylation, these PTMs can impose opposite fates on a substrate. For instance, phosphorylation stabilizes the human transcription factor Sp1, whereas sumoylation recruits the ubiquitin ligase RNF4, which induces ubiquitin-dependent proteasomal degradation of

Sp1 (*4, 8*). The plant transcription factor ABI5 is phosphorylated and activated by SnRK2.2 and SnRK2.3 kinases in response to ABA, whereas SIZ1-mediated sumoylation renders ABI5 inactive, probably by interfering with its phosphorylation (*9*). On the other hand, sumoylation can modulate protein kinase function without affecting its phosphorylation status. For instance, the insulin/IGF-1 activated protein kinase Akt is regulated by phosphorylation, ubiquitylation, acetylation and sumoylation. Akt sumoylation is Akt phosphorylation-dependent and sumoylation increases Akt kinase activity without affecting its phosphorylation level (*10, 11*).

Since SUMO itself and the SUMO machinery are also regulated by phosphorylation, protein kinases can be involved in sumoylation-phosphorylation regulatory feedback loops to better adjust the response of specific systems towards the cellular and whole organism demands.

The Snf1-Related protein Kinase 1 (SnRK1) is a central component that participates in plant developmental decisions as well as in the response to environmental stresses, to balance energy levels upon energy deprivation conditions (*1, 2*). Such central metabolic regulator needs to be tightly coordinated, promoting a concerted and timely activation of the pathway, though preventing its excessive activation, in accordance with the environmental and organism demands. The work described in this chapter integrates SnRK1 pathway activation and protein turnover in response to activating conditions. Furthermore, it suggests SnRK1 sumoylation is an intermediary step of a negative feedback loop to restrain SnRK1 signaling, preventing excessive activation and allowing an accurate response to energy deprivation. We hypothesize that a putative SnRK1-dependent phosphorylation of SIZ1 *in planta* may convey SnRK1 activation to the SUMO machinery, with a possible impact on SnRK1 and global sumoylation.

4.2 | Results

4.2.1 | SnRK1 activity triggers its degradation

We previously observed that inactive SnRK1α1 variants, such as SnRK1α1^{K48M} (K48 is responsible for the phosphotransfer activity) and the T-loop phosphomutant SnRK1α1^{T175A}, accumulate to higher levels than the WT SnRK1α1 protein (*1*) (**Figure** 4.1A), suggesting a connection between kinase activity and stability. By measuring protein half-life in the presence of cycloheximide in Col-0 cells, we found that the reason for overaccumulation of both inactive variants (SnRK1α1^{K48M} and SnRK1α1^{T175A}) was the lack of protein degradation, in comparison to the WT version of SnRK1α1 (**Figure** 4.1B). We next reasoned that SnRK1 degradation might be selectively induced or enhanced upon SnRK1 pathway activation. To evaluate this we determined the turnover of WT, SnRK1α1^{K48M} and SnRK1α1^{T175A} variants (all HA tagged constructs) when co-transfected with control DNA or with an active untagged SnRK1α1 construct in Col-0 cells. Importantly, SnRK1 pathway activation triggered by expression of untagged SnRK1α1 [**Figure** 3.1 and (*1, 12*)] but not by control DNA, induced degradation of inactive SnRK1α1^{K48M} and SnRK1α1^{T175A} proteins. This suggests that SnRK1 activity and/or SnRK1 pathway activation promotes SnRK1α1 turnover, possibly by acting *in trans* on the total SnRK1α1 pool (**Figure** 4.1C).

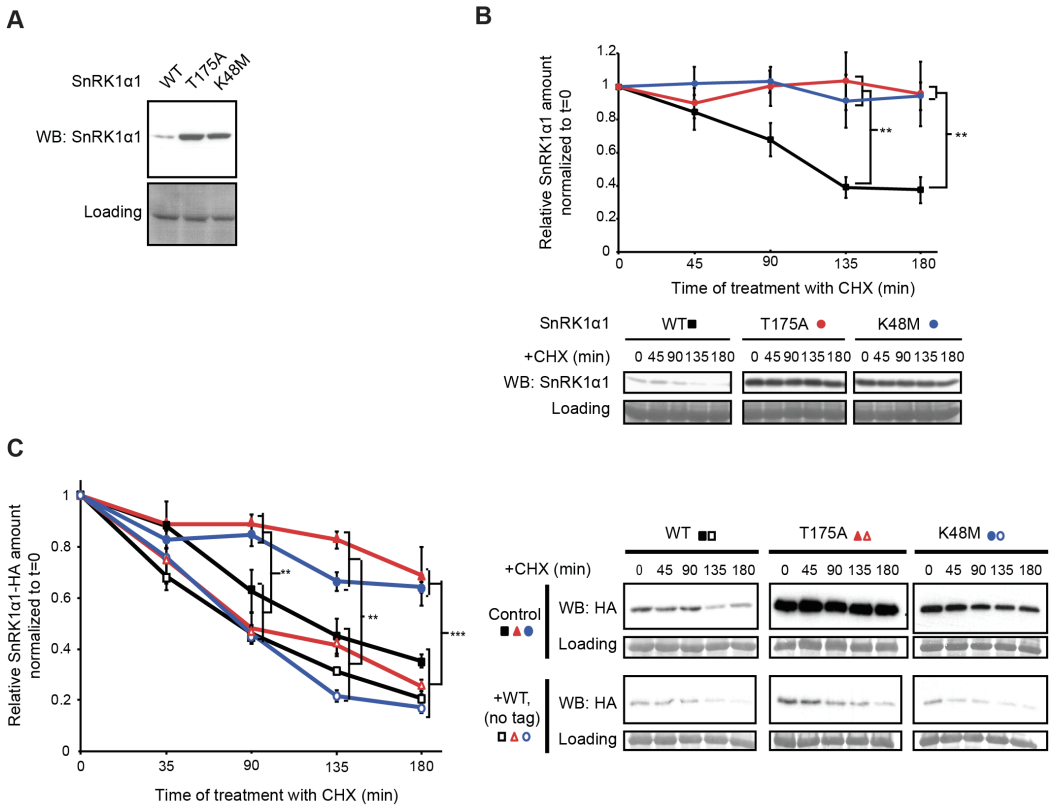

Figure 4.1 | SnRK1 activity triggers its degradation.

A. Inactive SnRK1α1 variants accumulate to higher levels than the WT protein. Accumulation of WT SnRK1α1 and of two inactive SnRK1α1^{T175A} and SnRK1α1^{K48M} mutants transiently expressed in Col-0 protoplasts, analyzed by Western-blot (WB) with anti-SnRK1α1 antibody. **B**. Only active SnRK1α1 undergoes degradation. WT (squares) or inactive (circles) SnRK1α1 variants were expressed in Col-0 protoplasts. Protoplasts were thereafter treated with cycloheximide (CHX), samples were harvested at the indicated time points, and analyzed by Western-blot (WB) with anti-SnRK1α1 antibody. The signal was quantified and normalized to the t=0 for each kinetics. **C**. As in B but HA-tagged SnRK1α1 variants (WT, squares; T175A, red triangles, K48M, blue circles) were co-expressed with a WT untagged variant (empty symbols) or with control plasmid (filled symbols). Data plotted are means (n≥3) and error bars are SEM. Statistical difference between kinetics at the different time points were analyzed through two-way ANOVA with Tukey's multiple comparison (*p<0.05, **p<0.01; ***p<0.001).

4.2.2 | Sumoylation restores degradation of inactive SnRK1α1 variants

Given the previously found interdependence between SnRK1α1 sumoylation and its ubiquitylation-mediated proteasomal degradation (**Chapter** 3), we hypothesized that the impaired turnover of inactive SnRK1α1 variants, observed in **Figure** 4.1B, was caused by a lack of sumoylation or, in the case sumoylation is occurring, by the absence of ubiquitylation-mediated proteasomal degradation downstream of sumoylation. To be able to distinguish between these two scenarios, we tested if we could restore a normal degradation of SnRK1α1 inactive variants by artificially providing the "SUMO signal". We expressed WT, SnRK1α1^{K48M}, and SnRK1α1^{T175A} variants as translational SUMO1 fusions ("SUMO mimetics", as in **Figure** 3.4F) in Col-0 cells, and determined their turnover. Interestingly, fusion of SUMO1 to inactive SnRK1α1 variants restored the degradation profile observed with active SnRK1α1, whilst a GFP-SUMO1 protein (control) was stable overtime, demonstrating a specific effect of the SUMO mimetic on SnRK1α1 stability (**Figure** 4.2A). This result suggests that the impaired turnover of inactive SnRK1α1 variants is caused by lack of sumoylation and that SnRK1α1 activity and/or SnRK1 pathway activation are a requirement for SnRK1 sumoylation and subsequent degradation.

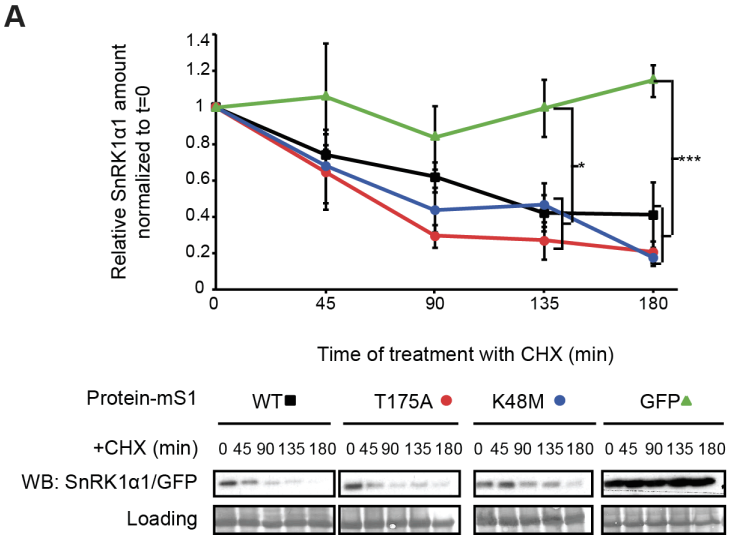

Figure 4.2 | Sumoylation restores degradation of inactive SnRK1α1 variants.

A. Inactive SnRK1α1 variants undergo degradation when expressed as SUMO-mimetics. SnRK1α1-mature SUMO1 (mS1) fusions (WT, squares; T175A, red circles, K48M, blue circles) or GFP fused to mS1 (green triangles, negative control) were expressed in Col-0 protoplasts. Protoplasts were thereafter treated with cycloheximide (CHX), samples were harvested at the indicated time points, and analyzed by Western-blot (WB) using anti-SnRK1α1 or anti-GFP antibodies. The signal was quantified and normalized to the t=0 for each kinetics. Stars denote statistical significance, as determined by two-way ANOVA with Tukey's multiple comparison (n≥3; error bars=SEM; *p<0.05, **p<0.01; ***p<0.001).

4.2.3 | Preliminary approaches to monitor endogenous SnRK1 protein turnover in energy deprivation (SnRK1 activation) conditions

Given that SnRK1 signaling is activated by energy deprivation [**Figure** 3.2A, (*1, 12*)] and that SnRK1 activation appears to trigger its own degradation (**Figure** 4.1), we decided to monitor the turnover of endogenous SnRK1, under control and activation conditions. The underlying hypothesis was that endogenous SnRK1 would be less stable under activating conditions due to increased sumoylation. To test this, we treated Col-0 and *siz1-2* protoplasts with control (2h light) or energy stress (2h darkness) conditions, and subsequently measured endogenous SnRK1α1 half-life in the presence of cycloheximide, the proteasome inhibitor MG132, or DMSO (mock) (**Figure** 4.3A). Despite the variability in SnRK1 degradation profile, we could sometimes visualize a small decrease of endogenous SnRK1α1 protein in dark-treated cells (**Figure** 4.3A), presumably as a result of SnRK1 activation by this stress (**Figure** 3.2A), and in accordance with the differential stability of active and inactive SnRK1α1 variants (**Figure** 4.1B). Furthermore, SnRK1α1 degradation in response to darkness was mostly diminished in the *siz1-2* mutant (**Figure** 4.3A), suggesting sumoylation could be a signal derived from SnRK1 activity that triggered its degradation. However, we failed to reproduce the differences regarding endogenous

SnRK1α1 protein accumulation in a consistent manner. Moreover, we also used a wide range of time points (to ensure detection of potentially transient changes), as well as detached leaves or liquid cultures of Arabidopsis seedlings, incubated with cyclohexamide and subjected to light and dark conditions, but no clear differences could be observed in SnRK1α1 protein accumulation overtime (not shown).

In order to determine if activation of the SnRK1 pathway would result into an increased accumulation of SnRK1α1-SUMO conjugates, we undertook two approaches. On one hand, we used Col-0 plants subjected to light (6h; control) or extended night (1h or 6h; energy stress) treatments to analyze SnRK1α1 accumulation and size profile in the corresponding nuclear extracts. Samples were processed to enrich for nuclear fractions since SUMO, the sumoylation machinery, and SUMO conjugates are particularly enriched in the nuclear compartment (*13*). Immunoblot analyses with anti-SnRK1α1 antibody revealed the accumulation of a high Molecular Weight (hMW) band in the nuclear fraction, relative to unmodified SnRK1α1, in response to energy stress (**Figure** 4.3B). The intensity of this band was stronger in the first hour of dark treatment while it was absent in control conditions (light), supporting the notion it could correspond to sumoylated SnRK1α1 (**Figure** 4.3B). However, the identity of SnRK1α1 hMW band should be specifically addressed. For instance, its disappearance in *siz1-2* nuclear fractions would suggest it corresponds indeed to SnRK1α1-SUMO conjugates. If further confirmed, this preliminary result may support the connection between SnRK1α1 activation in response to darkness and increased SnRK1α1 sumoylation, in the same energy stress conditions.

On the other hand, we treated *SnRK1α1-GFP* plants under light (control) and dark (energy stress) conditions, and performed GFP immunoprecipitations (IPs) to evaluate potential changes in the amount of SUMO1 conjugates associated with SnRK1α1-GFP immunoprecipitates. However, these experiments were not conclusive, as even though an accumulation of hMW SnRK1α1 forms and SUMO1 conjugates could sometimes be observed in response to dark stress

(D) as exemplified in **Figure** 4.3C, we failed to reproduce this observation in a consistent manner. Seedlings and leaf discs from *SnRK1α1-GFP* plants were also incubated in energy deprivation conditions, and in the presence of the proteasome inhibitor MG132, and subjected to GFP IPs. However, the plant material obtained with such approaches was much less abundant then the one retrieved with full rosettes, thereby hindering a reliable immunodetection of hMW SnRK1α1 forms and SUMO1 conjugates (not shown). Further attempts, perhaps employing stronger conditions to activate SnRK1 signaling (e.g. herbicide treatment, hypoxia, or the combination of both), specific cellular fractions (e.g. nucleus), different time points, and proteasome inhibitors may be required to tackle the accumulation of SnRK1α1-SUMO conjugates in response to energy stress and SnRK1 signaling activation.

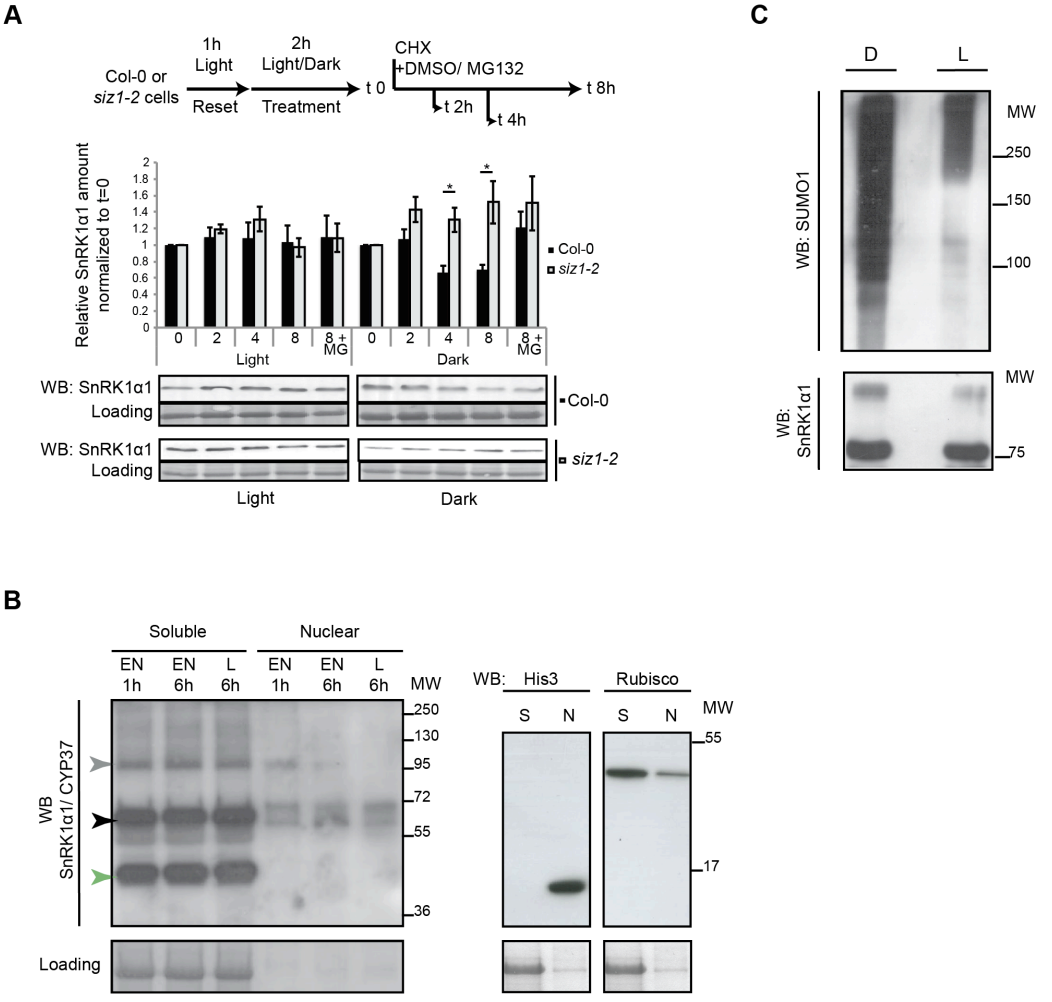

Figure 4.3 | SnRK1 activity triggers its sumoylation and turnover.

A. Following isolation, Col-0 and *siz1-2* protoplasts were rested for 1h under light, exposed to 2h of Light or Dark treatment, and subsequently treated with cyclohexamide (CHX), MG132 (MG) or DMSO (mock control). Samples were harvested at the indicated time points, and analyzed by Western-blot (WB) using anti-SnRK1α1 antibody. The signal was quantified and normalized to the t=0 for each kinetics. Data plotted are means and stars denote statistical significance, as determined by multiple *t*-tests using the Holm-Sidak method (n=4; error bars=SEM; *p<0.05). **B**. Full rosettes (~30 leaves) of 6-week-old Col-0 plants subjected to 1 or 6 hours of night extension (NE1h, NE6h; SnRK1α1 activating conditions), or to 6 hours of light (L6h; control), were used to separate soluble (S) and nuclei-enriched (N) fractions. These fractions were subsequently analyzed by SDS-PAGE and immunodetection with antibodies against SnRK1α1 and CYP37, a protein localized in the chloroplast that should be absent in the nuclear fraction. Green arrowhead indicates CYP37 protein, only present in "Soluble", black arrowhead indicates SnRK1α1 main band, and grey arrowhead, SnRK1α1 hMW bands. The panel on the right evidences nuclear enrichment in "N", through the immunodetection of Histone3 (His3) in this fraction, and a predominant presence of Rubisco in the "S" fraction, using the same protocol but in a parallel nuclear enrichment experiment. **C**. SnRK1α1-GFP was immunoprecipitated (IP) from leaf crude extracts of *SnRK1α1-GFP* plants treated with 3h of dark (D) or 3h of light (L), and analyzed by Western-Blot (WB) using antibodies against SnRK1α1 and SUMO1. WB, Western-blot; MW, molecular weight.

4.2.4 | SnRK1α1 phosphorylates SIZ1

Our previous results suggest that SnRK1 activation may trigger its sumoylation and subsequent turnover. However, how the SUMO machinery recognizes active SnRK1α1 is not yet understood. We hypothesized that the active kinase could phosphorylate a component of the SUMO pathway and thereby induce its own sumoylation. We searched for the presence of SnRK1 phosphorylation consensus motifs (*14, 15*) in the E3 ligase SIZ1 that confers specificity to SnRK1 sumoylation *in planta*, as previously shown (**Chapter** 2 and 3). We could detect seven SnRK1 phosphorylation motifs in SIZ1 (**Appendix**

Figure 2) and therefore decided to evaluate first if SnRK1 could phosphorylate SIZ1 to induce its own sumoylation. To this end, we performed *in vitro* kinase assays using recombinant SIZ1, SnRK1α1, and SnRK1 activating kinase 2 (SnAK2). SnAK2 was incubated with recombinant SnRK1α1 to promote its activation and, in agreement with previous reports, SnRK1α1 and SnAK2 crossphosphorylated [(*16*), **Figure** 4.4A]. A higher band corresponding to SIZ1 phosphorylation was detected when the three proteins were incubated together but not when SIZ1 was incubated alone or just with SnAK2 (**Figure** 4.4A). Similarly, recombinant SIZ1 was phosphorylated in the presence of SnRK1α1 immunoprecipitated from dark-treated *35S-SnRK1α1-HA* plants (*1*) (**Figure** 4.4B). The observed autophosphorylation of (active) immunoprecipitated SnRK1α1 has been previously reported (*12, 17*). These results support the hypothesis that SnRK1 may transduce its activation status through SIZ1 phosphorylation, thereby promoting its own sumoylation.

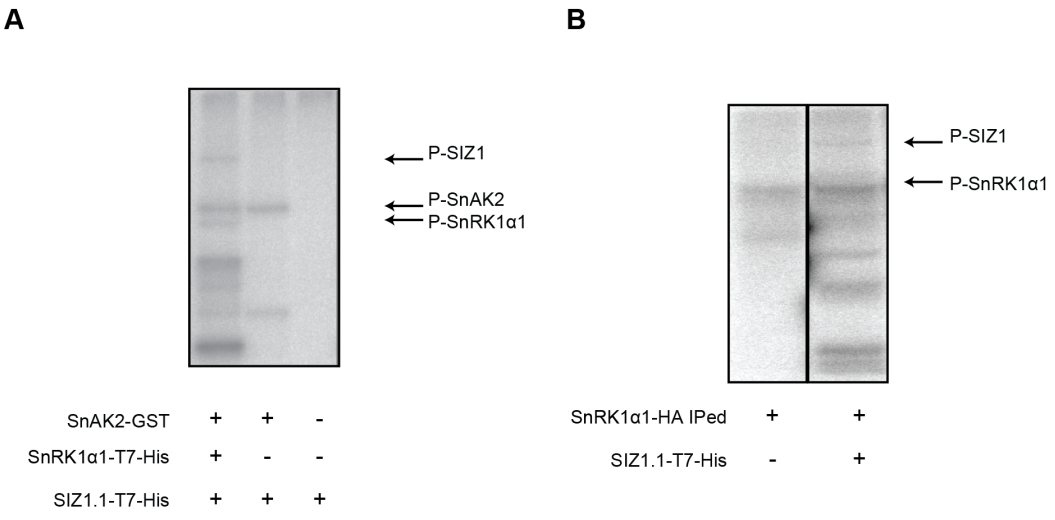

Figure 4.4 | SnRK1 phosphorylates SIZ1 *in vitro*.

A. Recombinant His-T7-SnRK1α1 (2μg) and GST-SnAK2-GST (0.2μg) were purified, and incubated in kinase activity buffer supplemented with γ-^{32}P-ATP in the presence of His-T7-SIZ1 (3ug) for 2h30m at 30ºC. Samples were then submitted to SDS-PAGE and autoradiography. The positions of phosphorylated SIZ1 (P-SIZ1), SnRK1α1 (P-SnRK1α1) and SnAK2 (P-SnAK2) are indicated. **B**. SnRK1α1-HA was immunoprecipitated from dark-treated *35S-SnRK1α1-HA* plants, and incubated in kinase activity buffer supplemented with γ-^{32}P-ATP for 1h at 30°C in the presence or absence of His-T7-SIZ1.1 (6ug). Samples were then submitted to SDS-PAGE and autoradiography. The positions of phosphorylated SIZ1 (P-SIZ1) and SnRK1α1 (P-SnRK1α1) are indicated.

To address the functional outcome of SIZ1 phosphorylation in SnRK1 sumoylation and SnRK1 pathway activation, we first aimed at identifying the residue(s) phosphorylated in SIZ1 in the *in vitro* kinase assays by mass spectrometry (MS). However, despite several attempts, we failed to detect SIZ1 phosphopeptides in our MS analyses, presumably due to the low phosphorylation signal together with a poor coverage of the protein in these analyses. As an alternative approach we generated SIZ1 variants harboring S/T to A (phosphomutant) or to D (phosphomimetic) mutations in putative SnRK1-dependent phosphorylation sites, in other SIZ1 phosphoresidues previously identified by MS (*18-22*), or in possible phosphorylation sites not covered in the MS analyses (**Appendix Figure** 2). These variants were then compared to WT SIZ1 for their ability to restore normal *pDIN6::LUC* reporter induction by transfected SnRK1α1 in *siz1-2*, as explained in **Figure** 3.1C. However, no clear differences were observed between WT or phosphomutant/ mimetic SIZ1 variants in a preliminary assay (**Figure** 4.5A), which may suggest that at least the targeted residues are not important for the repressive effect of SIZ1 on SnRK1α1 signaling. Further experiments are required to rule out SIZ1 phosphorylation as a possible mechanism connecting SnRK1 activity to its sumoylation. Additional replicates are needed and several possible SIZ1 phosphoresidues were not covered in this assay. The *in vitro* kinase assay

should also be used to test the abrogation of SnRK1-dependent phosphorylation of SIZ1 variants mutated in possible phosphoresidues (alone or in combination).

We also did preliminary assays to test if SnRK1α1 could phosphorylate other components of the SUMO pathway in Arabidopsis. For this purpose, we expressed in Col-0 cells various HA-tagged SUMO pathway components (E1 SUMO activating enzyme SAE1b, SAE2, or E2 SUMO conjugating enzyme SCE1) in the presence or absence of SnRK1α1. Proteins were thereafter resolved by Phos-Tag SDS-PAGE and immunodetected with a HA-antibody. Phos-Tag selectively retards phosphorylated proteins (*23*), allowing a clear separation between phosphorylated and non-phosphorylated forms of a given protein. However, no clear differences were observed in the migration pattern of SUMO machinery components in the presence or absence of SnRK1α1 (**Figure** 4.5B).

Finally, we reasoned that a putative regulation of the SUMO machinery by SnRK1 could have a broader impact on global sumoylation beyond the effect on SnRK1 itself. To test this, we induced transient systemic *snrk1* knockdown using virus-induced gene silencing (VIGS) (*1, 24*) of *SnRK1α2* in *snrk1α1-3* knockout seedlings (hereafter referred as *snrk1α1 snrk1α2* double mutant for simplicity), to circumvent the experimental limitation of obtaining *snrk1α* double loss-of-function mutants (*25-27*). Global SUMO1 profiles of control (Col-0), *siz1-2, snrk1α1 GFP* (VIGS against *GFP* in *snrk1α1-3 plants* as a control for VIGS), and *snrk1α1 snrk1α2* double mutant plants were analyzed after treatment of detached rosettes with several types of stress (darkness, heat, oxidative, ethanol, and salt) (*28-31*), or control conditions, and processing in 2X Laemmli solubilization buffer. Whereas no major differences were observed in the accumulation of SUMO1 conjugates in plants with diminished SnRK1 activity, *siz1-2* plants accumulated much less SUMO1 conjugates in stress conditions (**Figure** 4.5C), as previously described for this mutant (*32-36*).

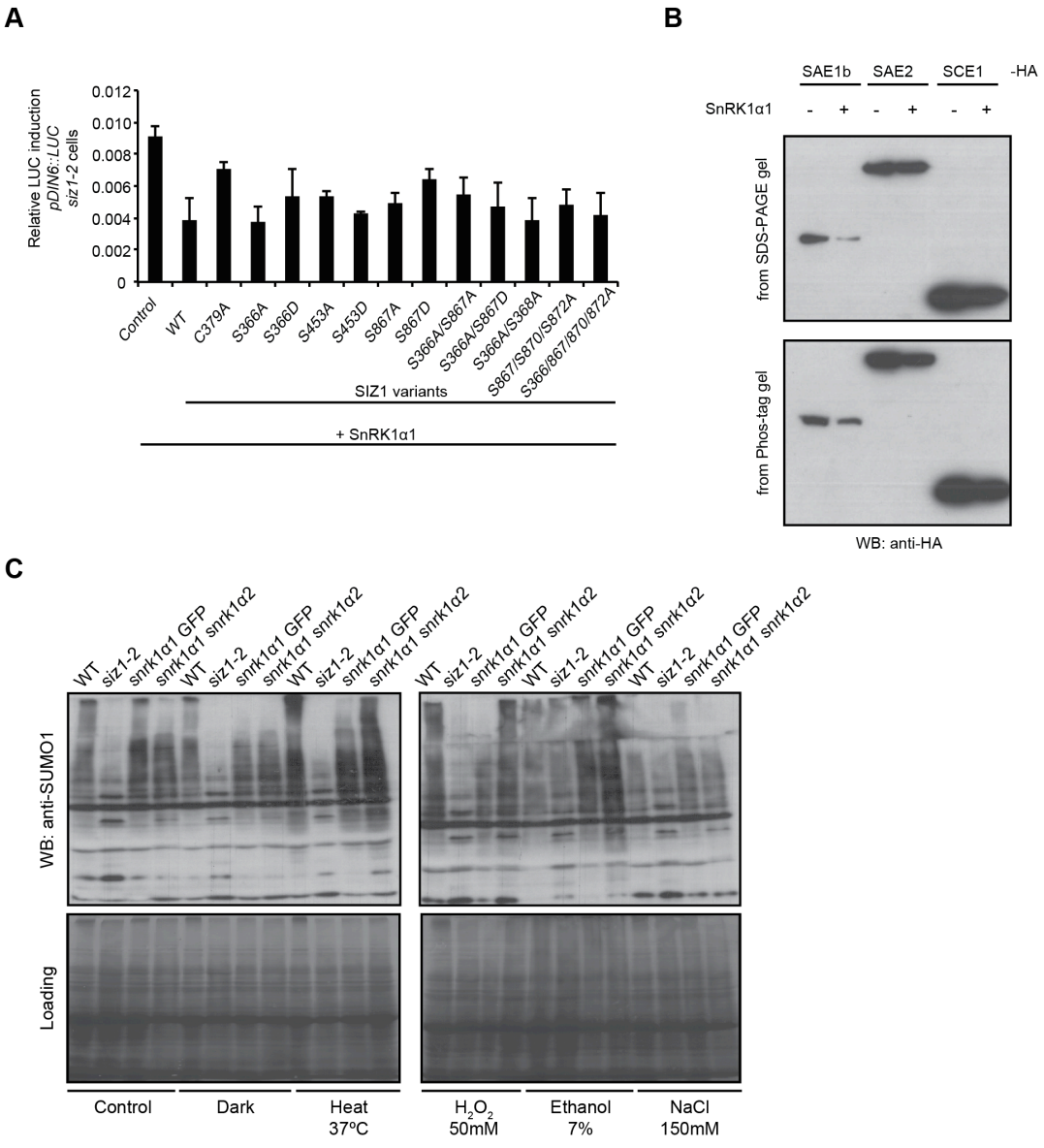

Figure 4.5 | SnRK1-dependent phosphorylation of SUMO pathway components and possible outcome.

A. Expression of SnRK1α1 triggers an overinduction of SnRK1 signaling in *siz1-2* that is rescued by the E3 ligase activity of SIZ1 (WT), but not by a catalytically inactive SIZ1 (C379A) variant. Several phosphomutant and phosphomimetic variants of SIZ1 were tested. **B**. HA tagged SUMO machinery components SAE1b, SAE2 and SCE1 were expressed alone or in combination

with SnRK1α1 in Col-0 protoplasts. Samples were then resolved through regular SDS-PAGE or Phos-tag SDS-PAGE and immunodetected with anti-HA antibody. **C**. Detached rosettes of WT (Col-0), *siz1-2*, *snrk1α1 GFP, and snrk1α1 snrk1α2* were incubated in control conditions or subjected to Dark, Heat (37ºC), oxidative (50mM H_2O_2), Ethanol (10%), or salt (150mM NaCl) stress for 1h. Samples were processed in 2X Laemmli buffer and analyzed by Western-blot (WB) with anti-SUMO1 antibody.

4.3 | Discussion

The activation of protein kinases is commonly coupled to their downregulation *via* the ubiquitin/proteasome system (*6*). Indeed, we provide evidence that SUMO-mediated degradation of SnRK1 is dependent on SnRK1 kinase activity. First, inactive SnRK1α1 variants are not degraded (**Figure** 4.1B) and therefore accumulate to higher levels than the active kinase (*1*) (**Figure** 4.1A). Nevertheless, upon SnRK1 pathway activation, attained by co-expression of an active SnRK1α1, the inactive SnRK1α1 variants recovered normal turnover (**Figure** 4.1C). Second, when expressed as SnRK1α1-SUMO1 fusions ("SUMO mimetics"), inactive SnRK1α1 variants are degraded like the WT SnRK1α1 (**Figure** 4.2A), suggesting that the reason for their impaired degradation is the lack of sumoylation. Finally, the turnover of active SnRK1α1 seems to be impaired in the *siz1-2* mutant (**Figure** 4.3A), suggesting that sumoylation may be an intermediate step between SnRK1 activity and its degradation. Collectively, these results suggest that SnRK1 activation initiates its downregulation through sumoylation-dependent ubiquitylation and proteasomal degradation. The prediction from this model would be that under conditions of high SnRK1 signaling activity such as dark stress, SnRK1 sumoylation and consequent degradation would be increased. Some of our preliminary experiments support such model, showing that destabilization of

endogenous SnRK1α1 occurs in cells subjected to energy stress (darkness), presumably as a result of SnRK1 activation (**Figure** 4.3A). We have also preliminary data that suggests an increase in SnRK1α1-SUMO conjugates upon energy deprivation (**Figure** 4.3B-C). However, the obtained differences are often subtle and prone to high variability, and hence our results on the endogenous protein are not yet conclusive. Probably there were technical limitations due to the quantification of small variations in protein amount, and to the degradation of untransfected protoplasts over long incubation times. A more sensitive loading control, with immunodetection of an endogenous and stable protein should be employed in future attempts. On the other hand, it is also possible that an increased rate of sumoylation, turnover and replenishment of SnRK1 protein does not result in the differential accumulation of SnRK1-SUMO conjugates, detected in a given time point. Further studies are needed to acquire a better temporal resolution (checking shorter and longer time points) of SnRK1 turnover, and upon different stress treatments (regarding the nature of the stress, but also the intensity and duration of the perturbation). For instance, a sensitive and dynamic pulse-chase labeling using SNAP-tag (*37, 38*) could be used to assess differences in SnRK1 turnover in living cells (Col-0 and *siz1-2*), and upon different stimuli.

Interestingly, SnRK1α is degraded in response to ABA in wheat roots (*39*). Given that ABA activates SnRK1 signaling (*12*) this suggests that SnRK1 degradation might be a general mechanism to reset SnRK1 signaling upon activation by different stimuli, preventing pathway overactivation, which might be deleterious for plant growth.

Activated kinases can be recognized for ubiquitylation and degradation by different mechanisms, often involving the generation of recognition motifs through phosphorylation, or their exposure through conformational changes (*6*). We show that sumoylation of active SnRK1α1 seems to be an intermediary step for its turnover, and that the active kinase phosphorylates SIZ1 *in vitro* (**Figure** 4.3A-B). This raises the possibility that the latter mechanism is used for

recognition of active SnRK1 by the SUMO machinery. Different SIZ1 phosphopeptides have been retrieved in phosphoproteomic studies (*18*-*22*), but the role of differentially phosphorylated SIZ1 remains unclear in plants. In other systems, phosphorylation was shown to directly modulate activity (*40*) or possibly localization (*41, 42*) of E3 SUMO ligases. Although not conclusively, we failed to show a clear impact of phosphorylation of specific SIZ1 residues in SnRK1α1 signaling pathway activation (**Figure** 4.5A), or of SnRK1-dependent phosphorylation on global sumoylation, in response to several types of stresses (**Figure** 4.5C). Further studies are required to address SnRK1-dependent SIZ1 phosphorylation *in planta*, and to clarify the functional outcome of this modification, namely on SnRK1 sumoylation and/or global sumoylation. Additionally, it is also possible that SnRK1 pathway activation is conveyed through SnRK1-dependent phosphorylation of other SUMO machinery components. Our preliminary tests showed unmodified SAE1b, SAE2 and SCE1, in the presence or absence of SnRK1α1 (**Figure** 4.5B). SnRK1 phosphorylation motifs can also be found in other SUMO pathway components such as SUMO proteases and SUMO itself (not shown), and further experiments should be made to clarify a possible regulation of sumoylation *via* SnRK1-dependent phosphorylation.

Recently, the insulin/IGF-1 activated protein kinase Akt was shown to be sumoylated, and this modification further enhanced kinase activity. Furthermore, active Akt phosphorylates SUMO1 and the SUMO conjugating enzyme Ubc9, and through both mechanisms regulates global sumoylation, including Akt and Ubc9 sumoylation, as well as substrate sumoylation specificity. The specific downstream sumoylation of phosphatase and tensin homolog (PTEN) serves as an endogenous mechanism to stop the positive feedback loop resulting from Akt activation and sumoylation (*10, 11*). Another interesting example of regulation through phosphorylation of SUMO pathway components, involves the phosphorylation of the E3 SUMO ligase Pc2 by its substrate, homeodomain interacting protein kinase 2 (HIPK2). HIPK2-dependent phosphorylation of Pc2

enhances its SUMO ligase activity towards HIPK2, creating a feedback regulatory mechanism (*40*). In a different case, phosphorylation of the E3 ligase PIAS1 requires, but does not seem to impact, its E3 ligase activity (*42, 43*). Besides the abovementioned mechanisms to convey SnRK1 kinase activity, phosphorylated residues on active SnRK1 or conformational changes associated with kinase activity, may create or expose a recognition motif for the SUMO machinery. Several phospho-residues were identified on catalytic SnRK1α subunits in phosphoproteomic studies, besides conserved T-loop phosphorylation (T175/T176) (*18-22, 44*). Phosphorylated residues on SnRK1α1 such as S176, S179 or Y182 (in the kinase domain), or S364 an S367 (in the regulatory domain), await functional characterization and may be eventually implied in a phosphorylation-dependent sumoylation of SnRK1. Similarly, identified phosphorylated residues on SnRK1 regulatory subunits (β1, β2 and βγ) (*18-22*) may putatively contribute to an interplay between phosphorylation and SnRK1 complex sumoylation. Another option may also include the downstream phosphorylation of SnRK1 targets that in turn could regulate the sumoylation pathway. For instance, the serine/arginine-rich (SR) splicing protein SF2/ASF was shown to stimulate SUMO conjugation of specific substrates in mammals (*45*). The Arabidopsis SR45 splicing protein interacts with the SUMO machinery in Y2H, but does not seem to be modified by sumoylation (*46*), suggesting it may rather have a role as a co-factor in sumoylation regulation. Furthermore, the SR45 splicing factor modulates SnRK1 stability (Carvalho, RF., submitted) but whether this depends on SnRK1 sumoylation and/or on SnRK1-dependent phosphorylation of SR45 remains to be tested. Finally, it is also possible that SnRK1 sumoylation is not directly induced by its activation status, but that is rather a consequence of the physical proximity between active SnRK1 and SUMO machinery, upon given stimuli (e.g. co-localization in the nucleus).

As previously addressed in Chapter 2 and Chapter 3 [see respective **Discussion**(s)], sumoylation has been described for SnRK1 orthologs in yeast

(SNF1) and mammals (AMPK). In AMPK, both catalytic (α1/α2) subunits are within a list of ~1600 human proteins found to be sumoylated using high-resolution MS (*47*). AMPKα1 sumoylation was detected in control samples and was significantly increased in response to heat shock, proteasome inhibition and SUMO protease inhibition treatments. It is known that several environmental stresses such as heat, oxidative stress and hypoxia result in ATP depletion and in the consequent activation of AMPK (*48*). Thus, similarly to SnRK1, AMPKα1 activation seems to enhance its sumoylation (upon heat stress) and is intimately connected to kinase turnover, as suggested by the enrichment of AMPKα1-SUMO conjugates upon proteasome inhibition. Sumoylation of the catalytic subunit AMPKα2 had a low intensity signal and was only detected upon MG132 treatment (*47*), suggesting it may similarly regulate kinase turnover and signal termination. In the case of SNF1, the Snf1 catalytic subunit was reported to be sumoylated and degraded in response to Snf1 inactivating conditions (glucose treatment) (*49*). Even though the authors conclude that sumoylation is important to reduce SNF1 levels when cells do no longer need SNF1 activity, the fact that the Mms21 SUMO ligase mutants also accumulate higher Snf1 levels under low glucose suggests that, as in the case of SnRK1 and AMPK, sumoylation of SNF1 catalytic subunit may also operate under activating conditions as a way to promote signal termination and prevent deleterious pathway overactivation.

However, distinct layers of regulation and functional outcomes may be attained through sumoylation of specific regulatory subunits or specific SNF1/AMPK/SnRK1 complexes. AMPKβ2 sumoylation was reported to enhance AMPK activity by increasing its phosphorylation (*50*). Furthermore, AMPKβ2 sumoylation and ubiquitylation appeared to be antagonistic, and possibly the same occurs with the SnRK1 regulatory subunit, SnRK1β2. On the other hand, SnRK1β1 and SnRK1β2 are differentially accumulated in the *siz1-2* mutant (**Figure** 3.4D), possibly due to distinct consequences of SUMO attachment.

Given the common downregulation of SNF1/AMPK/SnRK1 catalytic subunits by sumoylation, it is challenging to integrate diverse functional outcomes of individual regulatory subunits and whole complex sumoylation. One potential scenario is that complex composition influences its sumoylation, as the SUMO machinery may have different affinities towards distinct SNF1/AMPK/SnRK1 complexes and this might be partially due to their differential distribution within the cell. Alternatively, sumoylation may *per se* selectively determine SNF1/AMPK/SnRK1 complex composition in response to specific signaling cues, activating distinct complexes and consequently triggering their degradation.

In summary, the work here described has uncovered a negative feedback loop by which SnRK1 activity triggers its own SUMO-mediated proteasomal degradation. Furthermore, this feedback regulation allows to reset SnRK1 signaling to equilibrium, and to restrain stress responses over growth and developmental demands (*2, 51*), possibly taking into account the intensity and duration of stress signals. Such an intimate connection between kinase activity and turnover may be required for an accurate response to energy deprivation conditions, and seems to be evolutionarily conserved amongst SNF1/AMPK/SnRK1 kinases.

4.4 | Materials and Methods

A list of all primers, cloning steps and constructs used in this study is provided in **Appendix Table** 1.

4.4.1 | Plant Material, Growth Conditions and Virus-induced gene silencing (VIGS)

Unless otherwise specified, plants were grown in soil under a 12h light (100μE), 22°C/12h dark, 18°C regime. *Arabidopsis thaliana* plants used in this study are in the Columbia (Col-0) background such as Col-0 (WT), *siz1-2* (SALK_065397) (*52, 53*), and *snrk1α1-3* (described in **Chapter** 2), or in the Landsberg erecta (Ler) background for *35S-SnRK1α1-HA (1)*, and have been previously described. Virus-induced gene silencing (VIGS) of *SnRK1α2* or GFP (control) was performed in the *snrk1α1-3* background to generate *snrk1α1 snrk1α2* (*SnRK1α2* VIGS) or *snrk1α1 GFP* (GFP VIGS) plants. Virus-induced gene silencing (VIGS) was done as previously described (*24*). pTRV RNA1 and pTRV RNA2 (the latter containing gene specific fragments of -SnRK1α2 or -GFP) were introduced into *Agrobacterium tumefaciens* strain GV3101 and a 5mL culture was grown overnight at 28ºC in 50 mg/L gentamycin and 50 mg/L kanamycin. The culture was inoculated into 50mL LB medium containing antibiotics, 10mM MES, and 20μM acetosyringone and grown overnight in a 28ºC shaker. *A. tumefaciens* cells were harvested and resuspended in infiltration media (10mM MgCl2, 10mM MES, and 200μM acetosyringone), adjusted to an OD^{600nm} of 1.5, and left at room temperature for 3 to 4 h. Two- to three true-leaf seedlings of *snrk1α1-3* plants with approximately 2 weeks were used for VIGS. Agroinfiltration was performed after mixing 1:1 RNA1 and RNA2 Agrocultures, and infiltrating the entire leaf with a needleless 1mL syringe, into two leaves of each seedling. Plants were used for stress treatments at the age of 4-5 weeks.

4.4.2 | Antibodies and Protein Expression Analyses

The SnRK1α1 (1/500, anti-AKIN10, AS10919), Rubisco (1/5000, anti-RbcL, AS03037), Histone 3 (1/1000, anti-H3, AS10710) and CYP37 (1/2000, anti-PPIase CYP37, AS101589) antibodies were purchased from Agrisera. Anti-HA

(1/1000, Roche, #11867423001) and anti-GFP (1/500, A01388, GeneScript) antibodies were used to detect the corresponding tagged proteins, whereas anti-GST (1/2000, Sigma, #G7781) and anti-T7 (1/10000, #69522-3, Novagen) were used to immunoprecipitate the corresponding tagged proteins.

For immunoblotting all primary antibodies were diluted in 1% non-fat Milk in TBS (unless otherwise stated) and incubated with the membrane under gentle shaking for 12h at 4°C. Secondary antibodies (Jackson ImmunoResearch Lab, inc) were used at 1/10000 in 1% non-fat Milk in TBS for 1h at RT.

4.4.3 | Protoplast Transient Expression Assays

Protoplasts from Col-0 or *siz1-2* plants were isolated and transfected as already described (*54*). All effector constructs (**Appendix Table** 1) were generated by cloning the corresponding coding sequences into a pHBT95 vector harboring a C-terminal HA (*54*), except for the "SUMO mimetics" constructs that have no tag. The indicated mutations were introduced by site-directed mutagenesis and verified by sequencing. For endogenous protein quantifications (**Figure** 4.2B), protoplasts were incubated without transfection and collected at the described times. Cyclohexamide (Biochemica, A0879/0001; Ethanol stock) and MG132 (Sigma, C2211; DMSO stock) solutions were used at a final concentration of 100µM and 50µM, respectively.

For protein expression analyses, protoplasts were directly ressuspended in 4X Laemmli solubilization buffer (*55*) and boiled for 5min at 95°C. Samples were analyzed by SDS-PAGE or Phos-Tag SDS-PAGE, in which the Phos-Tag ligand selectively retards phosphorylated proteins [50 µM Phos-Tag ligand (Wako Chemicals GmbH, AAL-107, 304-93521) and 100 µM $MnCl_2$) (*23*)].

4.4.4 | Nuclear enrichment

Full rosettes from 6-week-old Col-0 plants were ground in liquid nitrogen and extracted with 15ml/rosette of Nuclear Enrichment Extraction buffer (EB) [20mM Tris-HCl pH6.8, 25% Glycerol (V/V), 1% Triton-X (V/V), 2.5mM $MgCl_2$, 20mM KCl, 2mM EDTA, 8.8% Sucrose (w/V), 0.5mM Spermidine, 30mM β-Mercapto-Ethanol, cOmplete protease inhibitor cocktail (one tablet/25mL), 1/500 (v/v) phosphatase inhibitor 2 (Sigma P5726) and 3 (Sigma P0044), 10mM NEM]. Liquid and homogenous plant extracts were filtered through four layers of Miracloth and kept on ice for 15-20min. Samples were thereafter cleared by centrifugation using a swing-out rotor (1000*g*, 4ºC, 10min). The supernatant, containing the "soluble fraction" was frozen (15-20µl of supernatant loaded per gel), and the pellet containing the nuclei was gently washed three times with 3ml of Nuclei Resuspension buffer (RB) [20mM Tris-HCl pH6.8, 25% Glycerol (V/V), 2.5mM $MgCl_2$, 0.5mM Spermidine, 30mM β-Mercapto-Ethanol, cOmplete protease inhibitor cocktail (one tablet/25mL), 1/500 (v/v) phosphatase inhibitor 2 (Sigma P5726) and 3 (Sigma P0044), 10mM NEM], and resuspended in 60ul of RB (20µl of nuclei enriched fraction loaded per gel). Prior to SDS-PAGE analysis, samples were boiled for 5min at 95°C with 4X Laemmli solubilization buffer (*55*).

4.4.5 | Plant Stress treatments

Detached rosettes of Col-0 (WT), *siz1-2*, *snrk1α1 snrk1α2*, or *snrk1α1 GFP* plants with 4 to 5 weeks, were incubated in small petri dishes with 10ml of *MilliQ* water and subjected to control or stress treatments for 1 hour. The following stresses were applied: darkness, heat (37ºC), oxidative stress (H_2O_2, 50mM), ethanol (10%), or salt stress (NaCl 150mM) (*28-31*). Plant material was frozen and subsequently processed in 2X Laemmli buffer with 8% β-Mercapto-Ethanol

and 50mM N-Ethylmaleimide (NEM), and boiled for 5min at 95°C. Samples were analyzed through SDS-PAGE and immunoblotting against SUMO1. Membranes were afterwards stained with Coomassie Brilliant Blue R250, and the loading of each lane was compared with the correspondent SUMO1 profile previously obtained.

4.4.6 | Quantification of immunoblot results

Membranes were analyzed by immunoblotting and then stained with Coomassie Brilliant Blue R250. Band intensity was quantified using Image J (http://imagej.nih.gov/ij/) and Gel Quant Net (http://biochemlabsolutions.com/GelQuantNET.html) softwares. The immunoblot intensities were normalized to the Coomassie staining intensity (referred as "loading"). Quantifications were normalized to the t=0 of each kinetics.

4.4.7 | Statistical Analyses

All statistical analyses were performed with the GraphPad Prism 6 software (GraphPad softwares).

4.4.8 | Recombinant Protein Production and Purification

Recombinant SnAK2-GST protein was purified from *E. coli* extracts using glutathione-agarose affinity chromatography (G4510; Sigma-Aldrich), according to the manufacturer's instructions and as previously described (*16*). SnRK1α1.1 and SIZ1.1 were cloned into pET28a (Novagen). Recombinant proteins were

produced in *E. coli* (BL21 rosetta) and purified using immobilized metal ion affinity chromatography (Ni-NTA, Qiagen) following the manufacturer's instructions and as previously described (*12*). Successful protein production and purification were verified by immunoblotting with anti-GST and anti-T7 antibodies.

4.4.9 | SnRK1α1 Immunoprecipitation and *in vitro* Kinase Assays

SnRK1α1 was immunoprecipitated from leaves of *35S-SnRK1.1-HA* plants treated for 1h in darkness. Plant material (1g) was extracted in 3 volumes of 1xPBS supplemented with 1mM EDTA, 0.05% Triton X-100, and 1/500 (v/v) plant-specific protease inhibitor cocktail (Sigma) and phosphatase inhibitor cocktail (Sigma). After centrifugation (20,000*g*, 4°C, 15min), the supernatant was recovered, and 1mg of total protein was incubated 2h at 4°C with 30µL of anti-HA affinity matrix. The matrix was washed three times with extraction buffer and resuspended in kinase assay buffer, of which one third was used for each reaction as follows.

For *in vitro* kinase assays, recombinant His-T7-SIZ1 (3µg) was incubated alone or with His-T7-SnRK1α1 (2µg) and/or GST-SnAK2 (0.2µg), for 2h at 30°C in kinase assay media [50mM Hepes-NaOH pH7.25, 10mM $MgCl_2$, 1mM DTT, 1/500 (v/v) plant-specific protease inhibitor cocktail (Sigma), 1/500 (v/v) phosphatase inhibitor 2 (Sigma P5726) and 3 (Sigma P0044), 100µM cold ATP and complemented with 2µCi of γ-^{32}P-ATP]. Immunoprecipitated SnRK1α1 was directly incubated (or not) with recombinant SIZ1 in kinase assay buffer, with 100µM cold ATP and 2µCi of γ-^{32}P-ATP, for 1h at 30°C. Reactions were stopped by addition of Laemmli buffer, and then boiled for 5 min at 95ºC. Proteins were resolved in an 8% SDS-PAGE gel, and detected using a phosphor image system (STORM 860; GE Healthcare).

4.4.10 | Accession Numbers

Sequence data can be found in the Arabidopsis Genome Initiative database under the following accession numbers: *SnRK1α1*, At3g01090; *SIZ1*, At5g60410*; SAE1b*, At5g50580; *SAE2*, At2g21470; *SCE1*, At3g57870; SUMO1, At4g26840; *DIN6*, At3g47340; *SnAK2*, AT3G45240.

Supplemental data

Supplemental Data includes Appendix Table 1.

Acknowledgements

I would like to acknowledge Elena Baena-González for guidance throughout all the work and careful reading of the chapter, and Pierre Crozet for contributing for the work here presented and for help with the figures. I would like to acknowledge the PAPPSO platform of the INRA at Gif/Yvette, France, for doing the MS analyses of phospho SIZ1. Furthermore, I am grateful to all Plant Stress Signaling group members for fruitful discussions, and to Vera Nunes for great plant care.

References

1. E. Baena-González, F. Rolland, J. M. Thevelein, J. Sheen, in *Nature*. (2007), vol. 448, pp. 938-942.
2. E. Baena-González, J. Sheen, in *Trends in Plant Science*. (2008), vol. 13, pp. 474-482.
3. X.-J. Yang, C.-M. Chiang, in *F1000Prime Rep*. (2013), vol. 5, pp. 45.
4. H. D. Ulrich, in *Mol Cell*. (2012), vol. 47, pp. 335-337.

5. Z. Guo, J. Kanjanapangka, N. Liu, S. Liu, C. Liu, Z. Wu, Y. Wang, T. Loh, C. Kowolik, J. Jamsen, M. Zhou, K. Truong, Y. Chen, L. Zheng, B. Shen, in *Mol Cell*. (2012), vol. 47, pp. 444-456.
6. Z. Lu, T. Hunter, in *Annu Rev Biochem*. (2009), vol. 78, pp. 435-475.
7. S.-H. Yang, A. Galanis, J. Witty, A. D. Sharrocks, in *EMBO J*. (2006), vol. 25, pp. 5083-5093.
8. Y.-T. Wang, W.-B. Yang, W.-C. Chang, J.-J. Hung, in *J Mol Biol*. (2011), vol. 414, pp. 1-14.
9. K. Miura, J. Lee, J. B. Jin, C. Y. Yoo, T. Miura, P. M. Hasegawa, in *Proc Natl Acad Sci USA*. (2009), vol. 106, pp. 5418-5423.
10. C. H. Lin, S. Y. Liu, E. H. Y. Lee, in *Oncogene*. (2015).
11. R. Li, J. Wei, C. Jiang, D. Liu, L. Deng, K. Zhang, P. Wang, in *Cancer Research*. (2013), pp. 1-33.
12. A. Rodrigues, M. Adamo, P. Crozet, L. Margalha, A. Confraria, C. Martinho, A. Elias, A. Rabissi, V. Lumbreras, M. González-Guzmán, R. Antoni, P. L. Rodriguez, E. Baena-González, in *The Plant Cell*. (2013), vol. 25, pp. 3871-3884.
13. J.-S. Seeler, A. Dejean, in *Nature Reviews Molecular Cell Biology*. (2003), vol. 4, pp. 690-699.
14. C. Sugden, P. G. Donaghy, N. G. Halford, D. G. Hardie, in *Plant Physiol*. (1999), vol. 120, pp. 257-274.
15. F. Vlad, B. E. Turk, P. Peynot, J. Leung, S. Merlot, in *Plant J*. (2008), vol. 55, pp. 104-117.
16. P. Crozet, F. Jammes, B. Valot, F. Ambard-Bretteville, S. Nessler, M. Hodges, J. Vidal, M. Thomas, in *J Biol Chem*. (2010), vol. 285, pp. 12071-12077.
17. R. P. Bhalerao, K. Salchert, L. Bakó, L. Okrész, L. Szabados, T. Muranaka, Y. Machida, J. Schell, C. Koncz, in *Proc Natl Acad Sci USA*. (1999), vol. 96, pp. 5322-5327.
18. W. R. Engelsberger, W. X. Schulze, in *Plant J*. (2012), vol. 69, pp. 978-995.
19. H. Nakagami, N. Sugiyama, K. Mochida, A. Daudi, Y. Yoshida, T. Toyoda, M. Tomita, Y. Ishihama, K. Shirasu, in *PLANT PHYSIOLOGY*. (2010), vol. 153, pp. 1161-1174.
20. T. Umezawa, N. Sugiyama, F. Takahashi, J. C. Anderson, Y. Ishihama, S. C. Peck, K. Shinozaki, in *Science Signaling*. (2013), vol. 6, pp. rs8.
21. P. Wang, L. Xue, G. Batelli, S. Lee, Y.-J. Hou, M. J. Van Oosten, H. Zhang, W. A. Tao, J.-K. Zhu, in *Proceedings of the National Academy of Sciences*. (2013), vol. 110, pp. 11205-11210.
22. Q. Yao, C. Bollinger, J. Gao, D. Xu, J. J. Thelen, in *Front. Plant Sci.* (2012), vol. 3, pp. 206.
23. E. Kinoshita, E. Kinoshita-Kikuta, T. Koike, *Nat Protoc.* (2009), vol. 4, pp. 1513-1521.
24. T. M. Burch-Smith, in *Plant Physiol*. (2006), vol. 142, pp. 21-27.
25. N. G. Halford, S. Hey, D. Jhurreea, S. Laurie, R. S. McKibbin, M. Paul, Y. Zhang, in *Journal of experimental botany*. (2003), vol. 54, pp. 467-475.
26. Y. Zhang, P. R. Shewry, H. Jones, P. Barcelo, P. A. Lazzeri, N. G. Halford, in *Plant J*. (2001), vol. 28, pp. 431-441.
27. R. Radchuk, V. Radchuk, W. Weschke, L. Borisjuk, H. Weber, in *Plant Physiol*. (2006), vol. 140, pp. 263-278.

28. J. Kurepa, J. M. Walker, J. Smalle, M. M. Gosink, S. J. Davis, T. L. Durham, D.-Y. Sung, R. D. Vierstra, in *J Biol Chem*. (2003), vol. 278, pp. 6862-6872.
29. L. Conti, G. Price, E. O'Donnell, B. Schwessinger, P. Dominy, A. Sadanandom, in *Plant Cell*. (2008), vol. 20, pp. 2894-2908.
30. H. C. Park, H. Kim, S. C. Koo, H. J. Park, M. S. Cheong, H. Hong, D. Baek, W. S. Chung, D. H. Kim, R. A. Bressan, S. Y. Lee, H. J. Bohnert, D.-J. Yun, in *Plant, Cell & Environment*. (2010), vol. 33, pp. 1923-1934.
31. M. J. Miller, M. Scalf, T. C. Rytz, S. L. Hubler, L. M. Smith, R. D. Vierstra, in *Mol Cell Proteomics*. (2012).
32. K. Miura, A. Rus, A. Sharkhuu, S. Yokoi, A. S. Karthikeyan, K. G. Raghothama, D. Baek, Y. D. Koo, J. B. Jin, R. A. Bressan, D.-J. Yun, P. M. Hasegawa, in *Proc Natl Acad Sci USA*. (2005), vol. 102, pp. 7760-7765.
33. C. Y. Yoo, K. Miura, J. B. Jin, J. Lee, H. C. Park, D. E. Salt, D.-J. Yun, R. A. Bressan, P. M. Hasegawa, in *PLANT PHYSIOLOGY*. (2006), vol. 142, pp. 1548-1558.
34. S. A. Saracco, M. J. Miller, J. Kurepa, R. D. Vierstra, in *PLANT PHYSIOLOGY*. (2007), vol. 145, pp. 119-134.
35. R. Catala, J. Ouyang, I. A. Abreu, Y. Hu, H. Seo, X. Zhang, N.-H. Chua, in *Plant Cell*. (2007), vol. 19, pp. 2952-2966.
36. C.-C. Chen, Y.-Y. Chen, I.-C. Tang, H.-M. Liang, C.-C. Lai, J.-M. Chiou, K.-C. Yeh, in *PLANT PHYSIOLOGY*. (2011), vol. 156, pp. 2225-2234.
37. D. L. Bodor, M. G. Rodríguez, N. Moreno, L. E. T. Jansen, in *Curr Protoc Cell Biol*. (2012), vol. Chapter 8, pp. Unit8.8.
38. L. E. T. Jansen, B. E. Black, D. R. Foltz, D. W. Cleveland, in *The Journal of Cell Biology*. (2007), vol. 176, pp. 795-805.
39. P. Coello, E. Hirano, S. J. Hey, N. Muttucumaru, E. Martinez-Barajas, M. A. J. Parry, N. G. Halford, in *Journal of experimental botany*. (2012), vol. 63, pp. 913-924.
40. A. Roscic, A. Möller, M. A. Calzado, F. Renner, V. C. Wimmer, E. Gresko, K. S. Lüdi, M. L. Schmitz, in *Molecular Cell*. (2006), vol. 24, pp. 77-89.
41. E. S. Johnson, A. A. Gupta, in *CELL*. (2001), vol. 106, pp. 735-744.
42. B. Liu, Y. Yang, V. Chernishof, R. R. O. Loo, H. Jang, S. Tahk, R. Yang, S. Mink, D. Shultz, C. J. Bellone, J. A. Loo, K. Shuai, in *CELL*. (2007), vol. 129, pp. 903-914.
43. F. Z. Watts, in *Chromosoma*. (2013).
44. M. K. Choudhary, Y. Nomura, L. Wang, H. Nakagami, D. E. Somers, in *Mol Cell Proteomics*. (2015).
45. F. Pelisch, J. Gerez, J. Druker, I. E. Schor, M. J. Muñoz, G. Risso, E. Petrillo, B. J. Westman, A. I. Lamond, E. Arzt, A. Srebrow, in *Proc Natl Acad Sci USA*. (2010), vol. 107, pp. 16119-16124.
46. N. Elrouby, G. Coupland, in *Proc Natl Acad Sci USA*. (2010), vol. 107, pp. 17415-17420.
47. I. A. Hendriks, R. C. J. D'souza, B. Yang, M. Verlaan-de Vries, M. Mann, A. C. O. Vertegaal, in *Nat Struct Mol Biol*. (2014).
48. D. G. Hardie, D. Carling, N. Halford, in *Semin Cell Biol*. (1994), vol. 5, pp. 409-416.
49. K. J. Simpson-Lavy, M. Johnston, in *Proc Natl Acad Sci USA*. (2013).
50. T. Rubio, S. Vernia, P. Sanz, in *Mol Biol Cell*. (2013), vol. 24, pp. 1801-1811.

51. B. Huot, J. Yao, B. L. Montgomery, S. Y. He, in *Mol Plant*. (2014), vol. 7, pp. 1267-1287.
52. J. M. Alonso, A. N. Stepanova, T. J. Leisse, C. J. Kim, H. Chen, P. Shinn, D. K. Stevenson, J. Zimmerman, P. Barajas, R. Cheuk, C. Gadrinab, C. Heller, A. Jeske, E. Koesema, C. C. Meyers, H. Parker, L. Prednis, Y. Ansari, N. Choy, H. Deen, M. Geralt, N. Hazari, E. Hom, M. Karnes, C. Mulholland, R. Ndubaku, I. Schmidt, P. Guzman, L. Aguilar-Henonin, M. Schmid, D. Weigel, D. E. Carter, T. Marchand, E. Risseeuw, D. Brogden, A. Zeko, W. L. Crosby, C. C. Berry, J. R. Ecker, *Science* (2003), vol. 301, pp. 653-657.
53. K. Miura, A. Rus, A. Sharkhuu, S. Yokoi, A. S. Karthikeyan, K. G. Raghothama, D. Baek, Y. D. Koo, J. B. Jin, R. A. Bressan, D. J. Yun, P. M. Hasegawa, *Proc Natl Acad Sci U S A* (2005), vol. 102, pp. 7760-7765.
54. S. D. Yoo, Y. H. Cho, J. Sheen, *Nat Protoc.* (2007), vol. 2, pp. 1565-1572.
55. U. K. Laemmli, *Nature* (1970), vol. 227, pp. 680-685.
56. P. Durek, R. Schmidt, J. L. Heazlewood, A. Jones, D. MacLean, A. Nagel, B. Kersten, W. X. Schulze, in *Nucleic Acids Research*. (2010), vol. 38, pp. D828-834.

CHAPTER 5

Concluding remarks and future perspectives

Plants are subjected to diverse environmental changes throughout their life cycle. Although stress responses are crucial for withstanding these changes, they may also compromise plant growth and influence development. Hence, limited resources should be adequately allocated in accordance with the internal and external demands. This delicate balance relies on accurate sensing of environmental cues and on complex signaling pathways, and is mediated by the crosstalk of several hormones, sugars and other metabolite effectors (*1*).

The plant Snf1-Related protein Kinase 1 (SnRK1) is a central kinase that senses and signals the energy levels of the cell, and is activated in response to starvation and energy depletion conditions (*2, 3*). Furthermore, SnRK1 has a privileged position at the interface of several stresses, hormonal, and metabolic signaling pathways at the whole organism level, and impacts plant growth and developmental decisions (*2-4*). The importance and centrality of SnRK1 is highlighted by its conservation across eukaryotes and by the fact that, in most organisms, the SnRK1 pathway is essential for viability (*2, 5-7*).

Yeast, mammalian and plant SNF1/AMPK/SnRK1 kinases are heterotrimeric complexes composed of an α-catalytic and β- and γ-regulatory subunits. Conservation of these complexes at the structural level overlays with common functionalities, and their regulation occurs through multiple mechanisms that impact kinase activity, stability, and/or subcellular localization. Such broad regulation confers flexibility to the SNF1/AMPK/SnRK1 kinases providing tissue, developmental, metabolic and/or environmental specificities (*8*). However, some of the members of this kinase group display very specific features that probably reflect divergent evolutionary outcomes, such as atypical subunits (*9-11*), allosteric regulation (*12*), or interaction with carbohydrates (*10, 13, 14*), amongst many others. In contrast to its mammalian and yeast orthologs, the plant SnRK1α T-loop phosphorylation/ dephosphorylation seems to be required but insufficient to determine its activation under stress, and subsequent inactivation once homeostasis is restored (*2, 15-17*). Furthermore, intrinsic SnRK1 kinase

activity appears unchanged under conditions that induce SnRK1 signaling as well as in *pp2c* mutants that display deficient repression of the SnRK1 pathway (*2, 15, 17*).

The work described in this thesis aimed at deciphering additional posttranslational regulatory mechanisms of the SnRK1 kinase that could explain its regulation in response to activating conditions. We focused on the modification of SnRK1 by the Small Ubiquitin-like modifier (SUMO), due to the presence of high probability SUMO attachment site (hpSAS) motifs on the SnRK1α1 catalytic subunit, and to the observation of high molecular weight (hMW) SnRK1α1 forms that could correspond to SnRK1α1-SUMO conjugates. Furthermore, SUMO pathway and SnRK1 signaling have important roles in the plant response to various biotic and abiotic stresses (*2, 4, 18-22*). Thus, we hypothesized that SUMO and SnRK1 could be entwined in the plant stress response, through sumoylation of the SnRK1 kinase, and possibly through SnRK1-dependent phosphorylation of SUMO pathway components.

Using several approaches we were able to determine that SnRK1 is sumoylated. SnRK1α1 interacts with the essential E2 SUMO conjugating enzyme (SCE1) in yeast two-hybrid assays (Y2H) and is sumoylated with SUMO1 and SUMO3 in several domains and multiple residues, in a system that reconstitutes the Arabidopsis SUMO pathway in *E. coli*. We also determined that other regulatory subunits of the SnRK1 complex (SnRK1β1 and SnRK1β2, but not SnRK1βγ) are similarly sumoylated in the *E. coli* system, raising the possibility that *in planta* protein group sumoylation targets the entire SnRK1 complex. Sumoylation of the SnRK1 subunits SnRK1α2 and SnRK1β3 remains to be determined, whereas the probably divergent and non-established SnRK1γ subunit was sumoylated in the *E.coli* system.

We were able to show that SnRK1α1 is sumoylated *in planta*. In GFP immunoprecipitates from *SnRK1α1-GFP* plants, SnRK1α1 hMW bands partially matched with SUMO1 bands in the same samples. Importantly, GFP immunoprecipitates from *SnRK1α1-GFP*$_{siz1-2}$ plants, which lack the E3 ligase

SIZ1 determinant for sumoylation specificity *in vivo*, were completely depleted of SUMO1 conjugates. In the same conditions SnRK1α1 hMW bands were strongly diminished, supporting their identity as SnRK1α1-SUMO1 conjugates. Thus, these data strongly suggest a SIZ1-dependent sumoylation of SnRK1α1 by SUMO1 *in planta*. For the *in vivo* detection of sumoylation we ground plant material in a mild denaturing buffer, through the usage of ionic detergents, to enable the subsequent immunoprecipitation (IP) step. The presence of the alkylating agent N-Ethylmaleimide (NEM) and of the proteasome inhibitor MG132 was crucial to enrich for the scarce and labile SnRK1α1-SUMO conjugates. However, such mild conditions allow protein non-covalent interactions and the co-immunoprecipitation of several SnRK1α1 interacting proteins, which may also be sumoylated. Indeed, we could assign a significant contribution to the SUMO1 signal in SnRK1α1-GFP IPs to SnRK1α1 interacting proteins, namely SnRK1β1 and SnRK1β2 regulatory subunits, which similarly to SnRK1α1 exhibit hMW bands and are likely sumoylated *in planta*. In SnRK1α1ΔKA1-GFP immunoprecipitates, SUMO1 signal intensity and SnRK1α1 hMW bands are strongly diminished but still present to some extent, evidencing that sumoylation still occurs in the remaining catalytic subunit. Removal of the KA1 domain of SnRK1α1 abrogates the interaction with regulatory subunits and probably with several other SnRK1α1 interacting proteins, but also one crucial lysine residue (K390) of SUMO attachment on SnRK1α1 is lost. The SUMO1 signal associated with SnRK1α1-GFP IPs can also result from non-covalent interactions between sumoylated proteins and putative SUMO interacting motifs (SUMO-SIM interactions) on SnRK1α1, or conversely by the interaction of SUMO moieties covalently attached to SnRK1α1 with SIMs in other (sumoylated) proteins. We could not detect SIM motifs in the SnRK1α1 subunit using a stringent search for SIMs type SIMa, SIMb or SIMr (*23*) or for the SIM motifs described by Sun and Hunter (*24*). However, additional *bona fide* SIM motif features await characterization and the SIM motifs present in the co-purified SnRK1 regulatory subunits (namely

SnRK1βγ) may be sufficient to convey SUMO-SIM non-covalent interactions, and contribute to the intensity of the SUMO1 signal obtained.

As previously mentioned, to unequivocally demonstrate sumoylation of a particular SnRK1 subunit, future analyses should employ plants expressing His-tagged SUMO1 or SUMO3 (*21, 25*) to perform SUMO pulldowns under denaturing conditions followed by immunoblots for the protein of interest. This would retrieve only components covalently bound to SUMO (as opposed to components interacting through non-covalent protein-protein interactions).

In any case, the extraction buffer used and the presence of both type of covalent and non-covalent protein interactions allowed a global insight into the massive SUMO1 signal associated with SnRK1α1 subunit *in planta.* Our results reinforce the idea that SUMO may act as a "glue", promoting or stabilizing interactions amongst groups of proteins and even establishing functional networks between sumoylated proteins and their noncovalent interactors (*26-30*). It will be extremely interesting to compare the SnRK1α1 interactome in the presence or absence of sumoylation (e.g. from *SnRK1α1-GFP* versus *SnRK1α1-GFP*$_{siz1-2}$ plants). Since SUMO can promote interactions but also act as a "repellent", the amount and identity of SnRK1α1 interacting proteins should vary in both backgrounds. Such knowledge should clarify our understanding of the functional and biological outcomes of SnRK1 sumoylation *in planta*.

Surprisingly, our preliminary results suggest sumoylation influences SnRK1 complex composition and its putative oligomerization. SnRK1 signaling is overactivated in *siz1-2* plants in response to energy stress and it will be interesting to correlate this overactivation with SnRK1 interacting partners, complex composition and oligomerization state in this mutant background.

Here we show a SIZ1-dependent sumoylation of SnRK1 by SUMO1, but we cannot exclude a possible sumoylation of SnRK1 by SUMO3 or SUMO5 *in planta*, due to the lack of good antibody tools, neither a role for the E3 ligase HPY2. Notwithstanding, the SUMO1 signal associated with SnRK1α1 can be fully attributed to the SIZ1 ligase activity in the conditions tested, as suggested

by its disappearance in immunoprecipitates from *SnRK1α1-GFP*$_{siz1-2}$ plants. As previously reported, the increase in SUMO1/SUMO2 conjugates associated with stress responses is mainly conveyed through the E3 SUMO ligase SIZ1 in plants (*18, 31*).

Similarly to the recently described sumoylation of yeast SNF1 and mammalian AMPK, our data suggest a possible sumoylation of the SNF1A Drosophila counterpart, and SnRK1 complex sumoylation *in planta*. Thus, the Small Ubiquitin-like modifier (SUMO) seems to have an expanding role in the regulation of the SNF1/AMPK1/SnRK1 family of protein kinases, conserved amongst eukaryotes.

Importantly, we determined that SIZ1-dependent sumoylation of SnRK1 by SUMO1 has a negative impact on SnRK1 pathway activation. Co-expression of SnRK1α1, SUMO1 and SIZ1 diminished the ability of SnRK1α1 to induce SnRK1 signaling. SnRK1 pathway was overactivated in *siz1-2* plants, as determined by qRT-PCR analysis of SnRK1 marker genes in response to dark treatment, as well as in the protoplast assay using *siz1-2* cells. We could observe that the negative impact of sumoylation occurred at the kinase level, since SnRK1 pathway activation induced by the downstream transcription factor GBF5 was not affected by SIZ1-dependent sumoylation. Furthermore, we show that the E3 SUMO ligase activity of SIZ1 is required to rescue the overactivation of SnRK1 signaling in *siz1-2*, which seems to be independent of the salicylic acid (SA) accumulation observed in this mutant.

We determined that SnRK1α1 intrinsic kinase activity was unchanged between WT and *siz1-2* plants, and that SnRK1 signaling overactivation in *siz1-2* could be attributed to the accumulation of SnRK1α1 protein in this background. Importantly, T-loop phosphorylation was increased proportionally to SnRK1α1 protein accumulation. Whereas SnRK1 subunits SnRK1α2 and SnRK1β1 also accumulated in *siz1-2*, the SnRK1β2 subunit did not, despite all of these being likely sumoylated *in planta*. Future studies should address the sumoylation of each SnRK1 complex subunit and its specific biochemical and

functional outcome *in planta*. This knowledge will contribute to integrate individual subunit regulation with regulation of the whole SnRK1 complex. Furthermore, specific features associated with the modulation of specific SnRK1 complexes may be clarified with such studies.

We observed that SnRK1α1 protein turnover was impaired in *siz1-2*, explaining protein kinase accumulation and signaling pathway overactivation in this mutant background. Importantly, a SUMO mimetic of SnRK1α1 restored a WT degradation profile to SnRK1α1 in *siz1-2*, supporting a connection between SnRK1α1 sumoylation and its degradation.

An increasing number of reports highlight the interplay between sumoylation and ubiquitylation (*32*-*36*), and we next assessed if SnRK1 sumoylation could be promoting its ubiquitylation and subsequent proteasomal degradation. Interestingly, ubiquitin conjugates co-purified with SUMO1 conjugates in immunoprecipitates from *SnRK1α1*-GFP plants, but were strongly diminished in *SnRK1α1-GFP*$_{siz1-2}$ IPs. This result suggests that SIZ1 sets a sumoylation-dependent ubiquitylation of SnRK1, possible through the action of SUMO-targeted ubiquitin ligases (STUbLs). Furthermore, as previously reported, we could also show that SnRK1α1 degradation occurs via the proteasome. One of the reasons why detection of SnRK1 sumoylation *in planta* was so challenging is probably due to the functional outcome of this modification in targeting SnRK1α1 to degradation. Besides the strategies employed to block SUMO proteases and enrich for the scarce SUMO conjugates, the utilization of MG132 revealed to be crucial to counteract proteasomal degradation of sumoylated and ubiquitylated SnRK1α1.

STUbLs bind sumoylated proteins via SUMO-SIM non-covalent interactions and further conjugate the sumoylated substrate with ubiquitin modifiers. In large-scale Y2H screens of Arabidopsis SUMO interacting proteins, six proteins were identified as the evolutionary and functional homologs of yeast STUbLs (*37*). Arabidopsis STUbLs (1-6) complemented to various degrees the *Schizosaccharomyces pombe* STUbL mutant *rfp1/rfp2*, evidencing partially non-

redundant functions that should be further dissected. Besides, plant-specific features were reported for STUbL4 (*37*). It will be interesting to address the role of STUbLs in SnRK1 sumoylation-mediated ubiquitylation. Mutant *stubl* plants should be analyzed regarding SnRK1 pathway activation and SnRK1 protein stability. These readouts should be correlated with the ubiquitylation and sumoylation profiles of SnRK1 in the respective mutants.

However, the role of other players in SnRK1 sumoylation should also be considered. The interaction between SnRK1α1 and the SUMO protease Early in short days 4 (ESD4) (*38, 39*) was reported in a Y2H screen (*40*). Future studies on SnRK1 sumoylation should also take into account such SUMO machinery component and explore, for instance, a possible accumulation of SnRK1-SUMO conjugates in *esd4* mutants and address its molecular and functional consequences. A delicate balance between the activity of SUMO proteases and STUbLs may exist at the level of SnRK1 sumoylation, since both molecular players may counteract the accumulation of sumoylated SnRK1. However, a putative SUMO protease and STUbL acting on SnRK1 may have antagonistic outcomes, since SnRK1 may be degraded through the action of a putative STUbL, and a SUMO protease may stabilize SnRK1 by antagonizing STUbLs action.

Furthermore, the E4 SUMO ligases PIAL1 and PIAL2, recently characterized to promote SUMO-chain formation in Arabidopsis (*28, 41*), may have a role in SUMO chain assembly on sumoylated SnRK1α1. Using the E4 SUMO ligase double mutant *pial1pial2* (*41*) may allow us to distinguish between multi- and polysumoylation as a requirement to putatively recruit STUbLs and subsequently ubiquitylate sumoylated SnRK1 *in planta*.

Whether SUMO conjugated to SnRK1 could fulfill other biological functions prior to SUMO targeted ubiquitylation and signal termination, remains an open question. If affirmative, the discrimination between both outcomes could be based on the (putative) length and/or topology of the attached SUMO chains (*42*). We could use the protoplast cell assay to block specific SUMO proteases

and STUbLs, and manipulate the E3 SIZ1 ligase and possibly E4 PIAL ligases, promoting SnRK1α1 sumoylation but preventing its proteolytic outcome. SnRK1 molecular and functional features should be addressed in such scenario.

A SUMO variant with mutated lysines could be a helpful tool to prevent SUMO chain extension or to modulate SUMO chain topology. Either alone or in fusion with SnRK1α1 (SUMO mimetic), this SUMO variant could be used to better dissect and characterize functional outcomes of SnRK1 sumoylation.

Our approach to block SnRK1α1 sumoylation through mutation of several lysine residues at the target level produced no effect regarding SnRK1 signaling activation and SnRK1 protein stability *in planta*. Probably, sumoylation at the whole SnRK1 complex level impairs such an approach, as similarly reported for other cases, and seemingly a characteristic feature of the SUMO pathway (*30, 43, 44*). Still, other readouts of SnRK1 activity beyond reporter gene activation remain to be assessed using the mutated lysine variants, for instance the phosphorylation level of direct targets of SnRK1 *in planta* (*45*).

We analyzed the loss of SnRK1 (SIZ1-dependent) sumoylation and its functional consequences using the *siz1-2* mutant. In another attempt to assess the functional relevance of this molecular mechanism *in planta,* we will analyze *SnRK1α1-OE* plant lines in the *siz1-2* background (*SnRK1*α1-OE_{siz1-2}). Since one of the endogenous mechanisms to repress SnRK1 signaling is lost in the *siz1-2* mutant, we expect SnRK1α1 overexpression in *SnRK1α1-*OE_{siz1-2} to be further enhanced in comparison to *SnRK1α1-OE*, in the Col-0 background. Accordingly, a true SnRK1α1 overexpressor in *SnRK1α1-*OE_{siz1-2} should exhibit higher severity of SnRK1-OE related phenotypes than the *SnRK1α1-OE* plants.

Conversely, in order to mimic SnRK1α1 sumoylation *in planta* we generated *SnRK1α1-SUMO-OE* plants. SnRK1α1 protein turnover and accumulation, SnRK1 pathway activation, and SnRK1α1-OE associated phenotypes will be compared in *SnRK1α1-OE* and *SnRK1α1-SUMO-OE* plants, with the expectation that *SnRK1α1-SUMO-OE* will behave as a weak overexpressor of SnRK1α1 due to the repressive effect associated with SnRK1α1 sumoylation.

Still, additional studies may be required to decipher the functional and biological implications of SIZ1-dependent sumoylation of SnRK1 *in planta*.

The fact that ubiquitylation is diminished but still present in the absence of SnRK1 sumoylation evidences that multiple E3 ubiquitin ligases may cooperatively regulate SnRK1 protein turnover and terminate kinase action, probably acting in accordance with distinct stimuli or other specificities (*46*).

Sumoylation also negatively regulates the stability of yeast Snf1 (*47*) and mammalian AMPKα (*48*), pointing to a conserved outcome of this posttranslational modification in the regulation of SNF1/AMPK/SnRK1 catalytic subunits.

Besides SnRK1 kinase stability, and consequent impact on SnRK1 signaling activation, it is also possible that sumoylation affects or is affected (see below) by kinase subcellular localization. Our preliminary studies suggest an enrichment of SnRK1α1 hMW forms in nuclear fractions, and further attempts should clarify if they correspond indeed to SnRK1α1-SUMO conjugates. Making use of *SnRK1α1-GFP* and *SnRK1α1-GFP*$_{siz1-2}$ plants, we can assess the impact of sumoylation on SnRK1α1 localization through microscopy techniques. Furthermore, the distribution of SnRK1α1 protein in *siz1-2* and WT backgrounds can be compared using subcellular fractionation protocols.

Importantly, we were able to show that SnRK1 kinase activity is intimately connected to its sumoylation, and subsequent ubiquitylation and protein turnover. Inactive SnRK1α1 mutants accumulate to a higher extent than the active form due to impaired turnover. However, their degradation rate can be restored to WT levels when co-expressed with active SnRK1α1, either due to a direct regulation in *trans* by the active kinase, or through an indirect effect derived from SnRK1 signaling activation. To be able to distinguish between these two scenarios we could test, for instance, the degradation rate of the inactive SnRK1α1 variants when the pathway is activated downstream of the SnRK1 kinase, through overexpression of the GBF5 transcription factor. Furthermore, fusion of SUMO1 to inactive SnRK1α1 mutants (SUMO mimetic)

restores a WT degradation profile, suggesting the impaired turnover is due to absence of sumoylation in inactive SnRK1α1 variants.

Endogenous SnRK1α1 protein degradation seems to be increased in response to dark-stress conditions, but further experiments are required to support this observation. Sumoylation could be one intermediary step in this process, since SnRK1α1 dark-induced turnover seems to be impaired in *siz1-2* cells. Future work should dissect the impact of different types of stress that converge as energy deprivation conditions, in active SnRK1 kinase turnover.

In protoplasts, the high induction of SnRK1 signaling upon SnRK1α1 transfection, in which sumoylated SnRK1 should get rapidly degraded, probably explains why we could not detect SnRK1α1-SUMO conjugates in this system. Maybe, when expressing SnRK1α1 in protoplasts of a yet to be determined STUbL mutant background, in the presence of the proteasome inhibitor MG132, and of a SUMO protease dominant negative version to block reversion of sumoylation, we could clearly see SnRK1α1 hMW bands in this system.

Moreover, further attempts should be made to analyze the differential accumulation of SnRK1α1-SUMO conjugates and SnRK1α1-ubiquitin conjugates upon SnRK1 signaling activation. We could not detect a clear difference in the accumulation of SUMO conjugates in GFP immunoprecipitates of *SnRK1α1-GFP* plants from light and sudden dark conditions. However, the detection of SnRK1α1 hMW bands after nuclear enrichment revealed an accumulation of these forms in SnRK1 activating conditions (extended dark) and their absence in SnRK1 repressing conditions (light). Combined strategies of enrichment and purification steps (e.g. nuclear fractionation followed by SnRK1α1 immunoprecipitation) might improve the detection of variable amounts of SnRK1α1-SUMO conjugates in response to different stimuli. Ideally, a quantitative approach could provide information on the stoichiometry and kinetics of SnRK1 sumoylation in different conditions, for instance through the combination of labeling methods, enrichment strategies and mass spectrometry analyses (*49*). As an example, Miller et al. recently used a quantitative

methodology with isobaric tag for relative and absolute quantification (iTRAQ) mass spectrometry, in conjunction with SUMO enrichment strategies, to quantify sumoylated proteins after heat stress in plants (*50*).

Interestingly, we could observe that active SnRK1α1 phosphorylates the E3 SUMO ligase SIZ1 *in vitro* and hypothesize this could be a way to signal SnRK1 pathway activation towards the SUMO machinery, promoting its sumoylation and subsequent turnover. How this modification affects SIZ1 ligase activity, and if it impacts SnRK1 or global sumoylation, remains to be determined. Additional studies are required to decipher the functional and biological implications of SnRK1-dependent phosphorylation of SIZ1 *in planta*. For instance, a thorough analysis of SIZ1 phosphomutants and phosphomimetics should give insights regarding the role of SIZ1 phosphorylation, and downstream consequences *in planta*. On the other hand, whether sumoylation depends or not on SnRK1 subcellular localization, could be assessed by monitoring SnRK1 sumoylation and/or stability in SnRK1 variants with distinct subcellular localization (e.g. plasma membrane, cytosol, nuclear). Such studies are already being launched.

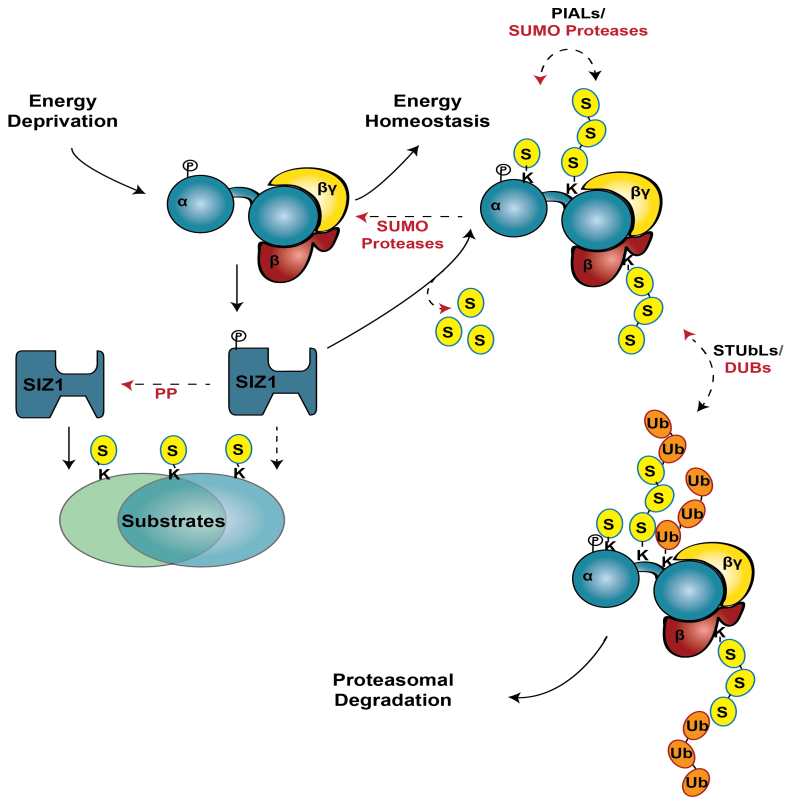

Figure 5.1 | Model of SnRK1 turnover mediated by sumoylation.

Upon energy stress, active SnRK1 regulates processes that promote energy homeostasis. As a consequence of its activity, possibly due to a SnRK1-mediated phosphorylation of SIZ1 and/or of other SUMO machinery components, SnRK1 is sumoylated on several subunits in a SIZ1-dependent manner. SIZ1 phosphorylation by SnRK1 may affect global sumoylation and substrate specificity. SnRK1 sumoylation can occur on multiple residues (multisumoylation) and possibly with the formation of SUMO chains (polysumoylation) mediated by the Arabidopsis E4 SUMO ligases PIALs. Sumoylated SnRK1 becomes ubiquitylated, possibly through the recruitment and activity of SUMO-Targeted Ubiquitin Ligases (STUbLs), and is degraded by the 26S proteasome. Sumoylation and ubiquitylation are reversible processes and thus specific SUMO proteases and deubiquitylases (DUBs) may counteract the attachment of the respective modifiers to SnRK1. Similarly, SnRK1-dependent phosphorylation of SIZ1 may be reverted by specific Protein Phosphatases (PP). The tight coupling between SnRK1 activity and its turnover may contribute to optimize the balance between stress/defense responses and biosynthetic growth-related processes in plants. Continuous or dashed lines represent molecular mechanisms and/or components identified or to be determined, respectively. In red, reversal of sumoylation (by SUMO Proteases), ubiquitylation (by deubiquitylases), or of phosphorylation (by protein phosphatases).

Overall, our aim to dissect a possible regulation of SnRK1 by sumoylation was based on the hypothesis that SnRK1 and SUMO could be entwined in the plant stress response, with the underlying idea that sumoylation could be a switch towards SnRK1 activation in energy-deprivation conditions. Surprisingly, we have unraveled an endogenous mechanism by which sumoylation represses SnRK1 signaling in the plant stress response. In many systems, protein kinase activity initiates signal termination through negative feedback loops and other mechanisms, in order to prevent deleterious effects derived from pathway overactivation. Likewise, sustained SnRK1 pathway activation may compromise growth and developmental transitions due to a metabolic switch towards catabolism and energy saving processes, with a deleterious impact on plant fitness and productivity. The work described in this thesis reveals SnRK1 activity

initiates its proteasomal-mediated degradation and adds yet another layer to the complex regulation of SnRK1 in the plant stress response.

Such molecular mechanism of signal termination, triggered by kinase activation-dependent sumoylation, may be conserved in yeast SNF1 and mammalian AMPK systems. The activation of AMPK pathway by heat stress correlates with an increment of AMPKα1-SUMO conjugates, which are mostly increased upon proteasome inhibition, suggesting their proteolytic fate (*48*). Furthermore, proteasome inhibition was recently shown to trigger AMPK activation (*51, 52*). In the yeast system, Snf1 sumoylation increases when cells are shifted from energy-deprivation (2% galactose, Snf1 activation) to energy replenishing (2% glucose, Snf1 inactivation) conditions. However, sumoylation-mediated turnover of Snf1 is also clearly important in Snf1 activating conditions, since yeast cells deficient on the SUMO ligase MMS21 accumulate more Snf1 when grown on 2% galactose (*47*). Collectively, sumoylation seems to terminate SNF1/AMPK/SnRK1-dependent energy signaling.

Whereas deleterious overactivation of the SnRK1 pathway seems to be counteracted by its sumoylation-mediated turnover in energy deficiency conditions, it will be important to clarify a possible role of sumoylation for the full clearance of SnRK1 signaling once homeostasis is restored. The dynamics of SnRK1 sumoylation upon reversal of the energy deficit should be analyzed, for instance, in plants switched from dark to light conditions, or after supplementation with sugars (energy) while still in the presence of the original stress (e.g. dark). As previously mentioned, a quantitative approach would be ideal to address the role of SnRK1 sumoylation in response to environmental and endogenous energy transitions.

References

1. B. Huot, J. Yao, B. L. Montgomery, S. Y. He, in *Mol Plant*. (2014), vol. 7, pp. 1267-1287.
2. E. Baena-González, F. Rolland, J. M. Thevelein, J. Sheen, in *Nature*. (2007), vol. 448, pp. 938-942.
3. E. Baena-González, J. Sheen, in *Trends in Plant Science*. (2008), vol. 13, pp. 474-482.
4. N. G. Halford, S. J. Hey, in *Biochem J*. (2009), vol. 419, pp. 247-259.
5. Y. Zhang, P. R. Shewry, H. Jones, P. Barcelo, P. A. Lazzeri, N. G. Halford, in *Plant J*. (2001), vol. 28, pp. 431-441.
6. N. G. Halford, S. Hey, D. Jhurreea, S. Laurie, R. S. McKibbin, M. Paul, Y. Zhang, in *Journal of experimental botany*. (2003), vol. 54, pp. 467-475.
7. R. Radchuk, V. Radchuk, W. Weschke, L. Borisjuk, H. Weber, in *Plant Physiol*. (2006), vol. 140, pp. 263-278.
8. M. Nietzsche, I. Schießl, F. Börnke, in *Front Plant Sci*. (2014), vol. 5, pp. 54.
9. M. Ramon, P. Ruelens, Y. Li, J. Sheen, K. Geuten, F. Rolland, in *Plant J*. (2013).
10. S. Emanuelle, M. I. Hossain, I. E. Moller, H. L. Pedersen, A. M. L. van de Meene, M. S. Doblin, A. Koay, J. S. Oakhill, J. W. Scott, W. G. T. Willats, B. E. Kemp, A. Bacic, P. R. Gooley, D. I. Stapleton, in *Plant J*. (2015), vol. 82, pp. 183-192.
11. C. Polge, M. Thomas, in *Trends Plant Sci*. (2007), vol. 12, pp. 20-28.
12. D. G. Hardie, in *Annu. Rev. Nutr.* (2014), vol. 34, pp. 31-55.
13. G. Polekhina, A. Gupta, B. J. W. Van Denderen, S. C. Feil, B. E. Kemp, D. Stapleton, M. W. Parker, in *Structure*. (2005), vol. 13, pp. 1453-1462.
14. A. Koay, B. Woodcroft, E. J. Petrie, H. Yue, S. Emanuelle, M. Bieri, M. F. Bailey, M. Hargreaves, J.-T. Park, K.-H. Park, S. Ralph, D. Neumann, D. Stapleton, P. R. Gooley, in *FEBS Letters*. (2010), vol. 584, pp. 3499-3503.
15. P. Coello, E. Hirano, S. J. Hey, N. Muttucumaru, E. Martinez-Barajas, M. A. J. Parry, N. G. Halford, in *Journal of experimental botany*. (2012), vol. 63, pp. 913-924.
16. S. Fragoso, L. Espíndola, J. Páez-Valencia, A. Gamboa, Y. Camacho, E. Martínez-Barajas, P. Coello, in *Plant Physiol*. (2009), vol. 149, pp. 1906-1916.
17. A. Rodrigues, M. Adamo, P. Crozet, L. Margalha, A. Confraria, C. Martinho, A. Elias, A. Rabissi, V. Lumbreras, M. González-Guzmán, R. Antoni, P. L. Rodriguez, E. Baena-González, in *The Plant Cell*. (2013), vol. 25, pp. 3871-3884.
18. P. H. Castro, R. M. Tavares, E. R. Bejarano, H. Azevedo, in *Cell Mol Life Sci*. (2012), vol. 69, pp. 3269-3283.
19. M. J. Mazur, H. A. Van Den Burg, in *Front. Plant Sci.* (2012), vol. 3, pp. 215.
20. J. Kurepa, J. M. Walker, J. Smalle, M. M. Gosink, S. J. Davis, T. L. Durham, D.-Y. Sung, R. D. Vierstra, in *J Biol Chem*. (2003), vol. 278, pp. 6862-6872.
21. M. J. Miller, G. A. Barrett-Wilt, Z. Hua, R. D. Vierstra, in *Proc Natl Acad Sci USA*. (2010), vol. 107, pp. 16512-16517.
22. R. Catala, J. Ouyang, I. A. Abreu, Y. Hu, H. Seo, X. Zhang, N.-H. Chua, in *Plant Cell*. (2007), vol. 19, pp. 2952-2966.
23. B. Vogt, K. Hofmann, in *Methods Mol Biol*. (2012), vol. 832, pp. 249-261.

24. H. Sun, T. Hunter, in *J Biol Chem*. (2012), vol. 287, pp. 42071-42083.
25. R. Budhiraja, R. Hermkes, S. Müller, J. Schmidt, T. Colby, K. Panigrahi, G. Coupland, A. Bachmair, in *PLANT PHYSIOLOGY*. (2009), vol. 149, pp. 1529-1540.
26. C.-M. Hecker, M. Rabiller, K. Haglund, P. Bayer, I. Dikic, in *J Biol Chem*. (2006), vol. 281, pp. 16117-16127.
27. O. Kerscher, in *EMBO reports*. (2007), vol. 8, pp. 550-555.
28. M. Novatchkova, K. Tomanov, K. Hofmann, H.-P. Stuible, A. Bachmair, in *New Phytol*. (2012), vol. 195, pp. 23-31.
29. S. Jentsch, I. Psakhye, in *Annu. Rev. Genet.* (2013).
30. I. Psakhye, S. Jentsch, in *CELL*. (2012), vol. 151, pp. 807-820.
31. S. A. Saracco, M. J. Miller, J. Kurepa, R. D. Vierstra, in *PLANT PHYSIOLOGY*. (2007), vol. 145, pp. 119-134.
32. M. Miteva, K. Keusekotten, K. Hofmann, G. J. K. Praefcke, R. J. Dohmen, in *Subcell Biochem*. (2010), vol. 54, pp. 195-214.
33. K. Uzunova, K. Göttsche, M. Miteva, S. R. Weisshaar, C. Glanemann, M. Schnellhardt, M. Niessen, H. Scheel, K. Hofmann, E. S. Johnson, G. J. K. Praefcke, R. J. Dohmen, in *J Biol Chem*. (2007), vol. 282, pp. 34167-34175.
34. M. Schnellhardt, K. Uzunova, V. N. Bade, A. Krause, S. R. Weisshaar, G. J. K. Praefcke, R. J. Dohmen, in *Methods Mol Biol*. (2012), vol. 832, pp. 81-92.
35. G. J. K. Praefcke, K. Hofmann, R. J. Dohmen, in *Trends in Biochemical Sciences*. (2012), vol. 37, pp. 23-31.
36. A. M. Sriramachandran, R. J. Dohmen, in *Biochim Biophys Acta*. (2013).
37. N. Elrouby, M. V. Bonequi, A. Porri, G. Coupland, in *Proc Natl Acad Sci USA*. (2013).
38. P. H. Reeves, G. Murtas, S. Dash, G. Coupland, in *Development*. (2002), vol. 129, pp. 5349-5361.
39. G. Murtas, P. H. Reeves, Y.-F. Fu, I. Bancroft, C. Dean, G. Coupland, in *Plant Cell*. (2003), vol. 15, pp. 2308-2319.
40. N. Elrouby, G. Coupland, in *Proc Natl Acad Sci USA*. (2010), vol. 107, pp. 17415-17420.
41. K. Tomanov, A. Zeschmann, R. Hermkes, K. Eifler, I. Ziba, M. Grieco, M. Novatchkova, K. Hofmann, H. Hesse, A. Bachmair, in *Plant Cell*. (2014), vol. 26, pp. 4547-4560.
42. C. M. Hickey, N. R. Wilson, M. Hochstrasser, in *Nat Rev Mol Cell Biol*. (2012), vol. 13, pp. 755-766.
43. H. R. Silver, J. A. Nissley, S. H. Reed, Y.-M. Hou, E. S. Johnson, in *DNA Repair*. (2011), vol. 10, pp. 1243-1251.
44. M. Sacher, B. Pfander, C. Hoege, S. Jentsch, in *Nature cell biology*. (2006), vol. 8, pp. 1284-1290.
45. C. Sugden, P. G. Donaghy, N. G. Halford, D. G. Hardie, in *Plant Physiol*. (1999), vol. 120, pp. 257-274.
46. Z. Lu, T. Hunter, in *Annu Rev Biochem*. (2009), vol. 78, pp. 435-475.
47. K. J. Simpson-Lavy, M. Johnston, in *Proc Natl Acad Sci USA*. (2013).
48. I. A. Hendriks, R. C. J. D'souza, B. Yang, M. Verlaan-de Vries, M. Mann, A. C. O. Vertegaal, in *Nat Struct Mol Biol*. (2014).
49. A. Ordureau, C. Münch, J. W. Harper, in *Mol Cell*. (2015), vol. 58, pp. 660-676.
50. M. J. Miller, M. Scalf, T. C. Rytz, S. L. Hubler, L. M. Smith, R. D. Vierstra, in *Mol Cell Proteomics*. (2012).

51. S. Jiang, D. W. Park, Y. Gao, S. Ravi, V. Darley-Usmar, E. Abraham, J. W. Zmijewski, in *Cellular Signalling*. (2015).
52. C.-S. Zhang, B. Jiang, M. Li, M. Zhu, Y. Peng, Y.-L. Zhang, Y.-Q. Wu, T. Y. Li, Y. Liang, Z. Lu, G. Lian, Q. Liu, H. Guo, Z. Yin, Z. Ye, J. Han, J.-W. Wu, H. Yin, S.-Y. Lin, S.-C. Lin, in *Cell Metabolism*. (2014), vol. 20, pp. 526-540.

Appendix

Appendix- Figure 1

```
CLUSTAL 2.1 multiple sequence alignment

K- hpSAS>91%
K- hpSAS<91%
K- sumoylated residues
K- sumoylated residues crucial for SnRK1α1 sumoylation in E. coli


Arabidopsis      Moss     Human    Drosophila       Yeast

SnRK1α1          Snf1a    AMPKα1   SNF1A            Snf1
SnRK1α2          Snf1b    AMPKα2


SnRK1α2          ------------------------------------MDHSSNRFGNNGVESILPNYKLGKT 25
SnRK1α1          ------------------------------------MDGSGTGS-RSGVESILPNYKLGRT 24
Snf1a            ------------------------------------MEAGGRPMGPATAEYYLPNYKLGKT 25
Snf1b            ------------------------------------MDSGGRPVAPVAVEYYLPNYKMGKT 25
AMPKα1           ---------------------------MRRLSSWRKMATAEKQKHDG-RVKIGHYILGDT 32
AMPKα2           ---------------------------------------MAEKQKHDG-RVKIGHYVLGDT 21
DmSNF1A          ---------------------------MPQMRAAAAAEAVAAGSANGQPLVKIGHYLLGAT 33
ScSnf1           MSSNNNTNTAPANANSSHHHHHHHHHHHHHHGHGGSNSTLNNPKSSLADGAHIGNYQIVKT 60
                                                                  : :* :  *

SnRK1α2.1        LGIGSFGKVKIAEHVVTGHKVAIKILNRRKIKNMEMEEKVRREIKILRLFMHPHIIRQYE 85
SnRK1α1.1        LGIGSFGRVKIAEHALTGHKVAIKILNRRKIKNMEMEEKVRREIKILRLFMHPHIIRLYE 84
Snf1a            LGIGSFGKVKVAEHSPTGHKVAIKILNRRKVKMMDMEEKVRREIKILRLFMHPHIIRLYE 85
Snf1b            LGIGSFGKVKVAEHTPTGHKVAIKILNRRKVKSMDMEEKVRREIKILRLFMHPHIIRLYE 85
AMPKα1           LGVGTFGKVKVGKHELTGHKVAVKILNRQKIRSLDVVGKIRREIQNLKLFRHPHIIKLYQ 92
AMPKα2           LGVGTFGKVKIGEHQLTGHKVAVKILNRQKIRSLDVVGKIKREIQNLKLFRHPHIIKLYQ 81
Dm               LGTGTFGKVKIGEHQITRVKVAVKILNRQKIKSLDVVGKIRREIQNLKLFRHPHIIKLYQ 93
Sc               LGEGSFGKVKLAYHTTTGQKVALKIINKKVLAKSDMQGRIEREISYLRLLRHPHIIKLYD 120
                 ** *:**:**:. *  *  ***:**:*:: :   ::  ::.***. *:*: *****: *:

SnRK1α2.1        VIETTSDIYVVMEYVKSGELFDYIVEKGRLQEDEARNFFQQIISGVEYCHRNMVVHRDLK 145
SnRK1α1.1        VIETPTDIYLVMEYVNSGELFDYIVEKGRLQEDEARNFFQQIISGVEYCHRNMVVHRDLK 144
Snf1a            VIETPADIFVVMEYVKSGELFDYIVEKGRLGEHEARRFFQQIVSGVEYCHRNMVVHRDLK 145
Snf1b            VIETPTDIFVVMEYVKSGELFDYIVEKQRLGEDEARRFFQQIVSGVEYCHRNMVVHRDLK 145
AMPKα1           VISTPSDIFMVMEYVSGGELFDYICKNGRLDEKESRRLFQQILSGVDYCHRHMVVHRDLK 152
AMPKα2           VISTPTDFFMVMEYVSGGELFDYICKHGRVEEMEARRLFQQILSAVDYCHRHMVVHRDLK 141
Dm               VISTPSDIFMIMEYVSGGELFDYIVKHGKLQEHQARRFFQQIISGVDYCHRHMIVHRDLK 153
Sc               VIKSKDEIIMVIEYAGN-ELFDYIVQRDKMSEQEARRFFQQIISAVEYCHRHKIVHRDLK 179
                 **.:  :: :::**. . ****** :. :: * ::*.:****:*.*:****: :******

SnRK1α2.1        PENLLLDSRCNIKIADFGLSNVMRDGHFLKTSCGSPNYAAPEVISGKLYAGPEVDVWSCG 205
SnRK1α1.1        PENLLLDSKCNVKIADFGLSNIMRDGHFLKTSCGSPNYAAPEVISGKLYAGPEVDVWSCG 204
Snf1a            PENLLLDSKSNVKIADFGLSNVMRDGHFLKTSCGSPNYAAPEVISGKLYAGPEVDVWSCG 205
Snf1b            PENLLLDSKWNVKIADFGLSNIMRDGHFLKTSCGSPNYAAPEVISGKLYAGPEVDVWSCG 205
AMPKα1           PENVLLDAHMNAKIADFGLSNMMSDGEFLRTSCGSPNYAAPEVISGRLYAGPEVDIWSSG 212
AMPKα2           PENVLLDAHMNAKIADFGLSNMMSDGEFLRTSCGSPNYAAPEVISGRLYAGPEVDIWSCG 201
Dm               PENLLLDHNMHVKIADFGLSNMMLDGEFLRTSCGSPNYAAPEVISGKLYAGPEVDIWSCG 213
Sc               PENLLLDEHLNVKIADFGLSNIMTDGNFLKTSCGSPNYAAPEVISGKLYAGPEVDVWSCG 239
                 ***:*** . : *********:* **.**:*****************:********:**.*

SnRK1α2.1        VILYALLCGTLPFDDENIPNLFKKIKGGIYTLPSHLSSEARDLIPRMLIVDPVKRITIPE 265
SnRK1α1.1        VILYALLCGTLPFDDENIPNLFKKIKGGIYTLPSHLSPGARDLIPRMLVVDPMKRVTIPE 264
Snf1a            VILYALLCGSLPFDDENIPNLFKKIKGGIYTLPSHLSPGARDLIPRMLLVDPMKRVTIPE 265
Snf1b            VILYALLCGSLPFDDENIPNLFRKIKGGIYTLPSHLSPGARDLIPRMLLVDPMKRVTIPE 265
AMPKα1           VILYALLCGTLPFDDDHVPTLFKKICDGIFYTPQYLNPSVISLLKHMLQVDPMKRATIKD 272
AMPKα2           VILYALLCGTLPFDDEHVPTLFKKIRGGVFYIPEYLNRSVATLLMHMLQVDPLKRATIKD 261
Dm               VILYALLCGTLPFDDEHVPTLFRKIKSGIFPIPEYLNKQVVNLVCQMLQVDPLKRANIEE 273
Sc               VILYVMLCRRLPFDDESIPVLFKNISNGVYTLPKFLSPGAAGLIKRMLIVNPLNRISIHE 299
                 ****.:**  *****: :* **::* .*::  *..*.  .  *: :** *:*::* .* :

SnRK1α2.1        IRQHRWFQTHLPRYLAVSPPDTVEQAK----------------KINEEIVQEVVN-MGFD 308
SnRK1α1.1        IRQHPWFQAHLPRYLAVPPPDTVQQAK----------------KIDEEILQEVIN-MGFD 307
```

b

```
Snf1a           IRQHPWFLNHLPRYLAVPPPDTTQQAK----------------RIDEEILERVVA-LNFD 308
Snf1b           IRQHPWFLNHLPRYLAVPPPDTLQQAK----------------RIDEEILERVVA-LNFD 308
AMPKα1          IREHEWFKQDLPKYLFPE--DPSYSST----------------MIDDEALKEVCEKFECS 314
AMPKα2          IREHEWFKQDLPSYLFPE--DPSYDAN----------------VIDDEAVKEVCEKFECT 303
Dm              IKKHEWFQKDLPAYLFPS--SIEQDSN----------------VIDTYAVAEVCTKFGVK 315
Sc              IMQDDWFKVDLPEYLLPPDLKPHPEEENENNDSKKDGSSPDNDEIDDNLVNILSSTMGYE 359
                * :. **  .** **     .   .                    *:   :  :   :

SnRK1α2.1       RNQVLESLRNR----TQNDATVTYYLLLDNRFRVPSGY------------LESEFQE--- 349
SnRK1α1.1       RNHLIESLRNR----TQNDGTVTYYLILDNRFRASSGY------------LGAEFQE--- 348
Snf1a           RDLLIDSLLNR----VQNKATVAYYLMLDNRRRLSNGY------------LCSEFNE--- 349
Snf1b           RVHLIESLLNR----VQNKATVAYYLMLDNRRRLSNGY------------LGSEFDE--- 349
AMPKα1          EEEVLSCLYNRN---HQDPLAVAYHLIIDNRRIMNEAK----------DFYLATSPPD--- 359
AMPKα2          ESEVMNSLYSGD---PQDQLAVAYHLIIDNRRIMNQAS----------EFYLASSPPSG-- 349
Dm              ETEVHNSLLSGD---PHDQLAIAYHLIIDNKRFADDAAN--QINEINNFFVAGSPPPPPP 370
Sc              KDEIYESLESSEDTPAFNEIRDAYMLIKENKSLIKDMKANKSVSDELDTFLSQSPPTFQQ 419
                .  : ..* .       :    :* *: :*:    .              :  .

SnRK1α2.1       -----TTDSGSNPMRT-----------------------------------PEAGASPVGHW 371
SnRK1α1.1       -----TMEG-TPRMHP-----------------------------------AESVASPVSHR 369
Snf1a           -----GKEHLMSPMD------------------------------------AFNGTPRSGY 369
Snf1b           -----GKEQSLSPMSPY----------------------------------GAHGGTPRSTY 372
AMPKα1          -----SFLDDHHLTR------------------------------------PHPERVPFLVAE 381
AMPKα2          -----SFMDDSAMHIPPGL--------------------------KPHPERMPPLIAD 376
Dm              PPVPQSSMDHQAPLATVTVGGGTSASSGTATPVPPVAGGTPSSTIPIRPHPERIAPMRDR 430
Sc              ----QSKSHQKSQVDHETAKQHARRMASAITQQRTYHQSPFMDQYKEEDSTVSILPTSLP 475


SnRK1α2.1       IPAHVDHYGLGARSQVP--------VDRKWALGLQSHAHPREIMNEVLKALQELNVCWKK 423
SnRK1α1.1       LPGLMEYQGVGLRSQYP--------VERKWALGLQSRAHPREIMTEVLKALQDLNVCWKK 421
Snf1a           PRTLTHMSSMDRRSASPSGLQHRVVAERKWVLGLQLRSHPKEIMNDVLKTLRDLGINWKK 429
Snf1b           PRSLIRTPSMDRRGSSSSVLQHRVVAERKWALGVQLRSHPKEIMSDVLDTLRKCDINWKK 432
AMPKα1          --TPRARHTLDELNPQKSKH--QGVRKAKWHLGIRSQSRPNDIMAEVCRAIKQLDYEWKV 437
AMPKα2          --SPKARCPLDALNTTKPKS--LAVKKAKWHLGIRSQSKPYDIMAEVYRAMKQLDFEWKV 432
Dm              QLAMSVQTSGGGAFPEKTARGGTPIKRAKWHLGIRSQSKPNDIMLEVYRAMKALSYEWKI 490
Sc              QIHRANMLAQGSPAASKISPLVTKKSKTRWHFGIRSRSYPLDVMGEIYIALKNLGAEWAK 535
                          .                 :* :*:: :: * ::* ::  :::  .  *

SnRK1α2.1       IG---HYNMKCRWVPG-------------LADGQNT-MVNNQL--HFRDESSIIEDDCAM 464
SnRK1α1.1       IG---HYNMKCRWVPNS------------SADGMLSNSMHDNN--YFGDESSIIENEAAV 464
Snf1a           TG---AYNLKCRWVAPGQNSNDTTAENHSLPDSPMAGSMPRASSCRWSSEQHGVSGSVAA 486
Snf1b           TG---AYNLKCRWVAPNQHLNDRASEHRGIPDSPMAGTTPRVSSGRWSSEQQGISGSVAS 489
AMPKα1          VN---PYYLRVRRKNPVTSTYSKMSLQLYQVDSRTYLLDFRSIDDEITEAKSGTATPQRS 494
AMPKα2          VN---AYHLRVRRKNPVTGNYVKMSLQLYLVDNRSYLLDFKSIDDEVVEQRSGSSTPQRS 489
Dm              IN---PYHVRVRRQNVKTGKFSKMSLQLYQVDAKSYLLDFKSLTNDEVEQ--GDDVIMES 545
Sc              PSEEDLWTIKLRWKYDIGNKTNTNEKIPDLMKMVIQLFQIETNNYLVDFKFDGWESSYGD 595
                 .    : :: *                   .

SnRK1α2.1       TS-----------------PTVIKFELQLYKAREEKYLLDIQR-VNGPQFLFLDLCAAFL 506
SnRK1α1.1       KS-----------------PNVVKFEIQLYKTRDDKYLLDLQR-VQGPQFLFLDLCAAFL 506
Snf1a           GNRDN----------ESGVESNVLKFELQLFKLREEKYLLDLQR-VVGPTYLFLDLCAAFL 536
Snf1b           GNKDD----------ESGVESNVLKFELQLFKMREEKYLLDLQR-VEGPTYLFLDLFSAFL 539
AMPKα1          GSVSNYRSCQRSDSDAEAQGKSSEVSLTSSVTSLDSSPVDLTPRPGSHTIEFFEMCANLI 554
AMPKα2          CSAAGLHRPRSSFDSTTAESHSLSGSLTGSLT--GSTLSSVSPRLGSHTMDFFEMCASLI 547
Dm              LTPP-------------------PLSVSGVMP---------LQP-TGHHTMEFFEMCAALI 577
Sc              DTTVS----------------NISEDEMSTFSA-----------------YPFLHLTTKLI 623
                 .                      .:                          *:.: : ::

SnRK1α2.1       TELRVI---- 512
SnRK1α1.1       AQLRVL---- 512
Snf1a           AELRVL---- 542
Snf1b           IELRVA---- 545
AMPKα1          KILAQ----- 559
AMPKα2          TTLAR----- 552
Dm              IQLAR----- 582
Sc              MELAVNSQSN 633
                  *
```

C

Appendix

Appendix-Figure 1**.** Protein Alignment of SnRK1α1 homologs. *Arabidopsis thaliana* (Arabidopsis) SnRK1α1 and SnRK1α2, *Physcomitrella patens patens* (Moss) Snf1a (Q6V8Y5) and Snf1b (Q6V8Y3), *Homo sapiens* (Human) AMPKα1 (Q13131) and AMPKα2 (P54646), *Drosophila melanogaster* (Drosophila, Dm) SNF1A (O18645) and *Saccharomyces cerevisae* (Yeast, Sc) Snf1 (P06782) protein sequences, were analyzed using the Clustal W2 multiple sequence alignment tool (http://www.ebi.ac.uk/Tools/msa/clustalw2/). Sequences were retrieved from UniprotKB Protein knowledgebase database (http://www.uniprot.org/uniprot), except for Arabidopsis proteins, whose sequence was retrieved from TAIR (www.arabidopsis.org). In the sequences, red underlined K(s) represent hpSAS >91%, blue underlined K(s) represent pSAS <91%, bold red K(s) represent sumoylated residues, bold red K(s) highlighted in yellow represent sumoylated residues crucial for SnRK1α1 sumoylation in *E. coli*. Blue italic underlined residues represent SIM1 and yellow italic underlined residues represent SIM2 motifs identified in yeast Snf1, in green italic underlined are the overlapped residues of both motifs. Below the alignment, asterisks (*) indicate amino acid residues conserved in all aligned sequences, colon (:) indicates conservation between groups of strongly similar properties, and period (.) indicates conservation between groups of weakly similar properties.

Appendix- Figure 2

Consensus recognition motif for SnRK1 kinases, from (*1*):

X	**M**	X	R
	L		K
	V		H
	F		R
	I		

X	X	**S**	X
		T	
			X

X	X	X	**L**
			F
			I
			M
			V

Phosphorylated residues are in bold type and underlined; basic residues at are underlined and hydrophobic residues are in bold type (*1*).

SIZ1.1_ At5g60410.1

MDLEANCKEKLSYFRIKELKDVL**T**QLGLSKQGKKQELVDRILTLLSDEQAARLLSKKNTV 60

AKEAVAKLVDDTYRKMQV**S**GASDLA**S**KGQVSSD**T**SNLKVKGEPEDPFQPEIKVRCVCGNS 120

LETDSMIQCEDPRCHVWQHVGCVILPDKPMDGNPPLPESFYCEICRLTRADPFWVTVAHP 180

L**S**PVRLTATTIPNDGASTMQSVERTFQITRADKDLLAKPEYDVQAWCMLLNDKVLFRMQW 240

PQYADLQVNGVPVRAINRPGGQLLGVNGRDDGPIITSCIRDGVNRISLSGGDVRIFCFGV 300

RLVKRR**T**LQQVLNLIPEEGKGETFEDALARVRRCIGGGGGDDNAD**S**D**S**DIEVVADFFGVN 360

LRCPM**S**GSRIKVAGRFLPCVHMGCFDLDVFVELNQRSRKWQCPICLKNY**S**VEHVIVDPYF 420

NRITSKMKHCDEEVTEIEVKPDGSWRVKFKRE**S**ERRELGELSQWHAPDGSLCPSAVDIKR 480

KMEMLPVKQEGY**S**DGPAPLKLGIRKNRNGIWEVSKPNTNGLSSSNRQEKVGYQEKNIIPM 540

SSSATGSGRDGDDASVNQDAIGTFDFVANGMELDSISMNVDSGYNFPDRNQSGEGGNNEV 600

IVLSDSDDENDLVITPGPAYSGCQTDGGLTFPLNPPGIINSYNEDPHSIAGGSSGLGLFN 660

DDDEFDTPLWSFPSETPEAPGFQLFRSDADVSGGLVGLHHHSPLNCSPEINGGYTMAPET 720

SMASVPVVPGSTGRSEANDGLVDNPLAFGRDDPSLQIFLPTKPDASAQSGFKNQADMSNG 780

LRSEDWISLRLGDSASGNHGDPATTNGINSSHQMSTREGSMDTTTETASLLLGMNDSRQD 840

KAKKQRSDNPFSFPRQKRSVRPRMYLSID**S**DSE 873

Appendix- Figure 2 | Predicted SnRK1 phosphorylation motifs, and phosphorylated residues retrieved from phosphoproteomics studies, in SIZ1.1 protein. Underlined are the predicted SnRK1 phosphorylation motifs encompassing T24, T94, S182, T307, S366, S410, S453 (putative phosphorylated residues are in bold, black). In red, bold, phosphorylated residues retrieved in several phosphoproteomic studies that include S79, S86, S346, S348, S493, and S870 (*2-6*). Functional domains of SIZ1 encompass the following residues: SAP (11-45), PD (112-168), PINIT (273-276), SP-RING (348-425), and SXS (604-606).

Appendix Table 1

Name	Number	AGI	Insert information (numbers of the corresponding primers)	Vector (Tag)	Description / usage	Reference
Clones used in this study						
Constructs for expression in protoplasts						
SnRK1α1	pEBG1	At3g01090.1	Previously described, see reference [CDS cloned into pHBT95 (498/709)]	pHBT95 (C-HA)	Expression of SnRK1α1 in protoplasts	(*7*)
SnRK1α1^{T175A}	pEBG2	At3g01090.1	Previously described, see reference [mutagenesis of pEBG1 (1444/1445)]	pHBT95 (C-HA)	Expression of SnRK1α1^{T175A} in protoplasts	(*7*)
SnRK1α1^{K48M}	pEBG3	At3g01090.1	Previously described, see reference [mutagenesis of pEBG1 (1377/1378)]	pHBT95 (C-HA)	Expression of SnRK1α1^{K48M} in protoplasts	(*7*)
SnRK1α1^{3K}	pPC54	At3g01090.1	Cloned from pPC55 (706/709)	pHBT95 (C-HA)	Expression of SnRK1α1$^{K34R/K63R/K390R}$ in protoplasts	
SnRK1α1^{8K}	pPC135	At3g01090.1	Cloned from pPC92 (706/709)	pHBT95 (C-HA)	Expression of SnRK1α1$^{K20R/K34R/K44R/K56R/K63R/K69R/K390R/K421R}$ in protoplasts	
mSUMO1	pLD24	At4g26840.1	CDS cloned into pHBT95 (759/440)	pHBT95 (N-Flag)	Expression of mature SUMO1 in protoplasts	
mSUMO3	pLD25	At5g55170.1	CDS cloned into pHBT95 (443/444)	pHBT95 (N-Flag)	Expression of mature SUMO3 in protoplasts	
mSUMO1^{AA}	pLD89	At4g26840.1	Cloned from pLD24 (759/835)	pHBT95 (N-Flag)	Intermediary step to generate SnRK1α1-mSUMO1^{AA}	
mSUMO1^{Q90A}	pLD92	At4g26840.1	Mutagenesis of pLD24 (833/834)	pHBT95 (N-Flag)	Expression of mature SUMO1^{Q90A} in protoplasts	
SnRK1α1-mSUMO1^{AA}	pLD87	At3g01090.1 / At4g26840.1	Cloned from pLD24 (759/835) to pEBG1	pHBT95	Expression of SnRK1α1-mSUMO1^{AA} in protoplasts	
SnRK1α1^{T175A}-mSUMO1^{AA}	pPC131	At3g01090.1 / At4g26840.1	Mutagenesis of pLD87 (1444/1445)	pHBT95	Expression of SnRK1α1^{T175A}-mSUMO1^{AA} in protoplasts	
SnRK1α1^{K48M}-mSUMO1^{AA}	pPC130	At3g01090.1 / At4g26840.1	Mutagenesis of pLD87 (1377/1378)	pHBT95	Expression of SnRK1α1^{K48M}-mSUMO1^{AA} in protoplasts	
GFP-mSUMO^{1AA}	pPC134	GFP / At4g26840.1	Subcloned GFP from pHBT-GFP-HA (plasmid 77 in Li et al., 2013, see reference) to pLD87	pHBT95	Expression of GFP-mSUMO1^{AA} in protoplasts	(*8*)
SIZ1	pLD28	At5g60410.1	CDS cloned into pHBT95 (495/496)	pHBT95 (C-HA)	Expression of SIZ1.1 in protoplasts	
SIZ1^{C379A}	pLD127	At5g60410.1	Mutagenesis of pLD28 (1382/1383)	pHBT95 (C-HA)	Expression of SIZ1.1^{C379A} in protoplasts	
SCE1	pLD27	At3g57870.1	CDS cloned into pHBT95 (489/490)	pHBT95 (C-HA)	Expression of SCE1 in protoplasts	
SnRK1α1-SCE1	pLD91	At3g01090.1/At3g57870.1	SCE1 StuI/StuI (809/490) cloned in frame with SnRK1α1 in pEBG1	pHBT95 (C-HA)	Expression of SnRK1α1-SCE1 in protoplasts	
SCE1-SnRK1α1	pLD93	At3g57870.1/At3g01090.1	SnRK1α1 StuI/StuI (649/709) cloned in frame with SCE1 in pLD27	pHBT95 (C-HA)	Expression of SCE1-SnRK1α1 in protoplasts	
SCE1-SnRK1α1ΔKA1-HA	pLD84	At3g57870.1/At3g01090.1	SnRK1α1ΔKA1 StuI/StuI (649/708) cloned in frame with SCE1 in pLD27	pHBT95 (C-HA)	Expression of SCE1-SnRK1α1ΔKA1 in protoplasts	

Name	Number	AGI	Insert information (numbers of the corresponding primers)	Vector (Tag)	Description / usage	Reference
SCE1$^{K15/154R}$	pLD104	At3g57870.1	Mutagenesis of pLD27 (912/913 and 973/974)	pHBT95 (C-HA)	Expression of SCE1$^{K15/154R}$ in protoplasts	
SnRK1α1-SCE1$^{K15/154R}$	pLD103	At3g01090.1/At3g57870.1	Mutagenesis of pLD91 (912/913 and 973/974)	pHBT95 (C-HA)	Expression of SnRK1α1-SCE1$^{K15/154R}$ in protoplasts	
SCE1$^{K15/154R}$-SnRK1α1	pLD105	At3g57870.1/At3g01090.1	Mutagenesis of pLD93 (912/913 and 973/974)	pHBT95 (C-HA)	Expression of SCE1$^{K15/154R}$-SnRK1α1 in protoplasts	
SCE1$^{K15/154R}$-SnRK1α1ΔKA1	pLD106	At3g57870.1/At3g01090.1	Mutagenesis of pLD84 (912/913 and 973/974)	pHBT95 (C-HA)	Expression of SCE1$^{K15/154R}$-SnRK1α1ΔKA1 in protoplasts	
HPY2	pEBG7	AT3G15150.1	CDS cloned into pHBT95 (BamHI/StuI)	pHBT95 (C-HA)	Expression of HPY2 in protoplasts	
GBF5	pEBG5	At2g18160.1	Previously described, see reference [CDS cloned into pHBT95 (GBF5_BamHI_F/GBF5_StuI_R)	pHBT95 (C-HA)	Expression of GBF5 in protoplasts	(*7*)
pDIN6::LUC	pEBG4	At3g47340	Previously described, see reference	pHBT95	Reporter gene construct (*pDIN6::LUC*) for following SnRK1 signaling in protoplasts	(*7*)
pUbq::GUS			Previously described, see reference	pHBT95	Control for protoplasts transfection efficiency (*pUbq::GUS*)	(*9*)
mER7 (Control DNA)			Previously described, see reference	pHBT95	Negative control for protoplast transfection (truncated GUS which is not expressed)	(*10*)
Constructs for E. coli assay - targets						
His-T7-SnRK1α1	pLD20	At3g01090.1	Cloned from pEBG1 (400/401)	pET28a	Expression of SnRK1α1 in the *E. coli* SUMOylation assay	
His-T7-SnRK1α1$^{K144/471R}$	pRB4	At3g01090.1	Mutagenesis of pLD20 (1013/1014 and 314/315)	pET28a	Expression of SnRK1α1$^{K144R/K471R}$ in the *E. coli* SUMOylation assay	
His-T7-SnRK1α1-KD	pRB3	At3g01090.1	Cloned from pEBG1 (400/593)	pET28a	Expression of SnRK1α1 Kinase Domain in the *E. coli* SUMOylation assay	
His-T7-SnRK1α1-KD$^{K34/63R}$	pPC38	At3g01090.1	Mutagenesis of pRB3 (738/739 and 740/741)	pET28a	Expression of SnRK1α1 Kinase Domain-$^{K34R/K63R}$ in the *E. coli* SUMOylation assay	
His-T7-SnRK1α1-RD	pRB1	At3g01090.1	Cloned from pEBG1 (736/401)	pET28a	Expression of SnRK1α1 Regulatory Domain in the *E. coli* SUMOylation assay	
His-T7-SnRK1α1-RD^{K390R}	pPC16	At3g01090.1	Mutagenesis of pRB1 (718/719)	pET28a	Expression of SnRK1α1 Regulatory Domain-^{K390R} in the *E. coli* SUMOylation assay	
His-T7-SnRK1α1^{3K}	pPC55	At3g01090.1	Mutagenesis of pLD20 (738/739; 740/741 and 718/719)	pET28a	Expression of SnRK1α1$^{K34R/K63R/K390R}$ in the *E. coli* SUMOylation assay	
His-T7-SnRK1α1^{8K}	pPC92	At3g01090.1	Mutagenesis of pPC55 (1138/1139; 1140/1141; 1142/1143; 1144/1145 and 720/721)	pET28a	Expression of SnRK1α1 $^{K20R/K34R/K44R/K56R/K63R/K69R/K390R/K421R}$	
His-T7-SnRK1β1	pPC104	At5g21170.1	Subcloned from pGBKT7::SnRK1β1 (from Martine Thomas) to pET28a	pET28a	Expression of SnRK1β1 in the *E. coli* SUMOylation assay	(*11*)
His-T7-SnRK1β2	pPC105	At4g16360.3	Subcloned from pGBKT7::SnRK1β2 (from Martine Thomas) to pET28a	pET28a	Expression of SnRK1β2 in the *E. coli* SUMOylation assay	(*11*)
His-T7-SnRK1γ	pPC107	At3g48530.1	Subcloned from pGBKT7::SnRK1γ (from Martine Thomas) to pET28a	pET28a	Expression of SnRK1γ in the *E. coli* SUMOylation assay	(*11*)
His-T7-SnRK1βγ	pPC108	At1g09020.1	Subcloned from pGBKT7::SnRK1βγ (from Martine Thomas) to pET28a	pET28a	Expression of SnRK1βγ in the *E. coli* SUMOylation assay	(*12*)

Name	Number	AGI	Insert information (numbers of the corresponding primers)	Vector (Tag)	Description / usage	Reference
His-T7-SNF1A-KD	pLD64	- -	Cloned from pLD39 (548/710)	pET28a	Expression of SNF1A Kinase Domain in the *E. coli* SUMOylation assay	
His-T7-SNF1A-RD	pLD68	- -	Cloned from pLD39 (727/549)	pET28a	Expression of SNF1A Regulatory Domain in the *E. coli* SUMOylation assay	
Constructs for E. coli assay - machinery						
SAE2 + SAE1A		pTK978	At2g21470.1 / At4g24940.1	pACYCDuet^{TM-1}	Expression of the machinery (E1) in the *E. coli* SUMOylation assay	(*13*)
SUMO1^{GG} + SCE1	pTK973	At4g26840.1 / At3g57870.1	AtSUMO**1**^{GG} / AtSCE1	pCDFDuet^{TM-1}	Expression of the machinery (E2 + SUMO1^{GG}) in the *E. coli* SUMOylation assay	(*13*)
SUMO1^{AA} + SCE1	pTK1017	At4g26840.1 / At3g57870.1	AtSUMO**1**^{AA} / AtSCE1	pCDFDuet^{TM-1}	Expression of the machinery (E2 + SUMO1^{AA}) in the *E. coli* SUMOylation assay	(*13*)
SUMO1^{RGG} + SCE1	mS1-RGG	At4g26840.1 / At3g57870.1	AtSUMO**1**^{RGG} / AtSCE1	pCDFDuet^{TM-1}	Expression of the machinery (E2 + SUMO1^{RGG}) in the *E. coli* SUMOylation assay	(*13*)
SUMO3^{GG} + SCE1	pTK975	At5g55170.1 / At3g57870.1	AtSUMO**3**^{GG} / AtSCE1	pCDFDuet^{TM-1}	Expression of the machinery (E2 + SUMO3^{GG}) in the *E. coli* SUMOylation assay	(*13*)
SUMO3^{AA} + SCE1	pTK1788	At5g55170.1 / At3g57870.1	AtSUMO**3**^{AA} / AtSCE1	pCDFDuet^{TM-1}	Expression of the machinery (E2 + SUMO3^{AA}) in the *E. coli* SUMOylation assay	(*13*)
SUMO3^{RGG} + SCE1	pKT1037	At5g55170.1 / At3g57870.1	AtSUMO**3**^{RGG} / AtSCE1	pCDFDuet^{TM-1}	Expression of the machinery (E2 + SUMO3^{RGG}) in the *E. coli* SUMOylation assay	(*13*)
Constructs for plant transformation						
PROM-5'UTR SnRK1α1	pLD40	At3g01090	Amplified from genomic DNA (557/558)	pDONR221 P1-P4	Entry clone with the promoter (2kb upstream of the ATG) of SnRK1α1	
*g*SnRK1α1.2-GFP	pLD33	At3g01090.2	Amplified from genomic DNA (664/709)	pHBT95 (C-GFP)	Intermediary clone for having the genomic sequence of SnRK1α1.2-GFP	
*g*SnRK1α1.2-GFP-att	pLD36	At3g01090.2	Cloned from pLD33 (546/547)	pDONR221	Entry clone with the genomic sequence of SnRK1α1 in frame with the CDS of the GFP	
3'UTR-TERM SnRK1α1	pLD41	At3g01090	Amplified from genomic DNA (559/560)	pDONR221 P4r-P3r	Entry clone with the terminator (1kb downsteam of the last codon) of SnRK1α1	
prom-*g*SnRK1α1-GFP-t*er*	pLD47	At3g01090.2	Multiple Site Gateway Recombination of pLD40, pLD36 and pLD41	pBm43GW0	Generation of *pSnRK1α1::SnRK1α1-GFP::tSnRK1α1/snrk1α1-3* and *pSnRK1α1::SnRK1α1-GFP::tSnRK1α1/siz1-2* plants	
SnRK1α1-DKA1-GFP	pLD66	At3g01090.1	Cloned from pEBG1 (498/708)	pHBT95 (C-ter GFP)	Intermediary clone for having the CDS of SnRK1α1-DKA1-GFP	

Name	Number	AGI	Insert information (numbers of the corresponding primers)	Vector (Tag)	Description / usage	Reference
SnRK1α1ΔKA1-GFP-att	pAE28	At3g01090.1	Cloned from pLD66 (279/547)	pDONR221	Entry clone with the CDS of SnRK1α1ΔKA1-GFP	
prom-SnRK1α1-ΔKA1-GFP-ter	pAE34	At3g01090.1	Multiple Site Gateway Recombination of pLD40, pAE28 and pLD41	pBm43GW0	Generation of *pSnRK1α1::SnRK1α1ΔKA1-GFP::tSnRK1α1/snrk1α1-3* plants	
mSUMO1^{AA}-SnRK1α1	pLD85	At4g26840.1+At3g01090.1	mSumo1^{AA} BamHI/StuI (837/838) +N-GFP-SnRK1α1 BamHI/StuI as backbone	pHBT95	Intermediary clone for having mSUMO1^{AA}-SnRK1α1	
mSUMO3^{AA}-SnRK1α1	pLD86	At5g55170.1+At3g01090.1	mSumo3^{AA} BamHI/StuI (838/840) +N-GFP-SnRK1α1 BamHI/StuI as backbone	pHBT95	Intermediary clone for having mSUMO3^{AA}-SnRK1α1	
SnRK1α1-mSUMO1^{AA}	pLD88	At3g01090.1+At5g55170.1	SnRK1α1-HA StuI/PstI as backbone + mSumo3^{AA} StuI/PstI (443/836)	pHBT95	Intermediary clone for having SnRK1α1-mSUMO1^{AA}	
mSUMO1^{AA}-SnRK1α1	pLD107	At4g26840.1+At3g01090.1	subcloned from pLD85a with BamHI/PstI and inserted in pCB302 plasmid BamHI/PstI	pCB302	Generation of *mSUMO1-SnRK1α1-OE* plants	
mSUMO3^{AA}-SnRK1α1	pLD108	At5g55170.1+At3g01090.1	subcloned from pLD86b with BamHI/PstI and inserted in pCB302 plasmid BamHI/PstI	pCB302	Generation of *mSUMO3-SnRK1α1-OE* plants	
SnRK1α1-mSUMO1^{AA}	pLD109	At3g01090.1+At3g57870.1	subcloned from pLD87a with BamHI/PstI and inserted in pCB302 plasmid BamHI/PstI	pCB302	Generation of *SnRK1α1-mSUMO1-OE* plants	
SnRK1α1-mSUMO3^{AA}	pLD110	At3g01090.1+At5g55170.1	subcloned from pLD88a with BamHI/PstI and inserted in pCB302 plasmid BamHI/PstI	pCB302	Generation of *SnRK1α1-mSUMO3-OE* plants	
mSUMO1^{AA}-GFP	pLD123	At4g26840.1+GFP	subcloned from pLD107 with StuI/PstI and inserted GFP StuI/PstI in this pCB302 pLD107 plasmid StuI/PstI	pCB302 (C-GFP)	Generation of *mSUMO1-GFP-OE* plants	
mSUMO3^{AA}-GFP	pLD124	At5g55170.1+GFP	subcloned from pLD108 with StuI/PstI and inserted GFP StuI/PstI in pCB302 pLD108 plasmid StuI/PstI	pCB302 (C-GFP)	Generation of *mSUMO3-GFP-OE* plants	
GFP-mSumo1^{AA}	pLD125	GFP+At3g57870.1	subcloned from pLD109 with BamHI/StuI and inserted GFP BamHI/StuI in pCB302 pLD109 plasmid BamHI/StuI	pCB302 (N-GFP)	Generation of *GFP-mSUMO1-OE* plants	
GFP-mSumo3^{AA}	pLD126	GFP+At5g55170.1	subcloned from pLD110 with BamHI/StuI and inserted GFP BamHI/Stulin pCB302 pLD110 plasmid BamHI/StuI	pCB302 (N-GFP)	Generation of *GFP-mSUMO3-OE* plants	
Constructs for Yeast-Two-Hybrid						
SCE1	pLD26	At3g57870.1	Cloned from pTK973 (491/490)	pGBKT7	Expression of GAL4 BD-SCE for Y2H	
SnRK1α1	pLD35	At3g01090.1	Cloned from pEBG1 (402/403)	pGADT7	Expression of GAL4 AD-SnRK1α1 full-length for Y2H	
SnRK1α1-KD	pLD49	At3g01090.1	Cloned from pEBG1 (402/561)	pGADT7	Expression of GAL4 AD-SnRK1α1 KD for Y2H	
SnRK1α1-RD	pLD34	At3g01090.1	Cloned from pEBG1 (447/403)	pGADT7	Expression of GAL4 AD-SnRK1α1 RD for Y2H	
SnRK1α1-RDΔKA1	pLD58	At3g01090.1	Cloned from pLD34 (447/672)	pGADT7	Expression of GAL4 AD-SnRK1α1 RDΔKA1 for Y2H	
SNF1A	pLD39	- -	Cloned from Drosophila cDNA (548/549)	pGADT7	Expression of GAL4 AD-SNF1A for Y2H	
SnRK1α1	- -	At3g01090.1	Previously described, see reference	pGBKT7	Expression of GAL4 BD-SnRK1α1 full-length for Y2H	(*14*)

Name	Number	AGI	Sequence
Primers used in this study			
Restriction or *att* sites introduced by PCR are marked in blue			
Cloning primers			
SnRK1α1ΔKA1-GFP attB1 Fw	279	At3g01090.1	GGGGACAAGTTTGTACAAAAAAGCAGGCTTAATGGATGGATCAGGCACAGGCAG
SnRK1α1-ATG BamHI Fw	400	At3g01090.1	CGGGATCCGATGGATCAGGCACAGGCAG
SnRK1α1 EcoRI Rv	401	At3g01090.1	CGGAATTCTCAGAGGACTCGGAGCTGAG
SnRK1α1 EcoRI Fw	402	At3g01090.1	CCGGAATTCATGGATGGATCAGGCACAGGC
SnRK1α1 BamHI Rv	403	At3g01090.1	CGCGGATCCGAGGACTCGGAGCTGAGCAAG
mSUMO1 PstI Rv	440	At4g26840.1	AAAACTGCAGTCAGCCACCAGTCTGATGG
mSUMO1 StuI Fw	759	At4g26840.1	AAGGCCTTCTGCAAACCAGGAGGAAG
mSUMO1AA PstI Rv	835	At4g26840.1	AAAACTGCAGTCAAGCAGCAGTCTGATGG
mSUMO3_StuI	443	At5g55170.1	AAGGCCTTCTAACCCTCAAGATGAC
mSUMO3_PstI	444	At5g55170.1	AAAACTGCAGTCAACCACCACTCATCGC
SnRK1α1 RD EcoRI Fw	447	At3g01090.1	CCGGAATTCGACGAGGAGATTCTCCAAG
SCE1_FP_Nco1	489	At3g57870.1	CATGCCATGGCTAGTGGAATCGCTCG
SCE1 StuI Rv	490	At3g57870.1	AAGGCCTGACAAGAGCAGGATACTGC
SCE1 EcoRI Fw	491	At3g57870.1	CGGAATTCGCTAGTGGAATCGCTCG
SCE1_StuI_Fw-ATG	809	At3g57870.1	AAGGCCTGCTAGTGGAATCGCTCG
SIZ1.1 NcoI Fw	495	At5g60410.1	CATGCCATGGATTTGGAAGCTAATTG
SIZ1.1 StuI Rv	496	At5g60410.1	AAGGCCTCTCAGAATCCGAGTCAATGG
SnRK1α1 BamHI Fw a	498	At3g01090.1	CGGGATCCATGGATGGATCAGGCACAGG
*g*SnRK1α1-GFP attB1 Fw	546	At3g01090.2	GGGGACAAGTTTGTACAAAAAAGCAGGCTTAATGTTCAAACGAGTAGATG
*g*SnRK1α1-GFP attB2 Rv	547	At3g01090.2	GGGGACCACTTTGTACAAGAAAGCTGGGTTTTACTTGTACAGCTCGTCC
SnRK1α1ΔKA1-GFP attB2 Rv	547	At3g01090.1	GGGGACCACTTTGTACAAGAAAGCTGGGTTTTACTTGTACAGCTCGTCC
PROM-5'UTR_*g*SnRK1α1 attB4 Fw	557	At3g01090.1	GGGGACAACTTTGTATAGAAAAGTTGTTTTAATCTTTGGTGTAGGCATCG
PROM-5'UTR_*g*SnRK1α1 attB1r Rv	558	At3g01090.1	GGGGACTGCTTTTTTGTACAAACTTGTGAGAATTTAGCGAGAATTAGG
TERM-3'UTR_*g*SnRK1α1 attB2r Fw	559	At3g01090.1	GGGGACAGCTTTCTTGTACAAAGTGGTTATACTAAACCGGACCTCTTC
TERM-3'UTR_*g*SnRK1α1 attB3 Rv	560	At3g01090.1	GGGGACAACTTTGTATAATAAAGTTGTACGAATCTTGGGGCGAATCCG
SnRK1α1 KD EcoRI Rv	561	At3g01090.1	CCGGAATTCAATCTTTTTTGCCTGTTGC
SnRK1α1 I293 EcoRI Rv	593	At3g01090.1	CCGGAATTCTCAAATCTTTTTTGCCTGTTGC

Name	Number	AGI	Sequence
*g*SnRK1α1 BamHI Fw	664	At3g01090.2	CGGGATCCATGTTCAAACGAGTAGATG
SnRK1α1 BamHI Fw b	706	At3g01090.1	CGGGATCCGGATGGATGGATCAGGCACAGG
SnRK1α1ΔKA1 StuI Rv	708	At3g01090.1	AAGGCCTTCTCTCAACAGGGTATTG
SnRK1α1D389_BamHI_Rv	672	At3g01090.1	CGCGGATCCTCTCTCAACAGGGTATTG
SnRK1α1 StuI Rv	709	At3g01090.1	AAGGCCTGAGGACTCGGAGCTGAGC
SnRK1α1 D294 BamHI Fw	736	At3g01090.1	CGCGGATCCGACGAGGAGATTCTCCAAGAAG
SNF1A_EcoR1_Fw	548	- -	CCGGAATTCCCCCAGATGAGGGCTGCG
SNF1A_EcoR1_Rp	549	- -	CCGGAATTCGCGAGCCAGTTGAATGATC
SNF1A-I300-XhoI-Rv	710	- -	CCGCTCGAGGATCACATTGGAGTCCTG
SNF1A-D301-BamHI-Fw	727	- -	CGGGATCCGACACCTACGCTGTGGCAG
GBF5_BamHI_F		At2g18160.1	CGGGATCCATGGCGTCATCTAGCAGCAC
GBF5_StuI_R		At2g18160.1	AAGGCCTATACATATTGATATCATTAG
SnRK1βγ_BamHI_F		At1g09020.1	CGGGATCCATGTTTGGTTCTACATTGG
SnRK1βγ _StuI_R		At1g09020.1	AAGGCCTAAGACCGAGCAGGAATTGG
Mutagenesis primers			
SnRK1α1^{-K48M} Fw	1377	At3g01090.1	TAAGGTTGCTATCATGATCCTCAATCGTCGC
SnRK1α1^{-K48M} Rv	1378	At3g01090.1	GCGACGATTGAGGATCATGATAGCAACCTTA
SnRK1α1^{-T175A} Fw	1444	At3g01090.1	GGTCATTTTTTGAAGGCAAGTTGTGGAAGT
SnRK1α1^{-T175A} Rv	1445	At3g01090.1	ACTTCCACAACTTGCCTTCAAAAAATGACC
SnRK1α1^{-K20R} Fw	1138	At3g01090.1	TCTACCAAATTACAGGCTTGGGAGAACTCTT
SnRK1α1^{-K20R} Rv	1139	At3g01090.1	AAGAGTTCTCCCAAGCCTGTAATTTGGTAGA
SnRK1α1^{-K34R} Fw	738	At3g01090.1	CCTTTGGTAGGGTGAGGATAGCTGAGCATGC
SnRK1α1^{-K34R} Rv	739	At3g01090.1	GCATGCTCAGCTATCCTCACCCTACCAAAGG
SnRK1α1^{-K44R} Fw	1140	At3g01090.1	ATTGACAGGACATAGGGTTGCTATCAAGATC
SnRK1α1^{-K44R} Rv	1141	At3g01090.1	GATCTTGATAGCAACCCTATGTCCTGTCAAT
SnRK1α1^{-K56R} Fw	1142	At3g01090.1	TCGTCGCAAAATCAGGAACATGGAGATGGAG
SnRK1α1^{-K56R} Rv	1143	At3g01090.1	CTCCATCTCCATGTTCCTGATTTTGCGACGA

Name	Number	AGI	Sequence
SnRK1α1^{-K63R} Fw	740	At3g01090.1	TGGAGATGGAGGAGAGAGTGAGGAGAGAGAT
SnRK1α1^{-K63R} Rv	741	At3g01090.1	ATCTCTCTCCTCACTCTCTCCTCCATCTCCA
SnRK1α1^{-K69R} Fw	1144	At3g01090.1	GAGGAGAGAGATCAGAATCTTGAGACTATTT
SnRK1α1^{-K69R} Rv	1145	At3g01090.1	AAATAGTCTCAAGATTCTGATCTCTCTCCTC
SnRK1α1^{-K144R} Fw	1013	At3g01090.1	TCACAGAGACCTCAGGCCTGAAAACTTGC
SnRK1α1^{-K144R} Rv	1014	At3g01090.1	GCAAGTTTTCAGGCCTGAGGTCTCTGTGA
SnRK1α1^{-K390R} Fw	718	At3g01090.1	CCCTGTTGAGAGAAGATGGGCTCTTGGAC
SnRK1α1^{-K390R} Rv	719	At3g01090.1	GTCCAAGAGCCCATCTTCTCTCAACAGGG
SnRK1α1^{-K421R} Fw	720	At3g01090.1	TGTATGTTGGAAGAGGATAGGGCACTACA
SnRK1α1^{-K421R} Rv	721	At3g01090.1	TGTAGTGCCCTATCCTCTTCCAACATACA
SnRK1α1^{-K471R} Fw	314	At3g01090.1	AAGTCGCCCAATGTTGTCCGTTTTGAAATTCAGTTGTAT
SnRK1α1^{-K471R} Rv	315	At3g01090.1	ATACAACTGAATTTCAAAACGGACAACATTGGGCGACTT
SIZ1.1^{-C379A} Fw	1382	At5g60410.1	GCTGGGAGATTTTTACCCGCTGTGCACATGGGCTGTTTTG
SIZ1.1^{-C379A} Rv	1383	At5g60410.1	CAAAACAGCCCATGTGCACAGCGGGTAAAAATCTCCCAGC
MUT_mSUMO1^{Q90A}_Fw	833	At4g26840.1	GATCGATGCGATGCTCCATGCGACTGGTGGCTGACTGCAG
MUT_mSUMO1^{Q90A}_Rp	834	At4g26840.1	CTGCAGTCAGCCACCAGTCGCATGGAGCATCGCATCGATC
Genotyping primers			
SnRK1α1-GABIa (LP)	374	At3g01090	CCAGCATAATAGAGAACGAAGC
SnRK1α1-GABIb (RP)	375	At3g01090	GTCCGGTTTAGTATTCAGAGG
GABI-08409-LB	722	--	ATATTGACCATCATACTCATTGC
SnRK1α1-seqF Fw	534	At3g01090	GAGATCCGGCAACACCCTTG
GABI1-RB-seq Rv	832	At3g01090	CATGTGTTGAGCATATAAGAAACC
SIZ1.1_Gen_RP	1568	AT5G60410.1	CACGACAGATGAAGCATTGTG
SIZ1.1_Gen_LP	1569	AT5G60410.1	GAGCTGAAGCATCTGGTTTTG
SALK LBb1 T-DNA primer	373	--	GCGTGGACCGCTTGCTGCAACT

Name	Number	AGI	Sequence
IMS2-Fw	828	At5g23020	GAGGAGAATCTCTGATGGATGG
IMS2-Rv	829	At5g23020	GATTTCAGCACCGTTCACCAC
qPCR primers			
AXP Fw	63	At2g33830	CTTCGACAAGCCTTCTCACC
AXP Rv	64	At2g33830	TCGTCGCTGTATAGCCAATC
DIN6 Fw	53	At3g47340	AACTTGTCGCCAGATCAAGG
DIN6 Rv	54	At3g47340	GGAACACGTGCCTCTAGTCC
TPS8 Fw	89	At1g70290	CCACAAGGTGTAAGCAAAGG
TPS8 Rv	90	At1g70290	CGCGTTCTACCATTTCTCG
ACT2 Fw	555	At3g18780	TTTGCAGGAGATGATGCTCCC
ACT2 Rv	556	At3g18780	GTCTTTGAGGTTTCCATCTCC
Virus Induced Gene Silencing (VIGS) primers			
KIN11VIGS-A		At3g29160	GGAATTCGTTTCTGTATATTTCTTCGCTC
KIN11VIGS-B		At3g29160	CGGGATCCAGTACTCTACACCAGATATTAT
GFPVIGS-A	--		CGGAATTCCCATCCTGGTCGAGCTGGAC
GFPVIGS-B	--		GGGGTACCCGTTGGGGTCTTTGCTCAGG

References

1. C. Sugden, P. G. Donaghy, N. G. Halford, D. G. Hardie, in *Plant Physiol*. (1999), vol. 120, pp. 257-274.
2. T. Umezawa, N. Sugiyama, F. Takahashi, J. C. Anderson, Y. Ishihama, S. C. Peck, K. Shinozaki, in *Science Signaling*. (2013), vol. 6, pp. rs8.
3. H. Nakagami, N. Sugiyama, K. Mochida, A. Daudi, Y. Yoshida, T. Toyoda, M. Tomita, Y. Ishihama, K. Shirasu, in *PLANT PHYSIOLOGY*. (2010), vol. 153, pp. 1161-1174.
4. W. R. Engelsberger, W. X. Schulze, in *Plant J*. (2012), vol. 69, pp. 978-995.
5. Q. Yao, C. Bollinger, J. Gao, D. Xu, J. J. Thelen, in *Front. Plant Sci.* (2012), vol. 3, pp. 206.
6. P. Durek, R. Schmidt, J. L. Heazlewood, A. Jones, D. MacLean, A. Nagel, B. Kersten, W. X. Schulze, in *Nucleic Acids Research*. (2010), vol. 38, pp. D828-834.
7. E. Baena-González, F. Rolland, J. M. Thevelein, J. Sheen, in *Nature*. (2007), vol. 448, pp. 938-942.
8. J.-F. Li, H. S. Chung, Y. Niu, J. Bush, M. McCormack, J. Sheen, in *The Plant Cell*. (2013).
9. S.-D. Yoo, Y.-H. Cho, J. Sheen, in *Nat Protoc*. (2007), vol. 2, pp. 1565-1572.
10. Y. Kovtun, W. L. Chiu, W. Zeng, J. Sheen, *Nature* (1998), vol. 395, pp. 716-720.
11. J. P. Bouly, L. Gissot, P. Lessard, M. Kreis, M. Thomas, in *Plant J*. (1999), vol. 18, pp. 541-550.
12. C. Polge, M. Jossier, P. Crozet, L. Gissot, M. Thomas, in *PLANT PHYSIOLOGY*. (2008), vol. 148, pp. 1570-1582.
13. S. Okada, M. Nagabuchi, Y. Takamura, T. Nakagawa, K. Shinmyozu, J.-i. Nakayama, K. Tanaka, in *Plant Cell Physiol*. (2009), vol. 50, pp. 1049-1061.
14. A. Rodrigues, M. Adamo, P. Crozet, L. Margalha, A. Confraria, C. Martinho, A. Elias, A. Rabissi, V. Lumbreras, M. González-Guzmán, R. Antoni, P. L. Rodriguez, E. Baena-González, in *The Plant Cell*. (2013), vol. 25, pp. 3871-3884.

ITQB-UNL | Av. da República, 2780-157 Oeiras, Portugal
Tel (+351) 214 469 100 | Fax (+351) 214 411 277

www.itqb.unl.pt